

**EVALUATING THE EFFECTS OF LEGACY PHOSPHORUS ON
DISSOLVED REACTIVE PHOSPHORUS LOSSES IN TILE-DRAINED
SYSTEMS**

by

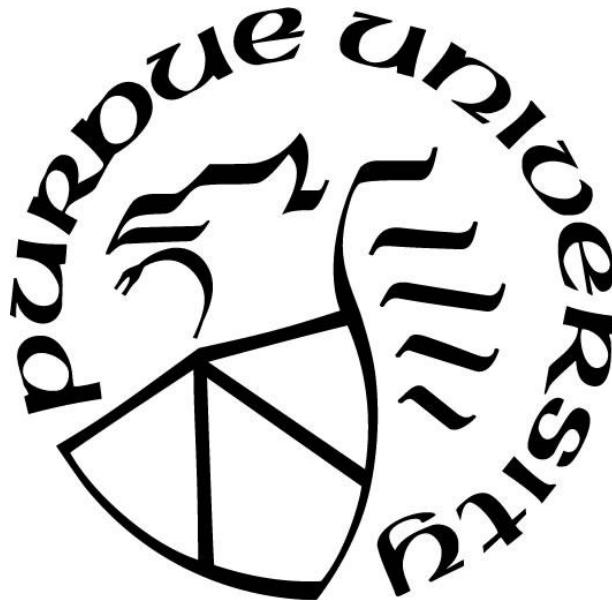
Pauline Welikhe

A Dissertation

Submitted to the Faculty of Purdue University

In Partial Fulfillment of the Requirements for the degree of

Doctor of Philosophy



Department of Agronomy

West Lafayette, Indiana

May 2020

THE PURDUE UNIVERSITY GRADUATE SCHOOL
STATEMENT OF COMMITTEE APPROVAL

Dr. Sylvie Brouder, Chair

Department of Agronomy

Dr. Jeffrey Volenec

Department of Agronomy

Dr. Ronald Turco

Department of Agronomy

Dr. Margaret Gitau

Department of Agronomy

Approved by:

Dr. Rich Grant

To Hennig Brandt

ACKNOWLEDGMENTS

Since joining Purdue University in the fall of 2016, I have received support and encouragement from many people. First, I would like to express gratitude to my major advisor: Professor Sylvie Brouder for allowing me to work on this research project, their support, guidance, advice, lots of valuable literature, and fruitful discussions. I wish to express my sincere thanks to Drs. Jeffrey Volenec, Ronald Turco, and Margaret Gitau for accepting .to be in my committee and their constructive discussion and contribution to my work. I am grateful to Dr. Linda Lee for admitting me to the Ecological Sciences and Engineering program and following my academic journey closely. I would like to thank my colleagues and all the staff in the Agronomy department for their help and friendship and for creating a conducive atmosphere that broadened my understanding of other cultures. Nicole De Armond gets a special mention for her tireless help from day one. Special thanks go to my parents (Mr. & Mrs. Welikhe) and sisters for their love and never-ending support. Also, this work was supported by the USDA NIFA NRI Managed Ecosystem Program grant (Award Number 2008-35101-19152), US DOE 2009 North Central Sun Grant Competitive Grants Program (Award Number DE-FG36-08GO88073), USDA NIFA Bioenergy CAP grant (Award Number 2011-68005-30411), and the 4R Research Fund of the Foundation for Agronomic Research (Project Number 2015-USA-4RN45) with additional support from a Purdue University Ecological Sciences and Engineering Lynn Fellowship, Bilsland Fellowship, and the Estate of Orpha M. Wickersham.

TABLE OF CONTENTS

LIST OF TABLES	8
LIST OF FIGURES	11
ABSTRACT	14
1. INTRODUCTION	16
1.1 Background and current knowledge gap	16
1.2 Research Objectives and Organization	18
1.3 References	22
2 DEVELOPMENT OF PHOSPHORUS SORPTION CAPACITY – BASED ENVIRONMENTAL INDICES FOR TILE-DRAINED SYSTEMS	28
2.1 Abstract	28
2.2 Introduction	29
2.3 Materials and Methods	32
2.3.1 Laboratory study	32
2.3.1.1 Soil selection and analysis	32
2.3.1.2 Data Analysis	33
2.3.2 Field study	34
2.3.2.1 Experimental site, Soil and Water Characterization	34
2.3.2.2 Data analysis	35
2.4 Results and Discussion	36
2.4.1 Laboratory study	36
2.4.1.1 Soil characteristics	36
2.4.1.2 Relationship among variables	36
2.4.1.3 Sorption pedotransfer function (pedoTF)	38
2.4.1.4 P release from soils	38
2.4.2 Field study	42
2.4.2.1 Soil characteristics	42
2.4.2.2 Phosphorus loss	44
2.5 Conclusions	45

2.6	References	46
3	USING ARTIFICIAL NEURAL NETWORKS TO IMPROVE PHOSPHORUS INDICES	55
3.1	Abstract	55
3.2	Introduction.....	56
3.3	Materials and Methods	59
3.3.1	Selection of ANN variables.	59
3.3.2	Study site and creation of datasets.....	59
3.3.3	Description and development of SP ANN-model	65
3.3.4	Relative importance analysis of input variables.....	67
3.3.5	PI performance	68
3.4	Results and Discussion	69
3.4.1	Performance of ANN.....	69
3.4.2	Relative importance of input variables on SP losses	72
3.4.3	Comparison of PI performance	76
3.5	Conclusion	78
3.6	References	80
4	DYNAMICS OF DISSOLVED REACTIVE PHOSPHORUS LOSS FROM PHOSPHORUS SOURCE AND SINK SOILS IN TILE-DRAINED SYSTEMS	90
4.1	Abstract	90
4.2	Introduction.....	90
4.3	Materials and Methods	94
4.3.1	Site description and nutrient management	94
4.3.2	Soils data.....	95
4.3.3	Flow and DRP concentration data collection.....	96
4.3.4	Calculations and statistical analysis	97
4.3.5	Determination of C-Q hysteresis loops.....	98
4.4	Results.....	100
4.4.1	Annual DRP loads and FDRP concentrations.....	100
4.4.2	Discharge events: General description, DRP loads, and FDRP concentrations	102

4.4.3	C-Q relationships	106
4.4.4	Hysteresis patterns	110
4.5	Conclusion	115
4.6	References	116
5	SYNTHESIS AND FUTURE WORK	124
5.1	References	128
APPENDIX		129
PUBLICATION		176

LIST OF TABLES

Table 2.1. Brief descriptions of P measures (indices) examined in this study.	30
Table 2.2. Pearson's correlation coefficients of Phosphorus sorption index (PSI) and soil properties of 73 archived soils samples used in the P sorption study.	37
Table 2.3. Mean and standard deviation (Std. dev.) for organic matter (OM), phosphorus (P) and aluminum (Al), phosphorus saturation ratio (PSR) and soil phosphorus storage capacity (SPSC) for archived soil samples from the 6 experimental sites (n=154 [†]).	39
Table 3.1. Categorical transport variables included in the empirical dataset, including name, brief description and rating values used in the study. Categories used were obtained from NASTRAT (IN-NRCS, 2013).	62
Table 3.2. Range of values for continuous input variables used for generating the theoretical dataset.	63
Table 3.3. Equations for multiplicative P index formulations used in the study.	69
Table 3.4. Testing and 10 fold-cross validation performance of the MLF ANN with increasing number of neurons in the hidden layer. The validation mean RMSE is the mean RMSE of the 10 folds analyzed during cross-validation.	69
Table 3.5. RMSE values for each fold during cross-validation.	72
Table 3.6. Results of the relative importance analysis for various site characteristics on annual flow-weighted mean DRP concentrations in tile effluent. Values in bold and in parenthesis represent Lemunyon and Gilbert (1993) weighting factors normalized to sum to 1.	73
Table 4.1. A brief description of no-till treatments at the Water Quality Field Station (WQFS) treatments (abbreviations and year of establishment, previous treatments (cropping systems and N rates) dating back to 1997, and P, N, and tillage management.	95
Table 4.2. Soil P storage capacity (SPSC) for surface soils (20 cm) reported in Welikhe et al. (2020). Negative SPSC and positive SPSC values are associated with P source and P sink soils, respectively. 2011, 2012, and 2013 are water years e.g. 2011 water year begins on 1 Oct 2010 and ends on 30 Sept 2013. Refer to Table 1 for description of treatments.	96
Table 4.3. The number of days with missing flow data for tiles in the study plots. The percentage of number of days with missing data per water year is presented parenthetically.	97
Table 4.4. Annual (water year) dissolved reactive phosphorus (DRP) loads in tile discharge. Plots with negative SPSC values (P source soils) are in bold. Refer to table 1 for description of treatments.	101
Table 4.5. Annual (water year) flow-weighted dissolved reactive phosphorus (FDRP) in tile discharge. Plots with negative SPSC values (P source soils) are in bold. Concentration above which eutrophication is accelerated i.e. > 0.02 mg P L ⁻¹ (Correll, 1999)) are italicized. Refer to Table 1 for description of treatments.	102

Table 4.6. General characteristics, DRP loads and FDRP concentrations, of the selected discharge events between October 2010 and September 2013 [†] . FDRP concentrations > 0.02 mg L ⁻¹ (concentration above which eutrophication is accelerated (Correll, 1999)) are italicized and in bold.....	103
Table 4.7. Pearson correlation matrix between general discharge event characteristics and the ΔR (%) and ΔC (%) parameters ^{††}	110
Table A.1 Soil classification and type of of phosphorus (P) inputs used at six (6) Purdue agricultural research centers (Davies (DPAC), Pinney (PPAC), Northeast (NEPAC), Southeast (SEPAC), Throckmorton (TPAC) and, Water Quality Field Station (WQFS)).	129
Table A.2. A brief description of current Water Quality Field Station (WQFS) treatments (abbreviations and year of establishment), any previous treatment (cropping system and N rates applied to maize) dating back to 1997, and P, N and tillage management. An estimate of the cumulative P ₂ O ₅ applied from 1997 – 2013 is shown parenthetically. Current N management identifies the N rates applied to perennial crops, sorghum, and continuous and rotated maize..	132
Table A.3. Univariate statistics of daily tile discharge (L day ⁻¹ plot ⁻¹) from 2010 - 2014 for each of the 48 tiles in the 12 treatments. Shaded rows represent tiles omitted from the study due to tile failure as evidenced by the low number of flow of flow days (< 5 % of total days studied). Italicized values represent outer fence values from Tukey's 1.5 IQR rule used to identify extreme outliers.	141
Table A.4 Univariate statistics of orthophosphate (DRP) concentrations (PO ₄ ⁻³ day ⁻¹ plot ⁻¹) from 2010 - 2014 for each of the forty-eight (48) tiles in the (12) treatments.....	143
Table A.5 Selected univariate statistic for the 73 archived soils samples used in the P sorption study including the phosphorus sorption index (PSI) and analytical results from routine analyses conducted in a commercial soil testing laboratory.	145
Table A.6 Change point values for the fitted nonlinear relationship between phosphorus saturation ratio (PSR) and water-soluble phosphorus (WSP) after removal of a random site's soils during statistical analysis (***significant at P≤ 0.001).....	147
Table A.7 Values for organic matter (OM), phosphorus (P), aluminum (Al), P saturation ratio (PSR), and soil P storage capacity (SPSC)for surface soils (20 cm) obtained from the monitored plots at the Water Quality Field Station (WQFS) for 2011 -2013 water years (e.g. October 1, 2010 – September 30, 2011 for 2011 water year).	148
Table A.8 Annual tile flow and tile drainage efficiencies (Q/P) for tiles in the study plots.	151
Table A.9 A brief description of current treatments at the Water Quality Field Station (WQFS) (abbreviations and year of establishment), any previous treatment (cropping system and N rates applied to maize) dating back to 1997, and P, N and tillage management. An estimate of the cumulative P ₂ O ₅ applied from 1997 – 2013 is shown parenthetically. Current N management identifies the N rates applied to perennial crops, sorghum, and continuous and rotated maize. (Table obtained from Welikhe et al. (2020)).....	166
Table A.10 Summary for Organic matter (OM) (%), phosphorus (P) (mg kg ⁻¹), Aluminum (Al) (mg kg ⁻¹), P saturation ratio (PSR) (unitless), Soil P storage capacity (SPSC) (L kg ⁻¹), and Annual	

flow-weighted mean DRP concentrations (fDRP) (mg L^{-1}) obtained from the monitored plots at the Water Quality Field Station (WQFS) for 2011 -2013 water years (e.g. Oct 1, 2010 – Sept 30, 2011 for 2011 water year). Cropping system abbreviation and management histories are provided in supplemental table S1. (Table obtained from Welikhe et al. (2020)) 167

Table A.11 Field data (empirical dataset) used to generate the theoretical dataset and for the calculation of PI values. Treatment (cropping system) abbreviation and management histories are provided in supplemental Table S1. Swine manure was applied at rates meant to supply $\sim 228 \text{ lbs N ha}^{-1} \text{ yr.}$ 168

LIST OF FIGURES

Figure 2.1 Relationship between (a) phosphorus saturation ratio (PSR) and water soluble phosphorus (WSP) of archived soil samples (< 20 cm depth) obtained from Davies (DPAC), Pinney (PPAC), Northeast (NEPAC), Southeast (SEPAC), Throckmorton (TPAC) and, the Water Quality Field Station (WQFS) (n=152). Parameter estimates (with standard errors in parentheses) and R^2 values for the fitted segmented line models (***) significant at the 0.001 probability level), (b) phosphorus saturation ratio (PSR) and annual flow weighted mean DRP (fDRP) for soil samples (20 cm depth) from the Water Quality Field Station (WQFS) plots (n=119). Parameter estimates (with standard errors in parentheses) and R^2 values for the fitted segmented line models (***) significant at the 0.001 probability level).....40

Figure 2.2. Relationship between (a) water soluble phosphorus (WSP) and soil phosphorus storage capacity (SPSC) of archived soil samples (< 20 cm depth) obtained from Davies (DPAC), Pinney (PPAC), Northeast (NEPAC), Southeast (SEPAC), Throckmorton (TPAC) and, the Water Quality Field Station (WQFS) (n=152). Dashed line locates zero SPSC values (proposed threshold), (b) annual flow-weighted DRP (fDRP) and soil phosphorus storage capacity (SPSC) for soil samples (20 cm depth) from the Water Quality Field Station (WQFS) plots (n=119). Dashed line locates zero SPSC values (proposed threshold).42

Figure 3.1. Neural interpretation diagram of the best MLP network structure with 11,7, and 1 neuron(s) in the input (I), hidden (H) and output (O) layers respectively. B1 and B2 are bias terms added to H and O layers. Black and grey lines represent positive and negative connections respectively, while line thickness represents the relative magnitude of each connection weight. Abbreviations are; STP= soil test P, PSR = P saturation ratio, SPSC = soil P storage capacity, FPR = Inorganic P fertilizer rate, FPA = Inorganic P fertilizer application method and timing, OPR = Organic P fertilizer rate, OPA = Organic P fertilizer application method and timing, SE = soil erosion, SR = surface runoff, SDP = subsurface drainage potential, DTW = distance to water body, and fDRP = Annual flow-weighted mean DRP concentrations.70

Figure 3.2. Selected MLF ANN parity plot for annual flow-weighted dissolved reactive phosphorus (fDRP) concentrations in tile discharge. The black line is the 1:1 ($y = x$) line.71

Figure 3.3. Observed annual flow-weighted mean DRP concentrations (fDRP) and predictions of SP loss risk calculated with the (a) Unweighted PI (PI_{NO}), (b) a PI weighted using Lemunyon and Gilbert (1993) weights (LG - weighted PI (PI_{LG})), and (c) a PI weighted using artificial neural network generated weights (ANN - weighted PI (PI_{ANN}))......77

Figure 4.1. Relationship between (a) daily discharge (mm) and daily dissolved reactive phosphorus (DRP) flux ($kg\ ha^{-1}$) presented on a log-log scale, and (b) event discharge (mm) and event dissolved reactive phosphorus (DRP) flux ($kg\ ha^{-1}$) presented on a log-log scale. Exponent (b) and coefficient (a) values are defined by Equation 2, and R^2 values were determined by linear regression on log transformed DRP flux and discharge values. Source and sink DRP represent DRP fluxes measured from P saturated (source) and unsaturated (sink) soils.....107

Figure 4.2. Plot of ΔC_{new} (%) versus ΔR (%) for the C-Q hysteresis loops of dissolved reactive phosphorus (DRP). The i , j , and k terms in the plot labels correspond to i th season (winter (W)),

spring (Sp), summer (Su), and fall (F)) in a water year (2011 (11), 2012 (12), and 2013 (13), the j th plot at the WQFS (10, 11, 12, 26, 30, 32, 43, and 44), and the k th discharge event for the specified plot. Table 5 provides detailed information on discharge events. Illustrations of the typical C-Q relationships (c, broken blue line; Q, continuous brown line) are presented for each of the regions A – D of the ΔC_{new} (%) versus ΔR plot. A few source DRP events showed clockwise hysteresis 112

Figure 4.3. A proposed conceptual model illustrating DRP loss in tile drained fields from, (a) P source soils, Panel 1, discharge at the start of the event when P rich event water (preferential flow) from the surface rapidly flows to tile drains; Panel 2, discharge during the event when P rich event water is mixed with P poor water from the soil matrix and shallow ground water, resulting in an overall dilution; Panel 3, when the discharge recedes and contributions from soil matrix and shallow ground water are absent, event water with high P concentrations continues, (b) P sink soils, Panel 1, discharge at the start of the event when P poor event water (preferential flow) from the surface rapidly flows to tile drains; Panel 2, discharge during the event when P poor waters (preferential, matrix, and shallow groundwater) mix; Panel 3, soil matrix and shallow ground water recede, event water with low P concentrations continues. 114

Figure A.1 A map showing the layout of plots at the Water Quality Field Station. The number at the top and bottom of each plot represents the plot and treatment number respectively. This study considered the 48 drainage lysimeter plots (plot number 1 - 48) only. Treatments 1 to 12 include; Native prairie mixture (Prairie), Miscanthus x giganteus (Mxg), continuous maize with residue removal (CM-RR), Switchgrass (Switch), continuous sorghum with residue removal (Sorgh), maize-soybean rotation trt#1 with residue return (MS-R1), soybean-maize rotation trt#1 with residue return (SM-R1), maize-soybean rotation trt#2 with residue return (MS-R2), soybean-maize rotation trt#2 with residue return (SM-R2), continuous maize with residue return and spring manure (CM-SpM), continuous maize with residue return and, fall manure (CM-FM) and continuous maize with residue return (CM) respectively (more details on previous crop, nutrient and tillage management can be found in Table S2 in the supplemental text). Letters A to H identify the instrumentation huts into which collection tiles drain. (Map obtained from; <https://ag.purdue.edu/agry/WQFS/Pages/map.aspx>) 131

Figure A.2 Missing daily follow data 134

Figure A.3 Unit circle resulting from principle component analysis of the different variables for the selected 73 soils. Relative positions of routinely determined soil test data (organic matter (OM), phosphorus (P), potassium (K), magnesium (Mg), calcium (Ca), log of H^+ concentrations (pH), cation exchange capacity (CEC), iron (Fe), aluminum (Al)) in the circle indicate the magnitude of direct association between these soil properties and phosphorus sorption index (PSI). Percentage value in parenthesis is the proportion of the total variance accounted for by each principle axis. 146

Figure A.4 Daily tile flow/discharge (m^3) from individual plots for the study period (beginning Oct 1, 2010 and ending on Sept 30, 2013). Gaps in graphs are a result of missing data either due to maintenance, flooding or equipment failure/error 152

Figure A.5. Boxplots of DRP concentration. Circles represent outliers, whiskers represent the 10th and 90th percentiles, the lower and upper edges of the boxes represent the 25th and 75th percentiles, and the horizontal line inside the boxes represents the median. Tile 42, 22, 23, 13, 2, 9, 38 and,

41, were omitted from the study due to tile failure. Current treatment abbreviations: Prairie, native prairie mixture with residue removed; Mxg, *Miscanthus x giganteus* established in 2008 ; CM - RR, continuous maize with residue removal; Switch, Switchgrass established in spring 2007; Sorgh, continuous sorghum with residue removal established in 2008; MS – R1,maize-soybean rotation trt#1 w/residue return; SM-R1, soybean-maize rotation trt #1 w/residue return; MS – R2, maize-soybean rotation trt#2 w/residue return; SM-R2, soybean-maize rotation trt #1 w/residue return; CM -SpM, continuous maize with residue return and spring manure applications; CM-FM, continuous maize with residue return and fall manure applications; CM, continuous maize with residue return. More details on previous crop, nutrient and tillage management can be found in Table S3 in the main text.....162

Figure A.6 Histogram and theoretical densities, Q-Q plot, empirical and theoretical cumulative distribution functions and P-P plots for the (a) Mehlich 3 soil test P log-normal (lnorm) distribution, (b) P saturation ratio normal (norm) distribution, and (c) Soil P storage capacity normal (norm) distribution.173

Figure A.7 Density plot showing the distribution of annual flow-weighted mean DRP values. 174

ABSTRACT

Eutrophication due to phosphorus (P) enrichment continues to be a primary water quality concern affecting freshwater and marine estuaries around the world. Excessive anthropogenic P inputs, driven by the need to meet the rising food and energy demands of a growing and increasingly urbanized population, have resulted in the buildup of P creating legacy (historical) P pools in agricultural landscapes. There is growing evidence that remobilization of accumulated legacy P can interfere with conservation efforts aimed at curbing eutrophication and improving water quality. Less is known about the magnitude and effects of these legacy P pools on dissolved reactive P (DRP) losses in tile-drained systems. This dissertation consists of three separate inquiries into how legacy P may affect DRP losses in tile drains. In the first inquiry, we examined the possibility of developing a suitable pedo-transfer function (pedoTF) for estimating P sorption capacity (PSC). Subsequent PSC-based indices (Phosphorus Saturation Ratio (PSR) and Soil Phosphorus Storage Capacity (SPSC)) were evaluated using daily water quality data from an in-field laboratory. The pedoTF derived from soil aluminum and organic matter accurately predicted PSC ($R^2 = 0.60$). Segmented-line models fit between PSR and soluble P (SP) concentrations in both desorption assays ($R^2 = 0.69$) and drainflows ($R^2 = 0.66$) revealed apparent PSR thresholds in close agreement at 0.21 and 0.24, respectively. Linear relationships were observed between negative SPSC values and increasing SP concentrations ($R^2 = 0.52$ and $R^2 = 0.53$ respectively), and positive SPSC values were associated with very low SP concentrations in both desorption assays and drainflows. Zero SPSC was suggested as a possible environmental threshold. Thus, PSC-based indices determined using a pedoTF could estimate the potential for SP loss in tile drains. Also, both index thresholds coincided with the critical soil test P level for agronomic P sufficiency (22 mg kg⁻¹ Mehlich 3 P) suggesting that the agronomic threshold could serve as an environmental P threshold. In the second inquiry, PSC-based indices in addition to other site characteristics present in a P index (PI), were used as inputs in the development of a multi-layer feed-forward artificial neural network (MLF-ANN). The MLF-ANN was trained, tested, and validated to evaluate its performance in predicting SP loss in tile drains. Garson's algorithm was used to determine the weight of each site characteristic. To assess the performance of ANN-generated weights, empirical data from an in-field laboratory was used to evaluate the performance of an unweighted PI (PI_{NO}), a PI weighted using Lemunyon and Gilbert weights (PI_{LG}), and an ANN-weighted PI (PI_{ANN}) in

estimating SP losses in tile effluent. The MLF-ANN provided reliable predictions of SP concentrations in tile effluent ($R^2 = 0.99$; RMSE = 0.0024). Soil test P, inorganic fertilizer application rate (FPR), SPSC, PSR, and organic P fertilizer application rate (OPR), with weights of 0.279, 0.233, 0.231, 0.097, and 0.084, respectively, were identified as the top five site characteristics with the highest weights explaining SP loss in tile discharge. These results highlighted the great contribution of both contemporary and legacy P sources to SP concentrations in tile discharge. Also, PI_{ANN} was the only PI with a significant exponential relationship with measured annual SP concentrations ($R^2 = 0.60$; $p < 0.001$). These findings demonstrated that MLF-ANNs coupled with Garson's algorithm, can accurately quantify weights for individual site characteristics and develop PIs with a strong correlation with measured SP in tile discharge. Finally, in the third inquiry, we compared DRP loads and flow-weighted mean DRP (FDRP) concentrations in P source and P sink soils and evaluated the predominant DRP concentration – discharge (C-Q) behavior in these soils on a daily and event scale. At the daily scale, C-Q patterns were linked to the soil P status whereby a chemostatic and dilution behavior was observed for P source and P sink soils, respectively. At the event scale, C-Q patterns were linked to soil P status, flow path connectivity, and mixing of event water, matrix water, and rising shallow groundwater. The predominant anti-clockwise rotational pattern observed on P source soils suggested that, as the discharge event progressed, contributions from P poor waters including matrix and shallow groundwater resulted in lower DRP concentrations on the rising limb compared to the falling limb. However, the variable flushing and dilution behavior observed on the rising limb suggested that, in addition to discharge and soil P status, rapid exchanges between P pools, the magnitude of discharge events (Q), and the relative number of days to discharge peak (D_{rel}) also regulated DRP delivery. On the other hand, the predominant non-hysteretic C-Q behavior in P sink soils suggest that DRP loss from these soils can be discounted. Our collective results highlight the need for nutrient and conservation practices focused on P drawdown, P sequestration, and P supply close to the crop needs, which will likely be required to convert P sources to sinks and to avoid the conversion of P sinks to sources.

1. INTRODUCTION

1.1 Background and current knowledge gap

In recent history, water quality success-stories from intensive conservation programs have seldom occurred. Freshwater eutrophication that occurs following phosphorus (P) enrichment and is characterized by harmful algal blooms, hypoxia, fish kills, and increased turbidity has become a common occurrence in many watersheds (Smith et al., 2006; Bennett & Schipanski, 2013). For example, despite over 30 years of conservation practices particularly for phosphorus (P) loss reduction in Lake Erie basin, Mississippi-Atchafalaya River basin, Chesapeake Bay watershed and, inland and coastal waters of Florida, there has been an increase in the magnitude and frequency of eutrophication in these waters (Sharpley et al., 2012; Dale et al., 2010; Reckhow et al., 2011; USEPA, 2011). Several likely causes for the increased cases of re-eutrophication of fresh-waters are being debated and closely scrutinized by the scientific, conservation and industrial communities (Smith et al., 2015). One suggested causal factor that has come under scrutiny is legacy P (Jarvie et al., 2013; Kleinman et al., 2011a; Sharpley et al., 2011; Mulla et al., 2008).

Legacy P is P accumulated from past surpluses in anthropogenic P inputs that are stored within agricultural soils and sediments and could potentially contribute to P release to the atmosphere, surface waters, and biomass (Kleinman et al., 2011; Sharpley et al., 2013; Chen et al., 2015). The main driver for excessive anthropogenic P inputs is the need to meet the rising food and energy demands of a growing and increasingly urbanized population (Chen et al., 2018). Indeed over the past several decades, in many watersheds across southern Europe, Midwestern United States, and China, inorganic P fertilizer additions is one of the major components of anthropogenic P inputs (Goyette et al., 2016; Chen et al., 2015; Hong et al., 2012; Russell et al., 2008). The heavy dependence on P fertilizers coupled with low crop P use efficiency has dramatically disrupted the P cycle (almost doubling P amounts in terrestrial systems) and ecosystem fluxes (Townsend & Porder, 2012; Elser & Bennett, 2011; Vitousek et al., 2009). Besides excessive inorganic P inputs, other anthropogenic activities have contributed to legacy P build up in soils. For example, the adoption of soil conservation measures that control soil erosion but inadvertently promote soil stratification, has caused P accumulations to be localized at the soil surface (Kleinman et al., 2011; Smith et al., 2015; Sharpley, 2016). Also, the intensification of

livestock production has resulted in manure inputs and localized organic P build up and imbalances. For example, in the Delmarva Peninsula soil P concentrations have increased to levels one order of magnitude greater than crop growth needs (Buda et al., 2010).

The reactivity of P as an anion results in its extremely high concentration in solid phases as compared to solution phases (Jones et al., 1984). Frossard et al. (1995) & Frossard et al. (2000) show that P sorption potential of sediments and soils is several orders of magnitude greater compared to the concentration of P in solution. Additionally, the major conduit for surplus P transfer i.e. riverine export flux, only transports a relatively small fraction of accumulated P (~3%; Zhang et al., 2015), which means that > 90% of anthropogenic P inputs are potentially stored in terrestrial and aquatic landscapes as built up legacy P pools (Chen et al., 2018; Goyette et al., 2016; Chen et al., 2015; Hong et al., 2012; Russell et al., 2008). Therefore, it is not surprising that, at the global scale, net P accumulation rates in agricultural soils increased to 8 Tg P year⁻¹ in 2000 from 1 Tg P year⁻¹ in 1950, with cumulative P of approximately 210 Tg P between 1970 and 2010 (Bouwman et al., 2013; Sattari et al., 2012). Even though these terrestrial, legacy P reserves may be the answer to diminishing phosphate reserves (projected to be exhausted in the next 50-100 years), they could also be responsible for widespread eutrophication (Steen, 1998; Smil, 2000 ; Carpenter, 2008). As added P accumulates and the P sorption capacity of a soil decreases, sorbed P is increasingly prone to release to soil solution (Sharpley, 1995; Hooda et al., 2000; Nair et al., 2004). This means that legacy P pools have the potential to be re-mobilized as dissolved reactive P (DRP), and act as a major source of P to fresh and coastal waters (Sharpley et al., 2005; McDowell & Sharpley, 2011).

Previously, leaching losses of DRP in tile drains was thought to be negligible because of the high sorption capacity of subsoils (Logan et al., 1980). However, recent studies show that the altered hydrology (i.e. low water tables, reduced surface runoff, increased subsurface drainage) in tile-drained systems greatly impacts the transport and fate of nutrients from agricultural soils, resulting in leaching losses of DRP especially from fields with long-term P applications (Radcliffe et al., 2015; King et al., 2015; Gentry et al., 2007; Kinley et al., 2007; Sims et al., 1998). Also, since tile drains act as direct conduits between fields and nearby water bodies, DRP export can be from a much larger area of the landscape compared to contributions from surface runoff (Heathwaite and Dils, 2000). In the humid and poorly drained regions of the Midwest United States (US), the installation of tile drains is a common and necessary practice for successful crop

production (Skaggs et al., 1994). Zucker and Brown, (1998) estimated that between 18 and 28 million ha of cropland in the Midwest US is tile-drained. However, Blann et al. (2009) indicate that the area of cropland with subsurface tile drains is likely significantly higher. In Indiana, based on the 2012 USDA-NASS Census of Agriculture, 7.5 million acres of the 14.7 million acres of farmland has some type of subsurface drainage present (e.g. tiles or ditches) (USDA-NASS, 2014). Given attempts to diminish soil P concentrations through phytomining and reduction or cessation of P inputs take decades or longer (McCollum, 1991; Schärer et al., 2007; Sharpley & Rekolainen, 1997), DRP losses in intensely tile-drained systems will persist. For example, in the Western Lake Erie Basin, increasing magnitude and frequency of re-eutrophication from the early 1990s has been directly linked to increasing inputs of DRP into the major river tributaries (Sandusky, Maumee and Raisin), the latter thought to be a consequence of the presence of legacy P and intensified tile drainage among other factors (Smith et al., 2015; King et al., 2015; Michalak et al., 2013; Baker et al., 2014; Scavia et al., 2014). Incidences such as the 2011 and 2014 record-setting algal blooms (Smith et al., 2015; Michalak et al., 2013) led to the governments of the United States and Canada to announce a new bi-national P target of 40% reduction in DRP and total P loads in spring (Annex 4, 2015). More research is needed to understand the impact of legacy P on DRP pollution loads and its effective integration into nutrient management measures. This is especially important in intensively tile-drained systems with long term histories of P application that are hypothesized to be critical source areas for DRP loss. This research will provide insight on how to quantify legacy P accumulation and identify P sink and P source soils, the importance of legacy P on eventual soluble P (SP) losses, and how legacy P affects DRP dynamics in tile drained systems. Findings from this research will help to optimize DRP loss management strategies as well as to control the expectations of stakeholders.

1.2 Research Objectives and Organization

This dissertation will focus on evaluating the effects of legacy P on DRP losses in tile-drained systems. The research is designed to analyze the relationship between P sorption capacity (PSC)- based environmental indices and DRP loss, the relative importance of a soil's P status to DRP loss compared to other site characteristics, and the effect a soil's P status has on DRP dynamics in tile-drained fields. The general and specific objectives, and hypotheses of each chapter are as follows:

- **Chapter 2**

- **Objective:** Determine the relationship between P sorption capacity (PSC)-based indices (Phosphorus Saturation Ratio (PSR) and Soil Phosphorus Storage Capacity (SPSC)) and edge-of-field DRP losses and to recommend environmental thresholds for water quality in tile-drained systems.
- **Specific objectives:**
 - To examine the possibility of developing a suitable pedo-transfer function (pedoTF) for estimating PSC using readily available soil test data
 - To ultimately evaluate the applicability and accuracy of laboratory determined threshold values at the field scale, especially where subsurface tile drains may exacerbate leaching losses.
- **Hypothesis:**
 - There will be a relationship identified between specific routinely determined chemical soil characteristics that estimates a soil's PSC.
 - PSC-based environmental thresholds will be identified above/below which DRP loss in tile-drained fields increases.
- **Rationale:**
 - In regions with long histories of fertilizer P addition such as the Midwest United States, PSC-based environmental indices can be relevant indicators of a soil's P status, particularly with increasing concern over the contribution of legacy P to increased eutrophication. Also, index thresholds identified could serve as environmental P thresholds for nutrient management.

- **Chapter 3**

- **Objective:** The study aimed to simulate soluble P concentrations in tile effluent using a multi-layer feed-forward artificial neural network (MLF-ANN) trained by the backpropagation algorithm and analyze the contribution of each site characteristics to eventual DRP loss.
- **Specific objectives:**

- To evaluate ANN model performance for predicting soluble P (SP) concentrations in tile effluent with selected site characteristics as predictor variables.
 - To determine ANN-generated WFs using Garson's algorithm and compare the performance of a PI with no WFs (PI_{NO}), a PI with WFs as proposed in the original Lemunyon and Gilbert PI (PI_{LG}), and a PI with ANN-generated WFs (PI_{ANN}), at predicting SP loss potential in tile discharge.
- **Hypothesis:**
 - SP in tile effluent will be accurately predicted by an ANN model trained by the backpropagation algorithm
 - Site characteristics related to a soil's P status will have greater contributions (weights) to eventual SP loss in tile effluent compared to site characteristics related to P movement off a field and P application methods.
 - The use of ANNs to determine PI weights is more efficient and ANN-generated weights will improve the relationship between calculated P index values and measured SP concentrations in tile effluent.
- **Rationale:**
 - To address the need to consider synergistic and antagonistic interactions among P index site characteristics when determining input factor weights.
- **Chapter 4**
 - **Objective:** The overall goal of this study was to quantify DRP losses from P source and P sink soils to tile drain waters, and assess patterns of loss as a function of discharge.
 - **Specific objectives:**
 - To determine DRP loads and flow-weighted mean DRP (FWDRP) concentrations from P source and sink soils at an annual and event-based time scale.
 - To evaluate the predominant concentration – discharge (C-Q) responses of DRP from P source and sink soils in tile discharge.
 - **Hypothesis:**

- P source and sink soils will differ in the DRP loads and FWDRP concentrations lost.
 - C-Q relationships in P source and P sink soils will differ.
- **Rationale:**
 - To elucidate solute pathways and investigate key components driving nutrient delivery in tile-drained systems to inform conservation practice and nutrient management recommendations in an effort to attain water quality goals.
- **Chapter 5**
 - **Conclusion and future work**
 - To synthesize and integrate the findings of the research conducted in this dissertation on the effects of Legacy P on DRP loss in tile-drained systems, highlight key findings and recommendations, and discuss future research needs.

1.3 References

- Annex 4 Objectives and Targets Task Team. (2015). Phosphorus Loading Targets for Lake Erie. Final Report to the Nutrients Annex Subcommittee. Great Lakes Water Quality Agreement, A. of 2012. <http://binational.net/wp-content/uploads/2015/06/nutrient.-T.pdf>. (accessed 27 D. 2018). (2015). *Phosphorus Loading Targets for Lake Erie*. 70.
- Baker, D. B., Confesor, R., Ewing, D. E., Johnson, L. T., Kramer, J. W., and Merryfield, B. J. (2014). Phosphorus loading to Lake Erie from the Maumee, Sandusky and Cuyahoga rivers: The importance of bioavailability. *Journal of Great Lakes Research*, 40(3), 502–517. <https://doi.org/10.1016/j.jglr.2014.05.001>
- Bennett, E. M., & Schipanski, M. E. (2013). The Phosphorus Cycle. *Fundamentals of Ecosystem Science*, (January), 159–178. <https://doi.org/10.1016/B978-0-08-091680-4.00008-1>
- Blann, K. L., Anderson, J. L., Sands, G. R., and Vondracek, B. (2009). Effects of agricultural drainage on aquatic ecosystems: A review. *Critical Reviews in Environmental Science and Technology*, 39(11), 909–1001. <https://doi.org/10.1080/10643380801977966>
- Bouwman, L., Goldewijk, K. K., Van Der Hoek, K. W., Beusen, A. H. W., Van Vuuren, D. P., Willems, J., and Stehfest, E. (2013). Exploring global changes in nitrogen and phosphorus cycles in agriculture induced by livestock production over the 1900-2050 period. *Proceedings of the National Academy of Sciences of the United States of America*, 110(52), 20882–20887. <https://doi.org/10.1073/pnas.1012878108>
- Buda, A. R., Church, C., Kleinman, P. J. A., Saporito, L. S., Moyer, B. G., and Tao, L. (2010). Using rare earth elements to control phosphorus and track manure in runoff. *Journal of Environmental Quality*, 39(3), 1028–1035. <https://doi.org/10.2134/jeq2009.0359>
- Carpenter, S. R. (2008). Phosphorus control is critical to mitigating eutrophication. *Proceedings of the National Academy of Sciences*, 105(32), 11039–11040. <https://doi.org/10.1073/pnas.0806112105>
- Chen, D., Hu, M., Guo, Y., and Dahlgren, R. A. (2015). Influence of legacy phosphorus, land use, and climate change on anthropogenic phosphorus inputs and riverine export dynamics. *Biogeochemistry*, 123(1–2), 99–116. <https://doi.org/10.1007/s10533-014-0055-2>
- Chen, D., Shen, H., Hu, M., Wang, J., Zhang, Y., and Dahlgren, R. A. (2018). Legacy Nutrient Dynamics at the Watershed Scale: Principles, Modeling, and Implications. In *Advances in Agronomy* (1st ed., Vol. 149). <https://doi.org/10.1016/bs.agron.2018.01.005>

- Dale, V. H., Kling, C. L., Meyer, J. L., Sanders, J., Stallworth, H., Armitage, T., and Wright, D. (2010). Hypoxia in the Northern Gulf of Mexico. In *Hypoxia in the Northern Gulf of Mexico*. <https://doi.org/10.1007/978-0-387-89686-1>
- Elser, J., & Bennett, E. (2011). Phosphorus cycle: A broken biogeochemical cycle. *Nature*, 478(7367), 29–31. <https://doi.org/10.1038/478029a>
- Frossard, E., Condron, L. M., Oberson, A., Sinaj, S., and Fardeau, J. C. (2000). Processes governing phosphorus availability in temperate soils. *Journal of Environment Quality*, 29(1), 15–23. <https://doi.org/10.2134/jeq2000.00472425002900010003x>
- Frossard, Emmanuel, Brossard, M., Hedley, M. J., and Metherell, A. (1995). Reactions Controlling the Cycling of P in Soils. *Phosphorus in the Global Environment: Transfers, Cycles, and Management*, (54), 107–138.
- Gentry, L. E., David, M. B., Royer, T. V., Mitchell, C. A., & Starks, K. M. (2007). Phosphorus Transport Pathways to Streams in Tile-Drained Agricultural Watersheds. *Journal of Environment Quality*, 36(2), 408. <https://doi.org/10.2134/jeq2006.0098>
- Hong, B., Swaney, D. P., Mörth, C. M., Smedberg, E., Eriksson Hägg, H., Humborg, C., and Bouraoui, F. (2012). Evaluating regional variation of net anthropogenic nitrogen and phosphorus inputs (NANI/NAPI), major drivers, nutrient retention pattern and management implications in the multinational areas of Baltic Sea basin. *Ecological Modelling*, 227, 117–135. <https://doi.org/10.1016/j.ecolmodel.2011.12.002>
- Hooda, P. S., Rendell, A. R., Edwards, A. C., Withers, P. J. A., Aitken, M. N., & Truesdale, V. W. (2000). Relating Soil Phosphorus Indices to Potential Phosphorus Release to Water. *Journal of Environment Quality*, 29(4), 1166. <https://doi.org/10.2134/jeq2000.00472425002900040018x>
- Goyette, J., Bennett, E. M., Howarth, R. W., and Maranger, R. (2016). Changes in anthropogenic nitrogen and phosphorus inputs to the St. Lawrence sub-basin over 110 years and impacts on riverine export. *Global Biogeochemical Cycles*, 30, 1000–1014. <https://doi.org/10.1002/2016GB005384>. Received
- Jones, C.A., Cole, C. V., Sharpley, A.N., Williams, J. R. (1984). *A Simplified Soil and Plant Phosphorus Model: I. Documentation*. *Soil Sci. Soc. Am. J.* 48:800-805.
- Heathwaite, A. L., and Dils, R. M. (2000). Characterising phosphorus loss in surface and subsurface hydrological pathways. *The Science of the Total Environment*, 251/252, 532–538.

- <https://doi.org/10.1177/014920638701300111>
- King, K. W., Williams, M. R., and Fausey, N. R. (2015). Contributions of Systematic Tile Drainage to Watershed-Scale Phosphorus Transport. *Journal of Environment Quality*, 44(2), 486. <https://doi.org/10.2134/jeq2014.04.0149>
- King, K. W., Williams, M. R., Macrae, M. L., Fausey, N. R., Frankenberger, J., Smith, D. R., and Brown, L. C. (2015). Phosphorus Transport in Agricultural Subsurface Drainage: A Review. *Journal of Environment Quality*, 44(2), 467. <https://doi.org/10.2134/jeq2014.04.0163>
- Kinley, R. D., Gordon, R. J., Stratton, G. W., Patterson, G. T., and Hoyle, J. (2007). Phosphorus losses through agricultural tile drainage in Nova Scotia, Canada. *Journal of Environmental Quality*, 36(2), 469–477. <https://doi.org/10.2134/jeq2006.0138>
- Kleinman, P. J. A., Sharpley, A. N., McDowell, R. W., Flaten, D. N., Buda, A. R., Tao, L., and Zhu, Q. (2011). Managing agricultural phosphorus for water quality protection: Principles for progress. *Plant and Soil*, 349(1–2), 169–182. <https://doi.org/10.1007/s11104-011-0832-9>
- Kleinman, P. J. A., Sharpley, A. N., Buda, A., McDowell, R., and Allen, A. (2011). Soil controls of phosphorus in runoff: Management barriers and opportunities. *Canadian Journal of Soil Science*, 91(3), 329–338. <https://doi.org/10.4141/cjss09106>
- McCollum, R. E. (1991). Buildup and Decline in Soil Phosphorus: 30-Year Trends on a Typic Umprabuilt. *Agronomy Journal*, 83(12563), 77–85. <https://doi.org/10.2134/agronj1991.00021962008300030011x>
- McDowell, R., & Sharpley, A. (2002). Availability of residual phosphorus in high phosphorus soils. *Communications in Soil Science and Plant Analysis*, 33:7-8, 1235-1246.
- Michalak, A. M., Anderson, E. J., Beletsky, D., Boland, S., Bosch, N. S., Bridgeman, T. B., and Zagorski, M. A. (2013). Record-setting algal bloom in Lake Erie caused by agricultural and meteorological trends consistent with expected future conditions. *Proceedings of the National Academy of Sciences*, 110(16), 6448–6452. <https://doi.org/10.1073/pnas.1216006110>
- Nair, V. D., Portier, K. M., Graetz, D. A., and Walker, M. L. (2004). An Environmental Threshold for Degree of Phosphorus Saturation in Sandy Soils. *Journal of Environment Quality*, 33(1), 107. <https://doi.org/10.2134/jeq2004.1070>
- Skaggs, R. W., Breve, M. A., and Gilliam, J. W. (1994). Hydrologic and Water Quality Impacts of Agricultural Drainage. *Critical Reviews in Environmental Science and Technology*, 24(1), 1–32. <https://doi.org/10.1080/10643389409388459>

- Radcliffe, D. E., Reid, D. K., Blombäck, K., Bolster, C. H., Collick, A. S., Easton, Z. M., and Smith, D. R. (2015). Applicability of Models to Predict Phosphorus Losses in Drained Fields: A Review. *Journal of Environment Quality*, 44(2), 614.
<https://doi.org/10.2134/jeq2014.05.0220>
- Reckhow, K. H., Norris, N. E., Budell, R.J., Di Toro, D. M., Galloway, J. N., Greening, H. (2011). *Achieving nutrient and sediment reduction goals in the Chesapeake Bay: An evaluation of program strategies and implementation*. Natl. Acad. Press, Washington, DC.
- Russell, M. J., Weller, D. E., Jordan, T. E., Sigwart, K. J., and Sullivan, K. J. (2008). Net anthropogenic phosphorus inputs: Spatial and temporal variability in the Chesapeake Bay region. *Biogeochemistry*, 88(3), 285–304. <https://doi.org/10.1007/s10533-008-9212-9>
- Sattari, S. Z., Bouwman, A. F., Giller, K. E., and Van Ittersum, M. K. (2012). Residual soil phosphorus as the missing piece in the global phosphorus crisis puzzle. *Proceedings of the National Academy of Sciences of the United States of America*, 109(16), 6348–6353. <https://doi.org/10.1073/pnas.1113675109>
- Scavia, D., Allan, J. D., Arend, K. K., Bartell, S., Beletsky, D., Bosch, N. S., et al. (2014). Assessing and addressing the re-eutrophication of Lake Erie: Central basin hypoxia. *Journal of Great Lakes Research*, 40(2), 226–246. <https://doi.org/10.1016/j.jglr.2014.02.004>
- Schärer, M., Stamm, C., Vollmer, T., Frossard, E., Oberson, A., Flühler, H., and Sinaj, S. (2007). Reducing phosphorus losses from over-fertilized grassland soils proves difficult in the short term. *Soil Use and Management*, 23(SUPPL. 1), 154–164. <https://doi.org/10.1111/j.1475-2743.2007.00114.x>
- Sharpley, A. N. and Rekolainen, S. (1997). Phosphorus in agriculture and its environmental implications. In *n H. Tunney, O. T. Carton, P. C. Brookes, and A. E. Johnston, eds. Phosphorus loss from soil to water*. CAB International, Wallingford, UK. Sharpley, (pp. 1–54).
- Sharpley, A. N. (1995). Dependence of runoff phosphorus on extractable soil phosphorus. *Journal of Environmental Quality*, 24(5), 920–926.
<https://doi.org/10.2134/jeq1995.00472425002400050020x>
- Sharpley, A. N., Kleinman, P. J. A., Flaten, D. N., & Buda, A. R. (2011). Critical source area management of agricultural phosphorus: Experiences, challenges and opportunities. *Water Science and Technology*, 64(4), 945–952. <https://doi.org/10.2166/wst.2011.712>

- Sharpley, A. N., Richards, P., Herron, S., and Baker, D. (2012). Case study comparison between litigated and voluntary nutrient management strategies. *Journal of Soil and Water Conservation*, 67(5), 442–450. <https://doi.org/10.2489/jswc.67.5.442>
- Sharpley A.N., McDowell R.W., Kleinman, P. J. A. (2005). Comments on “Amounts, Forms, and Solubility of Phosphorus in Soils Receiving Manure.” *Soil Science Society of America Journal*, 69(4), 1353. <https://doi.org/10.2136/sssaj2005.0077>
- Sharpley, A. N. (2016). Managing agricultural phosphorus to minimize water quality impacts. *Scientia Agricola*, 73(1), 1–8. <https://doi.org/10.1590/0103-9016-2015-0107>
- Sharpley, A. N., Jarvie, H. P., Buda, A., May, L., Spears, B., and Kleinman, P. (2013). Phosphorus Legacy: Overcoming the Effects of Past Management Practices to Mitigate Future Water Quality Impairment. *Journal of Environment Quality*, 42(5), 1308. <https://doi.org/10.2134/jeq2013.03.0098>
- Sims, J. T., Simard, R. R., and Joern, B. C. (1998). Phosphorus Loss in Agricultural Drainage: Historical Perspective and Current Research. *Journal of Environment Quality*, 27(2), 277. <https://doi.org/10.2134/jeq1998.00472425002700020006x>
- Smil, V. (2000). Phosphorus in the Environment: Natural Flows and Human Interferences. <https://doi.org/10.1146/annurev.energy.25:53-88>.
- Smith, D. R., King, K. W., and Williams, M. R. (2015). What is causing the harmful algal blooms in Lake Erie? *Journal of Soil and Water Conservation*, 70(2), 27A–29A. <https://doi.org/10.2489/jswc.70.2.27A>
- Smith, D. R., King, K. W., Johnson, L., Francesconi, W., Richards, P., Baker, D., and Sharpley, A. N. (2015). Surface Runoff and Tile Drainage Transport of Phosphorus in the Midwestern United States. *Journal of Environment Quality*, 44(2), 495. <https://doi.org/10.2134/jeq2014.04.0176>
- Smith, V. H., Joye, S. B., and Howarth, R. W. (2006). Eutrophication of freshwater and marine ecosystems. *Limnol. Oceanogr*, 51(2), 351–355. https://doi.org/10.4319/lo.2006.51.1_part_2.0351
- Steen, I. (1998). Phosphorus availability in the 21st Century: management of a non- renewable resource. *Phosphorus and Potassium*, Issue No:217(September-October, 1998), 25–31.
- Townsend, A. R., & Porder, S. (2012). Agricultural legacies, food production and its environmental consequences. *Proceedings of the National Academy of Sciences*, 109(16),

5917–5918. <https://doi.org/10.1073/pnas.1203766109>

United States Environmental Protection Agency (USEPA). (2011). Review of EPA's draft approaches for deriving numeric nutrient criteria for Florida's estuaries, coastal waters, and southern inland flowing waters. *USEPA Scientific Advisory Board, Washington, DC*, 1–4.

Retrieved from

[https://yosemite.epa.gov/sab/sabproduct.nsf/36a1ca3f683ae57a85256ce9006a32d0/C439B7C63EB9141F8525773B004E53CA/\\$File/FL+EC+Final+Methods+-+Chapters1-6.pdf](https://yosemite.epa.gov/sab/sabproduct.nsf/36a1ca3f683ae57a85256ce9006a32d0/C439B7C63EB9141F8525773B004E53CA/$File/FL+EC+Final+Methods+-+Chapters1-6.pdf)

United States Department of Agriculture - National Agricultural Statistics Services (USDA-NASS) (2014). Census of Agriculture. Retrieved May 2, 2018, from

https://www.agcensus.usda.gov/Publications/2012/Full_Report/Volume_1,_Chapter_1_State_Level/Indiana/

Vitousek P.M., Naylor, R., Crews, T., David, M. B., Drinkwater, L. E., Holland, E., Johnes, P. J., Katzenberger, J., Martinelli, L. A., Matson, P. A., Nziguheba, G., Ojima, D., Palm, C.A., Robertson, G. P., Sanchez, P. A., Townsend, A. R., and Zhang, F. S. (2009). Nutrient imbalances in agricultural development. *Science*, 324, 1519–1520.

<https://doi.org/10.1126/science.1170261>

Zhang, W., Swaney, D. P., Hong, B., Howarth, R. W., Han, H., and Li, X. (2015). Net anthropogenic phosphorus inputs and riverine phosphorus fluxes in highly populated headwater watersheds in China. *Biogeochemistry*, 126(3), 269–283.

<https://doi.org/10.1007/s10533-015-0145-9>

Zucker, L.A., and Brown, L. C. (1998). Agricultural drainage: Water quality impacts and subsurface drainage studies in the Midwest. Bulletin, 971-98. *University of Minnesota Extension, St. Paul, MN*.

2 DEVELOPMENT OF PHOSPHORUS SORPTION CAPACITY – BASED ENVIRONMENTAL INDICES FOR TILE-DRAINED SYSTEMS

This chapter was published in the Journal of Environmental Quality. It can be cited as; Welikhe, P., Brouder, S. M., Volenec, J. J., Gitau, M., & Turco, R. F. (2020). Development of phosphorus sorption capacity – Based environmental indices for Tile-drained systems. *Journal of Environmental Quality*, (January), 1–14. <https://doi.org/10.1002/jeq2.20044>

2.1 Abstract

The persistent environmental relevance of phosphorus (P) and P sorption capacity (PSC) on P loss to surface waters has led to proposals for its inclusion in soil fertility and environmental management programs. As fertility and environmental management decisions are made on a routine basis, the use of laborious P sorption isotherms to quantify PSC is not feasible. Alternatively, pedo-transfer functions (pedoTFs) estimate PSC from routinely assessed soil chemical properties. Our objective was to examine the possibility of developing a suitable pedoTF for estimating PSC and to evaluate subsequent PSC-based indices (Phosphorus Saturation Ratio (PSR) and Soil Phosphorus Storage Capacity (SPSC)) using data from an in-field laboratory where tile drain effluent is monitored daily. PSC was well predicted by a pedoTF derived from soil aluminum and organic matter ($R^2 = 0.60$). Segmented-line relationships between PSR and soluble P were observed in both desorption assays ($R^2 = 0.69$) and drainflows ($R^2 = 0.66$) with apparent PSR thresholds in close agreement at 0.21 and 0.24, respectively. Negative SPSC values exhibited linear relationships with increasing soluble P concentrations in both desorption assays and drainflows ($R^2 = 0.52$ and $R^2 = 0.53$ respectively) whereas, positive SPSC values were associated with low SP concentrations. Therefore, PSC-based indices determined using pedoTFs could estimate the potential for subsurface soluble P losses. Also, we determined that both index thresholds coincided with the critical soil test P level for agronomic P sufficiency (22 mg kg⁻¹ Mehlich 3 P) suggesting that the agronomic threshold could serve as an environmental P threshold.

2.2 Introduction

Over the last decade, persistent failure of intensive conservation programs to curb the eutrophication of fresh and coastal waters has led to increased debate and scrutiny of possible causes. One suggested cause is legacy P i.e., P that is present from past land-use activities or after changes in land use and management (Jarvie et al., 2013; Kleinman et al., 2011; Sharpley et al., 2013; Mulla et al., 2008). In many watersheds, agricultural land-use is mainly responsible for these elevated P levels (Sharpley, 2016). Historically, to increase agricultural production, P fertility strategies were centered on the concept of nutrient “Quantity” (soil solid phase) and “Intensity” (soil solution phase) and sought to overcome limited diffusion of P in soils through an intentional buildup of P quantity (Kleinman, 2017; Frossard et al., 1995; Olsen and Khasawneh, 1980). Breeuwsma and Silva (1992) postulated that fertilizer management to increase solid-phase P eventually saturated P sorption sites allowing more recently applied P to remain in the soluble P (SP) phase increasing its susceptibility to leaching.

Although P leaching losses from agricultural soils were originally thought to be negligible (Logan et al., 1980), recent studies have established leaching (especially in tile-drained fields with long-term, repeated P applications) as a significant pathway for P loss to surface waters (Gentry et al., 2007; Kinley et al., 2007; Sims et al., 1998). Subsurface tile drainage modifies soil hydrologic regimes, increases infiltration but creates direct conduits for transport of soil solutes to surface waters (King et al., 2015a). Also, in coarse-textured and cracking clay soils, the presence of significant preferential flow pathways exacerbates P loss through tile drains (Radcliffe et al., 2015). In consequence, knowing a soil’s P sorption capacity is crucial for the identification of potential, major P source areas.

Several measures of P sorption saturation have been developed (Table 2.1) and include the P saturation ratio (PSR) and the soil P storage capacity (SPSC) (Renneson et al., 2015; Nair and Harris, 2014; Wang et al., 2012; Nair and Harris, 2004). Unlike soil test phosphorus (STP), PSR indicates the potential of a soil to desorb P as it is estimated as the fraction of PSC occupied by sorbed P i.e., P/PSC (Beauchemin and Simard, 1999; Breeuwsma and Silva, 1992). Alternately, as a metric of remaining PSC before a soil crosses a P saturation threshold, SPSC directly estimates the remaining capacity of a soil to retain additional P (sink strength) (Nair and Harris, 2014). Information in Table 2.1 provides brief details on P measures/indices.

Table 2.1. Brief descriptions of P measures (indices) examined in this study.

Measure or index (abbrev.)	Intended purpose	Details	Key reference(s)
Soil test phosphorus (STP)	Assessing soil P fertility for crop growth and determining fertilizer recommendations	Routine extractions of labile P approximating quantities in soil expected to be available to a crop; common extractants are Morgan, Mehlich 1 and 3, Olsens, Bray, etc.	Morgan, 1941; Mehlich, 1953; Mehlich, 1984; Olsen et al., 1954; Bray and Kurtz, 1945.
Dissolved reactive P (DRP)	Direct measures of soluble P in soil solution and soil leachates	Direct analysis of a water samples for $\text{PO}_4^{3-}\text{-P}$ following filtration through 0.45 μm filter.	Pote and Daniel, 2000.
Water soluble P (WSP)	Predicting desorption of P from the soil to runoff water.	Extraction assessing solid-phase P that may readily desorb as soil solution P is removed by crop uptake, leaching, etc.; distilled water may be used as the extracting solution.	Bortolon et al., 2016; Sharpley et al., 2001; Davis et al., 2005.
Phosphorus Sorption Capacity (PSC)	Soil P fixation potential or total quantity of sorbed P in a P saturated soil.	Originally estimated as Q_{max} (sorption maximum) from multi-point P sorption isotherm fit with an empirical Langmuir model.	Olsen and Watanabe, 1957.
Phosphorus Sorption Index (PSI)	A single point sorption isotherm approach to directly estimate PSC where a fixed P conc. from the upper end of the multi-point isotherm is selected.	Estimated as the ratio of P added to the log of P concentration remaining in solution following a fixed equilibration period (e.g. 18 h); close correlations between Q_{max} and PSI have been observed	Bache and Williams, 1971
Phosphorus Saturation Ratio (PSR)	Estimate of P sorption saturation intended to reflect a soil's ability to retain newly introduced P and/or desorb solid phase P	Calculated as the fraction of PSC occupied by sorbed P (P/PSC); with sorbed P estimated by common STP protocols; explored for routine use with PSC estimated (PSC_{Est}) from proxy variables e.g. when based on Mehlich 1 (M1) extraction, $\text{PSR} = \text{M1P}/(\text{M1Al} + \text{M1Fe})$ or Mehlich 3 and equation 7	Nair, 2014.
Degree of Phosphorus Saturation (DPS)	Purpose similar to PSR	Calculated like PSR but with a scaling factor, α , applied to the proxy measures of Al and Fe in the determination of PSC. Also, unlike PSR, it is expressed as a percentage.	Beauchemin and Simard, 1999; Breeuwsma and Silva, 1992.
Soil Phosphorus Storage Capacity (SPSC)	Direct estimate of a soil's capacity to retain additional P (soil sink strength)	Requires identification of a threshold PSR value (d_0) above which soluble P starts to increase rapidly. Estimated as the product of PSC_{Est} and the difference between d_0 and a soil-specific PSR (equation 4)	Nair and Harris, 2014.

To derive these indicators, sorbed P and PSC need to be determined. Numerous studies have shown that recommended protocols for agronomic STPs (Mehlich 3-STP, Bray 1-STP, Olsen-STP etc.) are well correlated with total sorbed P in soils (Sims et al., 2000). Therefore, agronomic STPs have been used as approximations of sorbed P in environmental studies (Renneson et al., 2015; Houben et al., 2011; Hooda et al., 2000; Nair et al., 2004). For PSC determination, Olsen and Watanabe (1957) suggested that PSC could be estimated as the P sorption maximum (Q_{max}) determined from multi-point P sorption isotherm data fit to an empirical Langmuir model. The laborious nature of multipoint isotherms led Bache and Williams (1971) to

propose the use of the Phosphorus sorption index (PSI), a single-point sorption isotherm to estimate PSC based on its strong correlations with Q_{\max} ($r = 0.974$). A PSI determination involves PSC estimation at one P concentration (corresponding to the upper end of a multi-point isotherm) after a fixed equilibration period (Bache and Williams, 1971). Later studies reported similar, strong and significant correlations between Q_{\max} and PSI determined as a single-point measure of PSC (Brock et al., 2007; Zhou and Li, 2001; Mozaffari and Sims, 1994). However, since sorption isotherms are uneconomical, the proposed alternative is to predict PSC based on its relationships with soil physical and chemical properties (Tisdale and Nelson, 1993; Casson et al., 2006). For example, previous research has estimated PSC using proxies such as extractions of aluminum (Al) and iron (Fe) alone or in combination from neutral and acid ($\text{pH} < 8$) soils (van der Zee and van Riemsdijk, 1988; Maguire et al., 2001; Kleinman and Sharpley, 2002; Nair et al., 2004; Renneson et al., 2015) or of calcium (Ca) either alone or in combination with routine estimates of clay content and magnesium (Mg) in alkaline soils (Kleinman and Sharpley, 2002). Börling et al. (2001) and Maguire et al. (2001) showed that pedo-transfer functions (pedoTFs) developed by treating the PSC proxies as separate variables in linear regressions models better defined their relationship with directly measured PSC.

Regardless of the estimation method used during the determination of PSC-based indices, these indices have been used to define threshold values above (or below) which the risk of SP loss from soil to water strongly increases (Breeuwsma and Silva, 1992; McDowell and Sharpley, 2001; Nair et al., 2004; Nair and Harris, 2014). Yet, few studies have evaluated the field-scale performance of pedoTFs estimating PSC using data commonly available from commercial laboratories. In intensively drained agricultural regions such as the Midwest US there is a critical need for routine, economical indices to assess environmental risks from historic fertilizer regimes and legacy P. Our objectives were i) to examine the possibility of developing a suitable pedoTF for estimating PSC using readily available soil test data and ii) to evaluate the applicability and accuracy of laboratory-determined PSR and SPSC threshold values in fields with subsurface tile drains.

2.3 Materials and Methods

2.3.1 Laboratory study

2.3.1.1 Soil selection and analysis

Archived soil samples ($n = 154$) were obtained from Purdue Agricultural Centers (PACs) (Davis (DPAC), Pinney (PPAC), Northeast (NEPAC), Southeast (SEPAC), Throckmorton (TPAC) and the Water Quality Field Station (WQFS)). The soils included 2016 and 2011 fall samples from the WQFS and the PACs, respectively. The distribution of these agricultural centers provides broad representation of cropland soil types in Indiana (Supplemental Table S6.1).

The WQFS samples were obtained in the 0-20 cm layer (increment used for Indiana recommendations; Vitosh et al., 1995). Samples from other farms were obtained from both 0-10 and 10-20 cm layers as part of a nutrient stratification study. Routine chemical characterizations of samples were completed by a major commercial soil-testing laboratory (A&L Great Lakes Soil Testing Laboratory, Fort Wayne IN, <https://algreatlakes.com/> where, phosphorus (P), potassium (K), magnesium (Mg), calcium (Ca), aluminum (Al) and iron (Fe) were extracted using the Mehlich 3 method (Mehlich 1984) and analyzed by inductively coupled plasma (ICP) spectrometry (Chalmers and Handley, 2006), cation exchange capacity (CEC) was determined by summation of exchangeable K, Mg, Ca, and neutralizable acidity (Warnecke and Brown, 1998), soil $\text{pH}_{(\text{water})}$ was determined by the McLean (1982) procedure, and organic carbon (OC) was measured by the Walkley – Black procedure (Walkley, 1947; Walkley and Black, 1934) followed by percent organic matter (OM) determination ($\text{OM}\% = \text{OC}\% \times 1.72$) (Combs and Nathan, 1998). Given the time-consuming nature of PSI determination, a representative subset of 73 samples was selected for this analysis. The PSI was determined following the method of Bache and Williams (1971) as described by Sims (2009). Filtrate P concentrations were analyzed colorimetrically by the Murphy and Riley (1962) procedure using a SEAL AQ2 auto-analyzer method EPA-118-A Rev.5 (equivalent to USEPA method 365.1, Rev.2.0) (Seal Analytical, 2004). The PSI was calculated as:

$$PSI (L\ kg^{-1}) = \frac{x}{\log c} \quad [\text{Eq. 1}]$$

where, x is the amount ($\text{mg}\ \text{kg}^{-1}$) of added P adsorbed in the soil sample and c is the P concentration ($\text{mg}\ \text{L}^{-1}$) in the filtered equilibrium solution.

Water-soluble phosphorus (WSP), a proxy measure of dissolved reactive P (DRP) (Bortolon et al., 2016; Sharpley et al., 2001; Davis et al., 2005), was determined in all 154 soils as described for PSI and following the method of Self-Davis et al. (2009).

2.3.1.2 Data Analysis

In order to estimate PSC (PSC_{Est}) as a function of routinely measured proxy variables, principle component analysis (Webster, 2001) was used to evaluate correlations between soil PSI (equation 1) and corresponding soil chemical properties (OM, STP, K, Mg, Ca, pH, CEC, Fe and Al) of the 73 sample subset. A correlation matrix instead of a covariance matrix was used to eliminate the effects of different measurement units (James and McCulloch, 1990). Chemical properties strongly correlated with PSI ($r > 0.50$) were selected as possible predictor variables. Subsequently, stepwise regression analysis (forward and backward) was conducted with PSI as the dependent variable and the selected chemical properties as independent variables. At each step, variables that did not contribute significantly ($p > 0.05$) to model fit were eliminated. Least squares regression was used to build a pedoTF from selected independent variables (Neter et al., 1996). The fitness of the pedoTF was measured by the model's coefficient of determination. Once the pedoTF predicting PSC_{Est} was determined, the first of the PSC-based indices, the soil-specific PSR, was calculated directly as:

$$PSR = \frac{STP}{PSC_{Est}} \quad [Eq. 2]$$

with PSC_{Est} individually calculated for all 154 soils using the pedoTF equation applied to a given soil's chemical properties. Prior to the determination of PSC_{Est} all data were log-transformed to conform to normality.

Pearson's correlation coefficient was calculated to analyze the relationship between PSR and WSP. To estimate the second PSC-based index, the SPSC, the threshold PSR value or change point above which corresponding WSP starts to increase markedly needed to be identified. This relationship was modeled by a segmented-line model (equation 3) that describes the relationship

between two lines whose slopes on either side of the change point are significantly different ($P < 0.05$).

$$WSP = \begin{cases} a0 + b0 \text{ PSR}, & \text{PSR} \leq d0 \\ a1 + b1 \text{ PSR}, & \text{PSR} > d0 \end{cases} \quad [\text{Eq. 3}]$$

where, $a0$ and $a1$ are intercepts and $b0$ and $b1$ are slopes for the two segments and $d0$ is the PSR value at the change point. The $d0$ in the fitted model was directly estimated based on the data points while the other parameters ($a0$, $a1$, $b0$ and $b1$) were estimated using nonlinear least squares. The slope to the left of the change point ($b0$) is estimated as a function of $d0$ and other model parameters ($a0$, $a1$ and $b1$) to ensure that the two lines are joined at $d0$ (equation 4).

$$b0 = \frac{(a1 - a0) + b1 d0}{d0} \quad [\text{Eq. 4}]$$

A soil's SPSC was then calculated using $d0$ with soil specific PSC_{Est} and PSR (equation 2) as,

$$\text{SPSC} = (d0 - \text{PSR}) \times \text{PSC}_{\text{Est}} \quad [\text{Eq. 5}]$$

and Pearson's correlation coefficient was calculated to analyze the relationship between SPSC and WSP. Soil SPSC values range from positive values (unsaturated P sinks) to negative values (saturated P sources). However, unlike positive SPSC values, there exists strong, significant linear relationships between negative SPSC values and SP concentrations thus, an SPSC value of zero represents a potential threshold value below which SP concentration rapidly increases in soil solution (Nair and Harris, 2004). Therefore, to characterize the incremental risk to water quality once soils are P saturated, linear regression was used to model the relationship between WSP (independent variable) and SPSC (dependent variable) for $\text{SPSC} \leq 0$.

During the determination of PSR and SPSC, data were log-transformed to conform to normality, and Fisher information matrix was used to estimate standard errors from which confidence intervals were constructed. All statistical analyses were performed in R 3.4.0. (R Core Team, 2017).

2.3.2 Field study

2.3.2.1 Experimental site, Soil and Water Characterization

Among the sources of archived soils for the laboratory study, the WQFS was the only site equipped for direct monitoring of tile-drainage waters creating a unique opportunity to investigate SP loss from long-term, artificially-drained agricultural soils that have received either no P or

regular additions of inorganic or manure P. At the WQFS, 48 treatments plots are monitored continuously with data loggers for drainflow volumes; 24-hr flow-proportional drainage samples are collected whenever drainflow occurs. Soil samples (0 – 20 cm) are collected from each plot every fall at the start of each hydrologic year. Water samples are filtered and analyzed for DRP, the orthophosphate fraction that passes through a 0.45 µm filter (Pote and Daniel, 2000), using the Murphy and Riley (1962) method. Chemical characterizations of soil samples are conducted by commercial lab as described for the laboratory study. All data are archived in the Purdue University Research Repository. A full description of the WQFS facility, equipment, cropping systems, tile drainage water sampling and routine analytical protocols is presented in the supplemental material. All treatments were considered in this study for the 2011 – 2013 water years (e.g. October 1, 2010 – September 30, 2011 for water year 2011). (Note, WQFS soils used in the laboratory study were from 2016).

2.3.2.2 Data analysis

Archived flow and DRP data were reviewed and rectified for drainage tile and data logger malfunctions (flow) and values below detection limits (DRP). Outliers were identified and removed and occasional missing values were estimated (rectification and gap-filling methodologies presented in supplemental materials). Annual flow-weighted mean DRP concentrations (fDRP) were calculated as below;

$$fDRP = \frac{\sum_{j=1}^{365} (DRP_j \times V_j)}{\sum_{j=1}^{365} V_j} \quad [\text{Eq. 6}]$$

where, DRP_j ($j = 1, 2, 3, \dots, 365$ or 366 in a leap year) represents the DRP concentrations of tile drainage water collected on days with flow and V_j ($j = 1, 2, 3, \dots, 365$ or 366 in a leap year) represents the volume of flow recorded on a daily basis. To test the applicability and accuracy of the lab-derived pedoTF and PSR threshold the relationship between fDRP and PSR was modelled by a segmented-line model as shown below;

$$fDRP = \begin{cases} a0_f + b0_f PSR, & PSR \leq d0_f \\ a1_f + b1_f PSR, & PSR > d0_f \end{cases} \quad [\text{Eq. 7}]$$

where; $a0_f$ and $a1_f$ are intercepts and $b0_f$ and $b1_f$ are slopes for the two segments and $d0_f$ is the PSR value at which the linear relationship changes.

Linear regression was used to characterize the relationship between fDRP (independent variable) and SPSC (dependent variable) when SPSC values ≤ 0 as described above for the relationship between WSP and SPSC in the laboratory study. All statistical analyses were done in R 3.4.0. (R Core Team, 2017).

2.4 Results and Discussion

2.4.1 Laboratory study

2.4.1.1 Soil characteristics

The soils selected represented both well-managed and P-deficient cropland soils but also soils well in excess of sufficiency. The STP ranged from 1 to 104 mg kg⁻¹ with a mean of 44 mg kg⁻¹. Regionally, commercial P fertilizer is not recommended when STP is > 50 mg P kg⁻¹ (Indiana NRCS FOTG, 2013; Vitosh et al., 1995) for soils extracted with either Bray P1 or Mehlich 3 and P measured colorimetrically. Our studies measured P with inductively coupled plasma (ICP) spectrometry, an analytical method known to produce consistently higher values; the Mehlich 3 ICP value for the upper threshold for fertilizer applications is approximately 60 mg P kg⁻¹ (Mallarino, 2003). Therefore, the presence of soils with STP > 60 mg P kg⁻¹ suggests these soils provide a suitable range of STP to study both environmental P threshold values and potential risks of historic agronomic recommendations that predate current water quality concerns. The soils were generally acidic, saturated with basic cations (Ca²⁺, Mg²⁺ and K⁺) and with OM values < 6% as is typical of mollisols and alfisols which originally supported grasslands or forests (IDEM, 2007). The calculated PSI ranged between 419 and 598 L P kg⁻¹ (full analytical results, Supplemental Table S6.5).

2.4.1.2 Relationship among variables

Significant correlations with $r > 0.5$ were observed between PSI and OM, Mg, Ca, CEC and Al (Table 2.2), results consistent with other studies (Renneson et al., 2015; Zhang et al., 2005; Indiati and Diana, 2004; Nair et al., 2004; Kleinman and Sharpley, 2002; Börling et al., 2001; Maguire et al., 2001; Kleinman et al., 1999).

Table 2.2. Pearson's correlation coefficients of Phosphorus sorption index (PSI) and soil properties of 73 archived soils samples used in the P sorption study.

Variables ^{§§}	PSI	OM	P	K	Mg	Ca	pH	CEC	Fe	Al
PSI	1.00									
OM	0.57*	1.00								
P	-0.17	-0.23*	1.00							
K	0.43*	0.77	0.05	1.00						
Mg	0.53*	0.89*	-0.32*	0.75*	1.00					
Ca	0.54*	0.95*	-0.33*	0.76*	0.96*	1.00				
pH	-0.16*	-0.03	-0.08	0.08	-0.08	0.01	1.00			
CEC	0.59*	0.93*	-0.36*	0.75*	0.94*	0.96*	-0.04	1.00		
Fe	-0.19	0.07	0.49*	0.10	0.02	0.05	-0.14*	0.00	1.00	
Al	0.60*	0.57*	-0.15	0.60*	0.49*	0.51*	0.07*	0.63	-0.28*	1.00

* Significant relationships at a 0.05 probability level.

§§ Variable abbreviations and units: PSI, Phosphorus sorption index (L kg^{-1}); OM, Organic matter (%); P, Mehlich 3-P (mg kg^{-1}); K, Mehlich 3-K (mg kg^{-1}); Mg, Mehlich 3-Mg (mg kg^{-1}); Ca, Mehlich 3-Ca (mg kg^{-1}); CEC, cation exchange capacity (cmolc kg^{-1}); Fe, Mehlich 3-Fe (mg kg^{-1}); Al, Mehlich 3-Al (mg kg^{-1}).

Although we hypothesized that there would be a relationship between PSI and Fe, their association was not significant. Some studies have reported similar non-significant results (Brock et al., 2007; Sato et al., 2005). These studies postulated that changing P chemistry (shift from acidic to alkaline) within soils due to long-term manure amendments caused the lack of Fe significance in P sorption. One possible cause of this P chemistry shift is OM content whose effects on P sorption are documented as variable. For example, Bhatti et al. (1998) and Kang et al. (2009) reported OM decreases PSC (study OM values: 0.3 – 2.3% and > 4.9% respectively), while Ohno et al. (2007) found it increases PSC (1.8 – 18.1 OM%) and Borggaard et al. (1990) found it had no effect on PSC (0.16 – 3.4 OM%). When it affects PSC, OM outcompetes P for adsorption, complexing metal oxides and inhibiting adsorption sites or by forming metal-OM complexes with reactive sites for P adsorption (Jiao et al., 2007; Weng et al., 2012; Kang et al., 2009). In our study, the OM range was 0.9 to 6.1% and the low Fe concentrations compared to Al concentrations may have made adsorption sites on Fe oxides more susceptible to OM inhibition effects (Supplemental Table S6.5). The pH_{water} exhibited a significant negative correlation with PSI ($r = -0.16$, $P < 0.05$). This suggests that an increase in pH would reduce P sorption capacity of the soils as observed in

previous PSC studies in acidic to near-neutral soils (Maguire et al., 2001; Houben et al., 2011). Finally, no significant relationship existed between Mehlich 3 P and PSI (Table 2.2), which was consistent with previous studies (Laboski and Lamb 2004; Wang et al. 2015). This observation is understandable considering a soil's PSC is generally linked to exchangeable Fe, Al, and Ca concentrations, OM content, soil pH, clay content, and clay mineralogy (Laboski and Lamb 2004; Renneson et al., 2015; Wang et al. 2015).

2.4.1.3 Sorption pedotransfer function (pedoTF)

Principle component analysis found PSI plotted close to K, OM, Mg, Ca, CEC and Al (Supplemental Figure S6.3) confirming the existence of strong and direct relationships between PSI and these variables despite the possible presence of inter-relations among variables. Stepwise regression identified OM and Al as important independent variables with a best fit pedoTF model that accounted for 60% of PSC_{Est} variation as follows:

$$PSC_{Est} = 0.1 Al^{***} + 12.5 OM^{***} + 393.8^{***} \quad [Eq. 8]$$

with standard errors for Al and OM of 0.03 and 2.87, respectively. Both predictor variables (Al and OM) were highly significant ($P < 0.001$). However, we note that the selection and larger weighting of OM during stepwise regression, may be driven by its possible role as a dominant factor in CEC levels in the soils studied. Also, most of the treatments included in this study were under tilled corn – soybean rotations with residue return which could mean that management is the actual driver of PSC and OM is the measured covariable.

2.4.1.4 P release from soils

Estimated PSR (equation 2) ranged between 0 and 0.34 with lowest and highest values in soils from TPAC and PPAC, respectively (Table 2.3). The SPSC (equation 3) ranged between -85 to 207 L kg⁻¹; site means averaged -56.79 to 39.41 L kg⁻¹ with the most negative values, indicative of exceeded P storage capacity, observed on soils receiving either occasional inorganic fertilizer P applications or annual manure applications (treatment specific data not shown).

Table 2.3. Mean and standard deviation (Std. dev.) for organic matter (OM), phosphorus (P) and aluminum (Al), phosphorus saturation ratio (PSR) and soil phosphorus storage capacity (SPSC) for archived soil samples from the 6 experimental sites (n=154[†]).

Site ^{¶¶}	n	Statistics	OM	P	Al	PSR ^{##}	SPSC ^{##}	WSP ^{##}
			%	mg kg ⁻¹			L kg ⁻¹	mg L ⁻¹
DPAC	12	Mean	3.13	42.75	642.42	0.26	-33.2	0.1
		Std. dev.	0.5	26.8	70.68	0.04	24.24	0.05
NEPAC	19	Mean	2.22	61.95	723	0.3	-56.79	0.17
		Std. dev.	0.37	24.2	78.01	0.03	18.73	0.09
PPAC	17	Mean	1.74	64.47	651.18	0.31	-64.33	0.11
		Std. dev.	0.21	14.96	33.75	0.02	12.47	0.04
SEPAC	16	Mean	2.86	29	629.13	0.23	-8.46	0.08
		Std. dev.	1.4	17.59	236.03	0.09	56.5	0.08
TPAC	42	Mean	3.16	11.23	843.72	0.15	39.41	0.01
		Std. dev.	0.99	7.41	180.85	0.06	44.59	0.01
WQFS	48	Mean	4.76	29.3	787.3	0.22	-5.99	0.05
		Std. dev.	0.7	21.32	55.57	0.05	31.37	0.06

[†] Previously reported OM, P and Al values for the 73 soils used in the P sorption study (Supplemental Table S6.5) are included here.

^{¶¶} Site abbreviations DPAC, NEPAC, PPAC, SEPAC, TPAC and WQFS are for Davis Purdue Agricultural Center, Northeast PAC, Pinney PAC, Southeast PAC, Throckmorton PAC and the Water Quality Field Station, respectively.

^{##} PSR and SPSC are estimated by equations 2 and 3, respectively; WSP is determined after Self-Davis et al. (2009).

The WSP ranged from 0 to 0.31 mg L⁻¹ and had strong and significant correlations with PSR ($r = 0.66$, $P < 0.001$) and SPSC ($r = -0.67$, $P < 0.001$), similar to observations in other studies (Wang et al., 2016; Bortolon et al., 2016; Chakraborty et al., 2012; Nair et al., 2004). Relationship thresholds were observed when the PSC-based indices were plotted against WSP values. Once solid-phase P saturation has occurred, more SP remains in solution leading to a rapid increase in soluble P (Breeuwsma and Silva, 1992). In this study, the segmented line model (equation 3) related desorbed WSP to PSR with an R^2 of 0.69 ($P < 0.001$) (Figure 2.1a). The model identified a threshold PSR (d_0) of 0.21, below which there was very little P desorption and, above which, the concentration of WSP increased 1.3 mg P L⁻¹ for every unit increase in PSR (Figure 2.1a). The ratio of the slopes of the two segments of the model (b_1/b_0) suggests that after d_0 , solid-phase saturation, there is a 16-fold greater risk of solid-phase P release into the soil solution.

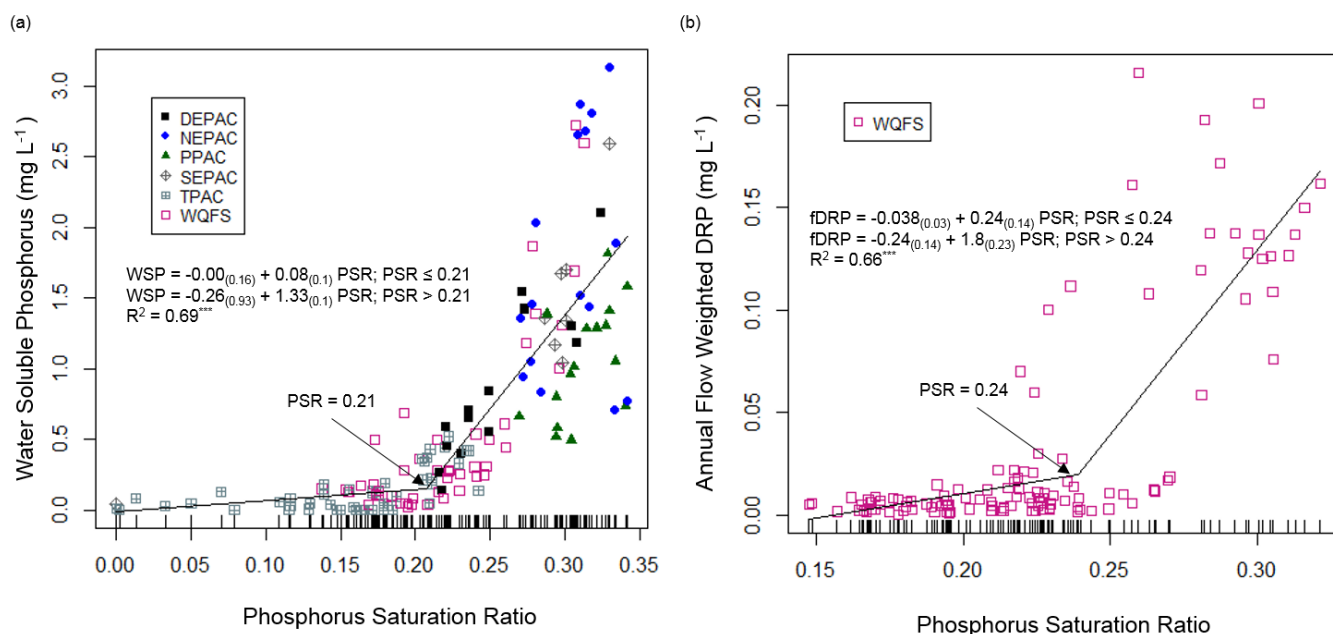


Figure 2.1 Relationship between (a) phosphorus saturation ratio (PSR) and water soluble phosphorus (WSP) of archived soil samples (< 20 cm depth) obtained from Davies (DPAC), Pinney (PPAC), Northeast (NEPAC), Southeast (SEPAC), Throckmorton (TPAC) and, the Water Quality Field Station (WQFS) (n=152). Parameter estimates (with standard errors in parentheses) and R^2 values for the fitted segmented line models (***) significant at the 0.001 probability level), (b) phosphorus saturation ratio (PSR) and annual flow weighted mean DRP (fDRP) for soil samples (20 cm depth) from the Water Quality Field Station (WQFS) plots (n=119). Parameter estimates (with standard errors in parentheses) and R^2 values for the fitted segmented line models (***) significant at the 0.001 probability level).

To test the robustness of $d0$, the segmented line model was iteratively fit to six subsets of the data, each with one experimental site removed. The PSR thresholds from analyses of the remaining five sites ranged from a $d0$ of 0.19 to 0.23 (WQFS and PPAC data removed, respectively); similar R^2 values were observed for all analyses (Supplemental Table S6.6). Thus, $d0$ identified using all sites (0.21; 95% confidence limits: 0.19 - 0.23) appears generally suitable for predicting P loss from various surface soils. Findings supporting the use of a single $d0$ PSR across a range of soils were reported by Dari et al., (2018) who observed that based on the confidence intervals of the thresholds determined for the soils analyzed (i.e. Alfisols, Entisols, Ultisols, Spodosols and Inceptisols), $d0$ values were essentially similar; therefore a threshold PSR of 0.1 was applicable. According to the authors, consistent threshold PSR values were observed

because the soils had similar P dynamics (i.e. acidic soils), and a similar soil test extractant (i.e. Mehlich 1 or Mehlich 3) was used.

Previous work by Provin (1996) on similar soils in Indiana reported threshold PSR as 0.23. In their laboratory study, P and PSC proxies (Al and Fe) used in PSR determination were extracted by the oxalate method (McKeague and Day, 1966). Provin's threshold is within the 95% confidence limit of our d_0 value (0.19 - 0.23). However, WSP values corresponding to d_0 in the two studies vary: 0.10 mg WSP L⁻¹ (Provin, 1996) and 0.21 mg WSP L⁻¹ (current study). Koopmans et al. (2002) and Fuhrman et al. (2005) suggest that these differences in WSP concentrations may reflect differences in soil: extractant ratios, extraction times and electrolytes present. Provin (1996) determined WSP by extracting soil with 0.01 M CaCl₂·2H₂O (1:25 mixture, shaken for 24 hours at 1200 rpm) whereas we extracted soil with distilled water (1:10 w:v ratio; 6000 rpm for 10 min) (Self-Davis et al., 2009). Nevertheless, both WSP values at d_0 exceeded the 0.05 mg P L⁻¹ guideline established by the USEPA as the upper limit of DRP concentrations suggested for protection of streams and lakes (USEPA, 2002).

Likewise, our analysis of WSP as a function of SPSC was generally in keeping with recent work. In previous studies, negative SPSC values were associated with significant increases in soluble P release from soils (Oladeji et al., 2007; Chakraborty et al., 2012; Andres and Sims, 2013; Nair and Harris, 2014). Similarly, in our study, negative SPSC values were associated with a significant linear increase in WSP loss ($R^2 = 0.52$) (Figure 2a).

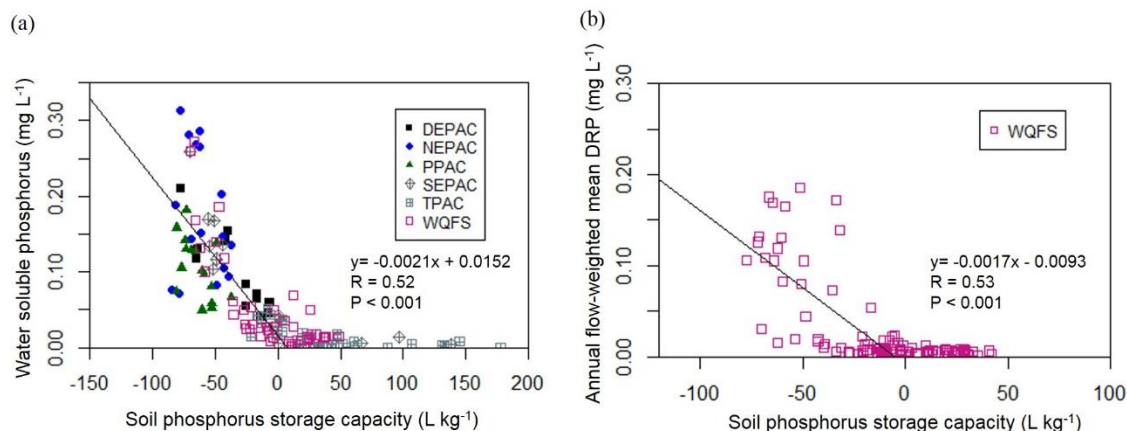


Figure 2.2. Relationship between (a) water soluble phosphorus (WSP) and soil phosphorus storage capacity (SPSC) of archived soil samples (< 20 cm depth) obtained from Davies (DPAC), Pinney (PPAC), Northeast (NEPAC), Southeast (SEPAC), Throckmorton (TPAC) and, the Water Quality Field Station (WQFS) (n=152). Dashed line locates zero SPSC values (proposed threshold), (b) annual flow-weighted DRP (fDRP) and soil phosphorus storage capacity (SPSC) for soil samples (20 cm depth) from the Water Quality Field Station (WQFS) plots (n=119). Dashed line locates zero SPSC values (proposed threshold).

Sites with no recent history of P management (i.e. TPAC) (Table 2.3)) had positive SPSC values with minimum P release to soil solution, a result consistently observed in prior work (Oladeji et al., 2007; Andres and Sims, 2013; Nair and Harris, 2014; Nair and Harris, 2004). Due to the rapid rate of change between negative SPSC and WSP compared to positive SPSC, zero SPSC has been suggested as an environmental threshold (Nair and Harris, 2004); our results support using a SPSC threshold value close or equal to zero as no significant linear relationship existed between WSP values less than 0.01 and SPSC.

2.4.2 Field study

2.4.2.1 Soil characteristics

The WQFS treatments with their varying P management resulted in a wide range of STP values (8 mg kg⁻¹ to 104 mg kg⁻¹) (analytical results by treatment plot, Supplemental Table S6.7). There were P-deficient soils where a response to P fertilizer would be expected in many crops (STP critical level < 22 mg kg⁻¹), soils with adequate P for crop growth (STP = 22 – 60 mg kg⁻¹) and soils with more than adequate P for crop growth (STP > 60 mg kg⁻¹) (values converted from colormetric analytical thresholds (Vitosh et al., 1995) to comparable ICP values after Pittman et al.,

2005). The OM and AI values were 3 - 6 % and 699 - 995 mg kg⁻¹, respectively. These P, AI and, OM values resulted in PSR and SPSC values ranging between 0.15 to 0.32 and -77.34 to 41.81 L kg⁻¹, respectively, representing both P unsaturated and saturated soils.

Plots with ICP STP values above 22 mg P kg⁻¹ (equivalent to the 15 mg P kg⁻¹ colorimetric value above which crops are not expected to respond to fertilizer P) had PSR and SPSC values above and below their respective index thresholds, with a general trend for PSR values to be higher and SPSC values to be most negative for continuous maize soils that received spring and fall manure applications (Supplemental Table S6.7). Previous studies also reported very high PSR values (Nair and Graetz, 2002) and very negative SPSC values (Nair and Harris, 2004) on soils with manure histories and very high STP levels. These index values above (for PSR) or below (for SPSC) threshold values suggest that soils in these plots are more prone to release DRP to drainage waters. Conversely, plots with STP values at or below 22 mg P kg⁻¹ mostly had P unsaturated soils (Supplemental Table S6.7). Finally, against expectations, two Prairie soils from the WQFS had negative SPSC values with STP values slightly above 22 mg P kg⁻¹ despite a complete absence of P application in the preceding 18+ years.

Our field-scale findings relating PSR and SPSC to STP, suggest that 22 mg kg⁻¹, the critical STP level for agronomic P sufficiency, could also serve as an environmental STP threshold with DRP loss in subsurface drainage expected to greatly increase once a soil's STP surpasses 22 mg P kg⁻¹. As previously mentioned, current agronomic guides recommend inorganic P fertilizer be applied until STP 60 mg kg⁻¹; for organic fertilizers, applications are permitted until STP \geq 230 mg kg⁻¹ (Indiana NRCS FOTG, 2013, ICP STP threshold estimated from colorimetric values after Pittman et al. (2005)). These recommendations are intended to allow farmers to maintain optimal conditions for crop growth and/or permit disposal of manure but may have adverse consequences for environmental quality. Indeed, relationships between agronomic critical STP levels and SP losses at concentrations greater than USEPA water quality guidelines have previously been documented. Duncan et al. (2017) found Ohio soils with STP values above the regionally recommended agronomic critical STP (Vitosh et al., 1995) were more likely to lose DRP at annual concentrations above the 0.05 mg P L⁻¹ USEPA mandated threshold (USEPA, 2002). Therefore, this study further highlights the urgent need identified by Duncan et al. (2017) to reanalyze the agronomic recommendations where the build-up or maintenance approach to fertilizer applications may turn soils into P sources, exacerbating DRP losses to surface waters.

2.4.2.2 Phosphorus loss

DRP concentrations in tile discharge ranged from 0.00 to 2.18 mg L⁻¹. However, in each tile, a few concentrations were identified as outliers (supplemental Figure S6.5). Annual flow-weighted mean DRP (fDRP) concentrations from study plots ranged from 0 to 0.216 mg L⁻¹ similar to those observed in other studies in the region (0.08 to 0.16 mg L⁻¹; King et al., 2015b). A detailed description of precipitation, tile discharge, and tile drain efficiencies during the study period is provided in the supplemental materials.

The segmented line model between PSR and fDRP identified a change point ($d0_f$) at 0.24 ($R^2 = 0.66$; 95% confidence limits; 0.22 - 0.25) (Figure 2.1b), slightly higher than the $d0$ of 0.21 (95% confidence limits; 0.19 - 0.23) identified in the laboratory study (Figure 2.1a). Additionally, the ratio of segment slopes ($b1_f/b0_f$) was half that in the PSR versus WSP model ($b1/b0$), 8 and 16, respectively. These differences in the models could be due to differences in soil-to-extractant ratios, extraction times and electrolytes present considering the field study was in a natural system (Koopmans et al., 2002; Fuhrman et al., 2005). Also, Nelson et al. (2005) suggested that absent data points at the extremes might affect the slope after the change point. In this respect, our in-field study lacked data points between 0 and 0.14 PSR (Figure 2.1b).

The fDRP concentration at $d0_f$ was 0.02 mg P L⁻¹ (Figure 2.1b), well below USEPA's 0.05 mg P L⁻¹ acceptable limit (USEPA, 2002). However, 0.02 mg P L⁻¹ has been identified as the P concentration above which lake water eutrophication is accelerated (Correll, 1999; Sharpley et al., 2003). This fDRP concentration was 10 times lower than the proxy WSP concentration observed at $d0$ in the laboratory study (0.21 mg P L⁻¹, Figure 1a). Numerous laboratory studies (Provin, 1996; Heckrath et al., 1995; Maguire and Sims, 2002; Nair et al., 2004; Hesketh and Brookes, 2000; McDowell and Condron, 1999; McDowell and Sharpley, 2001) have also reported WSP concentrations at PSR thresholds that were often above the USEPA mandates on acceptable SP concentrations. Yet, our study and others (e.g. Hesketh and Brookes, 2000; McDowell and Condron, 1999; McDowell and Sharpley, 2001) also consistently show that when P indices are modeled with fDRP in drainage water, the DRP concentrations at the PSR thresholds are often much lower compared to laboratory desorption assays. Interestingly, results presented in this study and elsewhere (Hesketh and Brookes, 2000; McDowell and Condron, 1999; McDowell and Sharpley, 2001) show that the laboratory determined PSR thresholds ($d0$) are in close agreement with that identified in the field ($d0_f$). However, for PSR to be an efficient management tool, the SP

concentrations associated with $d0_f$ and $d0$ should also be comparable. Therefore, further work is required to determine the best laboratory WSP assay that mimics DRP in drainage. We also note that other factors - varying rainfall intensities, subsoil interactions, presence of both surface and subsurface (matrix and preferential) flows etc. - may affect the eventual P concentrations in drainflow. Additionally, cumulative error in water sample handling, analysis and, gap-filling of flow and concentration data contribute to overall uncertainty in load and subsequent fDRP estimates (Harmel et al., 2006; Harmel and Smith, 2007).

Like the laboratory study (Figure 2a), soluble P represented by fDRP, increased linearly ($R^2=0.53$) with decreasing SPSC values (Figure 2b). However, positive soil SPSC values were associated with minimal fDRP release ($fDRP \leq 0.009 \text{ mg P L}^{-1}$). Thus, SPSC of 0 was also identified as the threshold SPSC value in the field study. The slope of the regression between SPSC and fDRP i.e. -0.0017 (95% confidence limits: -0.0021 to -0.0013) (Figure 2b), was slightly lower than the -0.0021 slope (95% confidence limits: -0.0026 to -0.0016) between SPSC and WSP (Figure 2a). These slopes were in close agreement suggesting that SPSC could accurately predict soluble P losses in tile drains.

2.5 Conclusions

Soil PSC is clearly an important parameter to consider when predicting soluble P concentrations in drainage waters. As data used in its estimation are not readily available from soil testing laboratories and national databases, its routine use in P loss risk assessment is greatly limited. The pedo-transfer approach to estimate PSC using data from routine soil analysis and the subsequent determination of PSC-based indices was found suitable for Midwestern USA soils and is recommended for a simple and fast risk assessment of soluble P losses from agricultural fields. Current P fertility strategies focused on buildup and maintenance of STP provides for the conversion of soils into P sources as shown in this study where even soils with STP levels considered optimal for crop growth were P saturated. Implementation of PSC-based indices or the suggested environmental STP threshold in soil fertility and environmental management programs could help avoid future soil P build up to levels that increase the risk of soluble P losses. Given the limited range of values examined, we recommend exploring a wider range of soils to develop a robust pedoTF for use in determining regional index thresholds which may be adopted as a dual-purpose P management tool.

2.6 References

- Andres, A. S. and J.T. Sims. 2013. Assessing potential impacts of a waste-water rapid infiltration basin system on groundwater quality: a delaware case study. *J. Environ. Qual.* 42: 391. <https://doi.org/10.2134/jeq2012.0273>.
- Bache, B. W., and E.G. Williams. 1971. A phosphate sorption index for soils. *J. Soil Sci.* 22 (3): 289–301. <https://doi.org/10.1111/j.1365-2389.1971.tb01617.x>.
- Beauchemin, S., and R. R. Simard. 1999. Soil phosphorus saturation degree: review of some indices and their suitability for p management in Québec, Canada. *Can. J. Soil Sci.* 79 (4): 615–25. <https://doi.org/10.4141/S98-087>.
- Bhatti, J. S., N. B. Comerford, and C. T. Johnston. 1998. Influence of oxalate and soil organic matter on sorption and desorption of phosphate onto a spodic horizon. *Soil Sci. Soc. Am. J.* 62 (4): 1089. <https://doi.org/10.2136/sssaj1998.03615995006200040033x>.
- Borggaard, O. K., S. S. Jørgensen, J. P. Møberg, and B. Raben-Lange. 1990. Influence of organic matter on phosphate adsorption by aluminium and iron oxides in sandy soils. *J. Soil Sci.* 41 (3): 443–49. <https://doi.org/10.1111/j.1365-2389.1990.tb00078.x>.
- Börling, K., E. Otabbong, and E. Barberis. 2001. Phosphorus sorption in relation to soil properties in some cultivated Swedish soils. *Nutr. Cycl. Agroecosyst.* 59 (1): 39–46. <https://doi.org/10.1023/A:1009888707349>.
- Bortolon, L., P. R. Ernani, E. S. O. Bortolon, C. Gianello, R. G. O. de Almeida, S. Welter, and D. A. Rogeri. 2016. Degree of phosphorus saturation threshold for minimizing p losses by runoff in cropland soils of Southern Brazil. *Pesquisa Agropecuaria Brasileira* 51 (9): 1088–98. <https://doi.org/10.1590/S0100-204X2016000900008>.
- Bray R.H., and L.T. Kurtz. 1945. Determination of total, organic and available forms of phosphorus in soils. *Soil Sci.* 59: 39–45.
- Breeuwsma, A. and S. Silva. 1992. Phosphorus fertilisation and environmental effects in the netherlands and the Po Region (Italy). Wageningen, The Netherlands. The Winard Staring Center for Integrated Land, Soil and Water Research. 39 p.
- Brock, E. H., Q. M. Ketterings, and P. J.A. Kleinman. 2007. Measuring and predicting the phosphorus sorption capacity of manure-amended soils. *Soil Sci.* 172 (4): 266–78. <https://doi.org/10.1097/ss.0b013e318032ab2e>.
- Casson, J. P., D. R. Bennett, S. C. Nolan, B. M. Olson, and G. R. Ontkean. 2006. Degree of

- phosphorus saturation thresholds in manure-amended soils of Alberta. *J. Environ. Qual.* 35 (6): 2212. <https://doi.org/10.2134/jeq2006.0085>.
- Chakraborty, D., V. D. Nair, W. G. Harris, and R. D. Rhue. 2012. Environmentally relevant phosphorus retention capacity of sandy coastal plain soils. *Soil Sci.* 177 (12): 701–7. <https://doi.org/10.1097/SS.0b013e31827d8685>.
- Correll, D. L. 1999. Phosphorus: a rate limiting nutrient in surface waters. *Poultry Sci.* 78 (5): 674–82. <https://doi.org/10.1093/ps/78.5.674>.
- Davis, R. L., H. Zhang, J.L. Schroder, J.J. Wang, M.E. Payton, and A. Zazulak. 2005. Soil characteristics and phosphorus level effect on phosphorus loss in runoff. *J. Environ. Qual.* 34 (5): 1640. <https://doi.org/10.2134/jeq2004.0480>.
- Duncan, E. W., K. W. King, M. R. Williams, G. A. LaBarge, L. A. Pease, D. R. Smith, and N. R. Fausey. 2017. Linking soil phosphorus to dissolved phosphorus losses in the midwest. *AEL* 2 (1): 0. <https://doi.org/10.2134/acl2017.02.0004>.
- Frossard, E., M. Brossard, M. J. Hedley, and A. Metherell. 1995. Reactions controlling the cycling of P in soils. *Phosphorus in the Global Environment: Transfers, Cycles, and Management*, no. 54: 107–38.
- Fuhrman, J. K., H. Zhang, J. L. Schroder, R. L. Davis, and M. E. Payton. 2005. Water-soluble phosphorus as affected by soil to extractant ratios, extraction times, and electrolyte. *Commun. Soil Sci. Plan.* 36 (7–8): 925–35. <https://doi.org/10.1081/CSS-200049482>.<https://doi.org/10.1081/CSS-200049482>.
- Gentry, L. E., M. B. David, T. V. Royer, C. A. Mitchell, and K. M. Starks. 2007. Phosphorus transport pathways to streams in tile-drained agricultural watersheds. *J. Environ. Qual.* 36 (2): 408. <https://doi.org/10.2134/jeq2006.0098>.
- Harmel, R.D., R.M. Cooper, R.L. Slade, J.G. Haney, and J.G. Arnold. 2006. Cumulative uncertainty in measured streamflow and water quality data for small watersheds. *T. ASABE* 49 (3): 689–701. <https://doi.org/10.13031/2013.20488>.
- Harmel, R. D. and P. K. Smith. 2007. Consideration of measurement uncertainty in the evaluation of goodness-of-fit in hydrologic and water quality modeling. *J. Hydrol.* 337 (3–4): 326–36. <https://doi.org/10.1016/j.jhydrol.2007.01.043>.
- Heckrath, G., P. C. Brookes, P. R. Poulton, and K. W. T. Goulding. 1995. Phosphorus leaching from soils containing different phosphorus concentrations in the Broadbalk experiment. *J.*

- Environ. Qual. 24 (5): 904. <https://doi.org/10.2134/jeq1995.00472425002400050018x>.
- Hesketh, N., and P. C. Brookes. 2000. Development of an indicator for risk of phosphorus leaching. J. Environ. Qual. 29 (1): 105–10. <https://doi.org/10.2134/jeq2000.00472425002900010013x>.
- Hooda, P. S., A. R. Rendell, A. C. Edwards, P. J. A. Withers, M. N. Aitken, and V. W. Truesdale. 2000. Relating soil phosphorus indices to potential phosphorus release to water. J. Environ. Qual. 29 (4): 1166. <https://doi.org/10.2134/jeq2000.00472425002900040018x>.
- Houben, D., C. Meunier, B. Pereira, and P. Sonnet. 2011. Predicting the degree of phosphorus saturation using the ammonium acetate-EDTA soil test. Soil Use Manag. 27 (3): 283–93. <https://doi.org/10.1111/j.1475-2743.2011.00353.x>.
- IDEM. 2007. Determining the fraction of organic carbon. IDEM September: 1–4. Indiana Department of Environmental Management, Office of Land Quality, Indianapolis, IN.
- Indiana NRCS FOTG. 2013. Conservation practice standard - Nutrient management. https://efotg.sc.egov.usda.gov/references/public/IN/590_Nutrient_Management.pdf
- Indiati, R., and G. Diana. 2004. Evaluating phosphorus sorption capacity of acidic soils by short-term and long-term equilibration procedures. Commun. Soil Sci. Plan. 35 (15–16): 2269–82. <https://doi.org/10.1081/LCSS-200030634>.
- James, F. C., and C. E. McCulloch. 1990. Multivariate analysis in ecology and systematics: panacea or pandora's box? Ann. Rev. Ecol. S. 21 (1): 129–66. <https://doi.org/10.1146/annurev.es.21.110190.001021>.
- Jarvie, H. P., A. N. Sharpley, P. J. A. Withers, J. T. Scott, B. E. Haggard, and C. Neal. 2013. Phosphorus mitigation to control river eutrophication: murky waters, inconvenient truths, and 'postnormal' science. J. Environ. Q. 42 (2): 295. <https://doi.org/10.2134/jeq2012.0085>.
- Jiao, Y., J. K. Whalen, and W. H. Hendershot. 2007. Phosphate sorption and release in a sandy-loam soil as influenced by fertilizer sources. Soil Sci. Am. 71 (1): 118. <https://doi.org/10.2136/sssaj2006.0028>.
- Kang, J., D. Hesterberg, and D. L. Osmond. 2009. Soil organic matter effects on phosphorus sorption: a path analysis. Soil Sci. Am. 73 (2): 360. <https://doi.org/10.2136/sssaj2008.0113>.
- King, K. W., M. R. Williams, M. L. Macrae, N. R. Fausey, J. Frankenberger, D. R. Smith, P. J. A. Kleinman, and L. C. Brown. 2015a. Phosphorus Transport in Agricultural Subsurface Drainage: A Review. *Journal of Environment Quality* 44 (2): 467. <https://doi.org/10.2134/jeq2014.04.0163>.

- King, K. W., M. R. Williams, and N. R. Fausey. 2015b. Contributions of systematic tile drainage to watershed-scale phosphorus transport. *J. Environ. Qual.* 44 (2): 486.
<https://doi.org/10.2134/jeq2014.04.0149>.
- Kinley, R.D., R. J. Gordon, G. W. Stratton, G. T. Patterson, and J. Hoyle. 2007. Phosphorus losses through agricultural tile drainage in Nova Scotia, Canada. *J. Environ. Qual.* 36, 469–477.
<https://doi.org/10.2134/jeq2006.0138>
- Kleinman, P. J. A. 2017. The persistent environmental relevance of soil phosphorus sorption saturation. *CURR. POLLUT. REP.* 3 (2): 141–50. <https://doi.org/10.1007/s40726-017-0058-4>.
- Kleinman, P. J. A., R. B. Bryant, and W. S. Reid. 1999. Development of Pedotransfer Functions to Quantify Phosphorus Saturation of Agricultural Soils. *Journal of Environmental Quality* 28 (6): 2026–30. <https://doi.org/10.2134/jeq1999.00472425002800060044x>.
- Kleinman, P. J.A., and A. N. Sharpley. 2002. Estimating soil phosphorus sorption saturation from Mehlich-3 data. *Commun. Soil Sci. Plan.* 33 (11–12): 1825–39. <https://doi.org/10.1081/CSS-120004825>.
- Kleinman, P. J. A, A. N. Sharpley, R. W. McDowell, D. N. Flaten, A. R. Buda, L. Tao, L. Bergstrom, and Q. Zhu. 2011. Managing Agricultural Phosphorus for Water Quality Protection: Principles for Progress. *Plant and Soil* 349 (1–2): 169–82.
<https://doi.org/10.1007/s11104-011-0832-9>.
- Koopmans, G. F., R. W. McDowell, W. J. Chardon, O. Oenema, and J. Dolfing. 2002. Soil phosphorus quantity-intensity relationships to predict increased soil phosphorus loss to overland and subsurface flow. *Chemosphere* 48 (7): 679–87. [https://doi.org/10.1016/S0045-6535\(02\)00146-7](https://doi.org/10.1016/S0045-6535(02)00146-7).
- Logan, T.J., G.W. Randall, and D.R.Timmons. 1980. Nutrient content of tile drainage from cropland in the north central region. North Central Regional Research Publication 268, September, 1980. Research Bulletin 1119. Ohio Agricultural Research and Development Center, Wooster, OH.
- Maguire, R. O., R. H. Foy, J. S. Bailey, and J. T. Sims. 2001. Estimation of the phosphorus sorption capacity of acidic soils in Ireland. *Eur. J. Soil Sci.* 52 (3): 479–87.
<https://doi.org/10.1046/j.1365-2389.2001.00394.x>.
- Maguire, R. O., and J. T. Sims. 2002. Soil testing to predict phosphorus leaching. *J. Environ. Qual.*

- 31 (5): 1601. <https://doi.org/10.2134/jeq2002.1601>.
- Mallarino, A. P. 2003. Field calibration for corn of the mehlich-3 soil phosphorus test with colorimetric and inductively coupled plasma emission spectroscopy determination methods. *Soil Sci. Soc. Am. Journal* 67 (6): 1928. <https://doi.org/10.2136/sssaj2003.1928>.
- McDowell, R.W., and L. M. Condrom. 1999. Developing a predictor for phosphorus loss from soil. . In: L. D. C. Urrie, editor, *Best soil management practices for production. Fertilizer and Lime Res. Centre 12th Annual Workshop*, Palmersto, North New Zealand. p. 153--164.
- McDowell, R.W., Sharpley, A.N., Kleineman, P.J.A. and Oburek, W.J. 2001. "Hydrological and Source Management of Pollutants at Thae Soil Profile Scale. In P.M. Flaygarth and S.C. McDowell, R.W., Sharpley, A.N., Kleineman, P.J.A. and Oburek, W.J. 2001. Hydrological and source management of pollutants at the soil profile scale. In: P. M. Flaygarth and S.C. Jarvis, editors, *Agriculture, hydrology and water quality*. CABI Pub, Wallingford, UK. p. 197 - 224.
- McDowell, R W, and A N Sharpley. 2001. Approximating phosphorus release from soils to surface runoff and subsurface drainage. *J. Environ. Qual.* 30 (2): 508–20. <https://doi.org/10.2134/jeq2001.302508x>.
- McKeague, J.A. & J. H. Day. 1966. Dithionite and oxalate extractable Fe and Al as aids in differentiating various classes of soils. *Can. J. Soil Sci.*, no. 46: 13–22.
- Mehlich, A. 1953. Determination of P, Ca, Mg, K, Na, and NH₄. North Carolina Soil Test Division (Mimeo). Raleigh, NC.
- Mehlich, A. 1984. Mehlich 3 soil test extractant: A modification of Mehlich 2 extractant. *Commun. Soil Sci. Plan.* 15 (12): 1409–16. <https://doi.org/10.1080/00103628409367568>.
- Morgan, M. F. 1941. *Chemical soil diagnosis by the universal soil testing system*. New Haven, CT: Bull. No. 450. Conn. Agric. Exp. Stn.
- Mozaffari, M. and J. T. Sims. 1994. Phosphorus availability and sorption in an atlantic coastal plain watershed dominated by animal-based agriculture. *Soil Sci.* 157 (2). https://journals.lww.com/soilsci/Abstract/1994/02000/Phosphorus_Availability_and_Sorpti_on_in_An.5.aspx.
- Mulla, D. J., A. S. Birr, N. R. Kitchen, and M. B. David. 2008. Limitations of evaluating the effectiveness of agricultural management practices at reducing nutrient losses to surface waters. Final Report: Gulf hypoxia and local water quality concerns workshop, 189–212.

- Murphy, J. and J.P. Riley. 1962. A modified single solution method for the determination of phosphate in natural waters. *Anal. Chem.* 27: 31–36. [https://doi.org/10.1016/S0003-2670\(00\)88444-5](https://doi.org/10.1016/S0003-2670(00)88444-5).
- Nair, V. D. 2014. Soil Phosphorus Saturation Ratio for Risk Assessment in Land Use Systems. *Frontiers in Environmental Science* 2 (April): 1–4. <https://doi.org/10.3389/fenvs.2014.00006>.
- Nair, V.D., and D.A. Graetz. 2002. Phosphorus saturation in spodosols impacted by manure. *J. Environ. Qual.* 31 (4): 1279. <https://doi.org/10.2134/jeq2002.1279>.
- Nair, V. D., and W. G. Harris. 2004. A capacity factor as an alternative to soil test phosphorus in phosphorus risk assessment. *New Zeal. J. Agr. Res.* 47 (4): 491–97. <https://doi.org/10.1080/00288233.2004.9513616>.
- Nair, V. D., K. M. Portier, D. A. Graetz, and M. L. Walker. 2004. An environmental threshold for degree of phosphorus saturation in sandy soils. *J. Environ. Qual.* 33 (1): 107. <https://doi.org/10.2134/jeq2004.1070>.
- Nair, V. D., and W. G. Harris. 2014. Soil phosphorus storage capacity for environmental risk assessment . *AAS* 2014: 1–10.
- Nelson, N. O., J. E. Parsons, and R. L. Mikkelsen. 2005. Field-scale evaluation of phosphorus leaching in acid sandy soils receiving swine waste. *J. Environ. Qual.* 34 (6): 2024. <https://doi.org/10.2134/jeq2004.0445>.
- Neter, J., M. Kutner, W. Wasserman, and C. Nachtsheim. 1996. *Applied linear statistical models* .4th Edition. Higher Education Group. Irwin. Chicago, Il.
- Ohno, T., B. R. Hoskins, and M. S. Erich. 2007. Soil organic matter effects on plant available and water soluble phosphorus. *Biol. Fert. Soils* 43 (6): 683–90. <https://doi.org/10.1007/s00374-006-0150-1>.
- Oladeji, Olawale O., George A. O'Connor, Jerry B. Sartain, and Vimala D. Nair. 2007. “Controlled Application Rate of Water Treatment Residual for Agronomic and Environmental Benefits.” *Journal of Environment Quality* 36 (6): 1715. <https://doi.org/10.2134/jeq2007.0160>.
- Olsen, S. R. and F. E. Khasawneh. 1980. Use and limitations of physical-chemical criteria for assessing the status of phosphorus in soils. In: F.E. Khasawneh et al., editors, *The role of phosphorus in agriculture*. ASA CSSA SSSA. Web. p. 361 - 404.
- Olsen, S.R., C.V. Cole, F.S. Watanabe, and L. A. Dean. 1954. Estimation of Available Phosphorus in Soils by Extraction with Sodium Bicarbonate. USDA Circular 939. U.S. Government

Printing Office, Washington D.C.

- Olsen, S.R. and Watanabe, F.S. 1957. A method to determine a phosphorus adsorption maximum of soils as measured by the langmuir isotherm. *Soil Sci. Soc. Am. J.* 21: 144–49.
- Pittman, J. J., H. Zhang, J. L. Schroder, and M. E. Payton. 2005. Differences of phosphorus in Mehlich 3 extracts determined by colorimetric and spectroscopic methods. *Comm. Soil Sci. Plan.* 36 (11–12): 1641–59. <https://doi.org/10.1081/CSS-200059112>.
- Pote, D.H. and T.C. Daniel. 2000. Analyzing for dissolved reactive phosphorus in water samples. In: J. L. Kovar and Pierzynski, G.M., editors, *Methods for phosphorus analysis for soils, sediments, residuals, and waters*. Southern Cooperative Series Bulletin, Virginia Tech University, Blacksburg. p. 91 - 93.
- Provin, T. L. 1996. Phosphorus retention in Indiana soils. (Order No. 9713586). Available from Dissertations & Theses @ CIC Institutions; ProQuest Dissertations & Theses Global. (304261374). Retrieved from <https://search.proquest.com/docview/304261374?accountid=13360>
- R Core Team. 2017. R: A language and environment for statistical computing. Vienna, Austria.: R Foundation for Statistical Computing. <https://www.r-project.org/>.
- Renneson, M., C. Vandenberghe, J. Dufey, J. M. Marcoen, L. Bock, and G. Colinet. 2015. Degree of phosphorus saturation in agricultural loamy soils with a near-neutral PH. *Eur. J. Soil Sci.* 66 (1): 33–41. <https://doi.org/10.1111/ejss.12207>.
- Sato, S., D. Solomon, C. Hyland, Q. M. Ketterings, and J. Lehmann. 2005. Phosphorus speciation in manure and manure-amended soils using xanes spectroscopy. *Environ. Sci. and Technol.* 39 (19): 7485–91. <https://doi.org/10.1021/es0503130>.
- <https://doi.org/10.1021/es0503130>.
- SEAL Analytical. 2004. O-Phosphate – P in drinking, saline and surface waters , and domestic and industrial wastes. AQ2 method EPA-118-A Rev. 5, SEAL Analytical, Mequon Technology Center 10520-C North Baehr Road Mequon, Wisc. 53092.
- Self-Davis, M.L., P. A. Moore and B. C. Joern. 2009. Water- or dilute salt-extractable phosphorus in soil. In: J. L. Kovar and Pierzynski, G.M., editors, *Methods for phosphorus analysis for soils, sediments, residuals, and waters*. Southern Cooperative Series Bulletin, Virginia Tech University, Blacksburg. p. 22–24.
- Sharpley, A. N. 2016. Managing agricultural phosphorus to minimize water quality impacts.

- Scientia Agricola 73 (1): 1–8. <https://doi.org/10.1590/0103-9016-2015-0107>.
- Sharpley, A. N., T. Daniel, T. Sims, J. Lemunyon, R. Stevens, and R. Parry. 2003. Agricultural phosphorus and eutrophication second edition agricultural phosphorus and eutrophication. Second Edition. U.S. Department of Agriculture, Agricultural Research Service, no. 149: 44.
- Sharpley, A. N., H. P. Jarvie, A. Buda, L. May, B. Spears, and P. J. A. Kleinman. 2013. Phosphorus legacy: overcoming the effects of past management practices to mitigate future water quality impairment. *J. Environ. Qual.* 42 (5): 1308. <https://doi.org/10.2134/jeq2013.03.0098>.
- Sharpley, A. N., R. McDowell, J. L. Weld, and P. J.A. Kleinman. 2001. Assessing site vulnerability to phosphorus loss in an agricultural watershed. *J. Environ. Qual.* 30: 2026–36. <https://doi.org/10.2134/jeq2001.2026>.
- Sims, J.T. 2009. A phosphorus sorption index. In: Kovar, J.L. and Pierzynski, G.M., Eds., *Methods for phosphorus analysis for soils, sediments, residuals, and waters*. Southern Cooperative Series Bulletin, Virginia Tech University, Blacksburg, 20–21.
- Sims, J.T., R. R. Simard, and B. C. Joern. 1998. Phosphorus Loss in Agricultural Drainage: Historical Perspective and Current Research. *J. Environ. Qual.* 27, 277. <https://doi.org/10.2134/jeq1998.00472425002700020006x>.
- Sims, J. T., A. C. Edwards, O. F. Schoumans, and R. R. Simard. 2000. Integrating soil phosphorus testing into environmentally based agricultural management practices. *J. Environ. Qual.* 29 (1): 60–71. <https://doi.org/10.2134/jeq2000.00472425002900010008x>.
- Tisdale, S. L. and W. L. Nelson. 1993. *Soil Fertility and Fertilizers*. New York: The Macmillan Company.
- USEPA. 2002. EPA water quality standards handbook, no. August: 2–3.
- Vitosh, M.L., J. W. Johnson, and D. B. Mengel. 1995. Tri-State fertilizer recommendations for corn, soybeans, wheat and alfalfa. Extension Bulletin E-2567 (New), July 1995 2567 (July): 1–4.
- Wang, Y. T., T. Q. Zhang, I. P. O’Halloran, C. S. Tan, and Q. C. Hu. 2016. A phosphorus sorption index and its use to estimate leaching of dissolved phosphorus from agricultural soils in Ontario. *Geoderma* 274 (January): 79–87. <https://doi.org/10.1016/j.geoderma.2016.04.002>.
- Wang, Y. T., T. Q. Zhang, I. P. O’Halloran, C. S. Tan, Q. C. Hu, and D. K. Reid. 2012. Soil Tests as Risk Indicators for Leaching of Dissolved Phosphorus from Agricultural Soils in Ontario. *Soil Science Society of America Journal* 76 (1): 220. <https://doi.org/10.2136/sssaj2011.0175>.

- Webster, R. 2001. Statistics to support soil research and their presentation. *Eur. J. Soil Sci.* 52 (2): 331–40.
- Weng, L., W. H. Van Riemsdijk, and T. Hiemstra. 2012. Factors controlling phosphate interaction with iron oxides. *J. Environ. Qual.* 41 (3): 628. <https://doi.org/10.2134/jeq2011.0250>.
- van der Zee, S.E.A.T.M., and W. H. van Riemsdijk. 1988. Model for long-term phosphate reaction kinetics in soil. *J. Environ. Qual.* 17 (1): 35. <https://doi.org/10.2134/jeq1988.00472425001700010005x>.
- Zhang, H., J. L. Schroder, J. K. Fuhrman, N. T. Basta, D. E. Storm, and M. E. Payton. 2005. Path and multiple regression analyses of phosphorus sorption capacity. *Soil Sci. Soc. Am. J.* 69 (1): 96. <https://doi.org/10.2136/sssaj2005.0096dup>.
- Zhou, M., and Y. Li. 2001. Phosphorus-sorption characteristics of calcareous soils and limestone from the Southern Everglades and adjacent farmlands. *Soil Sci. Soc. Am. J.* 65 (5): 1404. <https://doi.org/10.2136/sssaj2001.6551404x>.

3 USING ARTIFICIAL NEURAL NETWORKS TO IMPROVE PHOSPHORUS INDICES

3.1 Abstract

The phosphorus index (PI) was developed as a field-scale assessment tool used to identify critical source areas of phosphorus (P) loss, thus most states have adopted the PI as their strategy for targeted management and conservation practices for effective mitigation of P loss from agricultural landscapes to surface waters. Recent studies have focused on evaluating and updating PI weighting factors (WFs) to ensure agreement between final PI values and measured losses of P. Given that the WF of each site characteristic are determined individually without considering possible interactions, the goal of this study was to demonstrate how artificial neural networks (ANNs) that consider real-world interdependence can be used to determine WFs. Our specific objectives were to evaluate ANN performance for predicting soluble P (SP) concentrations in tile effluent using site characteristics as predictor variables, and to evaluate whether ANN-generated WFs can be used to improve PI performance. Garson's algorithm was used to determine the relative importance of each site characteristic to SP loss. Data from a monitored in-field laboratory was used to evaluate the ability of a PI with no WFs (PI_{NO}), a PI with WFs as proposed in the original Lemunyon and Gilbert PI (PI_{LG}), and a PI with ANN-generated WFs (PI_{ANN}), to estimate SP loss potential in tile discharge. Simulation results showed that the ANN model provided reliable estimates of SP in tile effluent ($R^2 = 0.99$; RMSE = 0.0024). The relative importance analysis highlighted the importance of prioritizing both contemporary and legacy P sources during P loss risk assessments. Unlike the other PIs, PI_{ANN} was able to provide reasonable estimates of SP loss potential as illustrated with significant exponential relationships ($R^2 = 0.60$; $p < 0.001$) between PI_{ANN} values and measured annual SP concentrations. These findings demonstrate that ANNs can be used to develop PIs with a strong correlation to measured SP.

3.2 Introduction

Phosphorus (P) enrichment of fresh surface waters is a major water quality concern in many watersheds because of its role as the limiting nutrient for harmful and nuisance algal blooms (Sharpley et al., 1994). Significant progress has been made towards limiting point source inputs of P to P-sensitive waters. However, there has been limited and in most cases elusive success in the remediation of non-point P sources; specifically diffuse P losses from agricultural fields (Dubrovsky et al., 2010; Kleinman et al., 2011). The coincidence of P source and transport factors (critical source areas) control P movement from agricultural fields to surface waters (Sharpley et al., 2011). Therefore, the success of mitigation efforts lies in creating a understanding and representation of these two factors in P loss risk assessment tools (Sharpley et al., 2012; Gburek et al., 2002).

In 1993, Lemunyon and Gilbert proposed the PI index to encompass source and transport factors controlling P movement from a field (Lemunyon and Gilbert, 1993). Initially, the PI served as a voluntary, simple, educational, and qualitative screening tool for farmer identification of fields with high potential risks of P loss to runoff (Lemunyon and Gilbert, 1993; Gburek et al., 2000). However, in response to the increasing water quality concern, the US Department of Agriculture's Natural Resource Conservation Service (NRCS) has added the P index (PI) concept to its National Nutrient Management Conservation Practice Standard (Code 590) as one of the options available to states for P loss risk assessment (USDA NRCS, 2011). In most of these states, the NRCS-Nutrient Management Standard (code 590) requires the determination of PI solely or in combination with an agronomic or threshold soil test P (STP) value, i.e. a PI determination has to be done once the agronomic or threshold STP is exceeded (Sharpley et al., 2003; Sharpley et al., 2012). The original PI by Lemunyon and Gilbert (1993) was made up of eight site characteristics: soil erosion, irrigation erosion, runoff class, STP, application rates and methods of both inorganic and organic P sources. Each site characteristics was assigned a weighting factor (WF) in such a way to reflect its relative importance in contributing to P loss in runoff, and a rating value i.e. 1 (low), 2 (medium), 4 (high) or, 8 (very high), to represent increasing risk level (Lemunyon and Gilbert, 1993). As an additive index, the final PI value for each site was obtained by multiplying each site characteristic's weight with the corresponding rating value and, summing up the resulting weighted characteristics (Lemunyon and Gilbert, 1993).

To adapt the PI, many states embarked on revising and evaluating the original PI to accommodate local conditions and priorities (Sharpley et al., 2003). These modifications include the incorporation of additional site characteristics (e.g. degree of phosphorus saturation, connectivity to water bodies, subsurface drainage, best management practices etc.), using measured field data to determine WFs, PI calculation (additive, multiplicative or component indices), and the interpretation of the final PI values (Sharpley et al., 2003; Osmond et al., 2012; Sharpley et al., 2013). This diversity in the PI formulation and interpretation for similar situations among states has led to concerted efforts to evaluate and validate existing PI's (Sharpley et al., 2013). One key finding from these evaluation studies is the great influence WFs assigned to site characteristics have on PI performance (Osmond et al., 2006). In consequence, these WFs have come under scrutiny especially given that in many state PIs, WFs were initially assigned based on the professional judgement of experts or adapted from pre-existing PIs in neighboring states (Bolster et al., 2012; Sharpley et al., 2013; Drewry et al., 2011; Sharpley et al., 2012). Recently, more states have used findings from studies investigating the relationships between each site characteristic and measured P loss data, to determine WFs leading to improved PI performance. For example, updated WFs based on measured P losses in the Kansas (soil erosion and STP WFs; Sonmez et al., 2009) and Arkansas (STP and soluble reactive P WFs; DeLaune et al., 2004) PIs, led to improved correlations between PI values and measured P losses.

In every state where WF determination was based on scientific data, the effect of each site characteristic on measured P loss was individually investigated (DeLaune et al., 2004; Sonmez et al., 2009; Bolster et al., 2012). Thus, the real-world synergistic and antagonistic effects among the PI source and transport characteristics were not considered (Gburek and Sharpley, 1998; Sharpley et al., 2011). Artificial neural networks (ANNs) together with relevant weight algorithms offers a novel approach to unravel and quantify complex nutrient loss dynamics in agricultural fields. An ANN is a computer-based system inspired by the learning process present in the vast network of neurons in the human brain (Lek and Guegan, 1999). Similar to the neural networks in a human brain, an ANN is made up of interconnected processing units (neurons) organized in a pre-determined topology (Lek and Guegan, 1999). An ANN can handle both qualitative and quantitative data, to analyze both linear and non-linear responses, and merge information (Schultz et al., 2000). Given this versatility, ANNs have recently received increased attention as potential tools suited to modeling input-output relationships in complex agricultural systems for which there is limited

understanding (Yang et al., 2018; Liakos et al., 2018). One area in which there is a growing trend in the use of ANNs is water quality modeling. Kaluli et al. (1998) successfully simulated nitrate leaching from agricultural fields and identified sub-irrigation, covercropping (corn and ryegrass) and a threshold nitrogen (N) rate (180 kg N ha^{-1}) as possible ways to greatly reduce nitrate leaching from fields. Salehi et al. (2000) used ANNs to predict nitrate losses in drain outflows with their results revealing that ANNs accurately predicted nitrate loss using fewer input parameters but that the ANN model itself was site-specific (not-transferable to other sites not studied). Kim et al. (2012) went further and compared the performance of ANNs with other existing nutrient models (Soil and Water Assessment Tool (SWAT) and the Haith's Generalized Watershed Loading Function (GWLF)). Their results revealed that ANNs were as accurate or sometimes much more accurate in predicting watershed nutrient loading for various management strategies compared to SWAT and GWLF. Results from these studies and others (Sharma et al., 2003; Kim and Gilley, 2008; Al-Mahallawi et al., 2012; Lallahem and Hani, 2017), suggest that ANNs can be used to model non-point source agricultural nutrient loss to surface and ground water. Additionally, building an ANN no longer requires advanced programming skills as several user-friendly ANN packages exist for use in open-source softwares e.g. NeuralNet (Marcus et al., 2018) and neuralnet (Wright et al., 2019) available for use in the R language environment (R Core Team, 2017).

Despite ANNs being more powerful predictive tools compared to traditional models such as linear regressions, multiple regressions, SWAT, GWLF etc., most researchers shy away from ANNs due to existing criticism that they are 'black boxes' (Olden and Jackson, 2002; Benítez et al., 1997). This is because once fitted, an ANN model does not provide insights or details on the underlying relationships, relative importance (weights) of each input variable and the structures of the covariates (inputs) with the modelled outcomes (Benítez et al., 1997). To overcome this weakness, numerous methods including partial derivatives (PaD), the profile and perturb method, connection weights approach, Garson's method, the classical and improved stepwise method can be used to interpret the connections and the contribution of ANN input factors (Olden & Jackson, 2002).

The study aimed to simulate soluble P (SP) concentrations in tile effluent using a multi-layer feed forward artificial neural network (MLF-ANN) trained by the backpropagation algorithm. The specific objectives of this study were to: (1) evaluate ANN model performance for predicting soluble P (SP) concentrations in tile effluent with selected site characteristics as

predictor variables and, (2) to determine ANN-generated WFs using Garson's algorithm and compare the performance of a PI with no WFs (PI_{NO}), a PI with WFs as proposed in the original Lemunyon and Gilbert PI (PI_{LG}), and a PI with ANN-generated WFs (PI_{ANN}), for predicting SP loss potential in tile discharge.

3.3 Materials and Methods

3.3.1 Selection of ANN variables.

The first step of this analysis was to determine the relevant site characteristics (input variables) governing soluble P loss (output variable) from tile drained fields. Selected input variables were selected to be consistent with the transport and loss potential components in the Indiana Nutrient and Sediment Transport Risk Assessment Tool (NASTRAT) (IN-NRCS, 2013). They include; one source variable (Bray/Mehlich 3 soil test P (STP) and seven transport variables (soil erosion (water) (SE), soil erosion (wind) (SEW), surface runoff class (SR), nitrate leaching index (NI), subsurface drainage potential (SDP), flooding frequency (FF), distance to waterbody (DTW)). In this study, we confined to the dominant input variables considered in previous P loss risk assessment studies (Nelson and Shober, 2011) thereby, eliminating SEW, FF and NI from consideration. To meet the minimum criteria for assessment for P loss risk potential established by United States Department of Agriculture Natural Resource Conservation Service in its Title 190 National Instruction, timing, rate and method of P (inorganic and organic) application were included in the analysis. The specific source variables were inorganic P fertilizer rate (FPR), inorganic P fertilizer application method and timing (FPA), organic P manure rate (OPR), and organic P manure application method and timing (OPA). Following the recommendation from Kleinman (2017) and Welikhe et al. (2020) to incorporate soil P sorption saturation into P loss risk assessment tools, P sorption capacity (PSC) - based environmental indices of P saturation ratio (PSR) and soil P storage capacity (SPSC)) were included as additional input variables. The output of interest was annual flow weighted mean DRP concentrations (fDRP) (mg L^{-1}).

3.3.2 Study site and creation of datasets

Once the ANN variables were identified, the next step was to generate datasets. The creation of a robust ANN, requires the use of a big dataset that can be sufficiently divided into training, testing and cross-validation subsets (Sinshaw et al., 2019; Berzina et al., 2009). Because

a sufficiently large dataset did not exist, this study followed the methods of Bolster et al. (2012) and Fiorellino et al. (2017), whereby an empirical dataset (small dataset) was used to generate a theoretical dataset (big dataset). These datasets were generated to represent well-managed agricultural fields with common cropping systems in Indiana. Here, well-managed agricultural fields refer to fields that adhere to state-established conservation practice standards for nutrient management and reduction of runoff and erosion processes (Indiana NRCS FOTG, 2013). The theoretical dataset with possible representative combinations of input and output variables was used to evaluate ANN performance for predicting SP losses in tile effluent while the empirical dataset consisting of actual (measured) site characteristics, was used to test whether ANN-generated weights improved PI performance.

The empirical dataset contained site characteristics, field management practices, soil and water quality data collected from tile-drained plots at the Water Quality Field Station (WQFS), Purdue University. Together the treatments at the WQFS (supplemental Table S7.1) provide an ideal opportunity to investigate P loss in tile effluent from well-managed fields that have received either no P or regular additions of either inorganic or organic P, and were either tilled or not tilled. Runoff and erosion is not monitored at the site therefore data on measured P loss via these pathways was not available. However, it is important to note that the facility has little variation in slope. For in-depth details on the WQFS facility, management histories, equipment and routine orthophosphate analytical protocols, see Ruark et al. (2009), Hernandez-Ramirez et al. (2011), and Welikhe et al. (2020).

Site characteristics and field management practices collected were those required as input into the ANN and PIs. Data were collected from the plots at the WQFS between 2011 – 2013 water years (e.g. Oct 1, 2010 – Sept 30, 2011 for water year 2011). In the NASTRAT (IN-NRCS, 2013), similar to the Lemunyon and Gilbert, (1993) PI, both P source and transport site characteristics are presented as categorical variables with discreet values assigned to each category. In Lemunyon and Gilbert, (1993) PI, these categories (low, medium, high, etc.) are further assigned a rating value using a base of 2 (low = 2^0 (1), high = 2^4 (16); Table 3.1) to represent increasing risk level from one category to the next. However, the use of categorical variables limits maximum values for P loss factors, and often results in arbitrary breakpoints in calculated index values (Nelson and Shober, 2012). Thus, when possible many PIs have resorted to using continuous variables instead

of categorical variables (Nelson and Shober, 2012). Therefore, this study chose to use continuous values for P source variables (except P application methods (FPA and OPA)).

Soil samples from WQFS were obtained in the 0 to 20 cm depth and sent to A&L Great Lakes Soil Testing Laboratory, Fort Wayne IN (<https://algreatlakes.com/>) for routine chemical characterization. Further details on methods used during chemical characterization can be found in Welikhe et al. (2020). A summary of data on P, aluminum (Al), organic matter (OM%), PSR, SPSC, and fDRP is presented in supplemental information (Table S7.1). Plots at the WQFS received either inorganic or organic P fertilizer applications (supplemental Table S7.1). Plots receiving inorganic P fertilizer applications did so at university recommended rates based on STP (Vitosh et al., 1995), while manured treatments received yearly additions of swine effluent at rates meant to supply $228 \pm 21 \text{ lbs N ha}^{-1} \text{ yr}^{-1}$. Rates of applied P were obtained from the WQFS field logs (supplemental Table S7.3). The P (inorganic and organic) application methods together with their assigned rating values include; no P applied (negligible category = 0), P placed with planter/injected deeper than 2 inches (5 cm) (very low category = 1), P incorporated immediately before crop (low category = 2), P incorporated > 3 months before crop or surface applied < 3 months before crop (medium category = 4), P surface applied > 3 months before crop (high category = 8). Field records show inorganic P (triple super phosphate; 0-45-0) was surface applied < 3 months before crop (~1 week or more before crop) and, when organic P was added, it was injected deeper than 2 inches (5 cm) therefore, these variables were assigned a value of 4 and 1 respectively in the dataset. However, on years when starter fertilizer (equal mix of urea ammonium nitrate (28-0-0) and liquid ammonium phosphate (10-34-0); 19-17-0) was used as only source of P, it was placed at planting 2 inches (5 cm) below the soil surface and was therefore assigned a value of 1.

In the empirical dataset, all transport variables were represented as categorical variables with each category assigned a rating value using a rating system of base 2 (Table 3.1). Based on field observations at the WQFS, soil erosion (SE), surface runoff (SR), subsurface drainage potential (SDP), and distance to a water body (DTW) were assigned the following rating values; 1, 0, 4, and 1, respectively. These category values reflect a low soil loss risk ($< 20 \text{ tons acre}^{-1} \text{ year}^{-1}$), a negligible risk of overland movement of soil solution from the site, a medium risk of SP losses through subsurface pathways, and that the plots at the site were > 100 ft (31 m) away from surface water, respectively.

Table 3.1. Categorical transport variables included in the empirical dataset, including name, brief description and rating values used in the study. Categories used were obtained from NASTRAT (IN-NRCS, 2013).

Variable [#]	Brief description	Rating values [‡]					
		0	1	2	4	8	16
Soil erosion (SE) (RUSLE 2) (tons/acre/year)	Soil loss estimated by the Revised Universal Soil Loss Equation (RUSLE2)		Low (< 20)		Medium (20 - 37)		High (> 37)
Surface runoff (SR) (unitless)	It represents the relative risk of movement of soil solution from a field. It is determined based on the interaction of two site characteristics; soil permeability and percent slope of the predominant soil in the field.	Negligible	Very low	Low	Medium	High	Very high
Subsurface drainage potential (SDP) (unitless)	It represents the relative risk of nutrient loss through subsurface pathways. It is determined from a matrix created using soil drainage class, depth to seasonal high water from the dominant soil in the field, and whether there are any surface tile inlets and artificial subsurface drainage. A minimum ranking of medium and high are assigned to fields with artificial subsurface drainage and surface tile inlets respectively.		Very low	Low	Medium	High	Very high
Distance to water body (DTW) (ft (m))	This variable is a measure of the nearest field distance to surface water (stream, river, pond, lake or perennial ditch).		Low (> 100 (31))		Medium (31 - 99 (9 - 30))		High (≤ 30 (9))

[‡] Rating values based on a rating system of base 2 like Lemunyon and Gilbert (1993).

[#] Detailed variable description and explanation of determination can be found in IN-NRCS (2013).

Like Bolster et al. (2012) and Fiorellino et al. (2017), the first step during theoretical dataset generation was the determination of the most accurate probability distribution function (*fpd*) for each variable based on recorded data in the empirical dataset. The range of each numerical variable was defined using the range observed in the empirical dataset to represent values that could potentially exist in well-managed fields (Table 3.2).

Table 3.2. Range of values for continuous input variables used for generating the theoretical dataset.

Variable	Abbreviation	Range
Mehlich 3 soil test P (mg kg ⁻¹)	STP	0 - 104
P saturation ratio (unitless)	PSR	0 - 0.34
Soil P storage capacity (L kg ⁻¹)	SPSC	-85 - 137.76
Annual flow-weighted mean DRP (mg L ⁻¹)	fDRP	0 – 0.216

The process of *f*pd selection and fitting to these observed values was done using different functions in the R package *fitdistrplus* (Delignette-Muller and Dutang, 2015 ; R Core Team , 2017). The adequate fit of the selected *f*pd's was examined with histograms and theoretical density plots (Q-Q plot, empirical and theoretical cumulative distribution functions and P-P plots) (supplemental Figure S1) (Delignette-Muller and Dutang, 2015). As there was no clear fit for fDRP, fDRP concentrations were generated using the 5th, 10th, 25th, 50th, 75th, 90th, 95th, 98th, and 99th percentiles (supplemental Figure S7.2).

Both inorganic and organic P fertilizers applications were considered in this study. For simplicity, this study only considered maize even though most fields in Indiana are under maize-soybean rotations. The assumption was that due to its higher yield potential and subsequent higher crop P removal rates, all P application rates determined using maize as a reference crop would encompass possible P application rates to soybean crops. In the state, inorganic fertilizer application rates are based on the tri-state fertilizer recommendations (Vitosh et al., 1995). These recommendations use observed STP and the potential yield of a selected crop (maize) to determine recommended inorganic P application rates for crops. The STP values generated using a log-normal distribution together with an average maize yield potential of 160 bu acre⁻¹ (10,080 kg ha⁻¹) were used to determine the corresponding inorganic P rates for the dataset. Dayton et al. (2017) used a similar average maize yield goal in their sensitivity analysis of the Ohio PI. Organic P rates are based on the organic nutrient guidelines in the Indiana NRCS Conservation Practice Standard code 590, which are also dependent on STP levels (Indiana NRCS FOTG, 2013). As per the guideline, organic P applications to soils with STP levels ≤ 50 mg kg⁻¹ are based on the current crop's (maize) nitrogen needs. Fields with STP levels between 51 – 100 mg kg⁻¹ and 101 – 200 mg kg⁻¹, are assigned organic P application rates that do not exceed $1.5 \times$ crop P₂O₅ removal rate and the crop P₂O₅ removal rate, respectively (Indiana NRCS FOTG, 2013). To simplify the

simulation, the study assumed that all manured fields received swine effluent similar to the WQFS, the reference experimental site. Subsequently, an N-based rate of 171 lbs P_2O_5 acre⁻¹ yr⁻¹ (192 kg P_2O_5 ha⁻¹ yr⁻¹) for swine effluent was determined for fields in the dataset with STP levels ≤ 50 mg kg⁻¹ following the steps outlined in Joern and Brichford (2003). Assuming that a corn-soybean rotation (with an average yield goal of 160 bu acre⁻¹ (10,080 kg ha⁻¹) for maize and 50 bu acre⁻¹ (3,350 kg ha⁻¹) for soybean similar to Dayton et al. (2017)) has an average crop removal rate of 50 lbs P_2O_5 acre⁻¹ yr⁻¹ (56 kg P_2O_5 ha⁻¹ yr⁻¹), fields with STP levels between 51 – 100 mg kg⁻¹ and 101 – 200 mg kg⁻¹ were assigned organic P rates of 75 lbs P_2O_5 acre⁻¹ yr⁻¹ (84 kg P_2O_5 ha⁻¹ yr⁻¹) and 50 lbs P_2O_5 acre⁻¹ yr⁻¹ (56 kg P_2O_5 ha⁻¹ yr⁻¹), respectively. Values for P application method and timing (FPA and OPA) were randomly assigned using modified uniform probability distributions. Based on the description of the five application methods in the empirical dataset and professional knowledge, the study assumed that 99% of fields in Indiana receive inorganic P applications which are surface applied < 3 months before crop and that there was an equal probability (0.25 %) of inorganic P being applied to a field using one of the remaining four methods. A similar distribution was used for organic P applications but since organic P applications represents < 20% of P applications in the region (King et al., 2017; Smith et al., 2018), 80% of the fields were assumed to receive no manure applications with the remaining fields having an equal probability (5%) of organic P being applied using any of the remaining methods.

Since data were not available for generation of transport variables, decision-making criteria based on information obtained from literature and professional knowledge was used to establish a distribution of possible values. Subsequently, values for SE, SR, SDP, and DTW, were randomly assigned using a modified uniform probability distribution based on assumptions made. According to USDA -NRCS (2015), recent estimates of annual soil loss by the Revised Universal Soil Loss Equation (RUSLE2) for croplands (both cultivated and uncultivated) in Indiana, is approximately 2.74 ± 0.16 tons acre⁻¹ year⁻¹. Therefore, the study assumed that most agricultural fields (99%) would be in the low soil loss category identified in the NASTRAT (< 20 tons acre⁻¹ year⁻¹; IN-NRCS, 2013), with the remaining fields having equal probabilities (0.5%) of being in the medium (20 - 37 tons acre⁻¹ year⁻¹) or high (> 37 tons acre⁻¹ year⁻¹) soil loss categories. Surface runoff classes (SR) are determined based on the interaction of two site characteristics; soil permeability and percent slope of the predominant soil in the field (IN-NRCS, 2013). Assuming that no agricultural fields are established on slopes > 10% and that most soils belong to the moderately

slow and slow soil permeability class similar to soils at the WQFS (Drummer silty clay loam and Raub silt loam), the study assigned equal probabilities (25%) to the negligible, very low, low, and medium surface runoff potential categories with zero probabilities of agricultural fields being established in areas with high and very high surface runoff potentials. Indiana NASTRAT guidelines specify that any fields with artificial subsurface drainage (at any depth) should automatically receive a medium drainage potential ranking while fields with surface tile inlets should automatically receive a high drainage potential ranking. Since approximately 80% of cropland in Indiana has some type of subsurface drainage (Blann et al., 2009), 80% of the fields in the dataset were classified as having a medium drainage potential with the rest of the fields having an equal probability (5%) of being in any of the remaining categories. Finally, for the distance to water body (DTW) variable, it was assumed that 90% of the fields were established at ≥ 100 feet (31 m) from surface water, with 5% between 31 – 99 feet (9 – 30 m) from surface water and the final 5% at ≤ 30 feet (9 m) from surface water.

Once, the distributions were determined, the dataset was generated by stochastic data generation (($n = 10,000$) using R 3.4.0. (R Core Team, 2017)), followed by logical selection of combination of inputs and outputs to represent possible physical and management conditions in well-managed agricultural fields.

3.3.3 Description and development of SP ANN-model

To predict SP losses, this study used a multi-layered feed forward (MLF) neural network structure. This is a popular network structure used in water resource applications such as the prediction of nutrient concentrations from runoff (Kim and Gilley, 2008), prediction of watershed nutrient loading (Kim et al., 2012), prediction of nitrate contamination of ground water (Ehteshami et al., 2016), and risk assessment of P loss (Berzina et al., 2009). An MLF ANN is typically organized in successive layers i.e. an input layer (independent variables), a hidden layer (connecting layer), and an output layer (dependent variables). Information flows unidirectionally through successive layers via adjustable connection weights (numeric weights) that recognize different patterns (Svozil et al., 1997). Most MLF ANNs contain one or more hidden layers but in many water quality studies, using one hidden layer is reasonable (Wu et al., 2015; Khalil et al., 2011). Using the inputs and output generated in the theoretical dataset, our MLF ANN is represented by the following equation (Equation 1);

$$fDRP = ANN [STP, PSR, SPSC, FPR, FPA, OPR, OPA, SE, SR, SDP, DTW] \quad [Eq. 9]$$

where $fDRP$ is the annual flow weighted mean DRP concentrations from tile effluent; STP is Mehlich 3 soil test P (mg kg^{-1}); PSR is P saturation ratio (unitless); SPSC is soil P storage capacity (L kg^{-1}); FPR is inorganic P fertilizer rate ($\text{lbs P}_2\text{O}_5 \text{ ha}^{-1}$); FPA is inorganic P fertilizer application method and timing; OPR is organic P manure rate ($\text{lbs P}_2\text{O}_5 \text{ ha}^{-1}$); OPA is organic P manure application method and timing ; SE is soil erosion ($\text{ton acre}^{-1} \text{ year}^{-1}$) ; SR is surface runoff ; SDP is subsurface drainage potential; and DTW is the distance to a water body (feet). In this study, neuralnet function (Wright et al., 2019; R Core Team, 2017), was used to create the MLF ANN trained by the backpropagation algorithm.

Given the inputs and output consisted of variables with different units and ranges, all data were scaled between 0 - 1 using the min-max normalization technique (Gopal et al., 2015). The datapoints (10,000) were randomly divided into two subsets, training set (60%) and testing set (40%). The training set was used to adjust the connection weights, biases, and optimum parameters, and the testing set was used to confirm the actual predictive power of the network. To train the MLF ANN, the backpropagation algorithm (Hecht-Nielsen, 1989) was used. This algorithm utilizes supervised training and compares its resulting outputs against target outputs, and propagates errors backwards through the systems to adjust the weights of the neurons in each layer and minimize the sum of square errors of the network (Hecht-Nielsen, 1989). In this study, initial default MLF ANN parameters included: the sum of squared error as the error function, 0.01 as the threshold for convergence (partial derivative of the error function to stop iteration), 100,000 as the stepmax (maximum number of steps of the training process), 1 as the number of the neurons in the hidden layer, resilient backpropagation (rprop+; the learning algorithm), and logistic function as the activation function. For additional details on network parameters, description, default settings and available options, see Wright et al. (2019). To ensure optimum network configuration, the activation function and number of neurons in the hidden layer were changed. The activation function was changed from logistic to softplus which has been shown to significantly improve model performance and convergence with fewer training steps compared to other standard functions (Zheng et al., 2015). Also, a trial and error approach was used to set the number of neurons in the hidden layer by varying them between $(2n^{1/2} + m)$ and $(2n + 1)$ (Fletcher and Goss, 1993), where n and m are the number of input and output variables (neurons) respectively, until the desired network accuracy was achieved. Finally, 10 fold cross-validation (Olden et al., 2008;

Chowdhury et al., 2002) was used to test network robustness across different samples and ensure the network was not overfit to a particular set of data. Network robustness has important implications particularly when the MLF ANN will be used for prediction purposes. An optimum network is the one that is robust across different samples (Olden et al., 2008). Therefore, this cyclic process of training (feed forward and error backpropagation), testing, and cross-validation, was repeated until the desired network accuracy was achieved.

During the optimization of the network, the goodness of fit between predicted and measured outputs was evaluated using the coefficient of determination (R^2) and the root mean square error (RMSE). The R^2 value indicates how well the network fits the data and accounts for the variability in prediction by the variables specified in the network. R^2 values > 0.9 , 0.8 to 0.9 and, 0.6 to 0.8, indicate a very satisfactory model, a fairly good model and an unsatisfactory model respectively (Lallahem and Mania, 2003). The RMSE indicates how close the predicted values are to the fitting line. The smaller the RMSE value, the closer the predicted value is to the observed value.

3.3.4 Relative importance analysis of input variables

Relative importance analysis is unique, as it not only quantifies relationships between input and output variables similar to common sensitivity analysis but it also considers the potential interactions among the input variables (Garson, 1991). Network weights determined from relative importance analysis are partially analogous to the coefficients in a linear model. Therefore, the combined effects of weights specific to an input variable represent its relative importance (weight) as a predictor variable (Garson, 1991). Garson's algorithm has been used in previous studies to determine the relative importance of input variables in an MLF ANN (Zheng et al., 2017; Grahovac et al., 2016; Giam and Olden, 2015; Zhou et al., 2015). This study used Garson's algorithm (garson function; package NeuralNetTools; Marcus et al., 2018) to partition the numerous ANN weights, and subsequently pool and scale (values ranging from 0 – 1) weights specific to each input variable to reflect their respective relative importance (Garson, 1991). All relative importance values were given in their absolute values.

3.3.5 PI performance

There is no existing PI in Indiana, therefore the first step in the analysis was to formulate a PI. Our study adopted a multiplicative PI formulation similar to the Pennsylvania PI. This formulation is a good representation of processes governing P loss from agricultural fields given it better represents the concept of critical source areas (Gburek et al., 2000; Sharpley et al., 2003). The multiplicative PI has the general form below:

$$PI = \sum_{i=1}^n (TW_i \cdot T_i) \cdot \sum_{j=1}^m (SW_j \cdot S_j) \quad [\text{Eq. 10}]$$

where T represents PI transport factors (soil erosion (SE), surface runoff (SR), subsurface drainage potential (SDP), distance to water body (DTW)), TW represents weights for the various transport factors, S represents PI sources (soil test P (STP), inorganic P fertilizer rate (FPR), inorganic P fertilizer application (FPA), organic P fertilizer rate (OPR), organic P fertilizer application (OPA)), SW represents weights for the source terms, n and m represent the number of transport and source factors, respectively. Given that relationships between SP and both PSR, SPSC have thresholds above/below which P loss increases to soil solution (Welikhe et al., 2020), we propose their inclusion into our multiplicative PI as follows; (1) for fields with PSR and SPSC values below and above the identified thresholds i.e. 0.21 and 0, respectively, the weighted PSR and SPSC values were subtracted from the total sum of source factors to indicate reduced risk of P loss from these fields, and (2) for fields with PSR and SPSC values above and below the identified thresholds, respectively, the weighted PSR and SPSC values were added to the total sum of source factors to indicate increased risk of P loss from these fields.

To evaluate whether the ANN-generated weights improve PI accuracy, we compared the performance of a PI weighted using ANN generated weights (PI_{ANN}), a PI weighted using the Lemunyon and Gilbert (1993) PI weights (PI_{LG}), and an unweighted (no weights) PI (PI_{NO}), at predicting observed fDRP concentrations in the empirical data set. Equations for the latter PI calculations are detailed in Table 3.3.

Table 3.3. Equations for multiplicative P index formulations used in the study.

PI	Equation
Unweighted PI (PI _(NO))	$(STP + (FPR \times FPA) + (OPR \times OPA)) \times (SE + SR + SDP + DTW)$
LG - weighted PI (PI _(LG))	$((STP \times 1) + ((FPR \times 0.75) \times (FPA \times 0.5)) + ((OPR \times 1) \times (OPA \times 1))) \times ((SE \times 1.5) + (SR \times 0.5) + (SDP \times 0.5) + (DTW \times 0.5))^{\ddagger}$
ANN - weighted PI (PI _(ANN))	$((STP \times W1) + (PSR \times W2) + (SPSC \times W3) + ((FPR \times W4) \times (FPA \times W5)) + ((OPR \times W6) \times (OPA \times W7))) \times ((SE \times W8) + (SR \times W9) + (SDP \times W10) + (DTW \times W11))^{\ddagger}$

[¥]Site characteristics not in the Lemunyon and Gilbert, (1993) PI, i.e. subsurface drainage potential (SDP) and distance to water body (DTW), were arbitrarily assigned weights of 0.5.

[‡]W1 to W11 represent the ANN generated weights.

All PI's were calculated using information (site characteristics and field management practices) from the empirical dataset. Like Sharpley et al. (2001), fDRP concentrations were subsequently regressed (exponential regression) against field PI scores (PI_{ANN}, PI_{NO}, and PI_{LG}). All regressions were performed using R 3.4.0. (R Core Team, 2017).

3.4 Results and Discussion

3.4.1 Performance of ANN

Based on Fletcher and Goss (1993) criteria, during network optimization, the number of neurons in the hidden layer was varied between 6 and 23. Results showed that an MLF ANN with 7 neurons in the hidden layer gave the lowest RMSE during both cross-validation and testing (Table 3.4).

Table 3.4. Testing and 10-foldcross validation performance of the MLF ANN with increasing number of neurons in the hidden layer. The validation mean RMSE is the mean RMSE of the 10 folds analyzed during cross-validation.

No. hidden neurons	Testing (R ²)	Testing (RMSE)	Validation (mean RMSE)
6	0.96	0.0028	7.2×10^{-6}
7	0.99	0.0024	5.2×10^{-6}
8	0.98	0.0014	4.9×10^{-4}
9	0.96	0.0033	5.3×10^{-4}

An increase in mean RMSE during cross-validation indicates model overfitting (fitting the noise in the training data) (Liu et al., 2007). In this study, as the number of neurons increased from 7, cross-validation mean RMSE increased (Table 3.4), indicating a decrease in network performance. Thus, the final network structure consisted of 11 neurons in the input layer, 7 neurons in the hidden layer, and 1 neuron in the output layer. The selected MLF ANN structure is presented in Figure 3.1. Given the numerous connection weights among the neurons (Figure 3.1), attempts to trace the direction and relative magnitude of weights between neurons were not successful.

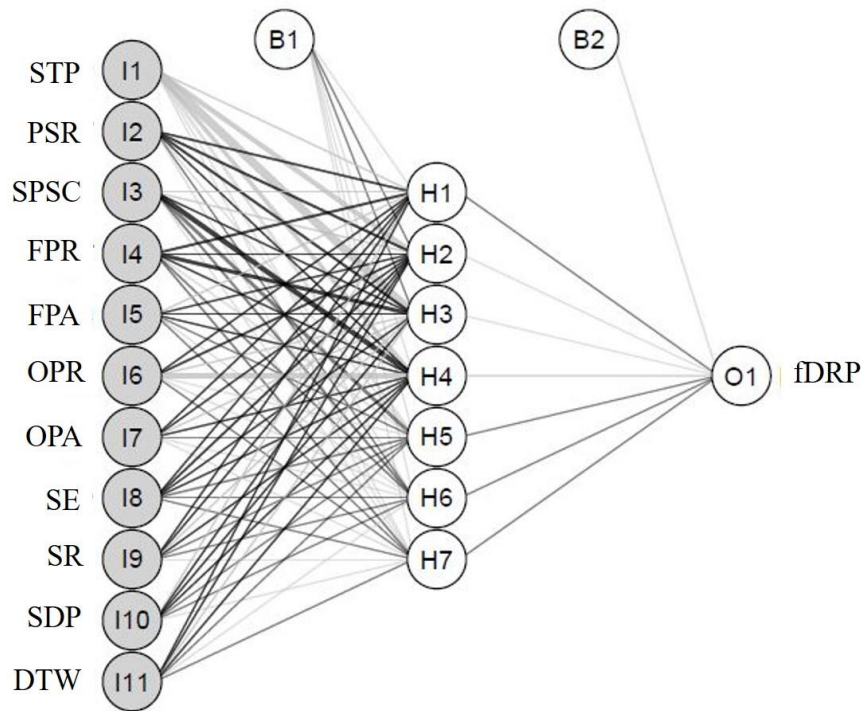


Figure 3.1. Neural interpretation diagram of the best MLP network structure with 11,7, and 1 neuron(s) in the input (I), hidden (H) and output (O) layers respectively. B1 and B2 are bias terms added to H and O layers. Black and grey lines represent positive and negative connections respectively, while line thickness represents the relative magnitude of each connection weight. Abbreviations are; STP= soil test P, PSR = P saturation ratio, SPSC = soil P storage capacity, FPR = Inorganic P fertilizer rate, FPA = Inorganic P fertilizer application method and timing, OPR = Organic P fertilizer rate, OPA = Organic P fertilizer application method and timing, SE = soil erosion, SR = surface runoff, SDP = subsurface drainage potential, DTW = distance to water body, and fDRP = Annual flow-weighted mean DRP concentrations.

The accurate performance of the selected MLF ANN is illustrated in Figure 3.2, where the simulated fDRP values were compared with the predicted fDRP values. The predicted and simulated values in the test set were very close to the 1:1 regression line ($y = x$, predicted fDRP = simulated fDRP), except for three data points that were underpredicted by the MLF ANN. An R^2 and RMSE value of 0.99 and 0.0024, respectively, for the test set, demonstrated a good linear fit, and confirmed the ability of the trained MLF ANN to predict new data precisely.

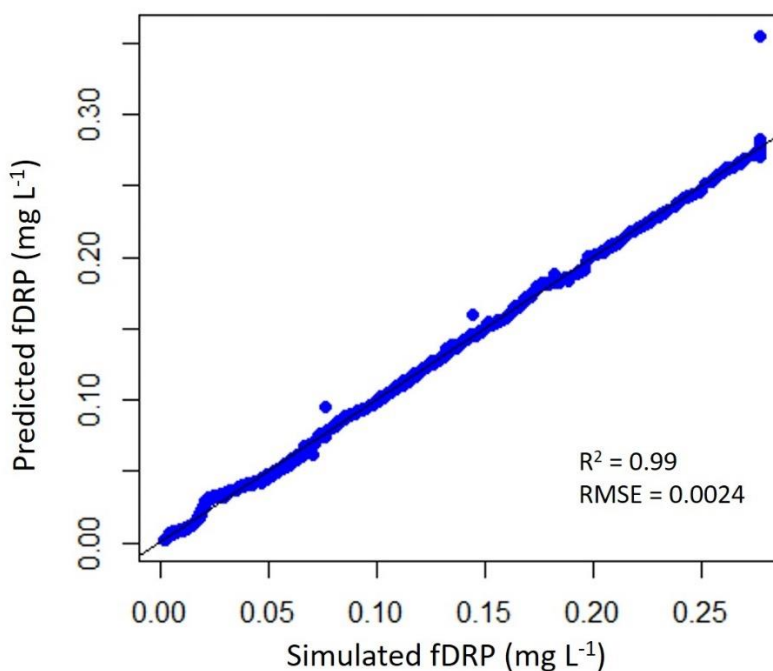


Figure 3.2. Selected MLF ANN parity plot for annual flow-weighted dissolved reactive phosphorus (fDRP) concentrations in tile discharge. The black line is the 1:1 ($y = x$) line.

A small variation in RMSE across folds during cross-validation indicates a robust network (Liu et al., 2007). The reasonably small variation in RMSE across folds in this study (Table 3.5) is evidence that the selected MLF ANN was quite robust. Much of the variation across fold RMSE values is associated with each fold having random initial starting seeds, and random split of the dataset into training and testing sets during the cross-validation process (Zhang et al., 1999).

Table 3.5. RMSE values for each fold during cross-validation.

Fold	RMSE
1	4.5×10^{-6}
2	4.8×10^{-6}
3	3.8×10^{-6}
4	7.5×10^{-6}
5	5.7×10^{-6}
6	8.0×10^{-6}
7	3.4×10^{-6}
8	5.4×10^{-6}
9	3.8×10^{-6}
10	4.6×10^{-6}

Kim and Gilley (2008) showed that ANNs trained with datasets that adequately represent the critical processes involved in nutrient loss to drainage waters achieved higher predictive ability. In the present study, the high predictive ability by the MLF ANN resulted from the use of a theoretical dataset whose variables were carefully generated and combined to represent conditions that could potentially exist in well-managed agricultural fields. This highlights the importance of a good dataset (simulated or measured) that accurately represents existing conditions in an area of interest during ANN model building.

3.4.2 Relative importance of input variables on SP losses

Table 3.6 presents the results of Garson's relative importance analysis of each site characteristic on SP losses in tile effluent. The latter algorithm uses absolute values of the connection weights to calculate variable importance; therefore, the values presented here do not provide the direction of the relationship between input and output variables (Garson, 1991).

Table 3.6. Results of the relative importance analysis for various site characteristics on annual flow-weighted mean DRP concentrations in tile effluent. Values in bold and in parenthesis represent Lemunyon and Gilbert (1993) weighting factors normalized to sum to 1.

Input	Abbrev.	Relative importance
<u>Source factors</u>		
Mehlich 3 soil test P	STP	0.279 (0.160)
P saturation ratio	PSR	0.097
Soil P storage capacity	SPSC	0.231
Inorganic P fertilizer rate	FPR	0.233 (0.120)
Inorganic P fertilizer application method and timing	FPA	0.007 (0.080)
Organic P fertilizer rate	OPR	0.084 (0.160)
Organic P fertilizer application method and timing	OPA	0.004 (0.160)
<u>Transport factors</u>		
Soil erosion	SE	0.043 (0.240)
Surface runoff	SR	0.008 (0.080)
Subsurface drainage potential	SDP	0.007
Distance to water body	DTW	0.006

Input variable contributions ranged from 0.004 to 0.279, with SP losses from well-managed fields being strongly governed by source factors (Table 3.6). As an indicator of total sorbed P in soils (Sims et al., 2000), STP has strongly been linked to SP losses in both surface runoff (e.g. in Pote et al., 1999) and subsurface drainage (e.g. in Duncan et al., 2017) waters. Our analysis revealed that STP had the greatest weight (0.279) on SP loss. This mainly reflects that the amount of bio-available P strongly influences SP losses in tile drains in well-managed agricultural fields. Phosphorus application rates have come under scrutiny as one of the reasons for increased P loss in agricultural watersheds (Smith et al., 2015). The MLF ANN identified FPR as the second most influential site characteristic with a weight of 0.233 (Table 3.6). The FPR are based on the Tri-state Fertilizer Recommendations (Vitosh et al., 1995). When these fertilizer recommendations were being developed, P fertilizer was relatively cheap in comparison to crop value; and under-

fertilization with its associated loss in yields was viewed as a higher economic risk than over-fertilization (Nelson, 1967). Therefore, historic recommendations included a safety factor to ensure yield potential would not be decreased across different soil types (Nelson, 1967; Vitosh et al., 1995). The result is that on many highly productive soils where Tri-state Fertilizer Recommendations are followed, it is very likely that inorganic P is applied at rates greater than crop demand which contributes to P enrichment of surface soils and subsequent P losses (Nizeyimana et al., 2001; Smith et al., 2015). The SPSC had a weight very close to FPR i.e. 0.231 and 0.233, respectively (Table 3.6). As an index of a soil's sink strength, the capacity dimension of SPSC takes into account previous P loading and enables the prediction of how much P a soil can sorb before becoming an environmental risk (Nair, 2014; Nair et al., 2015). The close weighting between FPR and SPSC indicates that in well-managed agricultural fields both contemporary (specifically inorganic P additions) and legacy P sources should be prioritized as top site characteristics for P loss risk assessment when developing strategies aimed at abating SP loss from fields. Compared to SPSC, PSR had a small relative importance of 0.097 to SP loss in well-managed fields which are not excessively P rich (maximum STP in the empirical dataset was 104 mg P kg^{-1}) (Table 3.6). This is consistent with previous work which showed that P sorption capacity has a bigger influence on SP loss potential in excessively P-rich soils (Reid et al., 2012; Bolinder et al., 2011). Even though not many fields in the region ($\sim 20\%$; King et al., 2017; Smith et al., 2018) receive organic P as simulated in the theoretical dataset, the relative importance analysis identified OPR (weight = 0.084) as the fifth most influential site characteristic (Table 6). Indiana soils with STP levels $\leq 50 \text{ mg kg}^{-1}$ receive N-based manure applications (Indiana NRCS FOTG, 2013). Research confirms that there is a higher P loss from fields receiving manure amendments applied at N-based application rates. These studies show that when manure is applied to meet the N requirements of a corn crop (N-based application), it results in the oversupply of P to soils because of the low N: P ratio in manures compared to most crops (King et al., 2018; Dodd and Sharpley, 2016; Toth et al., 2006). The influence that both organic (OPR) and inorganic P (FPR) rates have on SP loss emphasizes the significance of controlling P accumulation (i.e. contemporary P sources) in soils in order to control the amount of P that remains in solution and is susceptible to leaching once soil P sorption sites are saturated (Breeuwsma and Silva, 1992). With regards to P application methods, previous studies show that the potential for SP loss is exacerbated when either organic or inorganic P are surface applied, and it is generally reduced

when P materials are incorporated by injection, banding or tillage (Smith et al., 2016; Daverede et al., 2004). Compared to other source factors, both FPA and OPA were assigned very low weights i.e. 0.007 and 0.004, respectively. The low weights were expected given the potential for SP movement with either surface or subsurface runoff assigned in the theoretical dataset was not high. Also, the low weights assigned may be a reflection of the impact of the duration between the surface application of P fertilizers and runoff events. Findings by Smith et al. (2007) show that the shorter the duration between P fertilizer applications and runoff events, the greater the risk of P losses to surface water. Even though the most common P application method (especially for inorganic P) in Indiana is surface application, the timing of applications in these well-managed fields is such that runoff events do not occur soon after. This finding demonstrates the importance of considering the timing of P applications in addition to application methods in P loss risk assessments.

The transport site characteristics had low relative importance, compared to the source site characteristics (Table 3.6). This could be a reflection of the many widely adopted conservation practices aimed at reducing P movement from a field through reductions in erosion, runoff and P entrapment within fields (Dodd and Sharpley, 2016). Among the four transport variables, SE had the highest relative importance of 0.043, with the remaining transport site characteristics (SR, SDP, and DTW) all having relatively low impacts on SP losses in tile drains (Table 3.6). The high impact of SE may be the result of unintended consequences arising from the adoption of conservation practices. The conservation practices (e.g. no till, minimum till, cover cropping etc.) in the region have successfully reduced soil erosion, unfortunately this reduction in soil disturbance has inadvertently increased P loss (mainly SP loss) in tile drained fields due buildup of labile P in surface soils, especially on fields with long-term P applications (Jarvie et al., 2017; Dodd and Sharpley, 2016; Duiker and Beegle, 2006). Since 99% of the fields in the theoretical dataset were generated to represent fields with minimal annual soil loss, the latter unintended effect of reduced soil erosion on SP losses in tile drains, is a possible explanation of why soil erosion is the most important transport factor. The SR and SDP had relative importance values that were low, and close in magnitude to each other i.e. 0.008 and 0.007, respectively (Table 3.6). This result agrees with previously reported observations of SR and SDP contributions to SP losses. In many watersheds in the Midwest, there is an approximate 50-50 split between surface runoff and tile discharge contributions to stream flow (King et al., 2014). In these watersheds, previous studies

show that, in some settings, surface runoff and tile drains exported approximately equal amounts of DRP to streams (Ruark et al., 2012; King et al., 2014; Macrae et al., 2007). Finally, DTW was last in relative importance (0.006) among the transport factors (Table 3.6). Reid et al. (2018) show that the actual risk of SP loss to surface water depends on the distance and landscape characteristics between the point of SP release (edge of field) to the surface water, with higher risks being associated with shorter distances between these two points. In this study, the MLF ANN assigned the least relative importance to DTW since in the theoretical dataset, 90% of the fields were established at ≥ 100 feet (31m) from surface water (low risk category).

Overall, the ANN-generated WFs (WF_{ANN}) were different from the WFs assigned to site characteristics in the original PI (WF_{LG}) (Table 3.6). Unlike the WF_{LG} which were arbitrarily assigned (Lemunyon & Gilbert, 1993), the WF_{ANN} were assigned based on relationships identified between site characteristics and measured SP loss by the MLF ANN. The difference between WF_{LG} and WF_{ANN} , further highlight the need identified by the authors of the original PI (Lemunyon & Gilbert, 1993) to use field studies to more accurately assign WFs that reflect the contribution each site characteristic to P loss in an area of interest.

3.4.3 Comparison of PI performance

There was not a significant exponential relationship between index values and measured fDRP concentrations for both the PI_{NO} and PI_{LG} index formulations (Figure 3.3a and 3.3b). This indicated that both PI_{NO} and PI_{LG} poorly represented the risk of SP loss to tile discharge. According to the authors of the PI_{LG} , the function of input factor weights was to define each input's relative contribution to P loss risk (Lemunyon and Gilbert, 1993). Therefore, the poor performance of PI_{NO} (Figure 3a) was expected given the absence of weights that, much like coefficients in a linear model, describe the relationship between a predictor variable and its response variable (Sharpley et al., 2012; Garson, 1991). Lemunyon and Gilbert, (1993) acknowledged that weights in their PI were arbitrarily selected which explains the poor performance of PI_{LG} (Figure 3.3b). Ideally, to better capture P loss risk in a particular region, P index weights should be obtained from measured P loss data (Sharpley et al., 2012). This explains the significant exponential relationship observed between PI_{ANN} and measured fDRP concentrations (Figure 3.3c; $R^2 = 0.60$, $p < 0.001$). Previous studies for example, Eghball and Gilley (2001), DeLaune et al. (2004), and Sonmez et al. (2009), also reported improved PI performance when weights were based on measured P losses.

Distinct groups of data were observed when P loss data were plotted against both PI_{NO} and PI_{LG} (Figure 3.3a and 3.3b). Fiorellino et al. (2017) showed that the distinct groups of data observed when P loss data are plotted against calculated PI values, arise from the use of categorical variables which prevent calculated PI values from relating well with measured P loss data. Given that plots used in this study had similar values for transport factors, distinct groups of data separated out based on P application rates (both organic and inorganic) and their corresponding P application method categories.

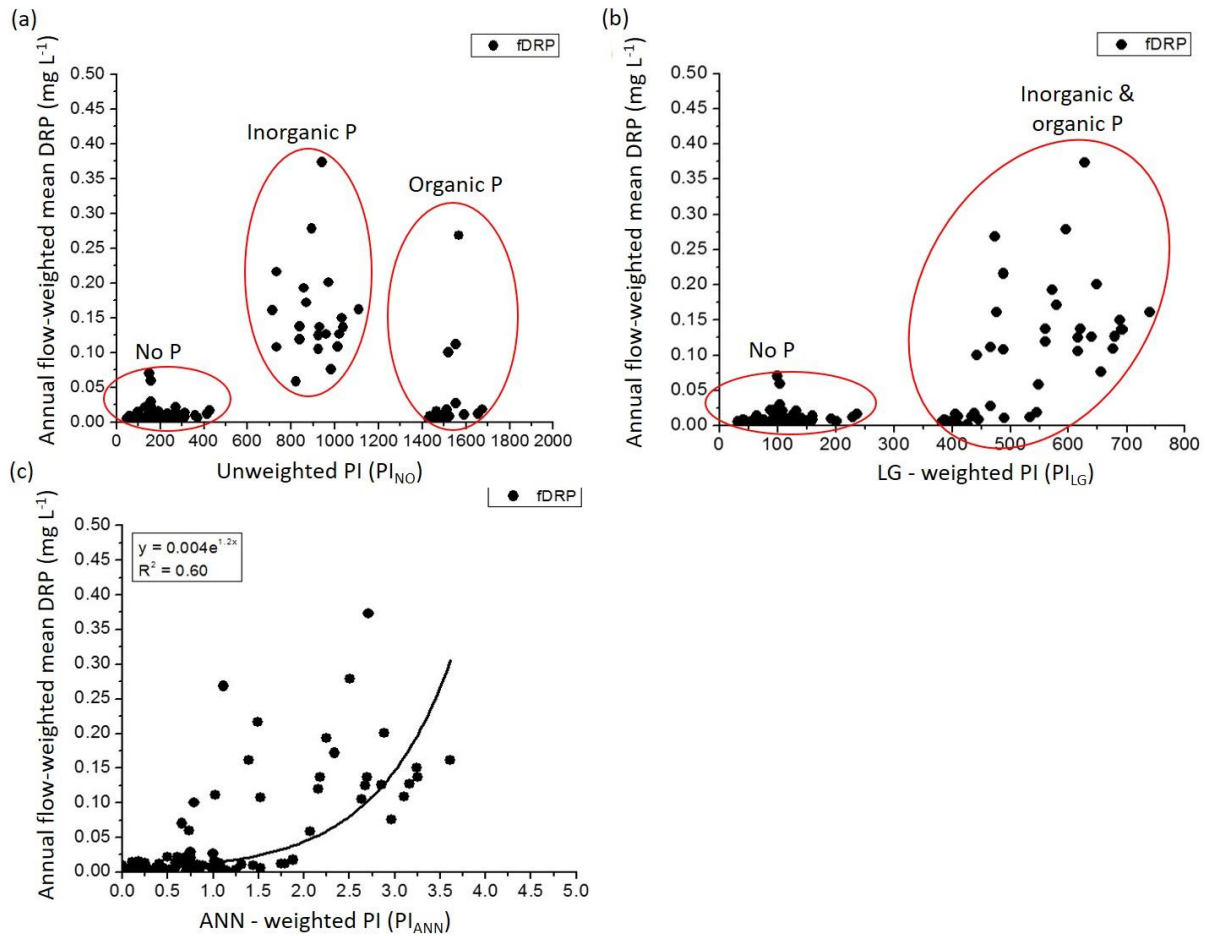


Figure 3.3. Observed annual flow-weighted mean DRP concentrations (fDRP) and predictions of SP loss risk calculated with the (a) Unweighted PI (PI_{NO}), (b) a PI weighted using Lemunyon and Gilbert (1993) weights (LG - weighted PI (PI_{LG})), and (c) a PI weighted using artificial neural network generated weights (ANN - weighted PI (PI_{ANN})).

Using the ANN-generated weights appeared to alleviate (to an extent) the distinct groups of data observed in the other two PIs (Figure 3.3). This observation highlights the importance of considering possible synergistic and antagonistic interactions between site characteristics during weight determination. Despite the improved relationship between PI_{ANN} and fDRP concentrations, there was still a significant amount scatter around the best fit line (Figure 3.3c). When Lemunyon and Gilbert (1993) came up with the PI concept, they did not intend for it to be used to quantitatively estimate actual P loss from a field but rather it was originally intended to be used as a tool to rate a field's relative risk to P loss based on the site characteristics. The significant amount of scattering still observed even with the use of WF_{SANN} , demonstrates the limitation of using a simple PI concept to model complex physical processes governing P loss. Yet, evaluating PI_{ANN} values against measured SP loss data was a reasonable approach for assessing its performance. Overall, the significant exponential relationship between PI_{ANN} and SP, shows that the proposed PI_{ANN} for well-managed agricultural fields was directionally and magnitudinally correct as is expected of PIs used to assess the risk of P loss (Sharpley et al., 2012).

3.5 Conclusion

The MLF ANN with 11-7-1 topology and trained by backpropagation, presented satisfactory predictive ability and robust generalization capacity for modeling complex SP loss through tile drains. Through analysis of relative importance, Garson's algorithm showed feasibility for evaluating the weights of eleven site characteristics and the results obtained were reasonable and consistent with known relationships between site characteristics and SP loss. Results from the relative importance analysis highlighted the need to prioritize both contemporary and legacy P sources when determining best management practices to minimize P loss from well-managed agricultural fields. Further, unlike the PI_{NO} and PI_{LG} , the PI_{ANN} had a significant exponential relationship with fDRP and was able to provide reasonable estimates of P loss in tile effluent. These findings suggest that modifications to a PI, such as WF_{SANN} , would likely improve the predictive ability of the risk assessment tool.

In the long-term, we propose the use of a wide range of measured field data representative of all fields in Indiana, not just well-managed fields, to allow for the identification of P risk categories in the final PI. Also, future research efforts should include all P forms (soluble, particulate, and total P) and consider P loss from all pathways not just through subsurface drainage. The authors

acknowledge that although this approach is rigorous, it is a relatively simple option for developing accurately weighted PIs that better reflect complex physical processes governing P loss. They note that the reliability of this approach will depend on the accuracy of the MLF ANN on which the weights are based and will be valid only over the range of conditions considered in the analysis. Also, as is common practice, the stochastic generation of the theoretical dataset from only one simulation (realization) raises the question on how representative the dataset is of existing conditions in well-managed agricultural fields. Guo et al. (2018) showed that a minimum of 25 simulations are needed to accurately capture statistical characteristics of climate during stochastic weather data generation. To our knowledge, no such study has been carried to identify the number of simulations needed to accurately capture statistical characteristics of soils and management data. Therefore, this study does not propose the adoption of these weights into an Indiana PI. Rather, we propose the use of the methods presented here during the development of a state PI, taking care that the MLF ANN used is trained and tested against measured P loss to improve PI accuracy.

3.6 References

- Al-Mahallawi, K., Mania, J., Hani, A., and Shahrour, I. (2012). Using of neural networks for the prediction of nitrate groundwater contamination in rural and agricultural areas. *Environmental Earth Sciences*, 65(3), 917–928. <https://doi.org/10.1007/s12665-011-1134-5>
- Benítez, J. M., Castro, J. L., and Requena, I. (1997). Are artificial neural networks black boxes? *IEEE Transactions on Neural Networks*, 8(5), 1156–1164. <https://doi.org/10.1109/72.623216>
- Berzina, L., Zujevs, A., and Sudars, R. (2009). Neural network approach in risk assessment of phosphorus loss. *Research for Rural Development*, 320–326.
- Blann, K. L., Anderson, J. L., Sands, G. R., and Vondracek, B. (2009). Effects of agricultural drainage on aquatic ecosystems: A review. *Critical Reviews in Environmental Science and Technology*, 39 (11), 909–1001. <https://doi.org/10.1080/10643380801977966>
- Bolinder, M. A., Simard, R. R., Beauchemin, S., and MacDonald, K. B. (2011). Indicator of risk of water contamination by P for Soil Landscape of Canada polygons. *Canadian Journal of Soil Science*, 80 (1), 153–163. <https://doi.org/10.4141/s99-040>
- Bolster, C. H., Vadas, P. A., Sharpley, A. N., and Lory, J. A. (2012). Using a Phosphorus Loss Model to Evaluate and Improve Phosphorus Indices. *Journal of Environment Quality*, 41 (6), 1758. <https://doi.org/10.2134/jeq2011.0457>
- Breeuwsma, A. and Silva, S. (1992). Phosphorus fertilisation and environmental effects in The Netherlands and the Po region (Italy). Wageningen, The Netherlands. The Winard Staring Center for Integrated Land, Soil, and Water Research. 39p.
- Chowdhury, P. R., and Shukla, K. K. (2002). On generalization and K-fold cross validation performance of MLP trained with EBPDT. *Lecture Notes in Computer Science (Including Subseries Lecture Notes in Artificial Intelligence and Lecture Notes in Bioinformatics)*, 2275, 352–359.
- Daverede, I. C., Kravchenko, A. N., Hoeff, R. G., Nafziger, E. D., Bullock, D. G., Warren, J. J., and Gonzini, L. C. (2004). Phosphorus runoff from incorporated and surface-applied liquid swine manure and phosphorus fertilizer. *Journal of Environmental Quality*, 33 (4), 1535–1544.
- Dayton, E. A., Holloman, C. H., Subburayalu, S., and Risser, M. D. (2017). Using Crop Management Scenario Simulations to Evaluate the Sensitivity of the Ohio Phosphorus Risk

- Index. *Journal of Environmental Protection*, 08 (02), 141–158.
<https://doi.org/10.4236/jep.2017.82012>
- DeLaune, P. B., Moore Jr., P. A., Carman, D. K., Sharpley, A. N., Haggard, B. E., and Daniel, T. C. (2004). Evaluation of the phosphorus source component in the phosphorus index for pastures. *Journal of Environmental Quality*, 33 (6), 2192–2200.
<https://doi.org/10.2134/jeq2004.2192>
- Delignette-Muller, M. L., and Dutang, C. (2015). Fitdistrplus : An R Package for Fitting Distributions . *Journal of Statistical Software*, 64 (4), 1–22.
<https://doi.org/10.18637/jss.v064.i04>
- Dodd, R. J., and Sharpley, A. N. (2016). Conservation practice effectiveness and adoption: unintended consequences and implications for sustainable phosphorus management. *Nutrient Cycling in Agroecosystems*, 104 (3), 373–392. <https://doi.org/10.1007/s10705-015-9748-8>
- Drewry, J. J., Newham, L. T. H., and Greene, R. S. B. (2011). Index models to evaluate the risk of phosphorus and nitrogen loss at catchment scales. *Journal of Environmental Management*, 92 (3), 639–649. <https://doi.org/10.1016/j.jenvman.2010.10.001>
- Dubrovsky, N. M., Burow, K. R., Clark, G. M., Gronberg, J. M., Hamilton, P. A., Hitt, K. J., Mueller, D. K., Munn, M. D., Nolan, B. T., Puckett, L. J., Rupert, M. G., Short, T. M., Spahr, N. E., Sprague, L. A. (2010). Nutrients in the Nation ’ s Streams and Groundwater , 1992 – 2004 National Water-Quality Assessment Program Circular 1350. In U.S. Geological Survey Circular 1350.
- Duiker, S. W., and Beegle, D. B. (2006). Soil fertility distributions in long-term no-till, chisel/disk and moldboard plow/disk systems. *Soil and Tillage Research*, 88 (1–2), 30–41.
<https://doi.org/10.1016/j.still.2005.04.004>
- Duncan, E. W., King, K. W., Williams, M. R., LaBarge, G. A., Pease, L. A., Smith, D. R., and Fausey, N. R. (2017). Linking Soil Phosphorus to Dissolved Phosphorus Losses in the Midwest. *AEL*, 2(1), 0. <https://doi.org/10.2134/ael2017.02.0004>
- Eghball, B., and Gilley, J. E. (2001). Phosphorus risk assessment index evaluation using runoff measurements. *Journal of Soil and Water Conservation*, 56 (3), 202–206. Retrieved from <http://www.scopus.com/inward/record.url?eid=2-s2.0-0035672646&partnerID=40&md5=faebe1d27de636c546a182f16a86c7d6>

- Ehteshami, M., Farahani, N. D., and Tavassoli, S. (2016). Simulation of nitrate contamination in groundwater using artificial neural networks. *Modeling Earth Systems and Environment*, 2 (1), 1–10. <https://doi.org/10.1007/s40808-016-0080-3>
- Fiorellino, N. M., McGrath, J. M., Vadas, P. A., Bolster, C. H., and Coale, F. J. (2017). Use of Annual Phosphorus Loss Estimator (APLE) Model to Evaluate a Phosphorus Index. *Journal of Environment Quality*, 46 (6), 1380. <https://doi.org/10.2134/jeq2016.05.0203>
- Fletcher D, G. E. (1993). Forecasting with neural networks: an application using bankruptcy data. *Inf Manage*, (24), 159–167.
- Garson, G. D. (1991). Interpreting neural-network connection weights. *AI Expert*, (6), 46–51.
- Gburek, W. J., Drungil, C. C., Srinivasan, M. S., Needelman, B. A., and Woodward, D. E. (2002). Variable-source-area controls on phosphorus transport: bridging the gap between research and design. *Journal of Soil and Water Conservation*, 57 (6), 534–543.
- Gburek, W. J., Sharpley, A. N., Heathwaite, L., and Folmar, G. J. (2000). Phosphorus management at the watershed scale: a modification of the phosphorus index. *Journal of Environment Quality*, 29, 130–144. <https://doi.org/10.2134/jeq2000.00472425002900010017x>
- Gburek, William J., and Sharpley, A. N. (1998). Hydrologic Controls on Phosphorus Loss from Upland Agricultural Watersheds. *Journal of Environment Quality*, 27 (2), 267. <https://doi.org/10.2134/jeq1998.00472425002700020005x>
- Giam, X., and Olden, J. D. (2015). A new R2-based metric to shed greater insight on variable importance in artificial neural networks. *Ecological Modelling*, 313, 307–313. <https://doi.org/10.1016/j.ecolmodel.2015.06.034>
- Gopal, S., Patro, K., & Kumar, K. (2015). Normalization: A Preprocessing Stage. Retrieved from <https://arxiv.org/ftp/arxiv/papers/1503/1503.06462.pdf>
- Grahovac, J., Jokić, A., Dodić, J., Vučurović, D., & Dodić, S. (2016). Modelling and prediction of bioethanol production from intermediates and byproduct of sugar beet processing using neural networks. *Renewable Energy*, 85, 953–958. <https://doi.org/10.1016/j.renene.2015.07.054>
- Guo, T., Mehan, S., Gitau, M. W., Wang, Q., Kuczek, T., & Flanagan, D. C. (2018). Impact of number of realizations on the suitability of simulated weather data for hydrologic and environmental applications. *Stochastic Environmental Research and Risk Assessment*,

- 32(8), 2405–2421. <https://doi.org/10.1007/s00477-017-1498-5>
- Hecht-Nielsen, R. (1989). Theory of the Backpropagation Neural Network-Based on “non-indent” by Robert Hecht-Nielsen, which appeared in Proceedings of the International Joint Conference on Neural Networks 1, 593–611, June 1989. © 1989 IEEE. In Neural Networks for Perception. <https://doi.org/10.1016/b978-0-12-741252-8.50010-8>
- Hernandez-Ramirez, G., Brouder, S. M., Smith, D. R., & Van Scoyoc, G. E. (2011). Nitrogen partitioning and utilization in corn cropping systems: Rotation, N source, and N timing. *European Journal of Agronomy*, 34 (3), 190–195. <https://doi.org/10.1016/j.eja.2010.12.002>
- IN-NRCS. (2013). Indiana Nutrient and Sediment Transport Risk Assessment Tool (NASTRAT).https://efotg.sc.egov.usda.gov/references/public/IN/Indiana_Nutrient_and_Sediment_Transport_Risk_Assessment_Tool.pdf.
- Indiana NRCS FOTG. 2013. Conservation practice standard - Nutrient management. https://efotg.sc.egov.usda.gov/references/public/IN/590_Nutrient_Management.pdf
- Jarvie, H. P., Johnson, L. T., Sharpley, A. N., Smith, D. R., Baker, D. B., Bruulsema, T. W., and Confesor, R. (2017). Increased soluble phosphorus loads to lake erie: unintended consequences of conservation practices? *Journal of Environment Quality*, 46 (1), 123. <https://doi.org/10.2134/jeq2016.07.0248>
- Joern, Brad C. and Brichford, S. L. (2003). Calculating Manure and Manure Nutrient Application Rates. Retrieved January 21, 2019, from Agronomy Guide Purdue University Extension Service website: <https://www.extension.purdue.edu/extmedia/AY/AY-277.html>
- Kaluli, J. W., Madramootoo, C. A., and Djebbar, Y. (1998). Modeling nitrate leaching using neural networks. *Water Science and Technology*, 38 (7 pt 6), 127–134. [https://doi.org/10.1016/S0273-1223\(98\)00614-3](https://doi.org/10.1016/S0273-1223(98)00614-3)
- Khalil, B., Ouarda, T. B. M. J., and St-Hilaire, A. (2011). Estimation of water quality characteristics at ungauged sites using artificial neural networks and canonical correlation analysis. *Journal of Hydrology*, 405 (3–4), 277–287. <https://doi.org/10.1016/j.jhydrol.2011.05.024>
- Kim, M., and Gilley, J. E. (2008). Artificial neural network estimation of soil erosion and nutrient concentrations in runoff from land application areas. *Computers and Electronics in Agriculture*, 64 (2), 268–275. <https://doi.org/10.1016/j.compag.2008.05.021>
- Kim, R. J., Loucks, D. P., and Stedinger, J. R. (2012). Artificial neural network models of

- watershed nutrient loading. *Water Resources Management*, 26(10), 2781–2797.
<https://doi.org/10.1007/s11269-012-0045-x>
- King, K.W., Williams, M.R., Smith, D.R., LaBarge, G.A., Reutter, J.M., Duncan, E.W., Pease, L.A., and Fausey, N. R. (2017). Directionally correct practices to address agricultural phosphorus loss in artificially drained landscapes. *Journal of Soil and Water Conservation*, 73(1), 38–50.
- King, K. W., Williams, M. R., LaBarge, G. A., Smith, D. R., Reutter, J. M., Duncan, E. W., and Pease, L. A. (2018). Addressing agricultural phosphorus loss in artificially drained landscapes with 4R nutrient management practices. *Journal of Soil and Water Conservation*, 73 (1), 35–47. <https://doi.org/10.2489/jswc.73.1.35>
- Kleinman, P. J. A., Sharpley, A. N., McDowell, R. W., Flaten, D. N., Buda, A. R., Tao, L., and Zhu, Q. (2011). Managing agricultural phosphorus for water quality protection: Principles for progress. *Plant and Soil*, 349 (1–2), 169–182. <https://doi.org/10.1007/s11104-011-0832-9>
- Lallahem, S., and Hani, A. (2017). Artificial neural networks for defining the water quality determinants of groundwater abstraction in coastal aquifer. *AIP Conference Proceedings*, 1814 (February 2017). <https://doi.org/10.1063/1.4976232>
- Lallahem, S., and Mania, J. (2003). A nonlinear rainfall-runoff model using neural network technique: Example in fractured porous media. *Mathematical and Computer Modelling*, 37 (9–10), 1047–1061. [https://doi.org/10.1016/S0895-7177\(03\)00117-1](https://doi.org/10.1016/S0895-7177(03)00117-1)
- Lek, S., and Guegan, J. F. (1999a). Artificial neural networks as a tool in ecological modelling, an introduction. 120, 1–9. Retrieved from papers2://publication/uuid/3E346E29-343B-4F88-819B-BC4BAF8AA6B1
- Lemunyon, J. L., and Gilbert, R. G. (1993). The concept and need for a phosphorus assessment tool. *Journal of Production Agriculture*, 6 (4), 483–486.
<https://doi.org/10.2134/jpa1993.0483>
- Liakos, K. G., Busato, P., Moshou, D., Pearson, S., and Bochtis, D. (2018). Machine learning in agriculture: A review. *Sensors (Switzerland)*, 18(8), 1–29.
<https://doi.org/10.3390/s18082674>
- Liu, Y., Starzyk, J. A., and Zhu, Z. (2007). Optimizing number of hidden neurons in neural networks. *Proceedings of the IASTED International Conference on Artificial Intelligence*

- and Applications, AIA 2007, 121–126.
- Marcus, A., Beck, W., & Beck, M. M. W. (2018). Package ‘ NeuralNetTools ’. <https://cran.r-project.org/web/packages/NeuralNetTools/NeuralNetTools.pdf>
- Nelson, N. O., and Shober, A. L. (2012). Evaluation of Phosphorus Indices after Twenty Years of Science and Development. (13), 1703–1710. <https://doi.org/10.2134/jeq2012.0342>
- Nelson, W. L. (1967). Nitrogen, phosphorus, and potassium - needs and balance for high yields. In ASA Special Publication number 9. Maximum Crop Yields - The Challenge, eds. D.A. Rohweder and S.E. Younts. 57-67. American Society of Agronomy.
- Nizeyimana, E. L., Petersen, G. W., Imhoff, M. L., Sinclair, H. R., Waltman, S. W., Reed-Margetan, D. S., and Russo, J. M. (2001). Assessing the Impact of Land Conversion to Urban Use on Soils with Different Productivity Levels in the USA. Soil Science Society of America Journal, 65, 391–402. <https://doi.org/10.2136/sssaj2001.652391x>
- Olden, J. D., and Jackson, D. A. (2002). Illuminating the “black box”: Understanding variable contributions in artificial neural networks. Ecological Modelling, 154, 135–150. [https://doi.org/10.1016/S0304-3800\(02\)00064-9](https://doi.org/10.1016/S0304-3800(02)00064-9)
- Olden, J. D., Lawler, J. J., and Poff, N. L. (2008). Machine learning methods without tears: A primer for ecologists. Quarterly Review of Biology, 83 (2), 171–193. <https://doi.org/10.1086/587826>
- Osmond, D. L., Cabrera, M. L., Feagley, S. E., Hardee, G. E., Mitchell, C. C., Mylavarapu, R. S., and Zhang, H. (2006). Comparing ratings of the southern phosphorus indices. Journal of Soil and Water Conservation, 61(6), 325–337.
- Osmond, D., Sharpley, A., Bolster, C., Cabrera, M., Feagley, S., Lee, B., and Zhang, H. (2012). Comparing phosphorus indices from twelve southern u.s. states against monitored phosphorus loads from six prior southern studies. Journal of Environment Quality, 41 (6), 1741. <https://doi.org/10.2134/jeq2012.0013>
- Peter J. A. Kleinman. (2017). The persistent environmental relevance of soil phosphorus sorption saturation. Current Pollution Reports, 3(2), 141–150. <https://doi.org/10.1007/s40726-017-0058-4>
- Pote, D.H., Daniel, T.C., Nichols, D.J., Moore, P.A., Sharpley, A.N., Miller, D.M., and Edwards, D. R. (1999). Seasonal and soil-drying effects on run-off phosphorus relationships to soil phosphorus. Soil Sci. Soc. Am. J., 63:1006–10. <https://doi.org/10.2136/sssaj1999.6341006x>

- R Core Team (2017). R: A language and environment for statistical computing. Retrieved from <https://www.r-project.org/>
- Reid, K., Schneider, K., and McConkey, B. (2018). Components of phosphorus loss from agricultural landscapes, and how to incorporate them into risk assessment tools. *Frontiers in Earth Science*, 6 (September), 1–15. <https://doi.org/10.3389/feart.2018.00135>
- Reid, D. K., Ball, B., and Zhang, T. Q. (2012). Accounting for the Risks of Phosphorus Losses through Tile Drains in a Phosphorus Index. *Journal of Environment Quality*, 41 (6), 1720. <https://doi.org/10.2134/jeq2012.0238>
- Ruark, M. D., Brouder, S. M., and Turco, R. F. (2009). Dissolved Organic Carbon Losses from Tile Drained Agroecosystems. *Journal of Environment Quality*, 38 (3), 1205. <https://doi.org/10.2134/jeq2008.0121>
- Salehi, F., Prasher, S. O., Amin, S., Madani, A., Jebelli, S. J., Ramaswamy, H. S., and Drury, C. F. (2000). Prediction of annual nitrate-n losses in drain outflows with artificial neural networks. *American Society of Agricultural Engineers*, 43(1987), 1137–1143.
- Schultz, A., Wieland, R., and Lutze, G. (2000). Neural networks in agroecological modelling - Stylish application or helpful tool? *Computers and Electronics in Agriculture*, 29 (1–2), 73–97. [https://doi.org/10.1016/S0168-1699\(00\)00137-X](https://doi.org/10.1016/S0168-1699(00)00137-X)
- Sharma, V., Negi, S. C., Rudra, R. P., and Yang, S. (2003). Neural networks for predicting nitrate-nitrogen in drainage water. *Agricultural Water Management*, 63 (3), 169–183. [https://doi.org/10.1016/S0378-3774\(03\)00159-8](https://doi.org/10.1016/S0378-3774(03)00159-8)
- Sharpley, A., C. Bolster, C. Conover, E. Dayton, J. Davis, Z. Easton, L. Good, C. Gross, P. Kleinman, A. Mallinaro, Moffitt, D., N. Nelson, L. Norfleet, D. Osmond, R. Parry, A. Thompson, P. Vadas., and M. W. (2013). Technical guidelines for assessing phosphorus indices,, representing Southern Cooperative Series bullutin 417. 81. Retrieved from <http://saaesd.ncsu.edu/docs/Assessing P Indices SERA17.pdf>
- Sharpley, Andrew N., Sims, J. T., Reddy, K. R., Chapra, S. C., Daniel, T. C., and Wedepohl, R. (1994). Managing agricultural phosphorus for protection of surface waters: issues and options. *Journal of Environment Quality*, 23 (3), 437. <https://doi.org/10.2134/jeq1994.00472425002300030006x>
- Sharpley, A., Beegle, D., Bolster, C., Good, L., Joern, B., Ketterings, Q., and Vadas, P. (2012). Phosphorus Indices: Why We Need to Take Stock of How We Are Doing. *Journal of*

- Environment Quality, 41 (6), 1711. <https://doi.org/10.2134/jeq2012.0040>
- Sharpley, A. N., McDowell, R. W., Weld, J. L., and Kleinman, P. J. A. (2001). Assessing site vulnerability to phosphorus loss in an agricultural watershed. *Journal of Environmental Quality*, 30 (6), 2026–2036.
- Sharpley, A. N., Weld, J. L., Beegle, D. B., Kleinman, P. J. A., Gburek, W. J., Moore, P. A., and Mullins, G. (2003). Development of phosphorus indices for nutrient management planning strategies in the United States. *Journal of Soil and Water Conservation*, 58 (3), 137–152. Retrieved from <http://www.scopus.com/inward/record.url?eid=2-s2.0-0141880335&partnerID=tZOtx3y1>
- Sharpley, A N, Weld, J. L., Beegle, D. B., Kleinman, P. J. A, Gburek, W. J., Moore, P. A, and Mullins, G. (2003). Development of phosphorus indices for nutrient management planning strategies in the United States. *Journal of Soil and Water Conservation*, 58(3), 137–152.
- Sharpley, Andrew N., Kleinman, P. J. A., Flaten, D. N., & Buda, A. R. (2011). Critical source area management of agricultural phosphorus: Experiences, challenges and opportunities. *Water Science and Technology*, 64 (4), 945–952. <https://doi.org/10.2166/wst.2011.712>
- Sims, J. T., Edwards, A. C., Schoumans, O. F., and Simard, R. R. (2000). Integrating soil phosphorus testing into environmentally based agricultural management practices. *Journal of Environmental Quality*, 29(1), 60–71. <https://doi.org/10.2134/jeq2000.00472425002900010008x>
- Sinshaw, T. A., Surbeck, C. Q., Yasarer, H., and Najjar, Y. (2019). Artificial neural network for prediction of total nitrogen and phosphorus in US lakes. *Journal of Environmental Engineering (United States)*, 145 (6), 1–11. [https://doi.org/10.1061/\(ASCE\)EE.1943-7870.0001528](https://doi.org/10.1061/(ASCE)EE.1943-7870.0001528)
- Smith, D. R., King, K. W., and Williams, M. R. (2015). What is causing the harmful algal blooms in Lake Erie? *Journal of Soil and Water Conservation*, 70 (2), 27A-29A. <https://doi.org/10.2489/jswc.70.2.27A>
- Smith, D. R., Owens, P. R., Leytem, A. B., and Warnemuende, E. A. (2007). Nutrient losses from manure and fertilizer applications as impacted by time to first runoff event. *Environmental Pollution*, 147 (1), 131–137. <https://doi.org/10.1016/j.envpol.2006.08.021>
- Smith, D.R., Wilson, R. S., King, K. W., Zwonitzer, M., McGrath, J. M., Harmel, R. D., and Johnson, L. T. (2018). Lake Erie, phosphorus, and microcystin: Is it really the farmer's

- fault? *Journal of Soil and Water Conservation*, 73 (1), 48–57.
<https://doi.org/10.2489/jswc.73.1.48>
- Smith, D. R., Harmel, R. D., Williams, M., Haney, R., and King, K. W. (2016). Managing Acute Phosphorus Loss with Fertilizer Source and Placement: Proof of Concept. *Ael*, 1(1), 0.
<https://doi.org/10.2134/ael2015.12.0015>
- Sonmez, O., Pierzynski, G. M., Janssen, K. A., Frees, L., Davis, B., Leikam, D., and Sweeney, D. W. (2009). A field-based assessment tool for phosphorus losses in runoff in Kansas. *Journal of Soil and Water Conservation*, 64 (3), 212–222.
<https://doi.org/10.2489/jswc.64.3.212>
- Svozil, D., Kvasnicka, V., and Pospichal, J. (1997). Introduction to multi-layer feed-forward neural networks. *CHemometrics and Intelligent Laboratory Systems*, 39, 43–62.
- Toth, J. D., Dou, Z., Ferguson, J. D., Galligan, D. T., and Ramberg, C. F. (2006). Nitrogen- vs. phosphorus-based dairy manure applications to field crops. *Journal of Environment Quality*, 35 (6), 2302. <https://doi.org/10.2134/jeq2005.0479>
- USDA -NRCS. (2015). 2015 National Resources Inventory. Retrieved May 5, 2019, from Natural Resources Conservation Service, Washington, DC. 31 October 2018 website: http://www.nrcs.usda.gov/Internet/NRCS_RCA/reports/nri_eros_in.html
- Vitosh, M.L., Johnson, J.W., Mengel, D. B. (1995). Tri-state Fertilizer Recommendations for Corn, Soybeans, Wheat and Alfalfa. Extension Bulletin E-2567 (New), (July), 1–4.
- Welikhe, P., Brouder, S. M., Volenec, J. J., Gitau, M., and Turco, R. F. (2020). Development and Evaluation of Phosphorus Sorption Capacity- based Environmental Indices. *Journal of Environmental Quality* <https://doi.org/10.1002/jeq2.20044>
- Wright, M. N., Suling, M., Mueller, S. M., and Wright, M. M. N. (2019). Package ‘neuralnet.’ <https://cran.r-project.org/web/packages/neuralnet/neuralnet.pdf>
- Wu, M. L., Wang, Y. S., and Gu, J. D. (2015). Assessment for water quality by artificial neural network in Daya Bay, South China Sea. *Ecotoxicology*, 24 (7–8), 1632–1642.
<https://doi.org/10.1007/s10646-015-1453-5>
- Yang, C., Na, J., Li, G., Li, Y., and Zhong, J. (2018). Neural network for complex systems: theory and applications. *Complexity*, 2018 (Dc), 1–2. <https://doi.org/10.1155/2018/3141805>
- Zhang, G., Hu, M. Y., Patuwo, B. E., and Indro, D. C. (1999). Artificial neural networks in bankruptcy prediction: general framework and cross-validation analysis. *European Journal*

- of Operational Research, 116 (1), 16–32. [https://doi.org/10.1016/S0377-2217\(98\)00051-4](https://doi.org/10.1016/S0377-2217(98)00051-4)
- Zheng, H., Yang, Z., Liu, W., Liang, J., and Li, Y. (2015). Improving deep neural networks using softplus units. Proceedings of the International Joint Conference on Neural Networks, 2015-Sept, 1–4. <https://doi.org/10.1109/IJCNN.2015.7280459>
- Zheng, Z. Y., Guo, X. N., Zhu, K. X., Peng, W., & Zhou, H. M. (2017). Artificial neural network – Genetic algorithm to optimize wheat germ fermentation condition: Application to the production of two anti-tumor benzoquinones. Food Chemistry, 227, 264–270. <https://doi.org/10.1016/j.foodchem.2017.01.077>
- Zhou, B., Vogt, R. D., Lu, X., & Xu, C. (2015). *Relative Importance Analysis of a Refined Multi-parameter Phosphorus Index Employed in a Strongly Agriculturally Influenced Watershed*. *Relative Importance Analysis of a Refined Multi-parameter Phosphorus Index Employed in a Strongly Agriculturally Influenc.* (March), 0–13. <https://doi.org/10.1007/s11270-014-2218-0>

4 DYNAMICS OF DISSOLVED REACTIVE PHOSPHORUS LOSS FROM PHOSPHORUS SOURCE AND SINK SOILS IN TILE-DRAINED SYSTEMS

4.1 Abstract

Understanding the processes controlling dissolved reactive phosphorus (DRP) loss in tile-drained systems is essential to better define critical source areas and inform nutrient and conservation practice recommendations. Concentration – discharge (C-Q) relationships have been used to infer solute sources, reactivity, proximity, and transport mechanisms governing solute fluxes. This study examined DRP C-Q relationships in phosphorus (P) source and P sink soils in an in-field laboratory where tile discharge from a hydrologically isolated soil volume is monitored daily. Our objective was to compare DRP loads and flow-weighted mean DRP (FDRP) concentrations in P source and sink soils and evaluate the predominant DRP C-Q behavior in these soils. At the daily scale, C-Q patterns were linked to the soil P status whereby, a chemostatic ($b = 1$) and dilution ($b < 1$) behavior was observed for P source and P sink soils, respectively. At the event scale, C-Q patterns were linked to soil P status, flow path connectivity, and mixing of event water, matrix water, and shallow groundwater. Source DRP events had variable hysteretic behavior with 21%, 7%, 6%, 9% and 15% exhibiting anticlockwise with dilution, anticlockwise with flushing, clockwise with dilution, clockwise with flushing, and no hysteresis behavior, respectively. These variable C-Q responses suggest that, in addition to discharge and soil P status, rapid exchanges between P pools, the magnitude of discharge events (Q), and the relative number of days to discharge peak (RL), also regulated solute delivery. On the other hand, the predominant non-hysteretic C-Q behavior in sink DRP events (67%), suggests that DRP loss from these soils can be discounted. Our results highlight the need for nutrient and conservation practices addressing P draw down, P sequestration, and P supply according to crop need, which will likely be required to convert P sources to sinks and to avoid the conversion of P sinks to sources.

4.2 Introduction

Phosphorus (P) is an essential element required for the growth of all living things, a role that has been exploited in crop production over the years. Leaching losses of dissolved reactive P (DRP), the biologically active orthophosphate fraction that passes through a 0.45 μm filter (Pote and Daniel, 2000), was historically discounted because of its rapid adsorption onto soil surfaces (Logan et al., 1980; Madison et al., 2014). However, recent studies have established leaching as a significant pathway for DRP losses to surface water especially in tile-drained fields with long-term, repeated phosphorus (P) applications (Gentry et al., 2007; Kinley et al., 2007; Sims et al., 1998). In poorly drained soils, tile-drained systems have significantly altered hydrology compared to naturally drained systems. Tile-drains lower water tables, reduce surface runoff, increase subsurface drainage, and consequently greatly impact the fate and transport of nutrients from drained agricultural fields (Radcliffe et al., 2015; King et al., 2015). In many watersheds in the Midwest United States and Canada, tile discharge constitutes approximately 50% of the streamflow. For example, King et al. (2014) found that tile discharge contributed 47% of annual watershed discharge in Ohio, and Macrae et al. (2007) reported that approximately 42% of annual watershed discharge in Ontario, Canada, originated from tile discharge. In these watersheds, the elevated levels of DRP in surface water links closely to the magnitude of tile discharge (King et al., 2014; Macrae et al., 2007). Indeed, studies have found that in some settings, tile drains exported equal amounts or more DRP loads as surface runoff. For example, Ruark et al. (2012) reported that in Wisconsin tiles supplied 16 to 58% of dissolved P loads. Similar elevated DRP loads from tile drains have been reported in other sites across North America and Europe (Gentry et al., 2007; Macrae et al., 2007; Gelbrecht et al., 2005).

These high DRP concentrations are often measured in tile discharge (Welikhe et al., 2020) despite the existing high P sorption capacity of subsoils (Djodjic et al., 2006). Phosphorus rich surface soils have been identified as the primary source of P to tile drains. For instance, Welikhe et al. (2020) showed that after a soil's P saturation ratio (PSR) exceeds a PSR threshold of 0.24 (i.e. attains solid phase P saturation), there was an 8-fold greater risk of DRP loss to tile discharge. Also, previous work (Uusitalo et al., 2001; Djodjic et al. 1999) using cesium-137 and phosphorus-33 isotopes, reported that elevated DRP concentrations in tile discharge originated from P-rich surface soils. The coincidence between elevated DRP concentrations and peak event water (new water) contribution to tile discharge, especially in no-till fields, suggests that the primary pathway

for DRP from surface soils to tile drains, is via macropore (preferential) flow pathways (Williams et al., 2016; Vidon and Cuadra, 2011; Simard et al., 2000). Further, Williams et al. (2016) hypothesized that P source soils could function as labile sources of P much like surface-applied P, resulting in DRP loss to tile drains throughout the year. Nevertheless, despite these studies highlighting the role of P soil status and macropore flow pathways on DRP export in tile-drained systems, no study has quantified DRP losses in tile discharge from P saturated (source) and P (unsaturated) sink soils and assessed the dynamics of DRP loss during discharge events. Therefore, understanding when and how DRP is being exported at the field scale from soils with different P status is critical for efficient decision making.

As nutrient concentrations exhibit varying responses to changing discharge rates (Godsey et al., 2009), previous studies have successfully used concentration (C) – discharge (Q) relationships to unravel active solute source areas and transport pathways in watersheds (Rose et al., 2018; Duncan et al. 2017; Bowes et al. 2015; Bende-Michl et al., 2013). Pioneer work by Johnson et al. (1969) on stream water chemistry, provides the framework for C-Q data analysis using power law fits i.e. $L = aQ^b$ (where, L = flux/load of solute or sediment, Q = discharge flow rate, and b = slope of $\log(L) - \log(Q)$ linear regression). The authors showed that the C-Q relationships can be classified as chemodynamic or chemostatic, depending on whether there is a significant or negligible variation in concentration, respectively, relative to discharge variation (Godsey et al., 2009; Rose et al., 2018). Large solute reservoirs associated with dissolution of geologic materials, and/ or anthropogenic-sourced solutes e.g. legacy stores of nitrate and phosphorus, linked to long-term, repeated land applications, are hypothesized to generate chemostatic C-Q relationships (Godsey et al. 2009; Basu et al. 2010; Thompson et al. 2011; Diamond, 2013). On the other hand, flushing C-Q behavior is observed when solute or particulate concentrations increase with discharge ($b > 1$), whereas a dilution C-Q behavior is observed when solute or particulate concentrations decrease with increasing discharge ($b < 1$) (Godsey et al., 2009; Bieroza et al., 2018).

One factor that causes the large dispersion in C-Q plots, is the presence of hysteresis due to existing source and transport limitations (Minaudo et al., 2019). These hysteretic patterns have been identified through visual inspection of graphical plots or through the use of metrics and indices that characterize and quantify hysteretic responses (Butturini et al., 2008; Lawler et al., 2006; Lloyd et al., 2016a; Lloyd et al., 2016b; Duncan et al. 2017). By classifying these C-Q

hysteretic patterns and their succession, studies gained additional information on processes controlling solute transport to streams. A study by Williams (1989) on hysteresis patterns of suspended sediment, was one of the first studies which outlined the most common shapes for hysteresis loops and provided possible explanations for their occurrence. The author classified the loops into five classes. The first class was described as a single-valued straight line, suggesting that sediment concentrations and discharge were synchronized. This shape could occur when sediment concentrations were plentiful. Class two was a clockwise loop, where peak sediment concentrations occur on the rising hydrograph limb. This shape suggests exhaustible sediment supply. On the other hand, Class three was an anticlockwise loop, where sediment peak concentrations lag discharge peak (i.e. solute concentrations are higher on the falling versus the rising hydrograph limb). This shape suggests differing transit times of sediment and water. Class four, was a mix of classes one and two i.e. a straight-line plus a loop which results from a change in C-Q relationship during a storm event possibly due to changes in sediment availability, storage, and transport. Class five was also a combination of class two and three resulting in loops with a figure-of-eight configuration. This shift in loop shape was also possibly caused by a shift in the relationship between discharge and sediment concentrations. Recent studies have further added possible explanations for the different loop shapes observed. For example, clockwise hysteresis could also suggest rapid mobilization, proximal sources to the stream, whereas anticlockwise hysteresis could also suggest transport-limited systems, distal solute sources, or an eventual mix of solute contributions from early, low concentration sources, and late, high concentration sources (Chanat et al., 2002; Bowes et al. 2005; Bieroza and Heathwaite, 2015; Vaughan et al., 2017).

In this study, nutrient and tile discharge data (daily resolution) collected over a 3-year period from tile-drained experiment plots were analyzed using both the power law and hysteresis indices to determine the daily and event scale C-Q behavior of DRP. Only no-till plots were considered in this study because tillage has been shown to disrupt macropore flow (Jarvis, 2007), which is the major flow pathway for DRP to tile drains especially in fine-textured soils (Beauchemin et al., 1998). Soil P storage capacity (SPSC) representing the soil P status determined in a previous study on the same study site (Welikhe et al., 2020), was used to designate field plots as P sources or P sinks. The overall goal of this study was to quantify DRP losses from P source and P sink soils to tile drain waters and assess patterns of loss as a function of discharge. Specific objectives include: (i) determination of DRP loads and flow-weighted mean DRP (FWDRP)

concentrations from P source and sink soils at an annual and event-based time scale, and (ii) evaluate the predominant C-Q responses of DRP from P source and sink soils in tile discharge.

4.3 Materials and Methods

4.3.1 Site description and nutrient management

The study was conducted between 1 Oct 2010 and 30 Sept 2013 (3-water years i.e. water year 2011, 2012, and 2013, each beginning on 1 October and ending on 30 September) at the Water Quality Field Station (WQFS), Purdue University. The predominant soil series at the site is Drummer silty clay loam with a small area (<2%) of Raub silty clay loam. Slopes range from 0 to 2%. At the WQFS, forty-eight treatments are arranged in a randomized complete-block design, with twelve treatments per block. The treatments consist of one native prairie mixture and eleven treatments representing common cropping systems in the Midwest United States. Of the twelve treatments, three treatments i.e. *Miscanthus x giganteus* (Mxg), continuous maize with residue removal (CM-RR), and switchgrass variety Shawnee (Switch), respectively, were considered in this study (Table 4.1). These treatments were not tilled before and during the monitoring period and had various P applications over the years. Since 1997, treatment CM-RR received approximately 10-gal acre⁻¹ of liquid starter fertilizer (17-17-0 [17% (w/w) N and 17% (w/w) P₂O₅] in 1997 and 19-17-0 [17% (w/w) N and 17% (w/w) P₂O₅] every year after) supplying 16 kg P₂O₅ with all maize plantings. Also, in April 2012, replicates in the treatment received 43 kg P₂O₅ ha⁻¹ from a 0-45-0 fertilizer application. Similar liquid starter fertilizer applications were done with all maize plantings in treatment Mxg and Switch from 1997 to 2008 and 2007, respectively, before the treatment plots were replaced with current treatments of miscanthus and switchgrass (Table 4.1). We note that at the WQFS, all commercial P fertilizer applications are based on Purdue University recommended rates that are dependent on soil test P levels (Vitosh et al., 1995).

Table 4.1. A brief description of no-till treatments at the Water Quality Field Station (WQFS) treatments (abbreviations and year of establishment, previous treatments (cropping systems and N rates) dating back to 1997, and P, N, and tillage management

Current treatment (abbrev./yr.est.)	Plot	Previous treatment (maize N rate, kg ha⁻¹ yr⁻¹)	Current N management (annual rate, kg ha⁻¹ yr⁻¹)	P management (Cumulative P₂O₅ applied 1997 - 2013; kg ha⁻¹)	Tillage practices
<i>Miscanthus x giganteus</i> (Mxg /2008)	11, 22, 32, 43	Annual soybean-maize rotation (180-P)	Spring broadcast urea (56)	Commercial fertilizer based on STP (265) + starter (272)	No till since 2008
Continuous maize w/residue removal (CM-RR /2008)	12, 23, 30, 46	Continuous maize w/ residue return (202-P)	Preplant UAN (180) + starter	Commercial fertilizer based on STP (180) + starter (80)	No till since 2008
Switchgrass var. Shawnee (Switch /2007)	10, 18, 26, 44	Annual soybean-maize rotation (180-P)	Spring broadcast urea (56)	Commercial fertilizer based on STP (180) + starter (80)	No till since 2007

4.3.2 Soils data

The values for Soil P storage capacity (SPSC) used in this study were determined (Equation 1) and reported by Welikhe et al. (2020) as follows;

$$SPSC = (d0 - PSR) \times PSC_{Est} \quad [\text{Eq. 11}]$$

where, $d0$ is a change-point PSR value of 0.21), PSR is an individual soil's P saturation ratio, and PSC_{Est} is a pedotransfer function used to accurately estimate a soil's P sorption capacity. Detailed descriptions of the determination of $d0$, PSR, PSC_{Est} , and chemical characterization of samples are available in Welikhe et al. (2020). The SPSC values range from negative to positive, where negative and positive values are estimates of loosely (easily desorbed) and firmly held legacy P in soils, respectively (Nair et al., 2015; Nair and Harris, 2014; Welikhe et al., 2020). Therefore, individual replicate SPSC values, were used to identify a soil's P status. For the purpose of this study, plots considered were those which consistently had negative SPSC values (P saturated referred to as P source soils in this work) or consistent positive SPSC values (P unsaturated referred to as P sink soils in this work) throughout the monitoring period. Therefore, plot 46 and 18 were excluded from this analysis because their P status varied throughout the study period. Table 4.2

shows the SPSC values determined for the study plots by Welikhe et al. (2020). Based on their SPSC values, plot 10, 11, and 12, were classified as P source soils while, plots 26, 30, 32, 43, and 44, were classified as P sink soils.

Table 4.2. Soil P storage capacity (SPSC) for surface soils (20 cm) reported in Welikhe et al. (2020). Negative SPSC and positive SPSC values are associated with P source and P sink soils, respectively. 2011, 2012, and 2013 are water years e.g. 2011 water year begins on 1 Oct 2010 and ends on 30 Sept 2013. Refer to Table 1 for description of treatments.

Current treatment (abbrev./yr.est.)	Plot	2011	2012	2013
		SPSC (L kg ⁻¹)		
Miscanthus x giganteus (Mxg/2008)	11	-10.0	-5.1	-6.6
	32	35.0	41.0	41.8
	43	20.6	23.8	28.4
Continuous maize w/residue removal (CM-RR/2008)	12	-10.9	-18.3	-7.8
	30	30.7	26.9	0.4
Switchgrass var. Shawnee (Switch/2007)	10	-2.6	-1.3	-2.6
	26	12.9	28.0	32.8
	44	11.9	29.5	22.4

4.3.3 Flow and DRP concentration data collection

In each treatment plot at the WQFS (10.8 × 48 m), an in-ground drainage lysimeter (24 × 9 m) was constructed as a bottomless clay box to create a hydrologically isolated area from which drain-flow would be collected. Lysimeter walls were constructed with Bentonite slurry to a depth of 1.5 m. Two, parallel, plastic tiles (collection tile and companion tile), 0.1 m in diameter, were installed at a depth of 0.9 m in the longitudinal centers of the plots. The collection tile drains the areas within the lysimeter while the companion tile drains the areas outside the lysimeter. The companion tile drains into a nearby drainage ditch while the collection tile drains into instrument huts where stainless steel tipping buckets are positioned at the end of the drains to measure hourly discharge volumes. The tipping buckets are fitted with a magnetic sensor switch to count the number of tips that are recorded by data loggers and summarized by the hour. The hourly tip counts were converted to discharge volumes using calibration values unique to each tipping bucket. Hourly discharge data were aggregated from noon to noon to create daily discharge data. A

statistical protocol and decision rule developed by Trybula (2012), was used to identify and eliminate non-functioning tiles from further analysis. Based on these criteria, tile 22 and 23 were eliminated from the rest of the study.

To best correspond with daily discharge volumes, 24-hr flow-proportional discharge water quality samples were collected whenever drain discharge occurred. Once retrieved, the water samples were immediately transported to the laboratory, filtered (0.45 μm filter), and filtrate DRP (orthophosphate) concentrations were analyzed colorimetrically by the Murphy and Riley (1962) procedure using a SEAL AQ2 auto-analyzer method EPA-118-A Rev.5 (equivalent to USEPA method 365.1, Rev.2.0) (Seal Analytical, 2004). Any samples not analyzed within 24 hours, were frozen. All discharge and corresponding DRP concentration data are archived in the Purdue University Research Repository (PURR). The data on daily tile discharge and DRP concentrations used for this study were retrieved from PURR and rectified by Welikhe et al. (2020). For a detailed description of flow processing, gap-filling of missing DRP values, handling of flow and DRP outliers, days with flooding, rainfall, and tile drain efficiencies, see Welikhe et al. (2020). In this study, missing daily discharge data was not gap filled. A summary of the number of missing days is presented in Table 4.3.

Table 4.3. The number of days with missing flow data for tiles in the study plots. The percentage of number of days with missing data per water year is presented parenthetically.

Tile	Days with missing flow data		
	2011	2012	2013
10	59 (16)	0 (0)	48 (13)
11	59 (16)	0 (0)	48 (13)
12	59 (16)	0 (0)	48 (13)
26	60 (16)	0 (0)	128 (35)
30	60 (16)	0 (0)	128 (35)
32	0 (0)	0 (0)	41 (11)
43	1 (0.3)	0 (0)	44 (12)
44	1 (0.3)	0 (0)	44 (12)

4.3.4 Calculations and statistical analysis

All statistical analysis was performed in R 3.4.0. (R Core Team, 2017). For a given tile, DRP loads were determined by multiplying the DRP concentration by the respective daily

discharge volume. Daily DRP loads were summed for each tile on an annual (water year) and event basis. Flow-weighted DRP concentrations (FDRP) were calculated as the summed loads divided by the summed flow volumes on an annual and event basis. For our purposes, an event was defined as a composite sample with a total discharge (Q) ≥ 100 liters (0.1 m^3) per event. Linear regression analysis (lm function) was used to characterize C-Q relationships between drainflow and DRP flux. The C-Q relationship was determined across two-time scales: daily and event, for each of the surface soil types (P source and P sinks). For each time scale, data were log-transformed (logTransform function) before regression analysis to test C-Q relationships for P source and P sink soils. The linear regression model was converted into a simplified expression based on the log-transformed data:

$$L = aQ^b \quad [\text{Eq. 12}]$$

where L is solute flux (daily or event scale), Q the is discharge flow rate (daily or event scale), a is the intercept of the linear regression of the non log-transformed values of DRP flux and discharge, and b is the slope of the linear relationship between the log-transformed values of DRP flux and discharge at daily or event scales. Ninety-five percent confident intervals of b (slope) were determined (confint function) to test whether b was significantly different from 1. b values less than, equal to, and greater than 1 indicate solute dilution (decrease with discharge), no effect (chemostasis), and accretion (increase with discharge) by increasing drainflow rates, respectively.

4.3.5 Determination of C-Q hysteresis loops

As previously mentioned, this study used low resolution (daily) data. Therefore, for our purpose, the following criteria were used to select discharge events to consider during hysteresis analysis: (1) having complete daily C and Q data for the entire discharge event, (2) discharge events with ≥ 3 days of c and Q data, (3) discharge events that did not have more than one peak, and (4) discharge events with a peak tile discharge rate greater than $1 \text{ mm day}^{-1} \text{ ha}^{-1}$. General characteristics of drainage events (ED, event duration; Δt , days since the previous event; Q , total event discharge; Q_{\max} , peak event discharge; Q_{ave} , average event discharge; D_{rel} , relative length (days) of the rising limb ($D_{\text{rel}} = (\text{days of the rising limb of the hydrograph} / \text{days of the entire hydrograph}) \times 100$), were determined.

For each discharge event, the analysis of DRP concentrations (C) versus discharge (Q) relationships, was performed with the approach proposed by Butturini et al. (2006) and Butturini

et al. (2008). Two simple, semi-quantitative descriptors of solute behavior: ΔC and ΔR , were used to describe the shapes, rotational patterns, and trends of DRP hysteretic loops during individual discharge events. The ΔC quantifies the relative changes in solute concentrations at the onset of discharge and peak flow. The ΔC (%) is calculated as:

$$\Delta C (\%) = \frac{C_s - C_b}{C_{max}} \times 100 \quad [\text{Eq. 13}]$$

where C_b and C_s are DRP concentrations at base flow and at peak discharge, respectively, and C_{max} is the highest DRP concentration observed in the tile during a discharge event. To adapt this parameter to tile discharge with no base flow, we replaced C_b with C_i , which is the DRP concentration at the beginning of the discharge event. Therefore, the modified ΔC (ΔC_{new}) was calculated as:

$$\Delta C_{new} (\%) = \frac{C_s - C_i}{C_{max}} \times 100 \quad [\text{Eq. 14}]$$

ΔC ranges between -100 to 100%, where $\Delta C < -10\%$, $-10\% \leq \Delta C \leq 10\%$, and $\Delta C > 10\%$, represent, solute dilution, neutral, and solute flushing, respectively (Butturini et al., 2008). A flushing solute trend is observed when solute concentrations increase with discharge ($b > 1$), whereas a dilution solute trend is observed when solute concentrations decrease with discharge ($b < 1$) (Godsey et al., 2009; Maher, 2011; Vaughan et al., 2017; Hoagland et al., 2017). The minimum ΔC i.e. -100%, is observed when $C_s = 0$ and $C_i = C_{max}$ while, the maximum ΔC i.e. 100% is observed when $C_s = C_{max}$ and $C_i = 0$.

The ΔR parameter (Equation 5) integrates information about the rotational pattern (R), and the area (A_h) of the C-Q loop.

$$\Delta R (\%) = (A_h \times R) \times 100 \quad [\text{Eq. 15}]$$

The A_h was determined (polyarea function), after standardizing discharge and concentrations values to a unity scale. An A_h value closer to zero suggests that the relationship pattern is more linear i.e. the concentrations in the rising limb are equal to the concentrations in the falling limb for the same discharge. When A_h value is closer to one, the area of the hysteresis loop is large and the concentrations in the rising and falling limb are different. R represents the rotational pattern of the C-Q hysteresis loop. If the hysteresis loop is clockwise, then $R = 1$, if anticklockwise, $R = -1$, and if there is no hysteresis or there is an unclear hysteresis (e.g. figure-

of-eight-shaped loops), $R = 0$. The ΔR also ranges between -100 to 100% where $\Delta R < -10\%$, $-10\% \leq \Delta R \leq 10\%$, and $\Delta R > 10\%$, represent, anticlockwise loop, no loop, and clockwise loop, respectively (Butturini et al., 2008). Clockwise hysteresis (i.e. higher solute concentrations on the rising versus the falling hydrograph limb), suggests an exhaustible solute supply (source-limited) from a proximal source or intense discharge, whereas anticlockwise hysteresis (i.e. solute concentrations are higher at the peak or on the falling versus the rising hydrograph limb) suggests transport-limited systems, distal solute sources, or sources that are in deeper subsurface zones. The relationship between the two hysteresis parameters and the recorded general discharge characteristics was analyzed using Pearson correlation analysis, to determine the controlling factors that influence DRP hysteresis in tile discharge at the event scale.

Finally, the variability of the two parameters (ΔC_{new} (%) and ΔR (%)) was presented in a two-dimensional plot of ΔC_{new} (%) versus ΔR (%), in which four regions can be identified based on the solute trend (dilution or flushing) and the hysteresis loop rotation (clockwise or anticlockwise). More details on the two-dimensional plot can be found in Butturini et al. (2006) and Butturini et al., (2008).

4.4 Results and discussion

4.4.1 Annual DRP loads and FDRP concentrations

Across plots and years, annual DRP loads measured in tile discharge ranged from 0 to $0.0272 \text{ kg ha}^{-1}$ (Table 4.4). Also, in most instances, annual DRP loads from P source soils (plot 10, 11, and 12) were an order of magnitude higher than annual DRP loads from P sink soils (remaining plots) but, in some years, plot 26 and 43 had DRP loads as high as P source soils (Table 4.4).

Table 4.4. Annual (water year) dissolved reactive phosphorus (DRP) loads in tile discharge. Plots with negative SPSC values (P source soils) are in bold. Refer to Table 1 for description of treatments.

Current treatment (abbrev./yr.est.)	Plot	2011	2012	2013
		DRP (kg ha ⁻¹)		
Miscanthus x giganteus (Mxg/2008)	11	0.0115	0.0272	0.0250
	32	0.0014	0.0037	0.0016
	43	0.0064	0.0106	0.0071
Continuous maize w/residue removal (CM- RR/2008)	12	0.0075	0.0121	0.0125
	30	0.0011	0.0029	0.0024
Switchgrass var. Shawnee (Switch/2007)	10	0.0079	0.0171	0.0076
	26	0.0104	0.0187	0.0096
	44	0.0070	0.0079	0.0000

In general, these loads were low compared to annual tile loads reported in previous studies in the Midwest, USA. For example, Gentry et al. (2007) reported annual DRP loads of 0.05 to 1.01 kg ha⁻¹ from similar soils (mollisols) in Illinois. Nevertheless, nutrient loads lost from crop production systems are dependent on discharge (Williams et al., 2014), therefore a possible reason for the differences in DRP loads are the higher tile drain efficiencies (annual tile discharge to rainfall ratio) observed in Gentry et al. (2007).

Annual FDRP concentrations from the study plots ranged from 0.0015 to 0.0228 mg L⁻¹ (Table 4.5) These concentrations were also low compared to FDRP concentrations of 0.08 to 0.16 mg L⁻¹ and 0.058 to 0.231 mg L⁻¹, reported for corn-soybean rotations on a Bennington silt loam and a Pewamo clay loam in Ohio, and on mollisols in Illinois, respectively (King et al., 2015; Gentry et al., 2007). In both study sites (Ohio and Illinois), producers applied P fertilizers every other year with corn plantings maintain optimum Bray P1/Mehlich 3P soil test levels for crop growth (King et al., 2015; Gentry et al., 2007). Welikhe et al. (2020) showed that, P source soils were more prone to desorbing P and had a greater risk of losing DRP to the tile drains. However, since SPSC and soil test P levels were not reported in King et al. (2015) and Gentry et al. (2007), and direct comparisons between P status of soils in these studies versus the present study could not be made, it is very likely that the build-up and maintenance approach to P fertilizer recommendation turned the soils in the Ohio and Illinois studies into P sources as highlighted in Welikhe et al. (2020). Soil type is another possible reason for the differences in FDRP lost to tile

discharge. Pewamo clay loam is the major soil (~ 60%) in tile drain contributing areas in the Ohio study (King et al., 2015). Soils with high clay content have a greater risk of losing DRP to tile drains, due to their high tendency to develop preferential flow pathways (Simard et al., 2000), which could explain the higher FDRP losses in those soils.

Table 4.5. Annual (water year) flow-weighted dissolved reactive phosphorus (FDRP) in tile discharge. Plots with negative SPSC values (P source soils) are in bold. Concentration above which eutrophication is accelerated i.e. $> 0.02 \text{ mg P L}^{-1}$ (Correll, 1999)) are italicized. Refer to Table 1 for description of treatments.

Current treatment (abbrev./yr.est.)	Plot	2011	2012	2013
		FDRP (mg L^{-1})		
Miscanthus x giganteus (Mxg/2008)	11	0.0056	0.0228	0.0219
	32	0.0015	0.0062	0.0028
	43	0.0017	0.0056	0.0043
Continuous maize w/residue removal (CM- RR/2008)	12	0.0045	0.0141	0.0178
	30	0.0018	0.0046	0.0056
Switchgrass var. Shawnee (Switch/2007)	10	0.0033	0.0130	0.0062
	26	0.0028	0.0081	0.0052
	44	0.0027	0.0062	0.0000

As expected, the P source soils in plot 10, 11, and 12, consistently lost higher FDRP concentrations throughout the monitoring period (Table 4.5). In the water year 2012 and 2013, FDRP concentrations $> 0.02 \text{ mg L}^{-1}$ were measured in tile discharge from plot 11. Correll, (1999) and Sharpley et al. (2003) reported that 0.02 mg P L^{-1} was the concentration above which eutrophication was accelerated. However, all annual FDRP concentrations were below USEPA's 0.05 mg P L^{-1} acceptable water quality limit (USEPA, 2002).

Accumulated P in soils becomes a water quality concern when there is active hydrology that mobilizes soil P and converts it from a crop nutrient resource to an offsite water pollutant (Sharpley et al. 2011). Because of the tile drains, all plots in the WQFS may be considered as hydrologically active and connected to surface waters. The labile legacy P in P source soils coupled with their hydrological connectivity turned these plots to critical source areas that need to be targeted during P management.

4.4.2 Discharge events: General description, DRP loads, and FDRP concentrations

Based on our discharge event criteria, a total of 75 events (30 on P source soils (plot 10, 11, and 12) and 45 on P sink soils (all other plots)) were selected (Table 4.6). Most of the events took place during fall (September 22 – 20 December), winter (December 21 – March 19), and spring (March 20 – June 20). During summer (June 21 – September 21), there was no discharge in most tiles except for tile 30, 43, and 44 in the summer of 2011. This discharge pattern is common in the region as a result of the interactions between precipitation, runoff, infiltration, and evapotranspiration (Gentry et al. 2007). Event discharge lasted an average of 3 or 4 days across tiles. Eight events lasted longer than the average duration (> 4 days per tile). The Q and Q_{\max} varied between 145 and 7993 L day⁻¹, and 77 and 4048 L day⁻¹. Across events, Q_{ave} ranged between 36 and 1995 L day⁻¹. Forty eight percent of the discharge events had D_{rel} values of 0%, indicating an abrupt rising limb. Previous studies in the region reported similar findings where tile discharge peaked early and abruptly during storm events (Gentry et al., 2000; Schilling et al., 2008). Table 4.6 summarises the main characteristics of all selected discharge events.

Table 4.6. General characteristics, DRP loads and FDRP concentrations, of the selected discharge events between October 2010 and September 2013[†]. FDRP concentrations > 0.02 mg L⁻¹ (concentration above which eutrophication is accelerated (Correll, 1999)) are italicized and in bold.

Plot no.	Water year (Oct 1 to Sept 30)	Event no.	Date	ED (days)	Δt (days)	Q (L event ⁻¹)	Q_{ave} (L day ⁻¹)	Q_{max} (L day ⁻¹)	D_{rel} (%)	DRP (kg ha ⁻¹)	FDRP (mg L ⁻¹)
10	2011	1	12/30 - 01/02	4	90	4106	1026	2431	0	0.0003	0.0017
10	2011	2	02/14 - 02/18	5	42	7086	1417	3030	40	0.0004	0.0012
10	2011	3	02/20 - 02/22	3	1	2984	995	2553	33	0.0002	0.0013
10	2011	4	02/27-03/01	3	4	4839	1613	4048	33	0.0004	0.0019
10	2011	5	03/04 - 03/07	4	2	4442	1111	4048	25	0.0005	0.0025
10	2011	6	03/09 - 03/11	3	1	3651	1217	3033	0	0.0005	0.0030
10	2011	7	04/26 - 04/29	4	2	7981	1995	4048	25	0.0025	0.0038
10	2012	8	12/04 - 12/06	3	2	2167	722	1477	33	0.0018	0.0176
10	2012	9	12/14 - 12/16	3	7	4991	1664	4048	33	0.0004	0.0002
10	2013	10	02/26 - 03/01	4	25	5763	1441	4048	0	0.0014	0.0051
10	2013	11	03/08 - 03/11	4	6	1417	354	724	50	0.0007	0.0102
Average				4						0.0008	0.0044

Table 4.6 continued

Plot no.	Water year (Oct 1 to Sept 30)	Event no.	Date	ED (days)	Δt (days)	Q (L event-1)	Qave (L day-1)	Qmax (L day-1)	Drel (%)	DRP (kg ha-1)	FDRP (mg L-1)
11	2011	1	12/30 - 01/01	3	90	1701	567	1503	0	0.0033	0.0420
11	2011	2	02/20 - 02/22	3	1	2195	732	1991	33	0.0003	0.0024
11	2011	3	02/27 - 03/01	3	1	3739	1246	3100	33	0.0004	0.0023
11	2011	4	03/04 - 03/07	4	2	3277	819	3100	25	0.0003	0.0024
11	2011	5	03/09 - 03/12	4	1	2686	671	2541	0	0.0004	0.0033
11	2011	6	03/15 - 03/17	3	2	1755	585	1641	0	0.0001	0.0010
11	2012	7	11/29 - 12/01	4	59	4495	1498	3100	0	0.0003	0.0015
11	2012	8	12/04 - 12/07	4	2	1625	406	1149	25	0.0028	0.0378
11	2012	9	12/14 - 12/16	3	6	3877	1292	3100	33	0.0001	0.0004
11	2012	10	12/30 - 01/01	3	8	753	251	465	0	0.0005	0.0153
11	2012	11	01/22 - 01/24	3	3	3120	1040	3100	33	0.0060	0.0418
11	2012	12	01/26 - 01/28	3	1	3249	1083	2607	0	0.0025	0.0168
11	2012	13	05/06 - 05/08	3	98	4805	1602	3100	33	0.0089	0.0401
11	2013	14	02/26 - 03/01	4	25	4459	1115	3100	0	0.0048	0.0233
Average				3						0.0022	0.0164
12	2011	1	03/15 - 03/17	3	2	1506	502	1052	0	0.0001	0.0014
12	2012	2	11/27 - 12/01	5	57	4485	897	2308	40	0.0035	0.0169
12	2012	3	12/04 - 12/06	3	2	638	213	436	33	0.0008	0.0255
12	2012	4	12/14 - 12/16	3	7	2586	862	2308	33	0.0001	0.0011
12	2012	5	12/30 - 01/01	3	8	489	163	236	33	0.0001	0.0047
12	2012	6	01/22 - 01/24	3	3	2415	805	2308	33	0.0019	0.0178
12	2012	7	01/26 - 01/28	3	1	3532	1177	1936	0	0.0019	0.0117
12	2012	8	05/06 - 05/08	3	98	1934	645	1867	33	0.0005	0.0051
Average				3						0.0011	0.0105
26	2011	1	12/29 - 01/02	5	89	7993	1599	3589	20	0.0005	0.0015
26	2011	2	03/15 - 03/18	4	2	4354	1089	3149	0	0.0003	0.0013
26	2011	3	06/20 - 06/22	3	3	2253	751	1207	0	0.0001	0.0014
26	2012	4	12/14 - 12/18	5	5	5527	1105	3589	20	0.0004	0.0014
26	2012	5	12/20 - 12/23	4	1	3144	786	1846	0	0.0002	0.0014
26	2012	6	12/30 - 01/02	4	6	3005	751	1550	0	0.0001	0.0008
26	2012	7	01/17 - 01/19	3	14	3990	1330	3589	0	0.0023	0.0126
26	2012	8	05/06 - 05/08	3	97	5043	1681	3589	33	0.0018	0.0075
26	2013	9	12/20 - 12/23	4	80	4305	1076	3331	0	0.0010	0.0049
26	2013	10	05/27 - 05/29	3	24	5317	1772	3589	0	0.0004	0.0014
26	2013	11	06/01 - 06/03	3	2	1039	346	562	33	0.0003	0.0063
Average				4						0.0007	0.0037

Table 4.6 continued

Plot no.	Water year (Oct 1 to Sept 30)	Event no.	Date	ED (days)	Δt (days)	Q (L event- 1)	Qave (L day-1)	Qmax (L day-1)	Drel (%)	DRP (kg ha-1)	FDRP (mg L- 1)
30	2011	1	12/30 - 01/01	3	90	944	315	917	0	0.0002	0.0047
30	2011	2	02/16 - 02/18	3	45	512	171	309	33	0.0000	0.0002
30	2011	3	04/26 - 04/28	3	2	1124	375	574	0	0.0002	0.0029
30	2011	4	06/20 - 06/22	3	3	2079	693	1449	33	0.0001	0.0014
30	2012	5	12/30 - 01/02	4	6	145	36	77	0	0.0000	0.0014
30	2012	6	01/17 - 01/19	3	14	414	138	392	0	0.0000	0.0048
30	2013	7	12/20 - 12/22	3	80	533	178	505	0	0.0003	0.0104
30	2013	8	02/26 - 03/05	8	25	1178	147	882	0	0.0004	0.0074
30	2013	9	05/27 - 05/29	3	24	2308	769	1509	0	0.0002	0.0014
30	2013	10	06/01 - 06/03	3	2	191	64	160	0	0.0004	0.0450
Average				4						0.0002	0.0080
32	2011	1	02/21 - 02/23	3	41	713	238	543	0	0.0001	0.0021
32	2011	2	02/28 - 03/02	3	4	1641	547	1444	0	0.0002	0.0022
32	2011	3	03/15 - 03/17	3	2	898	299	723	0	0.0000	0.0006
32	2012	4	11/28 - 12/01	4	58	2502	625	1444	25	0.0010	0.0090
32	2012	5	12/04 - 12/06	3	2	306	102	259	33	0.0002	0.0136
32	2012	6	12/14 - 12/16	3	7	1894	632	1444	33	0.0001	0.0007
32	2012	7	05/06 - 05/08	3	97	2935	978	1444	33	0.0005	0.0035
32	2013	8	02/26 - 03/03	6	25	3410	568	1444	0	0.0004	0.0027
32	2013	9	04/28 - 04/30	3	1	242	81	208	0	0.0000	0.0019
32	2013	10	05/27 - 05/29	3	26	2127	709	1444	0	0.0001	0.0014
Average				3						0.0003	0.0038
43	2011	1	12/30 - 01/03	5	33	4513	903	1825	20	0.0003	0.0014
43	2011	2	06/20 - 06/22	3	19	948	316	782	33	0.0001	0.0014
43	2012	3	12/04 - 12/07	4	1	3764	941	1875	25	0.0017	0.0096
43	2012	4	12/14 - 12/17	4	6	5317	1329	3554	25	0.0003	0.0014
43	2012	5	12/20 - 12/22	3	2	1593	531	941	0	0.0001	0.0014
43	2012	6	12/30 - 01/01	3	7	1923	641	972	33	0.0004	0.0041
43	2012	7	05/06 - 05/08	3	97	4993	1664	3554	0	0.0024	0.0105
43	2013	8	02/26 - 03/01	4	1	605	151	202	50	0.0001	0.0019
43	2013	9	03/09 - 03/11	3	7	2914	971	2119	33	0.0017	0.0125
Average				4						0.0008	0.0049

Table 4.6 continued

Plot no.	Water year (Oct 1 to Sept 30)	Event no.	Date	ED (days)	Δt (days)	Q (L event-1)	Q _{ave} (L day-1)	Q _{max} (L day-1)	D _{rel} (%)	DRP (kg ha-1)	FDRP (mg L-1)
44	2011	1	12/30 - 01/04	6	17	5366	894	2072	0	0.0003	0.0012
44	2011	2	06/20 - 06/22	3	19	2131	710	1561	33	0.0001	0.0014
44	2011	3	07/02 - 07/04	3	9	662	221	462	33	0.0000	0.0014
44	2012	4	11/22 - 11/24	3	6	1173	391	850	0	0.0008	0.0145
44	2012	5	12/30 - 01/02	4	5	1580	395	634	25	0.0001	0.0013
44	2012	6	01/17 - 01/19	3	14	2497	832	2072	0	0.0008	0.0068
Average				4						0.0004	0.0044

[†]ED, event duration; Δt , days since previous event; Q, total discharge; Q_{ave}, average event discharge; Q_{max}, peak event discharge; D_{rel}, relative length (days) of the rising limb; DRP, dissolved reactive phosphorus; FDRP, flow-weighted DRP concentrations.

Across all tiles, DRP loads and FDRP concentrations measured during selected discharge events ranged between 0 and 0.0089 kg P ha⁻¹ and 0.002 and 0.0401 mg P L⁻¹, respectively (Table 4.6). There was no distinct trend of loss for both DRP and FDRP in successive events in both P source and sink soils. However, when compared to P source soils, P sink soils had very low (some 0 kg ha⁻¹) event DRP loads (Table 4.6). Also, average FDRP concentrations from P source soils (with the exception of plot 10), were an order of magnitude higher than average FDRP concentrations from P sink soils (Table 4.6). The event FDRP concentrations were below USEPA's 0.05 mg L⁻¹ acceptable limit (USEPA, 2002), with a few events (7 events) having concentrations above the eutrophication acceleration limit 0.02 mg P L⁻¹ (Correll 1999; Sharpley et al., 2003).

4.4.3 C-Q relationships

The daily DRP flux from both P source and sink soils had a linear relationship with daily discharge when log-transformed ($R^2 = 0.61$ and $R^2 = 0.73$, respectively) (Figure 4.1a). The slope ($b = 0.93$) of the daily DRP – discharge relationship for source soils had a 95% confidence limit between 0.84 and 1.01, indicating that b was not significantly different from 1 and that DRP concentrations vary little compared to discharge (Figure 4.1a). According to Godsey et al. (2009), the observation of chemostasis implies that there is a mechanism at play in the catchment that is buffering variations in solute concentrations over a large range of discharge. Previous studies have shown that possible mechanisms include continuous weathering of bedrock for solutes such as magnesium, sodium, and calcium (Godsey et al. 2009), or the continuous release of legacy

nutrients (e.g. nitrates and phosphorus) in agricultural soils (Basu et al., 2010; Basu et al., 2011; Thompson et al., 2011). In Menezes-Blackburn et al. (2016), positive correlations ($r \geq 0.5$; $p \leq 0.01$) between P desorption rates and re-supply from solid phase with P concentrations in different tests (FeO strips, Olsen, oxalate, and NaOH-EDTA), suggested that P status was the main driver of P resupply from solid phase P into soil solution, and hence P bioavailability and lability. Sharpley et al. (1994) showed that these chronic transfer of DRP in runoff is symptomatic of long-term, repeated fertilizer and manure applications, which can lead to increases in solid phase P and ensuing desorption of solid phase P to runoff water. Thus, it is well-established that accumulated P in soils and DRP in surface and subsurface runoff are strongly tied (Vadas et al., 2005; Welikhe et al., 2020). In this study, soils classified as P source soils, were those with negative SPSC values. According to Nair et al. (2015), the magnitude of negative SPSC values are estimations of the loosely held legacy P stock in soils most prone to desorption into soil solution. Therefore, similar to other catchments with legacy nutrient stores, our source soils acted as mass stores that continually buffered DRP concentrations against changing discharge. The chemostatic behavior in P source soils, provides evidence to support Williams et al. (2016) hypothesis that P source soils could act as a source of labile P similar to surface-applied fertilizers, resulting in continuous delivery of DRP to tile drains throughout the year.

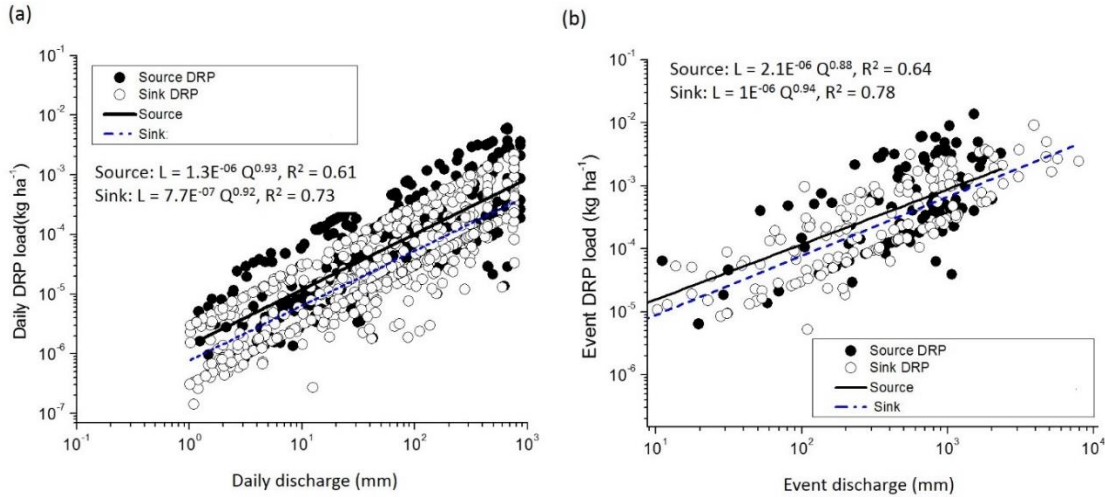


Figure 4.1. Relationship between (a) daily discharge (mm) and daily dissolved reactive phosphorus (DRP) flux (kg ha^{-1}) presented on a log-log scale, and (b) event discharge (mm) and event dissolved reactive phosphorus (DRP) flux (kg ha^{-1}) presented on a log-log scale. Exponent (b) and coefficient (a) values are defined by Equation 2, and R^2 values were determined by linear regression on log transformed DRP flux and discharge values. Source and sink DRP represent DRP fluxes measured from P saturated (source) and unsaturated (sink) soils.

The slope ($b = 0.92$) of the daily DRP – discharge relationship for sink soils had a 95% confidence limit between 0.87 and 0.96, indicating that b was significantly < 1 , and that lower DRP concentrations occurred in conjunction with high discharge totals (Figure 4.1a). However, the two slopes i.e. 0.93 and 0.92 of the daily DRP – discharge relationship for source and sink soils, respectively, were not significantly different (95% confidence limit between 0.88 and 0.96). Such a C-Q relationship suggests solute dilution which has been attributed to source limited or reaction rate-limited conditions (Godsey et al., 2009; Bieroza et al., 2018; Duncan et al., 2017). In P sink soils, the magnitude of positive SPSC values is an estimate of legacy P held in stable forms in these soils (Nair et al., 2015). Since desorption rates are much slower than sorption rates (Menezes-Blackburn et al., 2016), the dilution behavior in sink soils is primarily controlled by this hysteretic behavior of P between the solid and liquid phase in soils.

At the event scale, a similar linear relationship between DRP flux from both P source and sink soils and discharge when log-transformed was observed ($R^2 = 0.64$ and $R^2 = 0.78$, respectively) (Figure 4.1b). However, the slopes (b) of the log-log relationships highlighted a different (contrasting) DRP dynamic at the event scale compared to the daily scale. Previous authors (Ruark et al., 2009; Duncan et al., 2017), have also reported contrasting C-Q patterns when data are analyzed at different time scales e.g. daily, monthly, seasonal, or event time scales. These studies showed that the variation of C-Q relationships across different time scales results from the different processes influencing C-Q behavior at different temporal scales.

The slope ($b = 0.88$) of the event DRP – discharge relationship for source soils had a 95% confidence limit between 0.75 and 0.99, indicating that b was significantly < 1 i.e. a dilution effect (Figure 1b). On the other hand, the slope ($b = 0.94$) of the event DRP – discharge relationship for sink soils had a 95% confidence limit between 0.86 and 1.01, indicating that b was not significantly different from 1; i.e. chemostasis (Figure 4.1b). Although it is possible that the event-scale dilution ($b < 1$) observed in the P source soils could result from a single contribution of a high-source P pool that becomes increasingly exhausted throughout the event, the pervasive and persistent nature of legacy P in agricultural soils (Kleinman, 2017) make it unlikely that legacy stores become depleted on the timescale of an individual discharge event. On the other hand, the $b < 1$ may be the result of a dilution of the DRP-rich water from P-rich surface soils by P-poor ground water. Subsurface discharge water is composed of both shallow groundwater and precipitation water that has infiltrated through the soil and moved downwards either by matrix or

preferential flow (Stamm et al., 2002). Previous studies that used stable water isotopes and tracers to monitor movement of water into tile drains (Greve et al., 2012; Williams et al., 2016), showed that the initial contributions into tile discharge most likely originated from surface soils and moved through active preferential flow paths, but as the event progressed and the soil matrix neared saturation, tile discharge transitioned from predominantly event water (preferential flow) to a mixture of event, matrix flow and shallow groundwater. Even though water movement and mixing was not monitored in this study, the occurrence of lower DRP concentrations in conjunction with high discharge, suggests these concentrations may have been diluted by matrix and shallow ground water that are poor in P. This interpretation is supported by Williams et al. (2016), who observed that elevated DRP concentrations in tile discharge coincided with peak event water contribution from macropore flow pathways before the waters mixed along the flow pathway. Additionally, the effect of water table rise and antecedent soil moisture (both not measured in this study) on solute and hysteresis patterns was documented by Macrae et al. (2010) and Wagner et al. (2008) in their $\text{NO}_3 - \text{N}$ study where, instead of a solute dilution, they observed solute flushing (mobilization) because unlike P which is not vertically distributed in soils (Baker et al., 2017), rising water tables mobilized $\text{NO}_3 - \text{N}$ that is well-distributed in the soil matrix and is also found in high concentrations in shallow groundwater. On the other hand, the chemostatic behavior ($b = 1$) observed at the event scale in sink soils, suggests that these surface soils are just as P poor as matrix and shallow ground water. Since the stable forms of P in P sink soils are not readily desorbed (Nair et al., 2015), water from P sink surface soils would have similar low P concentrations as matrix and groundwater.

Our results from both timescales highlight the importance of P-rich surface soils and hydrological connectivity for DRP loss to tile drains. The continuous release of DRP from P source soils highlights how legacy P continues to undermine P mitigation efforts. Unfortunately, phytomining (growing and harvesting crops without P fertilization) takes decades or longer to draw down P (McCollum, 1991; Schärer et al., 2007; Sharpley & Rekolainen, 1997). On the other hand, there are a few more timely, and cost-effective materials arising as waste streams from various processes, which can be used to sequester P from P-rich soils. These materials include; fluidized gas desulfurization (FGD) gypsum, red muds, crushed concrete, and Fe gels etc. (Kleinman et al., 2019; Murphy & Stevens, 2010; Egemose et al., 2012; Chardon et al., 2012; Weng et al., 2012). Among these amendments, FGD gypsum has gained traction due to its added

benefit of acting as a source of sulfur, and because it can be used for the treatment of sea-salt impacted soils (Murphy & Stevens, 2010). However cost and possible adverse effects from the use of the remaining P amendments has hindered their adoption (Kleinman et al., 2019). Also, since macropores are the major pathway through which DRP is transported to tile drains, some studies recommend tillage to disrupt macropore flow pathways and decrease hydrological connectivity (Williams et al., 2016). Although tillage could potentially reduce DRP losses through tile discharge, it could also increase particulate P losses (Verbree et al., 2010), therefore it may not be a suitable conservation practice.

4.4.4 Hysteresis patterns

Table 4.7 presents the relationships between the discharge event characteristics and the C-Q hysteresis descriptors. ΔR was positively correlated to Q ($p < 0.05$) and D_{rel} ($p < 0.01$), suggesting that an increase in Q and D_{rel} would lead to a shift in loop trajectories from anticlockwise to clockwise. This observation has been reported in previous studies in which DRP anticlockwise loops were mostly associated with low discharge events (Williams et al., 2018; Bowes et al., 2005; Chow et al., 2017; Bieroza and Heathwaite, 2015). The ΔC_{new} was not significantly correlated with any of the discharge event characteristics.

Table 4.7. Pearson correlation matrix between general discharge event characteristics and the ΔR (%) and ΔC (%) parameters^{††}.

	ED	Δt	Q	Q_{ave}	Q_{max}	D_{rel}	ΔR (%)	ΔC_{new} (%)
ED	1.00							
Δt	0.10	1.00						
Q	0.10	0.01	1.00					
Q_{ave}	0.08	0.18	-0.10	1.00				
Q_{max}	0.15	0.12	-0.14	<i>0.93</i>	1.00			
D_{rel}	-0.06	-0.08	-0.12	0.11	0.09	1.00		
ΔR (%)	-0.06	0.13	<i>0.23</i>	-0.01	-0.15	<i>0.30</i>	1.00	
ΔC (%)	0.00	-0.08	-0.06	-0.04	-0.07	-0.19	-0.23	1.00

[†]Correlation is significant at $p < 0.001$ level for bold italic numbers, at $p < 0.01$ for bold numbers, at $p < 0.05$ for bold, italic and underlined numbers.

^{††}ED, event duration; Δt , days since previous event; Q , total discharge; Q_{ave} , average event discharge; Q_{max} , peak event discharge; D_{rel} , relative length (days) of the rising limb; ΔR (%), rotational pattern of hysteresis loops; ΔC (%), solute trends (neutral, dilution or flushing).

Figure 4.2 shows a plot of ΔC_{new} (%) and ΔR (%) that summarizes C-Q hysteresis loop types of the DRP from sink and source soils during the selected discharge events. Potential nutrient sources and delivery pathways to surface water are usually inferred from C-Q hysteresis loops where, clockwise hysteresis infers proximal sources with exhaustible solute supply or intense discharge, and anticlockwise hysteresis infers distal sources or transport-limited systems (Bowes et al. 2015). However, as noted by Williams et al. (2018), interpretation of hysteresis loops in tile-drained systems is more complex as even distant sources are directly connected to streams by tile drains. The use of low resolution data (daily sampling) did not accurately capture the variation in DRP concentrations (ΔC_{new} (%)). For example, for some events, initial Q was also Q_{max} in a discharge event therefore, $C_i = C_s$, resulting in discharge events whose solute trend (flushing or dilution) could not be determined given they plotted on the $y = 0$ line (Figure 4.2). These discharge events included 42% (30% anticlockwise, 12% clockwise) and 25% (18% anticlockwise, 7% clockwise) of source and sink DRP events, respectively. Of the remaining discharge events, our results show that hysteresis behavior of source DRP events was variable with 21%, 7%, 6%, 9% and 15% exhibiting anticlockwise with dilution, anticlockwise with flushing, clockwise with dilution, clockwise with flushing, and no hysteresis behavior, respectively. According to Williams et al. (2018) this variability in hysteresis behavior suggests that multiple flow pathways and transport mechanisms are involved in DRP loss to tile drains.

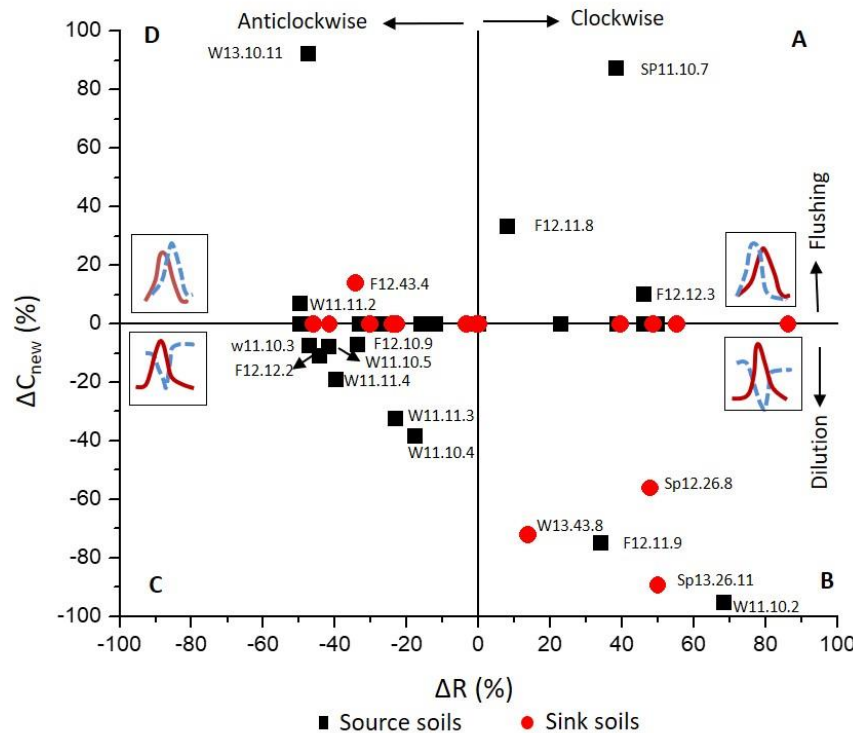


Figure 4.2. Plot of ΔC_{new} (%) versus ΔR (%) for the C-Q hysteresis loops of dissolved reactive phosphorus (DRP). The i , j , and k terms in the plot labels correspond to i th season (winter (W), spring (Sp), summer (Su), and fall (F)) in a water year (2011 (11), 2012 (12), and 2013 (13), the j th plot at the WQFS (10, 11, 12, 26, 30, 32, 43, and 44), and the k th discharge event for the specified plot. Table 5 provides detailed information on discharge events. Illustrations of the typical C-Q relationships (c, broken blue line; Q, continuous brown line) are presented for each of the regions A – D of the ΔC_{new} (%) versus ΔR plot. A few source DRP events showed clockwise hysteresis

The predominant anticlockwise and dilution pattern of source DRP events (region C of Figure 4.2) has two implications. First, tile drains facilitate the rapid transport of DRP from P rich surface soils and the contribution of event water to tile discharge (Vidon & Cuadra, 2011; Williams et al., 2016). Second, the mixing between event water, matrix water, and shallow groundwater, may delay the peak in DRP concentration thus a dilution of high DRP concentrations when waters mix results in anticlockwise hysteresis (high DRP concentrations on the falling limb versus the rising limb of the hydrograph) (Williams et al., 2018). The majority dilution pattern in source DRP events is consistent with our results i.e. $b < 1$, from the C-Q slope analysis at the event scale (Figure 4.1b). It reinforces our interpretation of the slopes of the C-Q relationships where the initial, high

DRP concentrations in event water progressively mixes with lower DRP concentrations in shallow ground water, resulting in a dilution as discharge approaches its peak. The anticlockwise hysteresis (illustration in region C of Figure 4.2) further shows that the dilution pattern reverses as discharge recedes, with soil matrix water and shallow groundwater progressively becoming disconnected from the tile drains, whereas event water from P-rich surface soils remains hydrologically connected through preferential pathways. In contrast, during other events, insufficient rise of shallow groundwater around tile-drains may prevent the mixing of P-rich and P-poor waters. This minimal mixing coupled with rapid transport of DRP and the contribution of event water to tile discharge, may result in clockwise hysteresis (high DRP concentrations on the rising limb versus the falling limb of the hydrograph) (Williams et al., 2018; Vidon & Cuadra, 2011; Williams et al., 2016). Also, our correlation results (Table 4.7) show that the shift from anticlockwise to clockwise hysteresis may be the result of an increase in Q and D_{rel} . Finally, the variation in DRP response could be the result of rapid exchanges between P pools due to sorption/desorption and biological processes under varying antecedent conditions (Williams et al., 2018). These variable hysteresis behavior and solute trend underscores the challenge of interpreting the contributing mechanisms to better manage DRP loss from P source soils in tile drained systems. However, we note that our results may be an artefact of low temporal resolution sampling.

Sink DRP events seemed to generally have no hysteresis or solute trend i.e. 67% of the events were plotted at the origin. These results support the chemostatic ($b = 1$) finding in the event C-Q slope analyses of sink soils. Among the remaining events whose solute trends were identified, 2% and 6% were anticlockwise with flushing and clockwise with dilution, respectively.

Based on these results, the proposed conceptual models illustrating DRP loss in P source and P sink soils are presented in Figure 4.3.

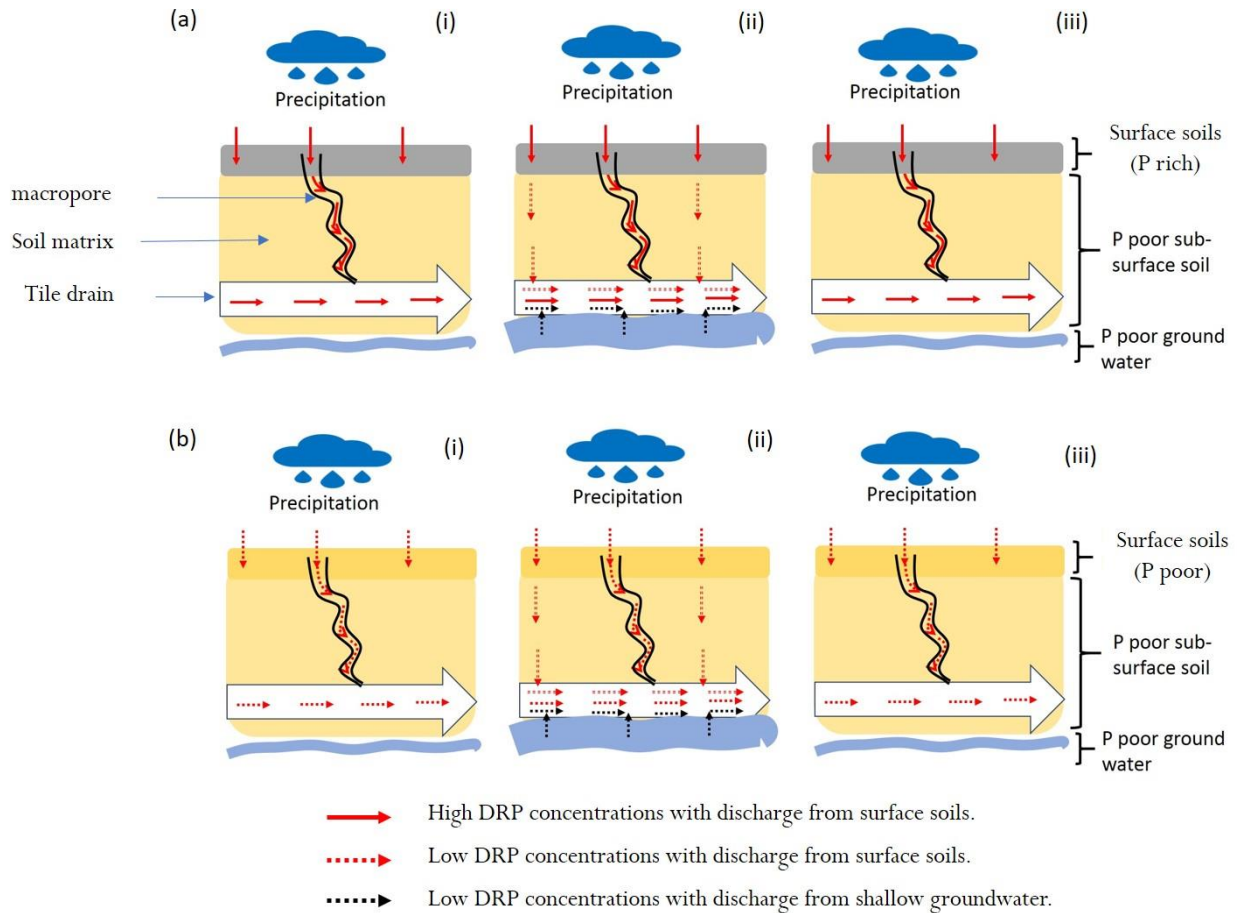


Figure 4.3. (a) A proposed conceptual model illustrating DRP loss in tile drained fields from P source soils, (i) discharge at the start of the event when P rich event water (preferential flow) from the surface rapidly flows to tile drains; (ii) discharge during the event when P rich event water is mixed with P poor water from the soil matrix and shallow ground water, resulting in an overall dilution; (iii) when the discharge recedes and contributions from soil matrix and shallow ground water are absent, event water with high P concentrations continues, (b) A proposed conceptual model illustrating DRP loss in tile drained fields from P sink soils, (i) discharge at the start of the event when P poor event water (preferential flow) from the surface rapidly flows to tile drains; (ii) discharge during the event when P poor waters (preferential, matrix, and shallow groundwater) mix; (iii) soil matrix and shallow ground water recede, event water with low P concentrations continues.

Even though tile drains are a major pathway for DRP loss as shown in this study and others (Welikhe et al., 2020; Gentry et al., 2007; Macrae et al., 2007; Gelbrecht et al., 2005), our results suggest that the water table dynamics during discharge events, soil P status, soil P stratification, the amount of discharge, and the number of days it takes to reach peak discharge, also control nutrient delivery and hysteresis patterns.

4.5 Conclusion

DRP C-Q relationships were examined within the context of soil P status to elucidate solute pathways and investigate key components driving nutrient delivery in tile drained systems. Our results showed that dynamics of DRP loss from P source and P sink soils in tile drained systems are different. Results from the daily C-Q slopes suggest that the differences in solute behavior and export during discharge events was regulated by solute reactivity, availability, and mobilization from surface soils. At the event scale, results from both C-Q slopes and hysteresis indices suggest that DRP behavior and export was regulated by DRP availability in surface soils, and the degree of mixing between event water, matrix water, and rising shallow groundwater. Also, changes in discharge event characteristics including Q and D_{rel} influenced DRP hysteresis. Despite the complex hysteresis behavior observed, findings suggest that mitigation of DRP loss from P source soils in tile-drained systems should involve both nutrient management practices aimed at P draw down (e.g. phytomining) and P sequestration. Even though, tillage has been proposed as a way to reduce hydrological connectivity between P rich surface soils and tile drains, it has not gained traction due to concerns over potential adverse impacts on particulate P loss. To avoid conversion of P-sink soils to P-source soils, 4R nutrient management practices with an emphasis on “feeding” the crop not the soil, will be needed. Due to low temporal resolution data, the current study only focused on single peak events; thus, future research analyzing DRP dynamics in both single and multi-peak discharge events is needed to increase understanding of P-loss patterns and inform nutrient management recommendations, and ultimately improve water quality.

4.6 References

- Baker, D. B., Johnson, L. T., Confesor, R. B., and Crumrine, J. P. (2017). Vertical stratification of soil phosphorus as a concern for dissolved phosphorus runoff in the lake erie basin. *Journal of Environmental Quality*, 46(6), 1287–1295. <https://doi.org/10.2134/jeq2016.09.0337>
- Basu, N. B., Destouni, G., Jawitz, J. W., Thompson, S. E., Loukinova, N. V., Darracq, A., and Rao, P. S. C. (2010). Nutrient loads exported from managed catchments reveal emergent biogeochemical stationarity. *Geophysical Research Letters*, 37(23), 1–5. <https://doi.org/10.1029/2010gl045168>
- Basu, N. B., Thompson, S. E., and Rao, P. S. C. (2011). Hydrologic and biogeochemical functioning of intensively managed catchments: a synthesis of top-down analyses. *Water Resources Research*, 47 (10), 1–12. <https://doi.org/10.1029/2011wr010800>
- Beauchemin, S., Simard, R. R., and Cluis, D. (1998). Forms And concentration of phosphorus in drainage water of twenty-seven tile-drained soils. *Journal Of Environmental Quality*, 27 (3), 721–728. <https://doi.org/10.2134/jeq1998.00472425002700030033x>
- Bende-Michl, U., Verburg, K., and Cresswell, H. P. (2013). High-frequency nutrient monitoring to infer seasonal patterns in catchment source availability, mobilisation and delivery. *Environmental Monitoring And Assessment*, 185(11), 9191–9219. <https://doi.org/10.1007/s10661-013-3246-8>
- Bieroza, M. Z., and Heathwaite, A. L. (2015). Seasonal Variation in phosphorus concentration-discharge hysteresis inferred from high-frequency in situ monitoring. In *Journal Of Hydrology* (Vol. 524). <https://doi.org/10.1016/j.jhydrol.2015.02.036>
- Bieroza, M. Z., Heathwaite, A. L., Bechmann, M., Kyllmar, K., and Jordan, P. (2018). The concentration-discharge slope as a tool for water quality management. *Science Of The Total Environment*, 630, 738–749. <https://doi.org/10.1016/j.scitotenv.2018.02.256>
- Bowes, M. J., Jarvie, H. P., Halliday, S. J., Skeffington, R. A., Wade, A. J., Loewenthal, M., and Palmer-Felgate, E. J. (2015). Characterising phosphorus and nitrate inputs to a rural river using high-frequency concentration-flow relationships. *Science Of The Total Environment*, 511, 608–620. <https://doi.org/10.1016/j.scitotenv.2014.12.086>
- Bowes, Michael J., House, W. A., Hodgkinson, R. A., and Leach, D. V. (2005). Phosphorus-discharge hysteresis during storm events along a river catchment: The River Swale, UK. *Water Research*, 39 (5), 751–762. <https://doi.org/10.1016/j.watres.2004.11.027>

- Butturini, A., Alvarez, M., Bernal, S., Vazquez, E., and Sabater, F. (2008). Diversity and temporal sequences of forms of doc and no₃- discharge responses in an intermittent stream: predictable or random succession? *Journal Of Geophysical Research: Biogeosciences*, 113(3), 1–10. <https://doi.org/10.1029/2008jg000721>
- Butturini, A., Francesc, G., Jérôme, L., Eusebi, V., and Francesc, S. (2006). Cross-site comparison of variability of doc and nitrate c-q hysteresis during the autumn-winter period in three mediterranean headwater streams: a synthetic approach. *Biogeochemistry*, 77(3), 327–349. <https://doi.org/10.1007/s10533-005-0711-7>
- Chardon, W. J., Groenenberg, J. E., Temminghoff, E. J. M., and Koopmans, G. F. (2012). Use of reactive materials to bind phosphorus. *Journal Of Environmental Quality*, 41(3), 636–646. <https://doi.org/10.2134/jeq2011.0055>
- Chow, M. F., Huang, J. C., and Shiah, F. K. (2017). Phosphorus dynamics along river continuum during typhoon storm events. *Water (Switzerland)*, 9(7), 1–15. <https://doi.org/10.3390/W9070537>
- Correll, D. L. (1999). Phosphorus: a rate limiting nutrient in surface waters. *poultry science*, 78(5), 674–682. <https://doi.org/10.1093/ps/78.5.674>
- Djodjic, F., Bergström, L., and Ulén, B. (2006). Phosphorus losses from a structured clay soil in relation to tillage practices. *Soil Use And Management*, 18(2), 79–83. <https://doi.org/10.1111/j.1475-2743.2002.tb00223.x>
- Djodjic, Faruk, Bergström, L., Ulén, B., and Shirmohammadi, A. (1999). Mode of transport of surface-applied phosphorus-33 through a clay and sandy soil. *Journal Of Environmental Quality*, 28(4), 1273–1282. <https://doi.org/10.2134/jeq1999.00472425002800040031x>
- Duncan, J. M., Band, L. E., and Groffman, P. M. (2017). variable nitrate concentration–discharge relationships in a forested watershed. *Hydrological Processes*, 31(9), 1817–1824. <https://doi.org/10.1002/hyp.11136>
- Duncan, J. M., Welty, C., Kemper, J. T., Groffman, P. M., and Band, L. E. (2017). Dynamics of nitrate concentration-discharge patterns in an urban watershed. *Water Resources Research*, 53 (8), 7349–7365. <https://doi.org/10.1002/2017wr020500>
- Egemose, S., Sønderup, M. J., Beinthin, M. V., Reitzel, K., Hoffmann, C. C., and Flindt, M. R. (2012). crushed concrete as a phosphate binding material: a potential new management tool. *Journal Of Environmental Quality*, 41(3), 647–653. <https://doi.org/10.2134/jeq2011.0134>

- Gelbrecht, J., Lengsfeld, H., Pöthig, R., and Opitz, D. (2005). Temporal and spatial variation of phosphorus input, retention and loss in a small catchment of Ne Germany. *Journal Of Hydrology*, 304(1–4), 151–165. <https://doi.org/10.1016/j.jhydrol.2004.07.028>
- Gentry, L. E., David, M. B., Royer, T. V., Mitchell, C. A., and Starks, K. M. (2007). Phosphorus transport pathways to streams in tile-drained agricultural watersheds. *Journal Of Environment Quality*, 36(2), 408. <https://doi.org/10.2134/jeq2006.0098>
- Gentry, L. E., David, M. B., Smith-Starks, K. M., and Kovacic, D. A. (2000). Nitrogen fertilizer and herbicide transport from tile drained fields. *Journal Of Environmental Quality*, 29 (1), 232–240. <https://doi.org/10.2134/jeq2000.00472425002900010030x>
- Godsey, S. E., Kirchner, J. W., and Clow, D. W. (2009). Concentration–discharge relationships reflect chemostatic characteristics of US catchments. *Hydrol. Process*, (23), 1844–1864. <https://doi.org/10.1002/hyp>
- Greve, A. K., Andersen, M. S., and Acworth, R. I. (2012). Monitoring the transition from preferential to matrix flow in cracking clay soil through changes in electrical anisotropy. *Geoderma*, 179–180, 46–52. <https://doi.org/10.1016/j.geoderma.2012.02.003>
- Jarvis, N. J. (2007). A review of non-equilibrium water flow and solute transport in soil macropores: principles, controlling factors and consequences for water quality. *European Journal Of Soil Science*, 58(3), 523–546. <https://doi.org/10.1111/j.1365-2389.2007.00915.x>
- Johnson, N. M., Likens, G. E., Bormann, F. H., Fisher, D. W., and Pierce, R. S. (1969). A working model for the variation in stream water chemistry at the hubbard brook experimental forest, New Hampshire. *Water Resources Research*, 5(6), 1353–1363. <https://doi.org/10.1029/wr005i006p01353>
- King, K. W., Fausey, N. R., and Williams, M. R. (2014). Effect of subsurface drainage on streamflow in an agricultural headwater watershed. *Journal Of Hydrology*, 519(Pa), 438–445. <https://doi.org/10.1016/j.jhydrol.2014.07.035>
- King, Kevin W., Williams, M. R., and Fausey, N. R. (2015). Contributions of systematic tile drainage to watershed-scale phosphorus transport. *Journal Of Environment Quality*, 44(2), 486. <https://doi.org/10.2134/jeq2014.04.0149>
- Kinley, R. D., Gordon, R. J., Stratton, G. W., Patterson, G. T., and Hoyle, J. (2007). Phosphorus losses through agricultural tile drainage in Nova Scotia, Canada. *Journal Of Environmental Quality*, 36 (2), 469–477. <https://doi.org/10.2134/jeq2006.0138>

- Kleinman, P. J. A. (2017). The persistent environmental relevance of soil phosphorus sorption saturation. *Current Pollution Reports*, 3 (2), 141–150. <https://doi.org/10.1007/s40726-017-0058-4>
- Kleinman, P. J. A., Fanelli, R. M., Hirsch, R. M., Buda, A. R., Easton, Z. M., Wainger, L. A., and Shenk, G. W. (2019). Phosphorus and the chesapeake bay: lingering issues and emerging concerns for agriculture. *Journal Of Environmental Quality*, 48 (5), 1191–1203. <https://doi.org/10.2134/jeq2019.03.0112>
- Lawler, D. M., Petts, G. E., Foster, I. D. L., and Harper, S. (2006). Turbidity dynamics during spring storm events in an urban headwater river system: The Upper Thame, West Midlands, UK. *Science Of The Total Environment*, 360 (1–3), 109–126. <https://doi.org/10.1016/j.scitotenv.2005.08.032>
- Lloyd, C. E. M., Freer, J. E., Johnes, P. J., and Collins, A. L. (2016a). Technical note: testing an improved index for analysing storm discharge-concentration hysteresis. *Hydrology And Earth System Sciences*, 20 (2), 625–632. <https://doi.org/10.5194/hess-20-625-2016>
- Lloyd, C. E. M., Freer, J. E., Johnes, P. J., and Collins, A. L. (2016b). Using hysteresis analysis of high-resolution water quality monitoring data, including uncertainty, to infer controls on nutrient and sediment transfer in catchments. *Science Of The Total Environment*, 543, 388–404. <https://doi.org/10.1016/j.scitotenv.2015.11.028>
- Logan, T.J., Randall, G. W., and Timmons, D. R. (1980). Nutrient content of tile drainage from cropland in the north central region. North Central Regional Research Publication 268, September, 1980. Research Bulletin 1119. Ohio Agricultural Research And Development Center, Wooster, Oh.
- Macrae, M. L., English, M. C., Schiff, S. L., and Stone, M. (2007). Intra-annual variability in the contribution of tile drains to basin discharge and phosphorus export in a first-order agricultural catchment. *Agricultural Water Management*, 92 (3), 171–182. <https://doi.org/10.1016/j.agwat.2007.05.015>
- Macrae, M. L., English, M. C., Schiff, S. L., and Stone, M. (2010). Influence of antecedent hydrologic conditions on patterns of hydrochemical export from a first-order agricultural watershed in Southern Ontario, Canada. *Journal Of Hydrology*, 389 (1–2), 101–110. <https://doi.org/10.1016/j.jhydrol.2010.05.034>
- Madison, A. M., Ruark, M. D., Stuntebeck, T. D., Komiskey, M. J., Good, L. W., Drummy, N.,

- and Cooley, E. T. (2014). Characterizing phosphorus dynamics in tile-drained agricultural fields of Eastern Wisconsin. *Journal Of Hydrology*, 519(Pa), 892–901.
<https://doi.org/10.1016/j.jhydrol.2014.08.016>
- Mccollum, R. E. (1991). Buildup and decline in soil phosphorus: 30-year trends on a typical umprabuilt. *Agronomy Journal*, 83 (12563), 77–85.
<https://doi.org/10.2134/agronj1991.00021962008300030011x>
- Menezes-Blackburn, D., Zhang, H., Stutter, M., Giles, C. D., Darch, T., George, T. S., and Haygarth, P. M. (2016). A holistic approach to understanding the desorption of phosphorus in soils. *Environmental Science And Technology*, 50(7), 3371–3381.
<https://doi.org/10.1021/acs.est.5b05395>
- Minaudo, C., Dupas, R., Gascuel-Oudoux, C., Roubéix, V., Danis, P. A., and Moatar, F. (2019). Seasonal and event-based concentration-discharge relationships to identify catchment controls on nutrient export regimes. *Advances In Water Resources*, 131 (July 2018), 103379.
<https://doi.org/10.1016/j.advwatres.2019.103379>
- Murphy, J. and Riley, J. P. (1962). A modified single solution method for the determination of phosphate in natural waters. *Analytical Chemistry Acta*, 27, 31–36.
[https://doi.org/10.1016/s0003-2670\(00\)88444-5](https://doi.org/10.1016/s0003-2670(00)88444-5)
- Murphy, P. N. C., and Stevens, R. J. (2010). Lime and gypsum as source measures to decrease phosphorus loss from soils to water. *Water, Air, And Soil Pollution*, 212 (1–4), 101–111.
<https://doi.org/10.1007/s11270-010-0325-0>
- Nair, V. D., Clark, M. W., and Reddy, K. R. (2015). Evaluation of legacy phosphorus storage and release from wetland soils. *Journal Of Environment Quality*, 44 (6), 1956.
<https://doi.org/10.2134/jeq2015.03.0154>
- Nair, V. D, and Harris, W. G. (2014). Soil phosphorus storage capacity for environmental risk assessment. *AAS 2014*: 1–10.
- Pote, D. H., and Daniel, T. C. (2000). Analyzing for dissolved reactive phosphorus in water samples. In: J. L. Kovar and Pierzynski, G. M., editors, *Methods of phosphorus analysis for soils, sediments, residuals and waters*. Southern Cooperative Series Bulletin, Virginia Tech University, Blacksburg. p, 91-93.
- R Core Team. (2017). R: A language and environment for statistical computing. retrieved from <https://www.r-project.org/>

- Radcliffe, D. E., Reid, D. K., Blombäck, K., Bolster, C. H., Collick, A. S., Easton, Z. M., and Smith, D. R. (2015). Applicability of models to predict phosphorus losses in drained fields: a review. *Journal Of Environment Quality*, 44 (2), 614. <https://doi.org/10.2134/jeq2014.05.0220>
- Rose, Lucy A., Karwan, Diana L., and Godsey, S. E. (2018). Concentration–discharge relationships describe solute and sediment mobilization, reaction, and transport at event and longer timescales. *Hydrological Processes*, 32(18), 2829–2844. <https://doi.org/10.1002/hyp.13235>
- Ruark, M. D., Brouder, S. M., And Turco, R. F. (2009). Dissolved organic carbon losses from tile drained agroecosystems. *Journal Of Environment Quality*, 38(3), 1205. <https://doi.org/10.2134/jeq2008.0121>
- Ruark, M., Madison, A., Madison, F., Cooley, E., Frame, D., Stuntebeck, T., and Komiskey, M. (2012). Phosphorus loss from tile drains: should we be concerned? University Of Wisconsin, 21. Retrieved From [Http://Fyi.Uwex.Edu/Drainage/Files/2015/09/P-Loss-From-Tile-Drains-Ppt.Pdf](http://fyi.uwex.edu/Drainage/Files/2015/09/P-Loss-From-Tile-Drains-Ppt.Pdf)
- Schärer, M., Stamm, C., Vollmer, T., Frossard, E., Oberson, A., Flühler, H., and Sinaj, S. (2007). reducing phosphorus losses from over-fertilized grassland soils proves difficult in the short term. *Soil Use And Management*, 23(Suppl. 1), 154–164. <https://doi.org/10.1111/j.1475-2743.2007.00114.x>
- Schilling, K.E., and Helmers, M. (2008). Tile drainage as karst: conduit flow and diffuse flow in a tile drained watershed. *J. Hydrol.*, 349:291–30. <https://doi.org/doi:10.1016/j.jhydrol.2007.11.014>
- SEAL Analytical. (2004). O-Phosphate – P in drinking, saline and surface waters , and domestic and industrial wastes. AQ2 method EPA-118-A Rev. 5, SEAL Analytical, Mequon Technology Center 10520-C North Baehr Road Mequon, Wisc. 53092
- Sharpley, A. N. and Rekolainen, S. (1997). Phosphorus in agriculture and its environmental implications. In N H. Tunney, O. T. Carton, P. C. Brookes, and A. E. Johnston, Eds. *Phosphorus Loss From Soil To Water*. Cab International, Wallingford, Uk. Sharpley, (Pp. 1–54).
- Sharpley, Andrew N., Sims, J. T., Reddy, K. R., Chapra, S. C., Daniel, T. C., and Wedepohl, R. (1994). Managing agricultural phosphorus for protection of surface waters: issues and

- options. *Journal Of Environment Quality*, 23 (3), 437.
<https://doi.org/10.2134/jeq1994.00472425002300030006x>
- Sharpley, A.N., Daniel, T., Sims, T., Lemunyon, J., Stevens, R., and Parry, R. (2003). *Agricultural phosphorus and eutrophication second edition agricultural phosphorus and eutrophication Second Edition*. U.S. Department Of Agriculture, Agricultural Research Service, (149), 44.
- Sharpley, Andrew N., Kleinman, P. J. A., Flaten, D. N., and Buda, A. R. (2011). Critical source area management of agricultural phosphorus: experiences, challenges and opportunities. *Water Science And Technology*, 64 (4), 945–952. <https://doi.org/10.2166/wst.2011.712>
- Simard, R. R., Beauchemin, S., and Haygarth, P. M. (2000). Potential for preferential pathways of phosphorus transport. *Journal Of Environmental Quality*, 29(1), 97–105.
<https://doi.org/10.2134/jeq2000.00472425002900010012x>
- Sims, J. T., Simard, R. R., and Joern, B. C. (1998). Phosphorus loss in agricultural drainage: historical perspective and current research. *Journal Of Environment Quality*, 27 (2), 277.
<https://doi.org/10.2134/jeq1998.00472425002700020006x>
- Stamm, C., Sermet, R., Leuenberger, J., Wunderli, H., Wydler, H., Flühler, H., and Gehre, M. (2002). Multiple tracing of fast solute transport in a drained grassland soil. *Geoderma*, 109 (3–4), 245–268. [https://doi.org/10.1016/s0016-7061\(02\)00178-7](https://doi.org/10.1016/s0016-7061(02)00178-7)
- Thompson, S. E., Basu, N. B., Lascrain, J., Aubeneau, A., and Rao, P. S. C. (2011). Relative dominance of hydrologic versus biogeochemical factors on solute export across impact gradients. *Water Resources Research*, 47 (7), 1–20. <https://doi.org/10.1029/2010wr009605>
- Trybula, E. 2012. Quantifying ecohydrologic impacts of perennial rhizomatous grasses on tile discharge: a plot level comparison of continuous corn, upland switchgrass, mixed prairie, and *Miscanthus X Giganteus*. (Order No. 1535171). Available From Dissertations & Theses @ Cic Institutions; Proquest Dissertations & Theses Global (1328160945). Retrieved From <https://search.proquest.com/docview/1328160945?accountid=13360>.
- USEPA (2002). EPA water quality standards handbook. (August), 2–3.
- Uusitalo, R., Turtola, E., Kauppi, T., and Lilja, T. (2001). Particulate phosphorus and sediment in surface runoff and drainflow from clayey soils. *Journal Of Environmental Quality*, 30 (2), 589–595. <https://doi.org/10.2134/jeq2001.302589x>
- Vadas, P. A., Kleinman, P. J. A., Sharpley, A. N., and Turner, B. L. (2005). Relating soil phosphorus to dissolved phosphorus in runoff: a single extraction coefficient for water

- quality modeling. *Journal Of Environmental Quality*, 34 (2), 572–580.
<https://doi.org/10.2134/jeq2005.0572>
- Verbree, D. A., Duiker, S. W., and Kleinman, P. J. A. (2010). Runoff losses of sediment and phosphorus from no-till and cultivated soils receiving dairy manure. *Journal Of Environmental Quality*, 39(5), 1762–1770. <https://doi.org/10.2134/jeq2010.0032>
- Vidon, P., and Cuadra, P. E. (2011). Phosphorus dynamics in tile-drain flow during storms in the US Midwest. *Agricultural Water Management*, 98 (4), 532–540.
<https://doi.org/10.1016/j.agwat.2010.09.010>
- Wagner, L. E., Vidon, P., Tedesco, L. P., and Gray, M. (2008). Stream nitrate and doc dynamics during three spring storms across land uses in glaciated landscapes of the Midwest. *Journal Of Hydrology*, 362 (3–4), 177–190. <https://doi.org/10.1016/j.jhydrol.2008.08.013>
- Welikhe, P., Brouder, S. M., Volenec, J. J., Gitau, M. and Turco, R. F. (2020). Development of phosphorus sorption capacity – based environmental indices for tile-drained systems. *Journal Of Environment Quality*, Jeq220044. <https://doi.org/10.1002/jeq2.20044>
- Weng, L., Van Riemsdijk, W. H., and Hiemstra, T. (2012). Factors controlling phosphate interaction with iron oxides. *Journal Of Environmental Quality*, 41(3), 628–635.
<https://doi.org/10.2134/jeq2011.0250>
- Williams, M., King, K., Ford, W. I., Buda, A., and Kennedy, C. (2016). Effect of tillage on macropore flow and phosphorus transport to tile drains. *Water Resources Research*, 52 (4), 2868–2882. <https://doi.org/10.1002/2015wr017650>.received
- Williams, M. R., Buda, A. R., Elliott, H. A., Hamlett, J., Boyer, E. W., and Schmidt, J. P. (2014). Groundwater flow path dynamics and nitrogen transport potential in the riparian zone of an agricultural headwater catchment. *Journal Of Hydrology*, 511, 870–879.
<https://doi.org/10.1016/j.jhydrol.2014.02.033>
- Williams, M. R., Livingston, S. J., Penn, C. J., Smith, D. R., King, K. W., and Huang, C. (2018). Controls of event-based nutrient transport within nested headwater agricultural watersheds of the Western Lake Erie Basin. *Journal Of Hydrology*, 559, 749–761.
<https://doi.org/10.1016/j.jhydrol.2018.02.079>

5 SYNTHESIS AND FUTURE WORK

This dissertation focused on evaluating the effects of legacy (historical) phosphorus (P) on dissolved reactive P (DRP) losses in tile-drained systems. For many decades, agricultural landscapes in the Midwest USA have heavily depended on anthropogenic P inputs to meet the growing demand for food and energy for a growing and increasingly urbanized global population. The result has been the buildup of P and subsequent saturation of solid-phase P sorption sites leading to subsequent P additions remaining in the soluble P phase, thereby increasing their susceptibility to leaching. In order to evaluate the effects of these P accumulations, research was needed to develop and evaluate P sorption capacity (PSC) – based environmental indices that could be used to identify P sink and source soils and quantify legacy P amounts in surface soils. Also, with the P index (PI) continuously being improved and evaluated, research was needed to compare the weights of PSC-based indices against other common PI site characteristics, to determine if there was indeed a need to incorporate these indices into a risk management tool for P losses. Finally, this research also sought to elucidate how a soil's P status i.e. P sink or P source, affects DRP dynamics on a daily and an event scale.

The pedo-transfer approach proved to be useful in determining a suitable function i.e. pedo-transfer function (pedoTF), that accurately estimated PSC ($R^2 = 0.60$) in neutral to slightly acidic Midwestern USA soils (mollisols and alfisols). These results suggest that PSC and subsequent PSC-based indices (P saturation ratio (PSR) and soil P storage capacity (SPSC)) could be determined routinely as simple and fast soluble P (SP) risk assessment tools. The coincidence of the identified PSR and SPSC thresholds with the critical soil test P (STP) level for agronomic P sufficiency (22 mg P kg^{-1}), suggests that the critical STP level for agronomic P sufficiency, could also serve as an environmental STP threshold above which DRP loss in subsurface drainage is expected to greatly increase. This finding highlights the need to reanalyze the buildup and maintenance approach to fertilizer and manure applications.

The observed, significant relationships between PSC-based indices and SP loss in tile drains, gave rise to the question of how important they were to SP loss in tile drains when compared to other P source and transport site characteristics considered in a P index. The successful prediction of SP loss by a multi-layered feed-forward artificial neural network (MLF-ANN) ($R^2 = 0.99$ and $\text{RMSE} = 0.0024$) allowed for the determination of the relative importance (weights) of

input factors using Garson's algorithm. Results from the relative importance analysis highlighted the importance of P source factors especially STP, inorganic P fertilizer application rate (FPR), SPSC, PSR, and organic P fertilizer application rate (OPR) which were the top five highest contributors to SP loss in tile drains. These findings highlighted the importance of closely monitoring and managing both contemporary and legacy P sources. When included in a multiplicative PI i.e. PI_{ANN} , the ANN-generated weights improved the performance of the PI in predicting SP loss risk potential when compared to PI_{NO} and PI_{LG} . This demonstrated that well trained ANNs coupled with weight algorithms have the potential to accurately weight input factors in a PI. There are many agricultural water quality models including, the Soil Water Assessment Tool (SWAT), Phosphorus Leaching from Soils to the Environment (PLEASE), Annual P Loss Estimator Tool (APLE), Agricultural Policy/ Environmental eXtender (APEX), Environmental Policy Integrated Climate (EPIC) (Qi & Qi, 2017). However, review of these models and others shows that they do not comprehensively represent either of the following processes; fate and transport of P in soils, subsurface drainage, and P transport to tile drains, thus limiting their use in simulating P loss in tile-drained systems (Qi & Qi, 2017). We showed in this study that supervised training of ANNs allows them to learn and simulate with high accuracy complex P loss dynamics in tile-drained fields, making ANNs more efficient water quality models compared to the aforementioned models.

Finally, driven by the need to incorporate PSC-based indices into a PI, this dissertation investigated DRP dynamics in P sink and P source soils. On a daily scale, P source and P sink soils exhibited chemostatic and dilution C-Q patterns, respectively. The chemostatic behavior in P source soils was indicative of a continuous buffering of DRP concentrations by P rich surface soils regardless of variations in discharge, while the dilution pattern in P sink soils indicated an exhaustible DRP source (low DRP concentrations) in P poor surface soils. At the event scale, predominant anti-clockwise rotational pattern in P source soils suggests that there was a mixing between P rich water (preferential flow) and P poor water (matrix and shallow groundwater) as the discharge event progressed, resulting in lower DRP concentrations on the rising limb compared to the falling limb. However, the variable flushing and dilution behavior observed on the rising limb suggested that, in addition to discharge and soil P status, rapid exchanges between P pools, the magnitude of discharge events (Q), and the relative number of days to discharge peak (D_{rel}), also

regulated DRP delivery. On the other hand, the predominant non-hysteretic C-Q behavior in P sink soils suggest that DRP loss from these soils will be minimal.

Overall, this research suggests that legacy P plays a great role in SP loss through tile drains. The risk of re-mobilization and release of legacy P increases once a soil's PSR and SPSC value exceeds or drops below identified index thresholds i.e. threshold PSR = 0.21 and threshold SPSC = 0, respectively. Also, even though it has been demonstrated that legacy P is one factor that contributes to the lack of water quality response to conservation efforts, surplus contemporary P sources (inorganic and organic P applications) that result from the current build up and maintenance approach to P applications used in university recommendations could be equally responsible. Therefore, to mitigate SP loss in tile drains, existing agronomic recommendations where the build-up or maintenance approach to fertilizer applications should be reanalyzed to avoid the conversion of P sink soils to P source soils. Also, phytomining and P sequestration will be needed to draw down P in P source soils.

This research focused on effects of legacy P on DRP losses in tile discharge only. Future research should consider legacy P effects on DRP losses via both surface and subsurface pathways. Also, soils with a wider range of chemical properties that represent existing conditions in the region should be used. Similarly, big empirical datasets will be needed to develop a robust MLF-ANN that could be used to determine the weights of a PI for Indiana. Finally, even though the daily water quality data satisfactorily identified DRP – discharge hysteretic rotations, to better understand the flushing or dilution patterns of DRP in P source soils, high temporal water quality data will be needed. Despite the data limitations (low spatial variability and temporal resolution), the WQFS research facility allowed for edge-of-field (EOF) monitoring of DRP which improved our understanding of the effects of legacy P on the fate and transport of DRP from tile-drained systems. Given the costs associated with the set-up and running of EOF monitoring sites such as the WQFS, it would be impractical to call for the establishment of numerous stand-alone sites to meet our data needs. A potential solution to the data needs would be regional cross-sectoral collaborations between private (land owners) and public organizations (land grant universities and research institutions). By extending EOF monitoring sites to real farms and streamlining processes such as soil sampling, soil testing, and variables to be monitored, a reliable database could be created with field-scale soils, management, and water quality information from a wide range of farming systems/management, topography, and hydrology. Such a database would provide

credible site-specific baseline information that would allow for the determination of regional environmental thresholds and PIs. For these collaborations to work, concerns around data-sharing among parties will need to be addressed to enforce mutual trust. Also, incentives to encourage participation will be needed.

5.1 References

- Qi, H., & Qi, Z. (2017). Simulating phosphorus loss to subsurface tile drainage flow: A review. *Environmental Reviews*, 25(2), 150–162. <https://doi.org/10.1139/er-2016-0024>

APPENDIX

SUPPLEMENTAL MATERIALS CHAPTER 2

Table A.1 Soil classification and type of of phosphorus (P) inputs used at six (6) Purdue agricultural research centers (Davies (DPAC), Pinney (PPAC), Northeast (NEPAC), Southeast (SEPAC), Throckmorton (TPAC) and, Water Quality Field Station (WQFS)).

Site	Soil series	Texture	U.S. Classification	P inputs from 2000 - 2012
DPAC	Blount	Silt loam	Aeric Epiaqualf	Inorganic P fertilizer [†]
	Pewamo	Silt loam	Typic Argiaquoll	
NEPAC	Rawson	Fine loamy	Oxyaquic Hapludalf	Inorganic P fertilizer [†]
	Haskins	Fine loamy	Aeric Epiaqualf	
WQFS	Drummer	Fine silty	Typic Endoaquoll	Variable P treatments: No P, Inorganic P [†] and Manure P [‡]
	Raub	Fine silty	Aquic Argiudoll	
TPAC	Toronto	Fine silty	Udolic Epiaqualf	No P inputs
PPAC	Sebewa	Fine loamy	Typic Argiaquoll	Inorganic P fertilizer [†]
	Cobbsfork			
SEPAC	k	Fine silty	Udolic Epiaqualf	Inorganic P fertilizer [†]

[†] P inputs based on soil test recommendations.

[‡] Manure applications based on crop nitrogen needs with fall or spring applications made annually from fall 1998– fall 2012 & spring 2013.

The Water Quality Field Station, Purdue University, West Lafayette, Indiana.

The WQFS features 48 plots (10.8 m wide × 48 m long) organized in a randomized complete-block design with 12 treatments and 4 replicates (Supplemental Figure S1). The soil series are Drummer silty clay loam and Raub silt loam with < 2 % slopes; these soils are among the major agricultural soils in northwestern Indiana. Since its inception (1992), all treatments (Supplemental Table S2) except a native prairie (Prairie), and continuous maize systems receiving either spring or fall manure (CM-SpM and CM-FM, respectively; supplemental Table S2) received commercial fertilizer P (P₂O₅) at university recommended rates based on STP (Vitosh et al., 1995). From 1998 to 2013, manured treatments received yearly additions of swine effluent at rates based on manure N content and a target N application rate of 255 ± 24 kg N ha⁻¹ yr⁻¹. Volume of manure applied per application was fairly consistent (63.3 ± 3.3 m³ ha⁻¹ yr⁻¹) but composition was highly variable averaging 4.05 and 1.45 g L⁻¹ total N and P₂O₅, respectively (Hernandez-Ramirez et al.,

2011). Based on the P_2O_5 composition of the manure and the number of spring or fall additions (16 or 14 respectively), the manured treatments [CM-SpM and CM-FM] received cumulative P_2O_5 applications of approximately 1461 kg ha^{-1} and 1278 kg ha^{-1} , respectively. Also, since 1997, 10-gal acre^{-1} of liquid starter fertilizer (17-17-0 [17% (w/w) N and 17% (w/w) P_2O_5] in 1997 and 19-17-0 [19% (w/w) N and 17% (w/w) P_2O_5] every year after) supplying $16 \text{ kg } P_2O_5 \text{ ha}^{-1} \text{ yr}^{-1}$ was applied with all maize plantings. Since its establishment, the Prairie has never received any fertilizer or manure additions. In all treatments except the Prairie, K, pH, other fertility attributes, weeds, pests and pathogens are managed to optimize productivity following university guides. Each of the 48 WQFS treatment plots contains a large in-ground drainage lysimeter (24 x 9 m) constructed as bottomless box with bentonite slurry walls extending to glacial till (1.5 m). Two, parallel plastic tiles (0.1 diameter) are installed in the longitudinal centers of the plots at 0.9 m below the soil surface. A collection tile only drains areas within each lysimeter while a companion tile drains plot area outside the lysimeter. Collection tiles drain into instrumentation huts where calibrated tipping buckets quantify drain flow volumes for each lysimeter. Data loggers automatically record the number of tips per bucket. Flow-proportional water samples were retrieved daily during flow events and were immediately transported to the laboratory and frozen (-10°C) if not analyzed within 24 hours. For additional details on the WQFS facility, equipment and routine analytical protocols, see Ruark et al. (2009) and Hernandez-Ramirez et al. (2011).

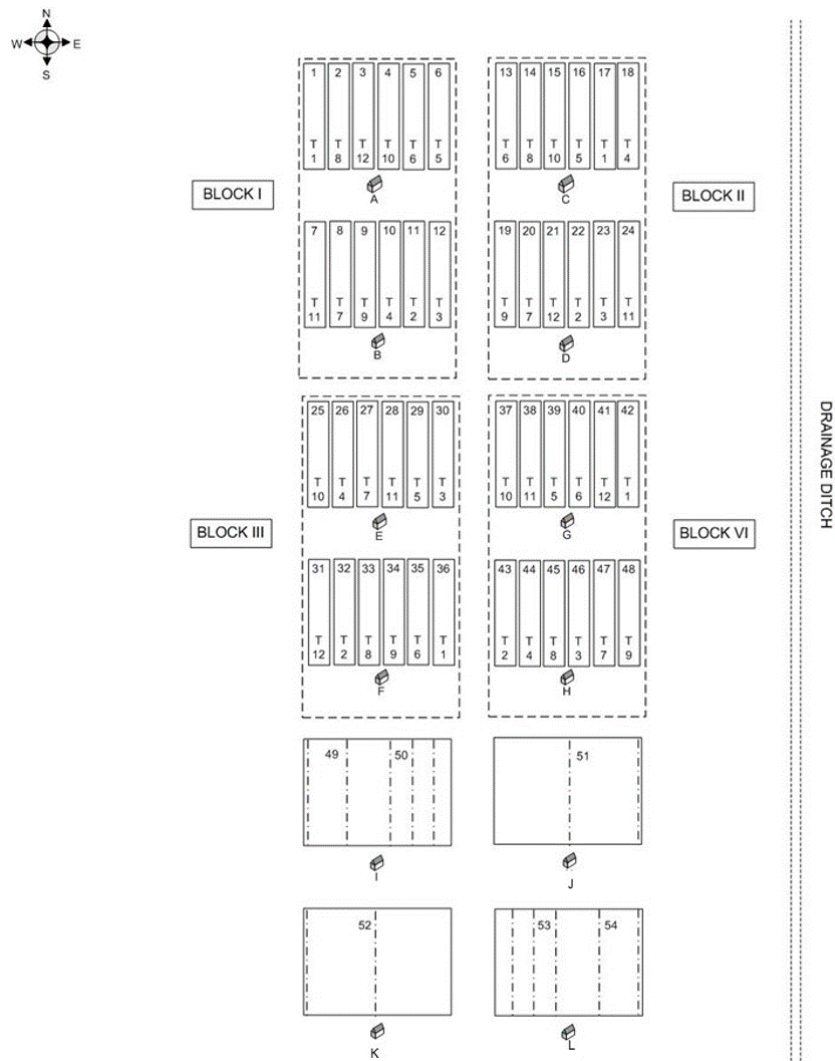


Figure A.1 A map showing the layout of plots at the Water Quality Field Station. The number at the top and bottom of each plot represents the plot and treatment number respectively. This study considered the 48 drainage lysimeter plots (plot number 1 - 48) only. Treatments 1 to 12 include; Native prairie mixture (Prairie), *Miscanthus x giganteus* (Mxg), continuous maize with residue removal (CM-RR), Switchgrass (Switch), continuous sorghum with residue removal (Sorgh), maize-soybean rotation trt#1 with residue return (MS-R1), soybean-maize rotation trt#1 with residue return (SM-R1), maize-soybean rotation trt#2 with residue return (MS-R2), soybean-maize rotation trt#2 with residue return (SM-R2), continuous maize with residue return and spring manure (CM-SpM), continuous maize with residue return and, fall manure (CM-FM) and continuous maize with residue return (CM) respectively (more details on previous crop, nutrient and tillage management can be found in Table S2 in the supplemental text). Letters A to H identify the instrumentation huts into which collection tiles drain. (Map obtained from; <https://ag.purdue.edu/agry/WQFS/Pages/map.aspx>)

Table A.2. A brief description of current Water Quality Field Station (WQFS) treatments (abbreviations and year of establishment), any previous treatment (cropping system and N rates applied to maize) dating back to 1997, and P, N and tillage management. An estimate of the cumulative P₂O₅ applied from 1997 – 2013 is shown parenthetically. Current N management identifies the N rates applied to perennial crops, sorghum, and continuous and rotated maize.

Current Treatment (abbrev. /yr. est.) [§]	Previous Treatment (maize N rate, kg ha ⁻¹ yr ⁻¹) [¶]	Plots [#]	P management (cumulative P ₂ O ₅ applied 1997-2013; kg ha ⁻¹) ^{††}	Current N management (annual rate, kg ha ⁻¹ yr ⁻¹)	Tillage
Native prairie mixture (Prairie /1993)	NA	1, 17, 36, 42	No fert. (0)	No fert. (0)	No till since 1993
<i>Miscanthus x giganteus</i> (Mxg /2008)	Annual soybean- maize rotation (180- P)	11, 22 , 32,43	Commercial fertilizer based on STP (180) + starter (80)	Spring broadcast urea (56)	No till since 2008
Continuous maize w/ residue removal (CM-RR /2008)	Continuous maize w/ residue return (202-P)	12, 23 , 30,46	Commercial fertilizer based on STP (265) + starter (272)	Preplant UAN (180) + starter	No till since 2008
Switchgrass var. Shawnee (Switch /2007)	Annual maize- soybean rotation (180-P)	10,18, 26,44	Commercial fertilizer based on STP (180) + starter (80)	Spring broadcast urea (56)	No till since 2007
Continuous sorghum w/ residue removal (Sorgh /2008)	Continuous maize w/ residue return (157-S)	6,16, 29,39	Commercial fertilizer based on STP + starter (176)	Preplant UAN (180)	Till
Maize-soybean rotation trt#1 w/ residue return (MS- R1 /1997)	NA	5, 13 , 35,40	Commercial fertilizer based on STP (265) + starter (144)	Preplant UAN (157) + starter	Till
Soybean-maize rotation trt#1 w/ residue return (SM-R1)	NA	8,20, 27,47	Commercial fertilizer based on STP (265) + starter (128)	Preplant UAN (157) + starter	Till
Maize-soybean rotation trt#2 w/ residue return (MS- R2 /1997)	NA	2,14, 33,45	Commercial fertilizer based on STP (265) + starter (144)	Sidedress UAN (135) + starter	Till
Soybean-maize rotation trt#2 w/ residue return (SM- R2 /1997)	NA	9 ,19, 34,48	Commercial fertilizer based on STP (265) + starter (128)	Sidedress UAN (135) + starter	Till
Continuous maize w/ residue return & spring manure (CM-SpM /1998)	NA	4,15, 25,37	16 yr annual spring swine effluent (approx. 1461) + starter (272)	Preplant swine effluent (avg. 255) + starter	Till
Continuous maize w/ residue return & fall manure (CM- FM /1998)	NA	7,24, 28, 38	14 yr annual fall swine effluent (approx. 1278) + starter (272)	Post-harvest swine effluent (avg. 255) + starter	Till
Continuous maize w/ residue return (CM /1997)	NA	3,21, 31, 41	Commercial fertilizer based on STP (265) + starter (272)	Preplant UAN (180) + starter	Till

[§] Treatments other than the Prairie were variable and not consistently maintained prior to 1997

[¶] N rates are only for the maize year in a rotation with P or S following the rate indicating a preplant or sidedress application. Not application (NA) indicates a treatment was maintained from 1997 – 2013.

[#] An italicized plot number indicates a tile line that ceased to function, and the plot was therefore eliminated from analysis of relationships between soluble P in drainage water and measures of soil P saturation.

^{††} Cumulative P₂O₅ added as commercial fertilizer differs among cropping systems as perennial crops did not receive applications. Cumulative starter P₂O₅ varies reflecting the number of times maize was grown on a specific treatment and includes current and previous systems. Cumulative P₂O₅ applied as manure differs as there were 16 spring applications but only 14 fall applications reflecting weather and termination of both manure treatments in fall 2013; quantities are based on an estimated amount of 91.3 kg P₂O₅ ha⁻¹ per application.

Flow and Orthophosphate Concentration Data: Cleaning, rectification, and gap filling

The flow data had been previously converted from hourly tip counts to flow volumes using calibration values unique to each tipping bucket and a statistical protocol and criteria were developed for identifying and eliminating from further analysis individual tiles suspected of failing to function properly (protocol and criteria described in supplemental information). For the timeframe of this study, one of the four replicate tiles in all but four treatments (CM-SpM, SM-R1, Sorgh and Switch retained four replicates, supplemental Table S3) was eliminated from analyses of relationships between annual flow-weighted DRP and PSR or SPSC. Outliers in the raw data (flow and concentration) were identified and adjusted using Tukey's 1.5 IQR rule (Seo et al., 2006) before their use.

The 5-year records of flow and orthophosphate concentration were evaluated individually for each of the 48 treatment tiles. The number of days with missing flow data for a specific treatment tile ranged between 1 – 62, 1 – 39, 1 – 33, 40 – 129 and 2 – 73 days (not necessarily consecutive days) in 2010, 2011, 2012, 2013 and, 2014 respectively (Supplemental Figure S6.2). These gaps were of two general reasons. The first reason for data loss was equipment failure/malfunction due to flooding damage, leaking tipping buckets, freezing conditions etc. The second major reason for loss was the intentional removal of data loggers for maintenance, construction etc. mostly during days when little to no flow was anticipated. Occasionally, maintenance and repairs lasted far longer than anticipated and/or weather forecasts for periods of dry conditions were inaccurate and, in general, intentional removal of data loggers and not their malfunction accounted for a greater proportion of missing data.

(a)

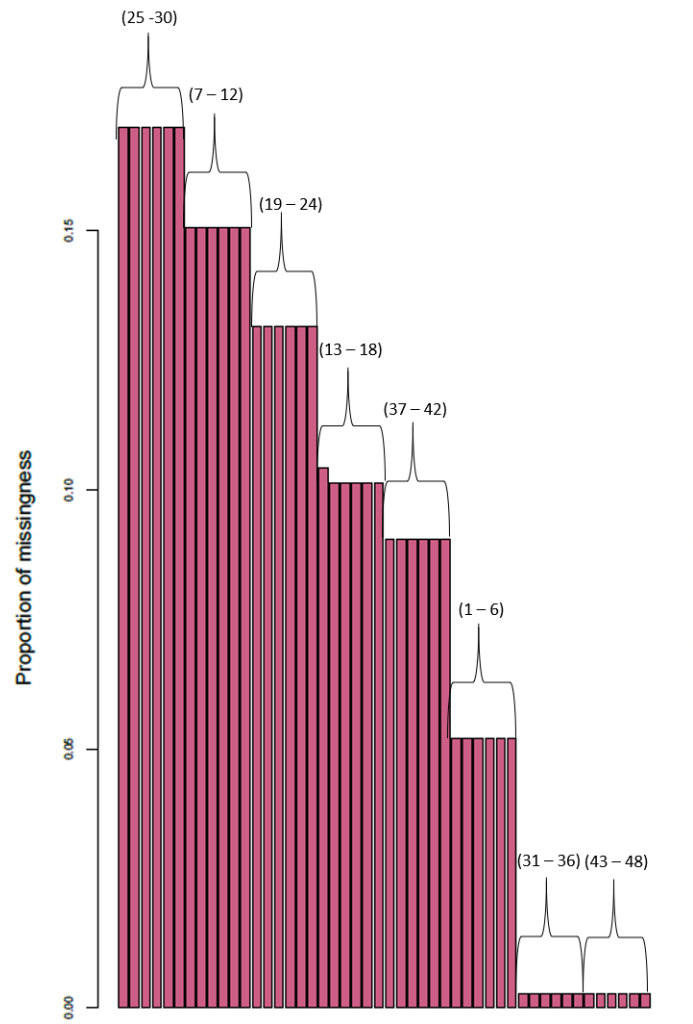


Figure A.2 Missing daily flow data

(a) A bar plot displaying the proportion missing daily flow data in each tile (tile numbers in parenthesis) for water year 2010 whereby, a proportion of 0 and 1 represents zero missing daily flow data and 365 (366 for leap year) missing daily flow data respectively.

Figure A.2 continued

(b)

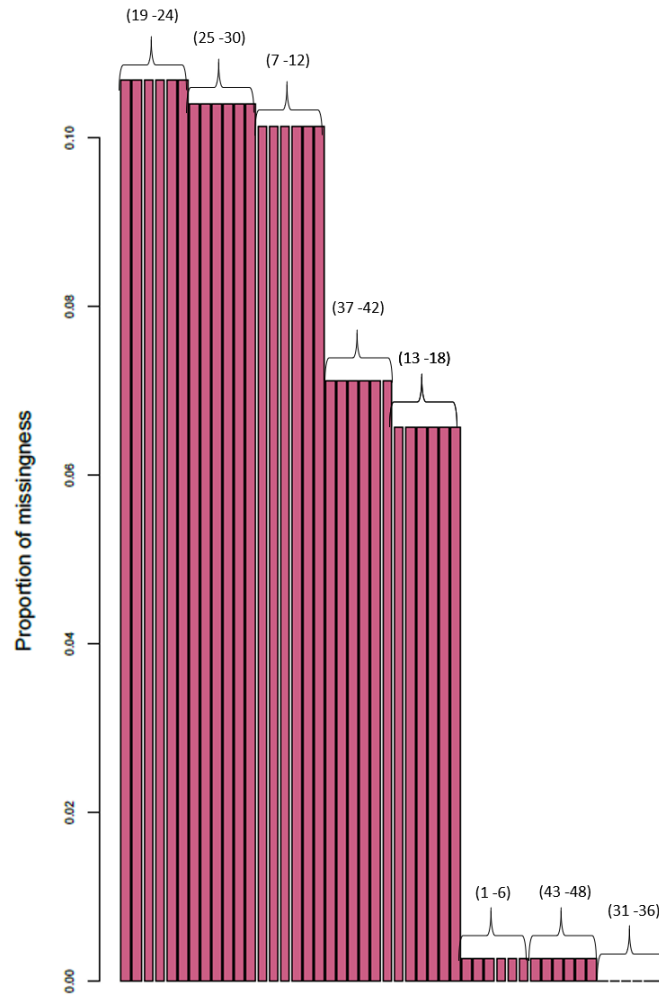


Figure S6.2 (b) A bar plot displaying the proportion missing daily flow data in each tile (tile numbers in parenthesis) for water year 2011 whereby, a proportion of 0 and 1 represents zero missing daily flow data and 365 (366 for leap year) missing daily flow data respectively.

Figure A.2 continued

(c)

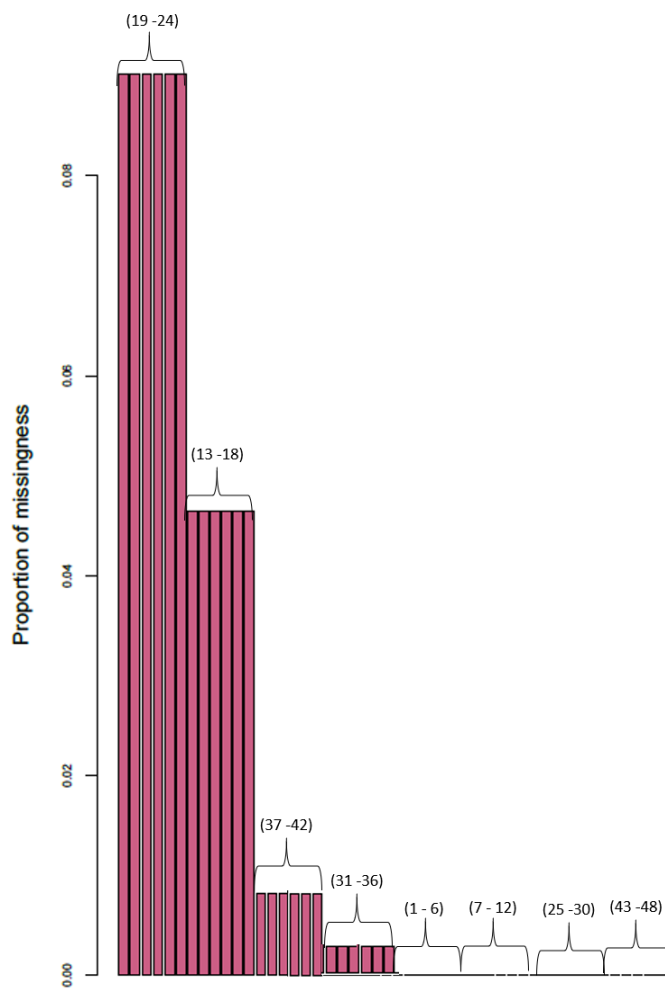
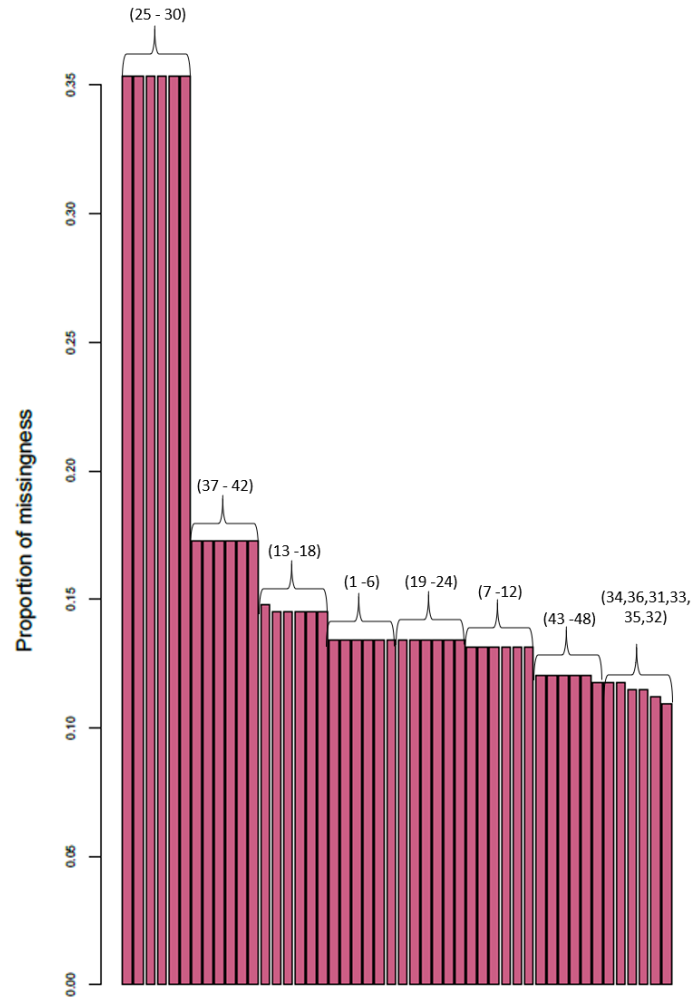


Figure S6.2 (c) A bar plot displaying the proportion missing daily flow data in each tile (tile numbers in parenthesis) for water year 2012 whereby, a proportion of 0 and 1 represents zero missing daily flow data and 365 (366 for leap year) missing daily flow data respectively.

Figure A.2 continued

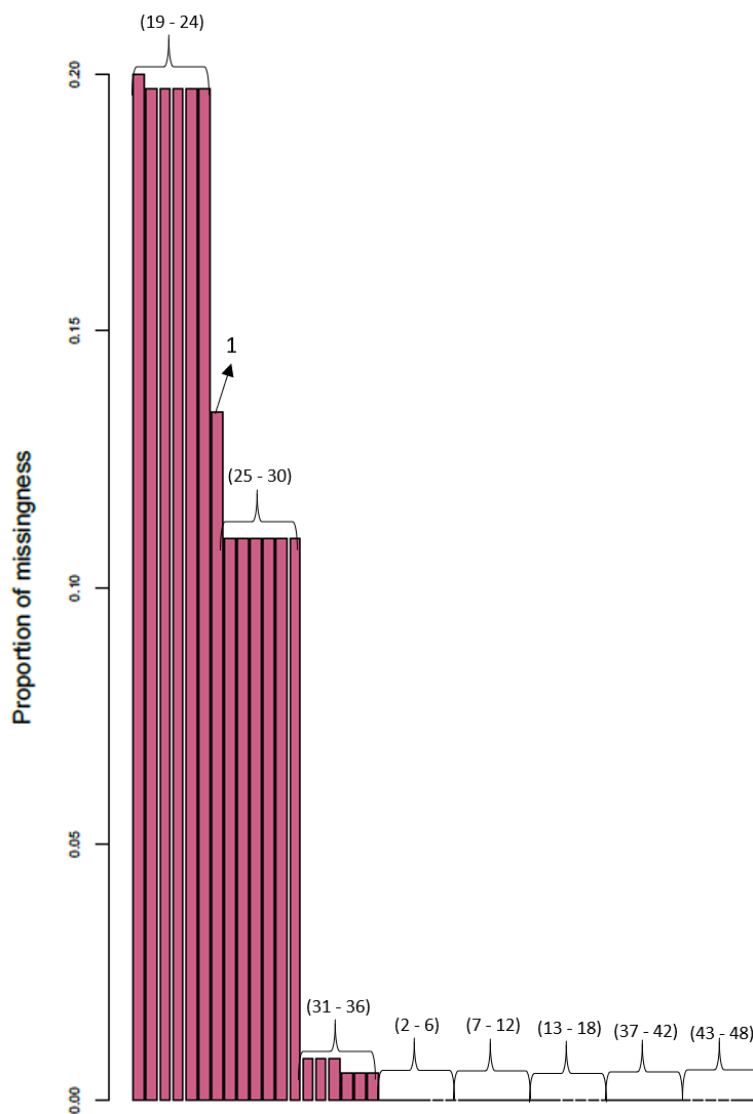
(d)



(d) A bar plot displaying the proportion missing daily flow data in each tile (tile numbers in parenthesis) for water year 2013 whereby, a proportion of 0 and 1 represents zero missing daily flow data and 365 (366 for leap year) missing daily flow data respectively.

Figure A.2 continued

(e)



(e) A bar plot displaying the proportion missing daily flow data in each tile (tile numbers in parenthesis) for water year 2014 whereby, a proportion of 0 and 1 represents zero missing daily flow data and 365 (366 for leap year) missing daily flow data respectively

Initial rectification of flow data involved cross-referencing data logger records with daily field notes and assigning zero flow when data loggers were inoperable, but field notes indicated a specific tile had “no flow (NF) and no sample (NS)” for a specific day. Then, for each treatment tile, univariate statistics for the 5-year (1826 days) record of flow data was used to identify specific

tiles that may no longer be functioning properly. Among the individual tiles the percent (%) of non-zero flow days ranged from 1% to 36% (Supplemental Table S6.3). Apart from corn/soybean rotation – switchgrass (Switch), continuous corn-sorghum (Sorgh), soybean/corn rotation 2 (SM-R2) and continuous corn spring manure (CM-SpM)) treatments, all other treatments had at least one of their replicates (plots/tiles) with < 91 days of flow data i.e. < 5% of the total days considered in this study. These plots (tiles) were numbers 2, 9, 13, 22, 23, 38, 41 and 42 (supplemental Table S6.3). A previous long-term (1997 – 2008) flow data and field log analysis also reported < 5% days with flow data for the same tiles and suggested 5% be the criteria for identifying failed tile function (Trybula 2012). In consequence, this study omitted data from these plots from further analysis.

For the 40 individual tiles remaining in the study, missing drainflows were accounted for as follows:

- 1) If missing data were because of a flooding event, Tukey's 1.5 Interquartile Range (IQR) rule ($[Q3 \text{ (Third quartile)} + 1.5] \times IQR$) (Tukey 1977) applied to the univariate statistical results was used as a conservative estimate of tile flow. The resulting value of the top whisker (outer fence), which ranged from 809 to 4618 L-1 day-1 plot-1 (supplemental Table S6.3) was assigned as the daily flow volume for each tile during any flooding event (six (6) flooding events; May 22 and June 22, 2010, April 20, May 31 and June 21, 2011 and, April 19, 2013),
- 2) If the missing period was < 1 day (24 hours), linear interpolation was done to gap fill the missing hours of data, and
- 3) When the missing period was > 1 day, auto-regressive integrated moving average (ARIMA) was used because flow data showed signs of non-stationarity due to the presence of seasonality.

Here we note, ARIMA has been employed in studies modeling seasonal time series data in hydrology since it performs preliminary differencing of data to make it stationary (Hyndman, 2014; Katimon et al., 2017; Nasir et al., 2017). The AR (auto regressive) and MA (moving averages) components of the model tailor it to the data i.e. the AR regresses the variable on its past values while MA represents model error as a linear combination of past error terms (Hyndman, Rob and Athanasopoulos 2014). The I (integrated) represents differencing a series to make it stationary i.e.

subtracting its current values from previous values (Hyndman, Rob and Athanasopoulos 2014). The `auto.arima` function in R was used (Hyndman, Rob and Athanasopoulos 2014).

Missing daily DRP concentrations and measured concentrations below detection limits were accounted for as follows:

- 1) For missing concentration not separated by more than 10 days of zero flow from a preceding or following recorded value, the recorded was assigned as the missing value,
- 2) For a missing concentration found between two recorded values (< 10 days before and after and separated by days with zero flow) was assigned their average,
- 3) A missing concentration separated by more than 10 days from a measured value was assigned the mean annual concentration for that tile, and
- 4) All negative concentrations (concentrations below the limit of detection (LOD, $0.002 \text{ mg P L}^{-1}$)) were substituted by the LOD divided by the square root of 2 ($^{\text{LOD}}/\sqrt{2}$) (Croghan and Egeghy 2003). There were no positive numbers below the limit of detection.

Outliers in the raw data (flow and concentration) were identified using Tukey's 1.5 IQR rule where anything above the outer fence ($[Q3 \text{ (Third quartile)} + 1.5] \times \text{IQR}$) is deemed a possible outlier (Seo et al., 2006; Tukey, 1977). This method was selected because of its simplicity and because it does not make any distributional assumptions (Loureiro et al. 2016). As the data were right-skewed, the lower fence ($[Q3 \text{ (Third quartile)} - 1.5] \times \text{IQR}$) was not considered. Outliers were re-adjusted to the value of the outside fence (supplement Table S6.3 & S6.4) for each tile before their use in the study.

Table A.3. Univariate statistics of daily tile discharge ($\text{L day}^{-1} \text{ plot}^{-1}$) from 2010 - 2014 for each of the 48 tiles in the 12 treatments. Shaded rows represent tiles omitted from the study due to tile failure as evidenced by the low number of flow of flow days ($< 5\%$ of total days studied). Italicized values represent outer fence values from Tukey's 1.5 IQR rule used to identify extreme outliers.

Treatment [†]	Plot #	Non-zero flow days	Mean	Std error	Std. Dev	Min	10th Percentile	1 st Quartile	Median	3 rd Quartile	90th Percentile	Max	Skewness	Kurtosis	Tukey's outer fence
(L day ⁻¹ plot ⁻¹)															
Prairie	1	105	335	49	500	1	2	17	71	501	1193	2311	2	2	1228
	17	130	1093	129	1472	1	2	36	466	1591	3198	7168	2	3	3923
	36	191	382	47	648	2	6	19	67	504	1226	3268	2	6	1231
	42	76	169	37	320	1	2	2	24	173	435	1638	3	8	431
Mxg	11	151	949	120	1469	1	3	28	242	1257	3168	7502	2	4	3100
	22	56	248	70	523	1	1	3	21	312	629	3449	4	23	776
	32	201	470	52	743	2	4	11	130	584	1487	3495	2	4	1444
	43	225	1053	93	1389	1	5	79	533	1469	2883	8846	2	6	3554
CM - RR	12	177	786	98	1304	1	2	19	192	934	2636	6701	2	6	2308
	23	43	132	41	267	1	1	2	6	119	393	1416	3	11	295
	30	243	489	57	891	1	2	9	42	609	1507	6064	3	11	1509
	46	297	375	41	709	1	1	5	66	355	1203	4326	3	8	880
Switch	10	157	1281	136	1702	1	6	73	577	1663	3519	9517	2	5	4048
	18	330	405	46	828	1	2	14	75	332	1174	6010	3	11	809
	26	256	1197	108	1733	1	4	56	414	1469	3639	8729	2	4	3589
	44	267	706	67	1099	2	5	51	218	859	2000	7344	3	7	2072
Sorgh	6	105	667	90	927	1	6	49	273	925	1827	5109	2	6	2239
	16	150	897	108	1324	1	2	22	253	1149	2732	8176	2	6	2841
	29	102	271	43	439	1	1	6	45	420	738	2495	2	7	1041
	39	362	565	51	976	2	3	10	91	666	1948	4761	2	5	1650
MS – R1	5	193	1283	111	1545	1	18	136	664	1723	3375	9054	2	4	4104
	13	23	62	18	87	1	1	3	21	84	203	267	1	0	206
	35	193	351	44	618	2	2	9	47	415	1166	3483	2	6	1024
	40	178	610	71	946	1	5	29	129	920	1951	7223	3	13	2258
SM – R1	8	191	226	33	453	1	1	8	42	200	863	3239	3	15	489
	20	124	586	111	1238	1	1	2	32	506	1926	9834	4	24	1261
	27	245	476	50	780	1	1	7	89	609	1522	4252	2	5	1511
	47	395	953	63	1249	1	8	110	489	1241	2537	7152	2	5	2937
MS – R2	2	68	566	112	920	1	1	3	207	795	1451	4664	3	8	1982
	14	146	888	96	1157	1	4	29	413	1361	2616	7087	2	5	3360

Table A.3 continued

	33	666	378	26	675	1	6	19	97	395	1108	5736	3	12	959
	45	427	639	47	970	1	3	23	204	858	1983	7609	2	8	2112
SM – R2	9	79	492	91	808	1	1	4	144	792	1371	5626	4	18	1974
	19	101	975	139	1394	1	2	68	423	1145	2822	8859	3	9	2760
	34	521	620	46	1054	2	8	38	194	680	1849	7332	3	11	1643
	48	152	850	93	1147	1	2	12	352	1340	2484	5068	2	2	3331
CM -SpM	4	137	1095	129	1511	1	2	42	495	1718	3119	9311	2	6	4231
	15	316	1459	117	2082	1	11	103	543	2095	4333	16332	3	9	5084
	25	345	1054	102	1898	1	7	33	201	1198	3536	12605	3	9	2946
	37	155	357	53	661	2	2	3	16	431	1091	3875	3	7	1074
CM - FM	7	120	1089	139	1524	1	1	12	405	1832	3143	9919	2	8	4563
	24	95	1191	155	1508	1	17	104	515	1910	3369	8410	2	4	4618
	28	159	601	83	1043	1	1	6	120	796	2018	7346	3	14	1981
	38	78	113	19	164	1	1	1	8	226	383	541	1	0	562
CM	3	144	1119	132	1585	1	9	37	430	1775	3221	9061	2	6	4381
	21	122	1119	136	1506	1	5	65	513	1447	3014	8878	3	9	3519
	31	214	728	71	1036	2	2	28	281	1032	2070	4769	2	3	2537
	41	80	206	37	329	1	1	4	31	330	655	1427	2	3	819

†Current treatment abbreviations: Prairie, native prairie mixture with residue removed; Mxg, *Miscanthus x giganteus* established in 2008 ; CM -RR, continuous maize with residue removal; Switch, Switchgrass established in spring 2007; Sorgh, continuous sorghum with residue removal established in 2008; MS – R1,maize-soybean rotation trt#1 w/residue return; SM-R1, soybean-maize rotation trt #1 w/residue return; MS – R2, maize-soybean rotation trt#2 w/residue return; SM-R2, soybean-maize rotation trt #1 w/residue return; CM -SpM, continuous maize with residue return and spring manure applications; CM-FM, continuous maize with residue return and fall manure applications; CM, continuous maize with residue return. More details on previous crop, nutrient and tillage management can be found in supplemental Table S6.2.

Table A.4 Univariate statistics of orthophosphate (DRP) concentrations ($\text{PO}_4^{3-} \text{ day}^{-1} \text{ plot}^{-1}$) from 2010 - 2014 for each of the forty-eight (48) tiles in the (12) treatments.

Treatment [‡]	Plot #	Days with conc.	Days with no conc.	Mean	Std error	Std Dev	Min	1 st Quartile	Median	3 rd Quartile	Max	Skewness	Kurtosis	Tukey's outer fence
(PO ₄ ³⁻ L ⁻¹ day ⁻¹ plot ⁻¹)														
Prairie	1	63	42	0.0123	0.0023	0.0185	0.0000	0.0034	0.0071	0.0138	0.1192	3.6207	15.9739	0.0294
	17	117	13	0.0215	0.0062	0.0670	0.0000	0.0042	0.0071	0.0160	0.6931	8.7478	83.7761	0.0337
	36	148	43	0.0177	0.0052	0.0632	0.0000	0.0040	0.0071	0.0071	0.6588	8.1459	73.9137	0.0118
	42	12	64	0.1068	0.0654	0.2267	0.0030	0.0212	0.0378	0.0656	0.8198	2.5575	5.1665	0.1322
Mxg	11	99	52	0.0664	0.0297	0.2953	0.0002	0.0040	0.0071	0.0192	2.1810	6.3655	40.4393	0.0420
	22	17	39	0.0284	0.0119	0.0492	0.0005	0.0070	0.0080	0.0220	0.1851	2.1831	3.7038	0.0445
	32	108	93	0.0120	0.0040	0.0416	0.0000	0.0022	0.0071	0.0071	0.4118	8.4031	76.1442	0.0145
	43	148	77	0.0130	0.0048	0.0585	0.0000	0.0030	0.0071	0.0071	0.6320	9.1629	88.0011	0.0133
CM -RR	12	118	59	0.0156	0.0022	0.0240	0.0000	0.0035	0.0071	0.1550	0.1550	3.2056	12.0460	0.3823
	23	8	35	0.0408	0.0116	0.0329	0.0000	0.0164	0.0326	0.0612	0.1010	0.5305	-1.2786	0.1284
	30	157	86	0.0103	0.0016	0.0205	0.0000	0.0049	0.0071	0.0071	0.2278	8.0894	78.6391	0.0104
	46	148	149	0.0175	0.0068	0.0824	0.0000	0.0031	0.0071	0.7590	0.7590	8.1513	66.4956	1.8929
Switch	10	106	51	0.0091	0.0011	0.0115	0.0000	0.0020	0.0071	0.0089	0.0601	2.5682	7.0800	0.0193
	18	171	159	0.0097	0.0014	0.0178	0.0000	0.0026	0.0071	0.0071	0.1560	5.5812	36.2600	0.0139
	26	179	77	0.0107	0.0016	0.0215	0.0000	0.0030	0.0071	0.0071	0.1837	5.3259	32.9125	0.0133
	44	198	69	0.0219	0.0104	0.1465	0.0000	0.0022	0.0071	0.0071	1.9040	11.4474	138.4656	0.0145
Sorgh	6	86	19	0.0081	0.0012	0.0109	0.0000	0.0020	0.0071	0.0071	0.0662	3.0616	10.5902	0.0148
	16	171	-21 [§]	0.0094	0.0025	0.0324	0.0000	0.0028	0.0071	0.0071	0.4177	11.7489	144.5102	0.0136
	29	14	88	0.1495	0.0573	0.2145	0.0000	0.0071	0.0106	0.2326	0.6240	1.0680	-0.4351	0.5709
	39	182	180	0.0108	0.0037	0.0494	0.0000	0.0039	0.0071	0.0071	0.6680	12.9284	168.9077	0.0119
MS - R1	5	145	48	0.0134	0.0059	0.0705	0.0000	0.0030	0.0071	0.0071	0.8450	11.3243	130.3815	0.0133
	13	1	22	0.0000	—	—	0.0000	0.0000	0.0000	0.0000	0.0000	—	—	0.0000
	35	98	95	0.0089	0.0032	0.0314	0.0000	0.0020	0.0071	0.0071	0.3103	9.0734	84.0242	0.0148
	40	116	62	0.0193	0.0064	0.0687	0.0000	0.0050	0.0071	0.0149	0.7326	9.6652	97.0223	0.0298
SM - R1	8	80	111	0.0270	0.0084	0.0748	0.0000	0.0047	0.0071	0.0142	0.6224	6.4641	47.4688	0.0285
	20	49	75	0.0281	0.0122	0.0855	0.0007	0.0043	0.0092	0.0200	0.6007	6.1236	37.9947	0.0436
	27	155	90	0.0124	0.0033	0.0410	0.0000	0.0028	0.0071	0.0071	0.4350	8.1122	74.3631	0.0136
	47	248	147	0.0102	0.0028	0.0435	0.0000	0.0040	0.0071	0.0071	0.6793	14.6800	222.1478	0.0118
MS - R2	2	32	36	0.0239	0.0071	0.0401	0.0000	0.0019	0.0071	0.0217	0.1583	2.0419	3.2190	0.0514
	14	98	48	0.0087	0.0012	0.0123	0.0000	0.0023	0.0071	0.0071	0.0938	4.2592	23.3419	0.0143
	33	316	350	0.0131	0.0047	0.0828	0.0000	0.0030	0.0071	0.0071	1.4312	16.0769	269.8663	0.0133

Table A.4 continued

	45	230	197	0.0124	0.0036	0.0553	0.0000	0.0020	0.0071	0.0760	0.7844	12.2585	163.7676	0.1870
	9	38	41	0.0188	0.0055	0.0336	0.0000	0.0053	0.0071	0.0185	0.1810	3.6662	13.5665	0.0383
SM – R2	19	78	23	0.0195	0.0023	0.0200	0.0000	0.0071	0.0130	0.0240	0.0976	1.8827	3.2711	0.0494
	34	287	234	0.0087	0.0012	0.0210	0.0000	0.0029	0.0071	0.0071	0.2860	9.7302	112.6247	0.0134
	48	85	67	0.0173	0.0085	0.0783	0.0000	0.0040	0.0071	0.0076	0.7231	8.6254	74.7594	0.0130
	4	85	52	0.0770	0.0129	0.1189	0.0003	0.0090	0.0297	0.0790	0.6360	2.5144	6.4988	0.1840
CM - SpM	15	206	110	0.0166	0.0018	0.0252	0.0000	0.0057	0.0071	0.0154	0.1601	3.2931	12.2072	0.0300
	25	222	123	0.0236	0.0034	0.0506	0.0000	0.0040	0.0071	0.0158	0.3706	4.1684	19.9547	0.0335
	37	48	107	0.0789	0.0139	0.0965	0.0000	0.0086	0.0410	0.1075	0.4389	1.7738	3.0610	0.2559
	7	62	58	0.1907	0.0274	0.2154	0.0013	0.0550	0.1287	0.2320	1.0590	2.2549	5.3988	0.4975
CM - FM	24	77	18	0.0978	0.0136	0.1190	0.0000	0.0231	0.0533	0.1081	0.5990	1.9339	3.7070	0.2356
	28	84	75	0.1052	0.0142	0.1303	0.0000	0.0196	0.0598	0.1404	0.5802	1.9730	3.5699	0.3216
	38	9	69	0.3150	0.1146	0.3439	0.0000	0.1300	0.2207	0.3834	1.1448	1.4082	0.9018	0.7635
	3	94	50	0.0153	0.0059	0.0573	0.0000	0.0029	0.0071	0.0071	0.5517	8.7189	78.4339	0.0134
CM	21	83	39	0.0177	0.0033	0.0303	0.0000	0.0055	0.0082	0.0170	0.2430	5.2804	34.5444	0.0343
	31	129	85	0.0131	0.0033	0.0370	0.0000	0.0038	0.0071	0.0071	0.3434	7.2978	56.9091	0.0121
	41	21	59	0.00	0.0361	0.1653	0.0000	0.0071	0.0261	0.0760	0.7635	3.3321	10.9337	0.1794

*Current treatment abbreviations: Prairie, native prairie mixture with residue removed; Mxg, *Miscanthus x giganteus* established in 2008 ; CM -RR, continuous maize with residue removal; Switch, Switchgrass established in spring 2007; Sorgh, continuous sorghum with residue removal established in 2008; MS – R1,maize-soybean rotation trt#1 w/residue return; SM-R1, soybean-maize rotation trt #1 w/residue return; MS – R2, maize-soybean rotation trt#2 w/residue return; SM-R2, soybean-maize rotation trt #1 w/residue return; CM -SpM, continuous maize with residue return and spring manure applications; CM-FM, continuous maize with residue return and fall manure applications; CM, continuous maize with residue return. More details on previous crop, nutrient and tillage management can be found in supplemental Table S2[§]A negative value resulted from there being days with recorded concentrations but missing flow data

Table A.5 Selected univariate statistic for the 73 archived soils samples used in the P sorption study including the phosphorus sorption index (PSI) and analytical results from routine analyses conducted in a commercial soil testing laboratory.

Variable ^{‡‡}	mean	Std. dev	median	min	max	Range
PSI (L kg ⁻¹)	509.7	39.9	503.9	419.4	597.6	178.3
OM (%)	3.1	1.4	2.8	0.9	6.1	5.2
P (mg kg ⁻¹)	44.4	25.6	38.0	1.0	104.0	103.0
K (mg kg ⁻¹)	104.1	45.3	98.0	35.0	213.0	178.0
Mg (mg kg ⁻¹)	443.7	252.7	317.0	144.0	867.0	723.0
Ca (mg kg ⁻¹)	1888.2	971.2	1532.0	611.0	3647.0	3036.0
pH _(water)	6.4	0.5	6.0	4.4	7.2	2.8
CEC (cmolc kg ⁻¹)	16.2	8.1	14.1	5.6	31.0	25.4
Fe (mg kg ⁻¹)	164.3	44.6	159.0	101.0	327.0	226.0
Al (mg kg ⁻¹)	700.1	138.5	719.0	323.0	991.0	668.0

‡‡ Variable analytical details: PSI is estimated as described by Bache and Williams (1971); soil test P and macronutrient cations are from Mechlich 3-ICP analysis, pH was determined in water, OM was determined as described by Watson and Brown (2011) after organic carbon determination by the Walkley-Black procedure (Walkley, 1947; Walkley and Black, 1934), and CEC was estimated by summing the milliequivalent (meq) exchangeable bases per 100 g (cmolc kg⁻¹) and the milliequivalent (meq) exchangeable acidity per 100 g (cmolc kg⁻¹).

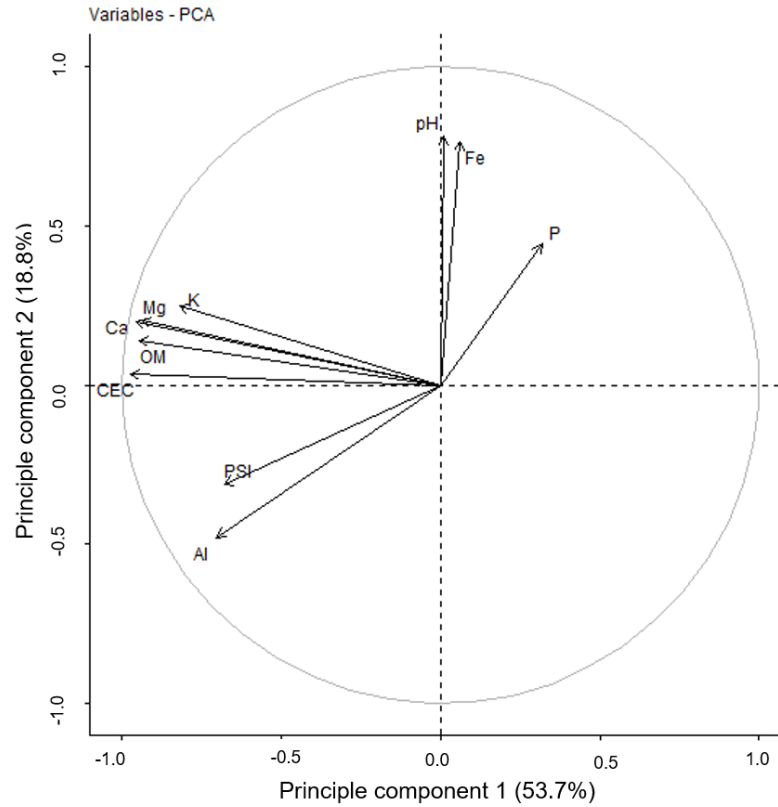


Figure A.3 Unit circle resulting from principle component analysis of the different variables for the selected 73 soils. Relative positions of routinely determined soil test data (organic matter (OM), phosphorus (P), potassium (K), magnesium (Mg), calcium (Ca), log of H^+ concentrations (pH), cation exchange capacity (CEC), iron (Fe), aluminum (Al)) in the circle indicate the magnitude of direct association between these soil properties and phosphorus sorption index (PSI). Percentage value in parenthesis is the proportion of the total variance accounted for by each principle axis.

Table A.6 Change point values for the fitted nonlinear relationship between phosphorus saturation ratio (PSR) and water-soluble phosphorus (WSP) after removal of a random site's soils during statistical analysis (***)significant at $P \leq 0.001$)

Omitted site	Change point	R ²
DEPAC	0.21	0.68
NEPAC	0.21	0.74
PPAC	0.23	0.77
SEPAC	0.21	0.66
TPAC	0.21	0.61
WQFS	0.19	0.67

Table A.7 Values for organic matter (OM), phosphorus (P), aluminum (Al), P saturation ratio (PSR), and soil P storage capacity (SPSC) for surface soils (20 cm) obtained from the monitored plots at the Water Quality Field Station (WQFS) for 2011 -2013 water years (e.g. October 1, 2010 – September 30, 2011 for 2011 water year).

Current treatment (abbrev)	Plot no.	2011 water year					2012 water year					2013 water year				
		OM	P	Al	PSR	SPSC	OM	P	Al	PSR	SPSC	OM	P	Al	PSR	SPSC
Native prairie mixture (Prairie)	1	4.8	27	846	0.23	-12.02	5.1	26	860	0.22	-9.46	5.3	29	845	0.23	-14.54
	17	4.7	23	758	0.22	-5.55	4.7	26	821	0.23	-10.68	5.3	24	855	0.22	-5.26
	36	4.9	14	788	0.18	19.06	4.2	11	785	0.17	28.87	5	16	820	0.19	13.31
<i>Mixcanthus x giganteus</i> (Mxg)	11	4.6	26	900	0.22	-10.04	5	24	922	0.22	-5.10	5.4	25	895	0.22	-6.61
	32	3.3	9	734	0.16	35.01	3.1	8	798	0.15	41.03	3.6	8	753	0.15	41.81
	43	4.2	13	767	0.18	20.63	3.7	12	811	0.17	23.76	4.1	11	770	0.17	28.37
Continuous maize w/residue removal (CM – RR)	12	5.3	27	862	0.23	-10.89	5.2	32	969	0.24	-18.34	5.6	26	932	0.22	-7.79
	30	4.1	11	927	0.17	30.73	4.2	12	934	0.17	26.88	4.5	21	932	0.21	0.44
	46	4.9	22	846	0.21	-1.93	4.3	17	916	0.20	10.03	5.4	25	906	0.22	-6.50
Switchgrass var. Shawnee (Switch)	10	4.8	22	810	0.21	-2.57	5	22	883	0.21	-1.30	5.4	23	889	0.21	-2.61
	18	5	23	810	0.22	-4.30	4.9	17	838	0.20	10.41	4.9	14	805	0.18	19.31
	26	3.6	15	816	0.19	12.91	3.8	11	801	0.17	28.04	4	10	779	0.16	32.78
	44	4.4	16	816	0.19	11.90	4.2	11	824	0.17	29.47	4.8	13	787	0.18	22.37
Continuous sorghum w/residue removal (Sorgh)	6	3.7	15	843	0.19	13.55	3.9	17	859	0.20	8.31	4.6	32	888	0.24	-20.21
	16	4.2	25	821	0.22	-9.89	4.8	37	806	0.25	-27.60	4.7	36	751	0.25	-27.03
	39	4.6	34	860	0.24	-23.40	4.5	31	916	0.24	-18.62	4.8	28	869	0.23	-13.53
Maize-soybean rotation trt #1 w/residue return (MS – R1)	5	3.8	16	839	0.19	10.69	3.7	16	875	0.19	10.88	4.4	28	944	0.23	-13.64
	35	3.7	12	809	0.17	23.73	3	12	793	0.18	21.35	3.7	16	825	0.19	10.23
	40	5.1	33	888	0.24	-20.74	5.2	33	840	0.24	-21.03	5.1	28	915	0.23	-12.49
Soybean-maize rotation trt#1 w/residue return (SM – R1)	8	4.9	20	882	0.21	3.10	4.8	23	896	0.22	-3.72	5.5	27	934	0.22	-9.79
	20	5.3	31	886	0.23	-17.37	5.7	31	854	0.23	-17.01	6	33	839	0.24	-19.75
	27	3.7	16	831	0.19	10.31	3.4	11	788	0.17	26.68	4	11	760	0.17	27.95
	47	4.1	20	814	0.21	0.47	4.7	15	815	0.19	15.68	4.9	19	883	0.20	5.60
Maize-soybean rotation trt#2 w/residue return (MS – R2)	14	4.8	27	849	0.23	-11.99	4.9	24	856	0.22	-6.02	4.8	32	846	0.24	-20.22
	33	3	10	802	0.16	30.16	3.1	11	761	0.17	25.32	3.3	12	827	0.18	22.82
	45	4.3	25	849	0.22	-9.35	3.9	21	809	0.21	-2.43	4.6	20	794	0.21	1.38
Soybean-maize rotation trt#2 w/residue return (SM – R2)	19	4.9	41	904	0.25	-31.51	4.6	51	922	0.27	-42.53	5.3	52	888	0.27	-42.53
	34	3.3	11	811	0.17	26.73	3	10	756	0.17	29.42	3.5	17	781	0.20	6.19
	48	4.6	26	782	0.23	-11.33	3.6	25	727	0.23	-12.50	5	26	778	0.23	-10.58

Table A.7 continued

Continuous maize	4	4.3	59	815	0.28	-50.85	4.8	83	811	0.31	-66.38	4.6	92	833	0.31	-71.53
w/residue return &	15	4.6	89	836	0.31	-69.92	4.5	79	769	0.30	-64.76	4.7	104	818	0.32	-77.34
spring manure (CM -	25	4.1	74	824	0.30	-62.04	4.2	91	763	0.32	-72.07	3.9	73	776	0.30	-62.11
SpM)	37	4.3	56	786	0.28	-48.57	3.9	68	774	0.30	-58.74	4.9	64	803	0.29	-53.79
Continuous maize	7	5.4	62	849	0.28	-51.20	5.1	88	932	0.31	-68.23	5.5	76	995	0.29	-60.27
w/residue return & fall	24	4.9	59	836	0.28	-49.64	5.1	73	785	0.30	-59.94	5.5	81	827	0.30	-64.18
manure (CM – FM)	28	3.4	38	819	0.26	-31.95	3.5	41	782	0.26	-35.62	4.1	41	813	0.26	-33.87
Continuous maize	3	3.8	20	846	0.21	0.09	4.8	26	967	0.22	-8.96	4.4	28	918	0.23	-13.89
w/residue return (CM)	21	5.1	43	888	0.26	-33.60	5	48	906	0.26	-38.99	5.6	50	915	0.27	-39.99
	31	3.7	13	819	0.18	20.06	3.8	13	774	0.18	19.68	4.2	16	822	0.19	11.50

Precipitation, discharge, and tile drain efficiencies

Over the 3 water years examined at the WQFS, average annual precipitation was 836 mm, which is slightly lower than the long-term (30-year) average precipitation of 939.8 mm in Northern Indiana (Scheeringa 2002). On average, 20%, 12% and, 8% of annual precipitation was discharged as tile flow in 2011, 2012 and 2013 with tile drain efficiencies ranging between 0 to 59% (discharge (Q)/rainfall (P); Supplemental Table S6.8). These tile drain efficiencies are similar to others reported in the Midwest United States (13 % to 37 % at same site; Ruark, 2006 and 11 % to 87 % in Ohio; King et al., 2016). Since snowmelt data were unavailable, they were not included in the calculations of tile drain efficiency. Therefore, years with significant snowmelt may have resulted in overestimation of Q/P values. Tile flow from all plots exhibited a pattern of high flow events during winter and spring months compared to summer months (supplemental Figure S6.4). This pattern is common in the region and it has been attributed to the interaction among rainfall, infiltration, evapotranspiration and runoff (Gentry et al., 2007; Williams et al., 2015).

In all tiles, standard deviations exceeded the means (Supplemental Table S6.3), signifying high flow variability. Tile flows had positively skewed distributions indicating a tendency for low daily flow events to outnumber high daily flow events and the strong influence of unusually large flow events (extended right tail). This distribution is common in flow data due to a left bound of zero (no negative flow) and the presence of high outliers (Pagano and Garen, 2004; Tomer et al., 2003; Gotway et al., 1994).

Table A.8 Annual tile flow and tile drainage efficiencies (Q/P) for tiles in the study plots.

Plot/Tile	Water years					
	2011		2012		2013	
	Annual tile flow (m ³)	Q/P [¶] (%)	Annual tile flow (m ³)	Q/P [¶] (%)	Annual tile flow (m ³)	Q/P [¶] (%)
1	10	5	5	3	6	2
3	48	23	27	14	19	8
4	45	21	22	11	27	11
5	60	29	36	18	29	12
6	15	7	0	0	13	6
7	50	24	16	8	11	5
8	8	4	3	1	3	1
10	52	25	28	14	27	11
11	44	21	26	13	25	10
12	36	17	19	9	15	6
14	27	13	20	10	17	7
15	123	59	81	41	58	25
16	45	22	28	14	20	8
17	0	0	40	20	27	11
18	19	9	14	7	12	5
19	58	28	15	8	19	8
20	36	17	7	4	4	2
21	38	18	20	10	16	7
22	36	17	20	10	25	10
25	80	39	36	18	38	16
26	79	38	50	25	40	17
27	32	15	6	3	7	3
28	29	14	14	7	12	5
30	14	6	13	7	9	4
31	41	20	25	13	19	8
32	20	9	13	7	12	5
33	41	20	25	13	26	11
34	61	29	33	17	31	13
35	13	6	9	5	6	3
36	23	11	14	7	13	6
37	16	7	6	3	5	2
39	31	15	22	11	14	6
40	25	12	15	8	11	5
43	82	39	41	21	35	15
44	57	27	28	14	0	0
45	62	30	29	15	33	14
46	17	8	10	5	11	5
47	116	56	64	32	44	19
48	50	24	12	6	40	17
Avg.	42	20	23	12	20	8

Q/P = annual discharge to rainfall ratio with rainfall of 209, 197 and, 236 m³ in 2011, 2012 and 2013 respectively

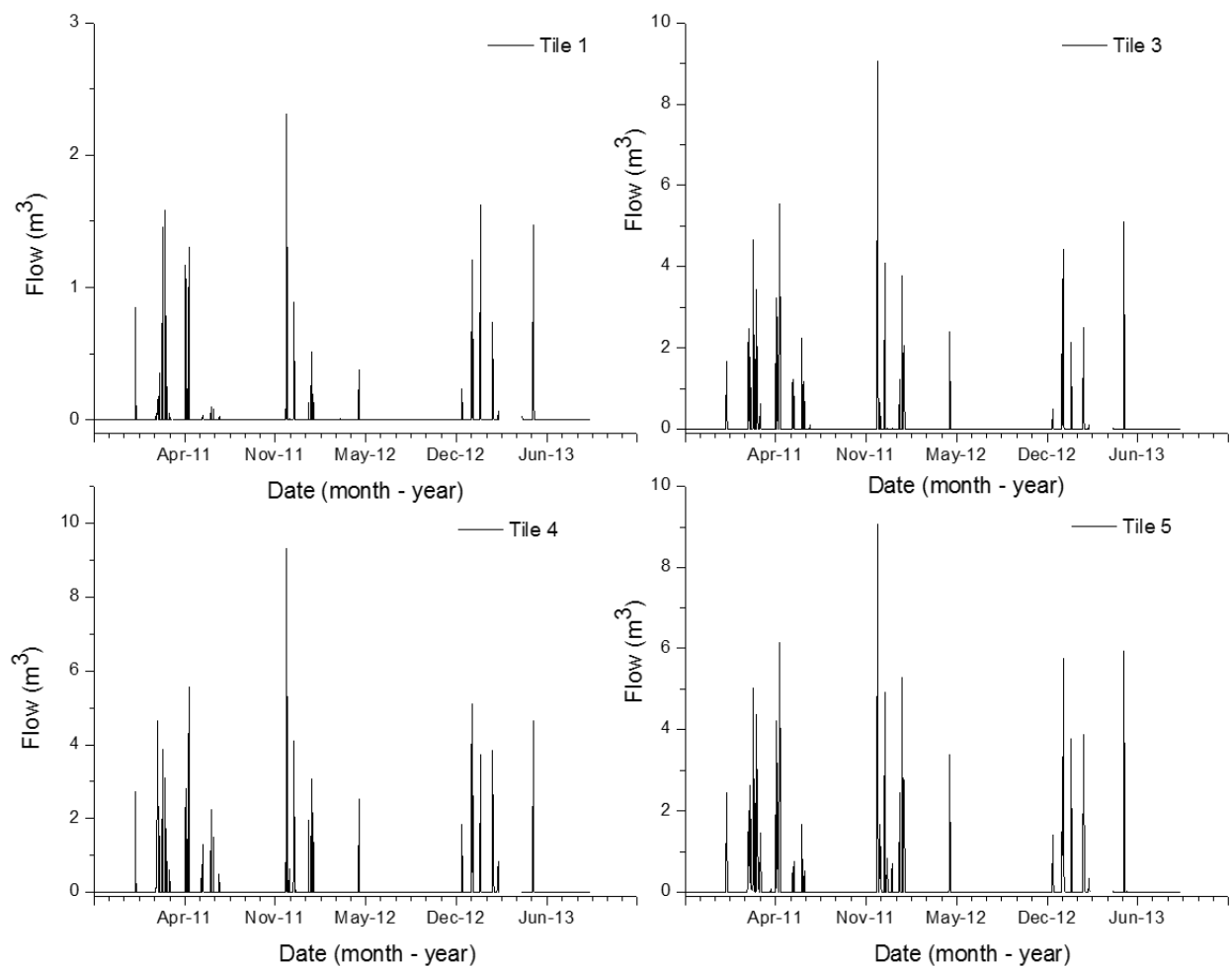


Figure A.4 Daily tile flow/discharge (m^3) from individual plots for the study period (beginning Oct 1, 2010 and ending on Sept 30, 2013). Gaps in graphs are a result of missing data either due to maintenance, flooding or equipment failure/error

Figure A.4 continued

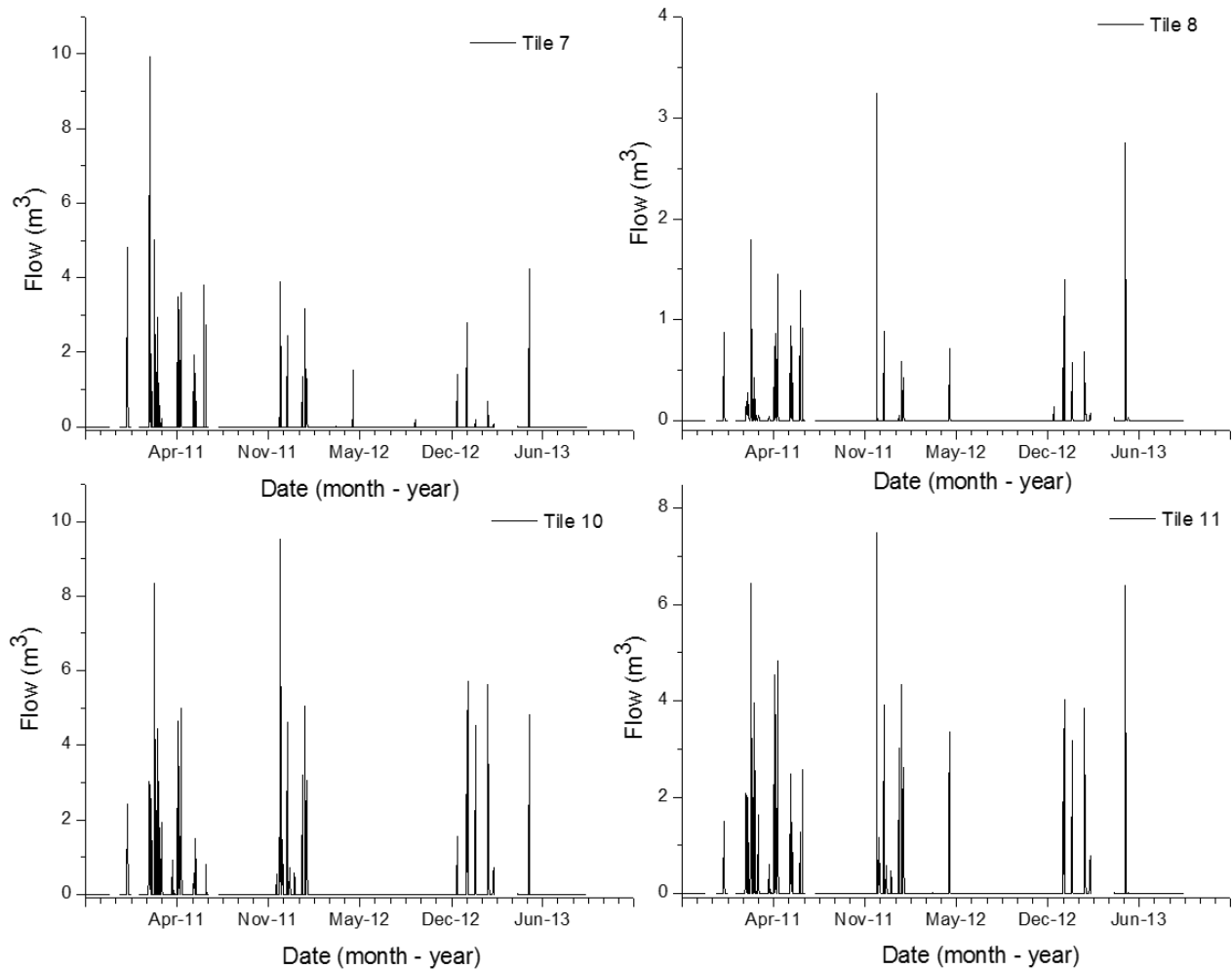


Figure A.4 continued

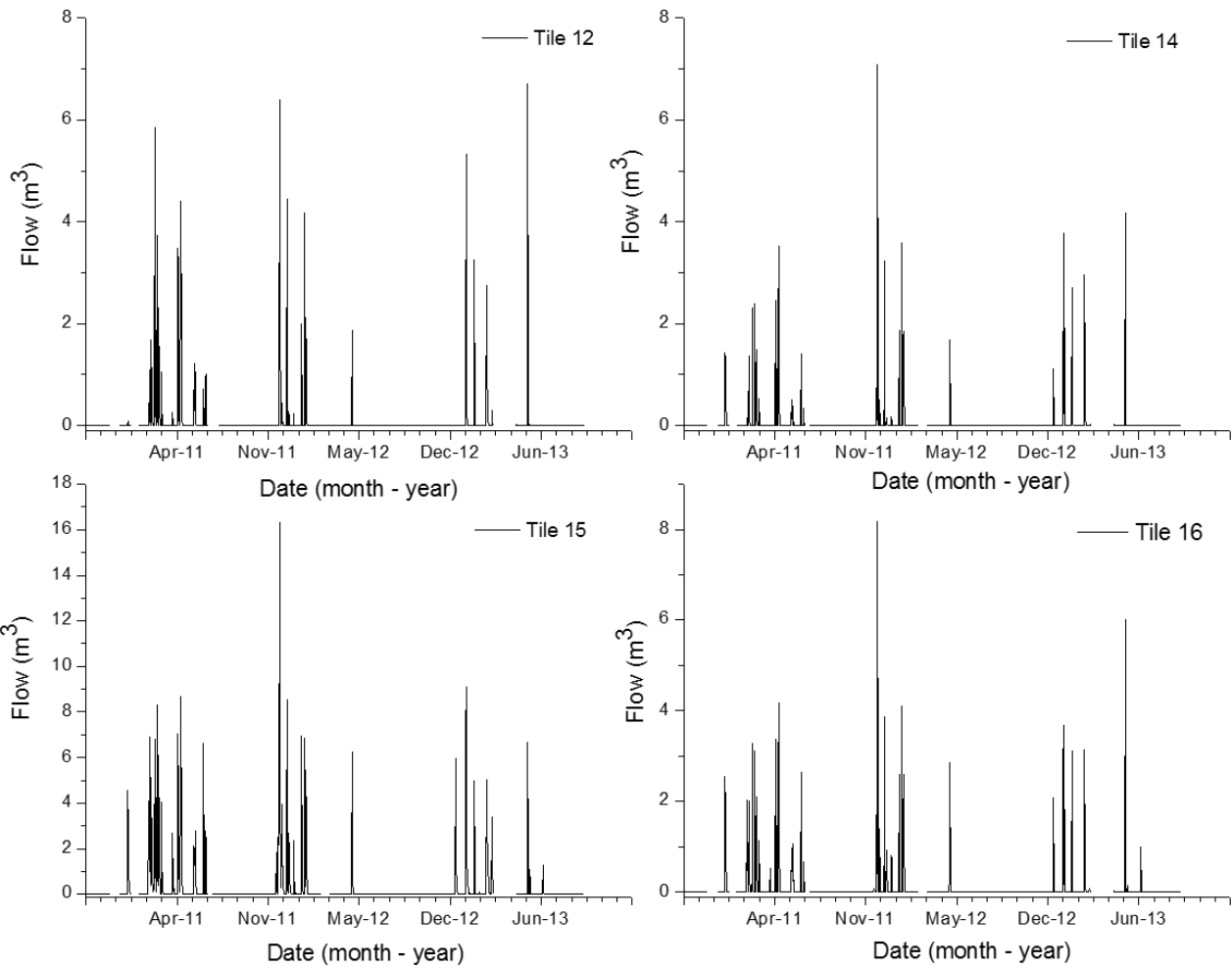


Figure A.4 continued

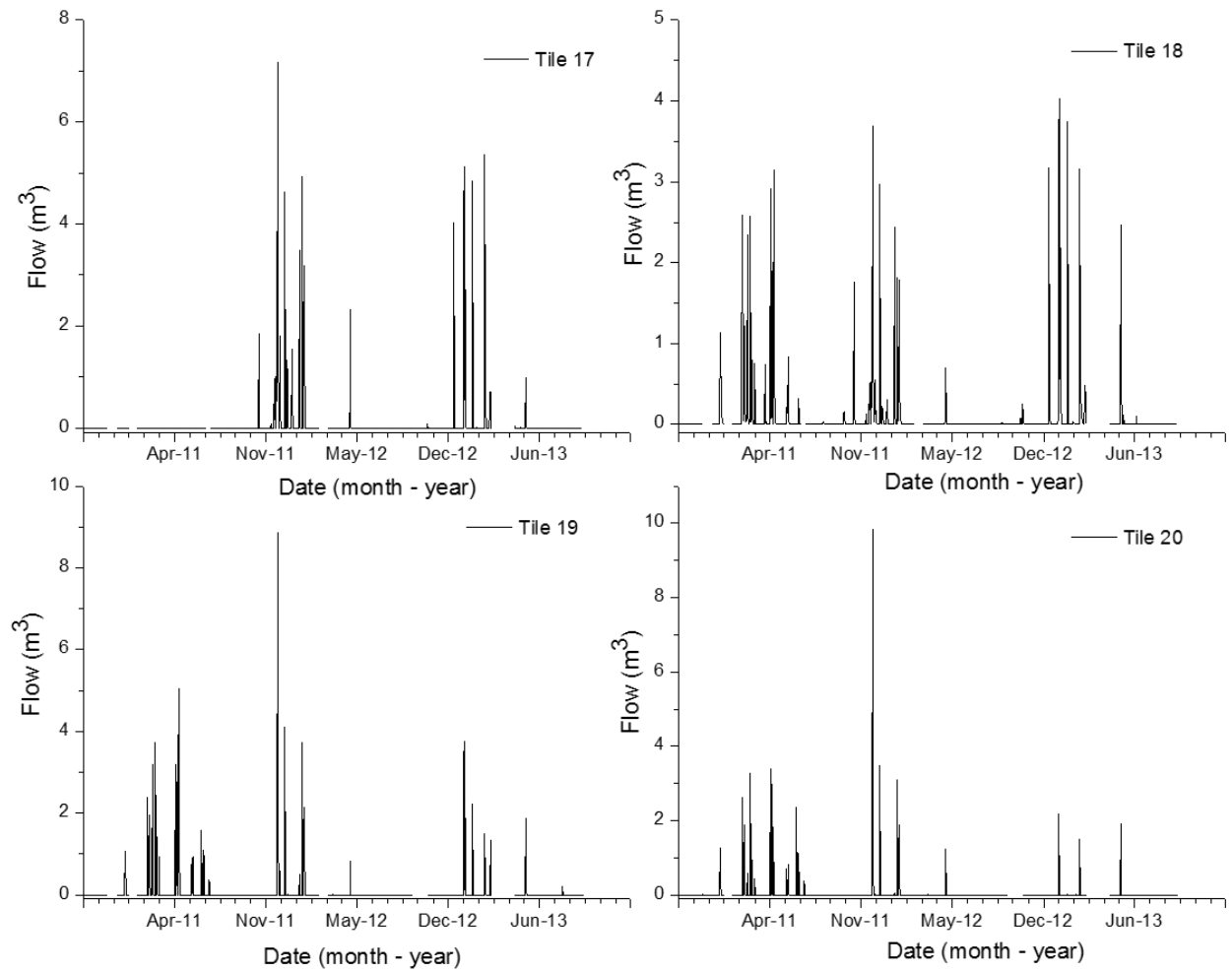


Figure A.4 continued

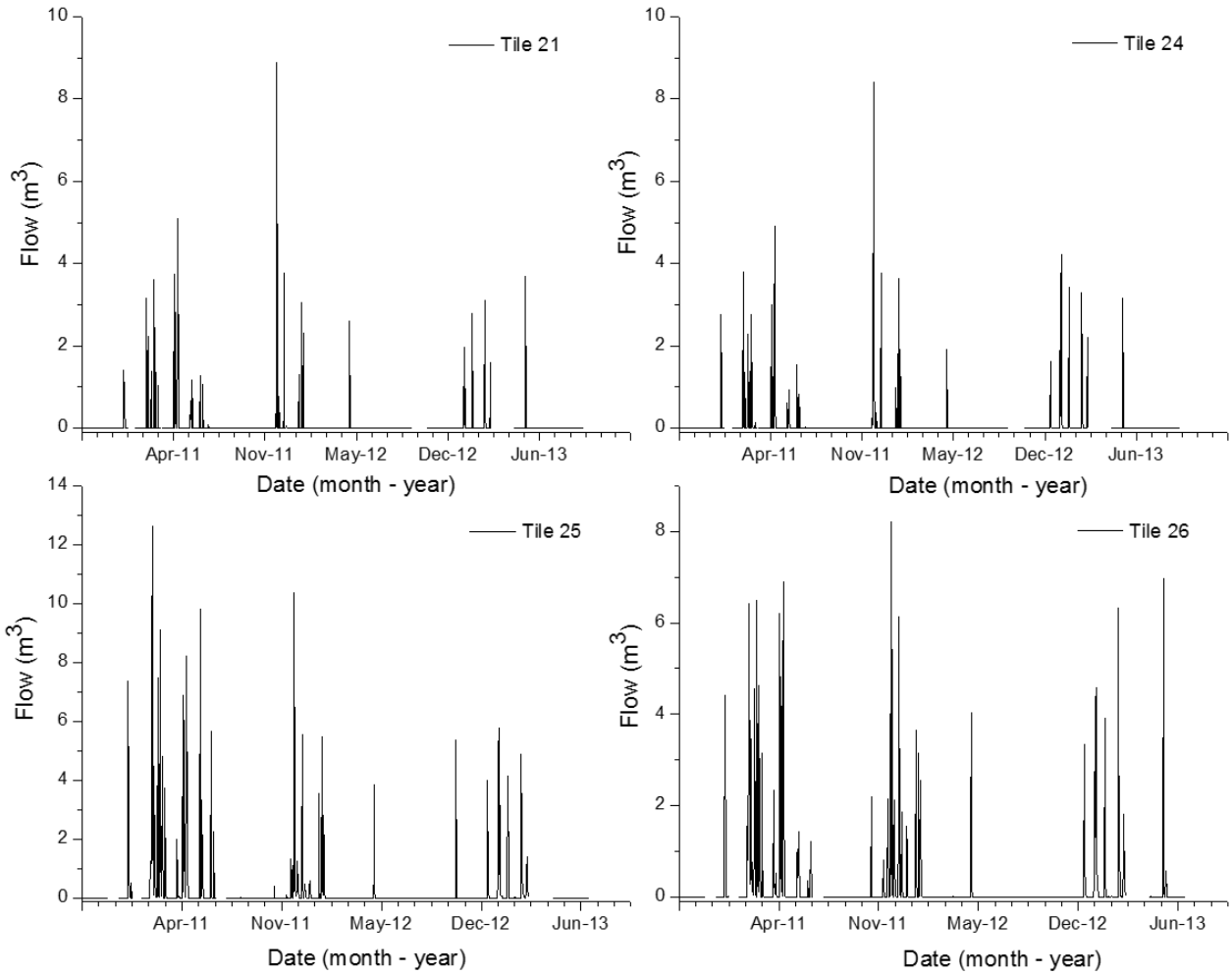


Figure A.4 continued

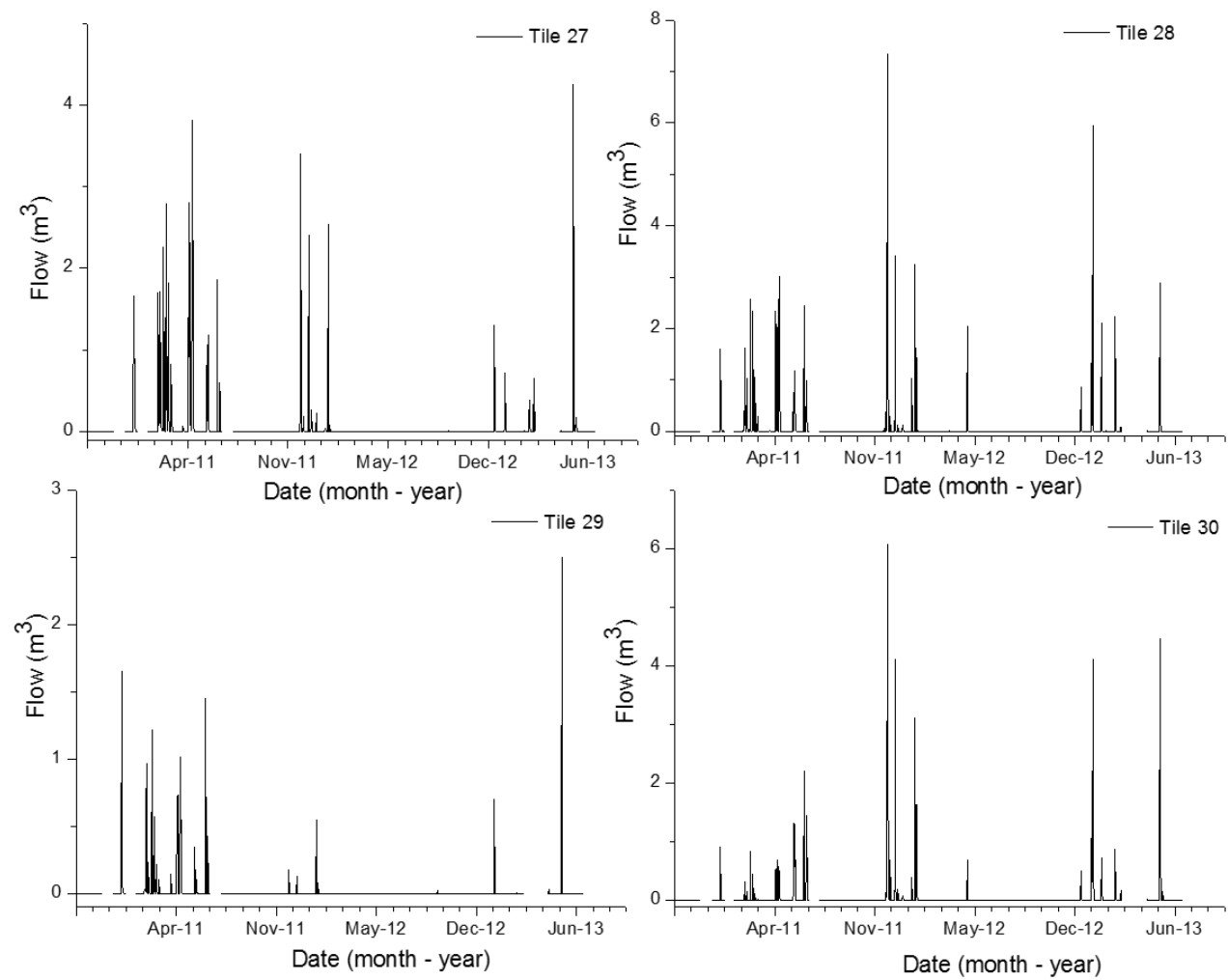


Figure A.4 continued

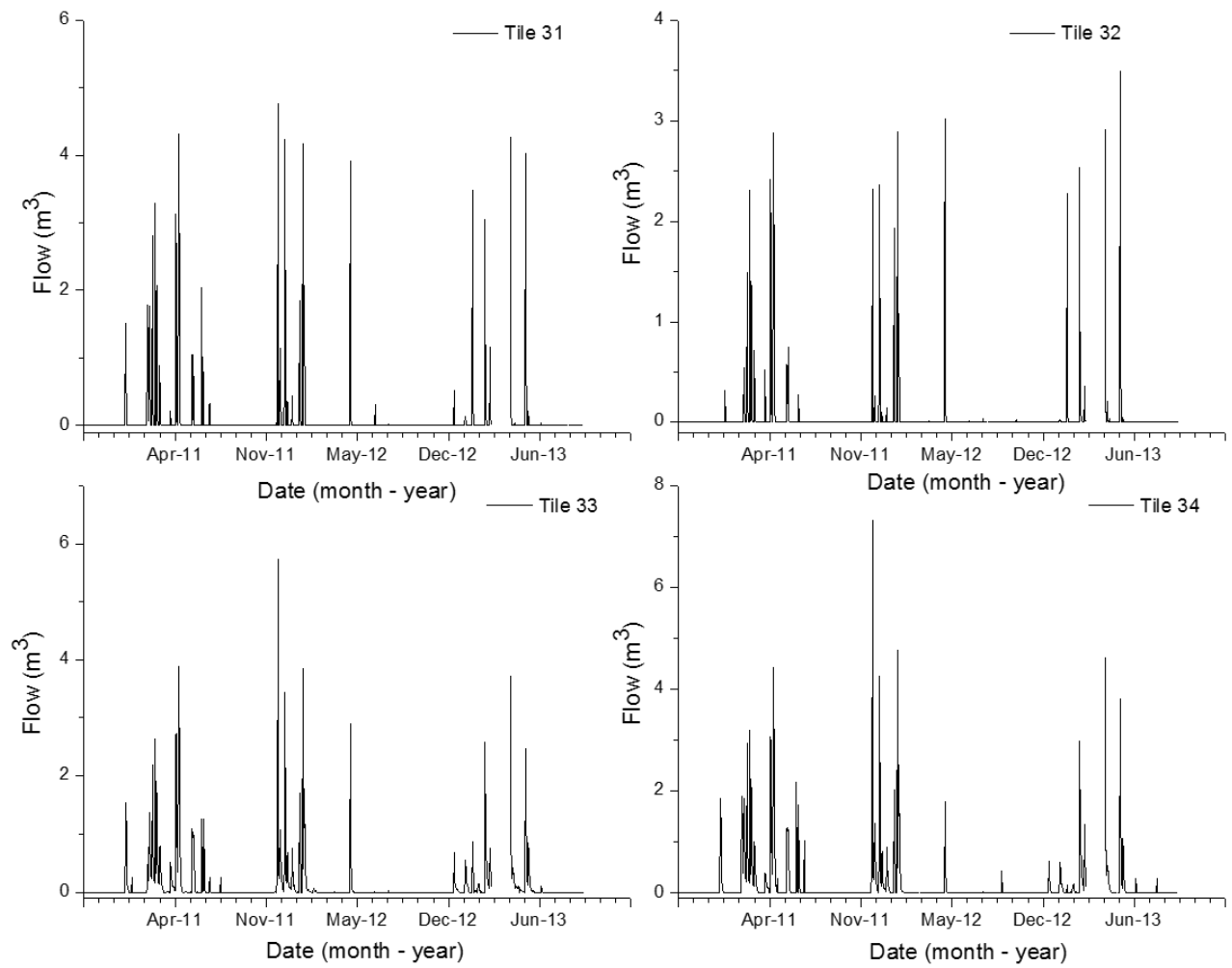


Figure A.4 continued

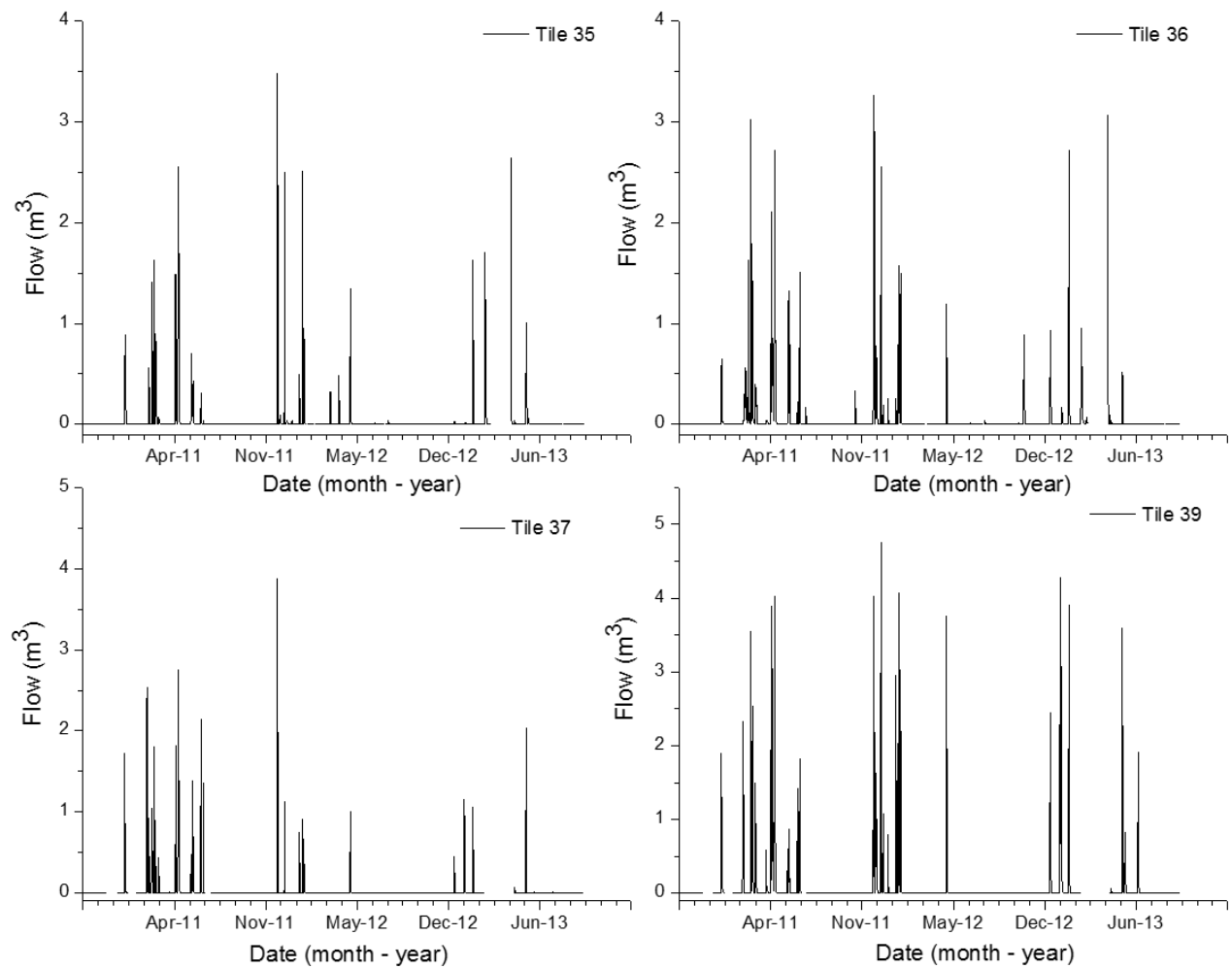


Figure A.4 continued

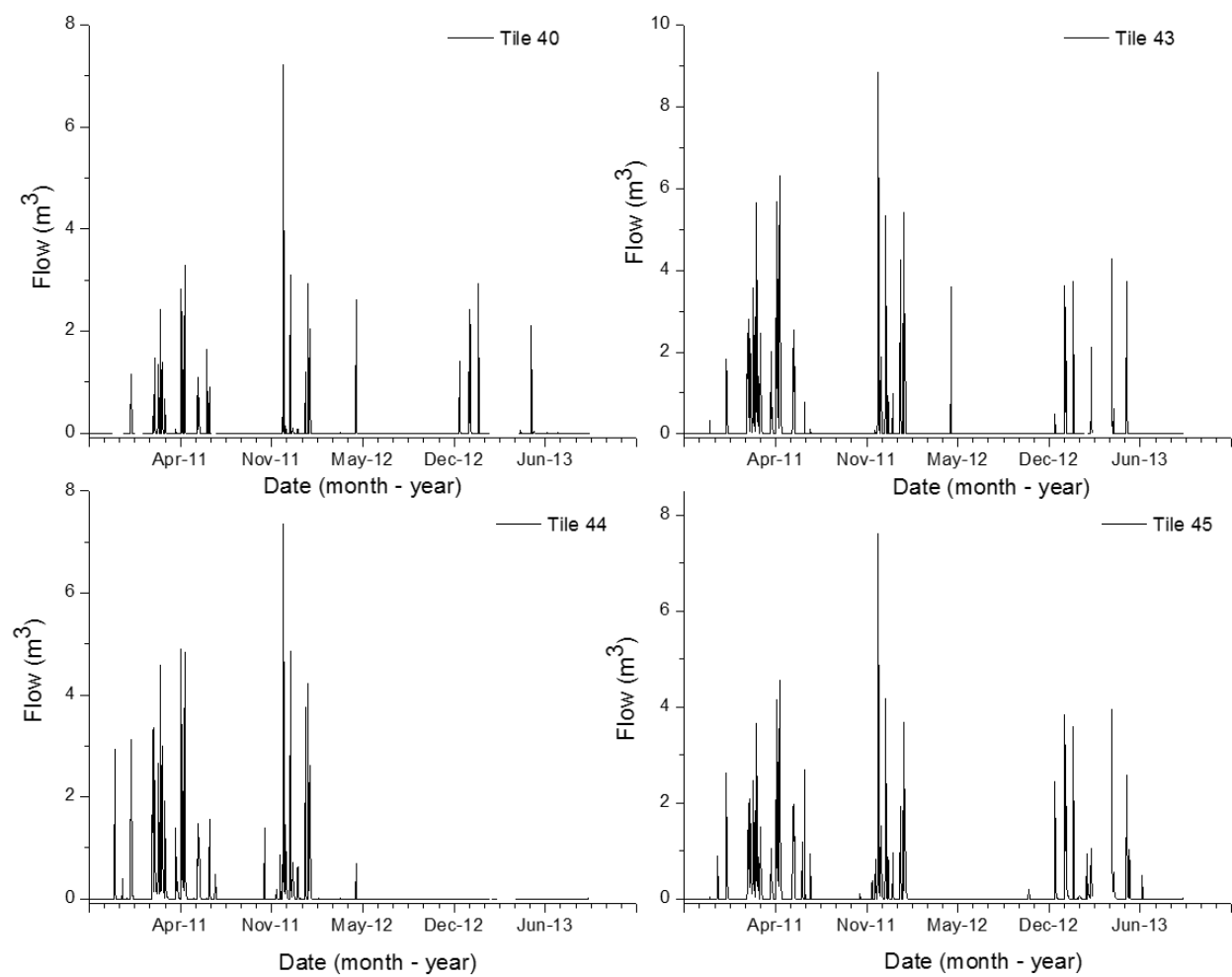
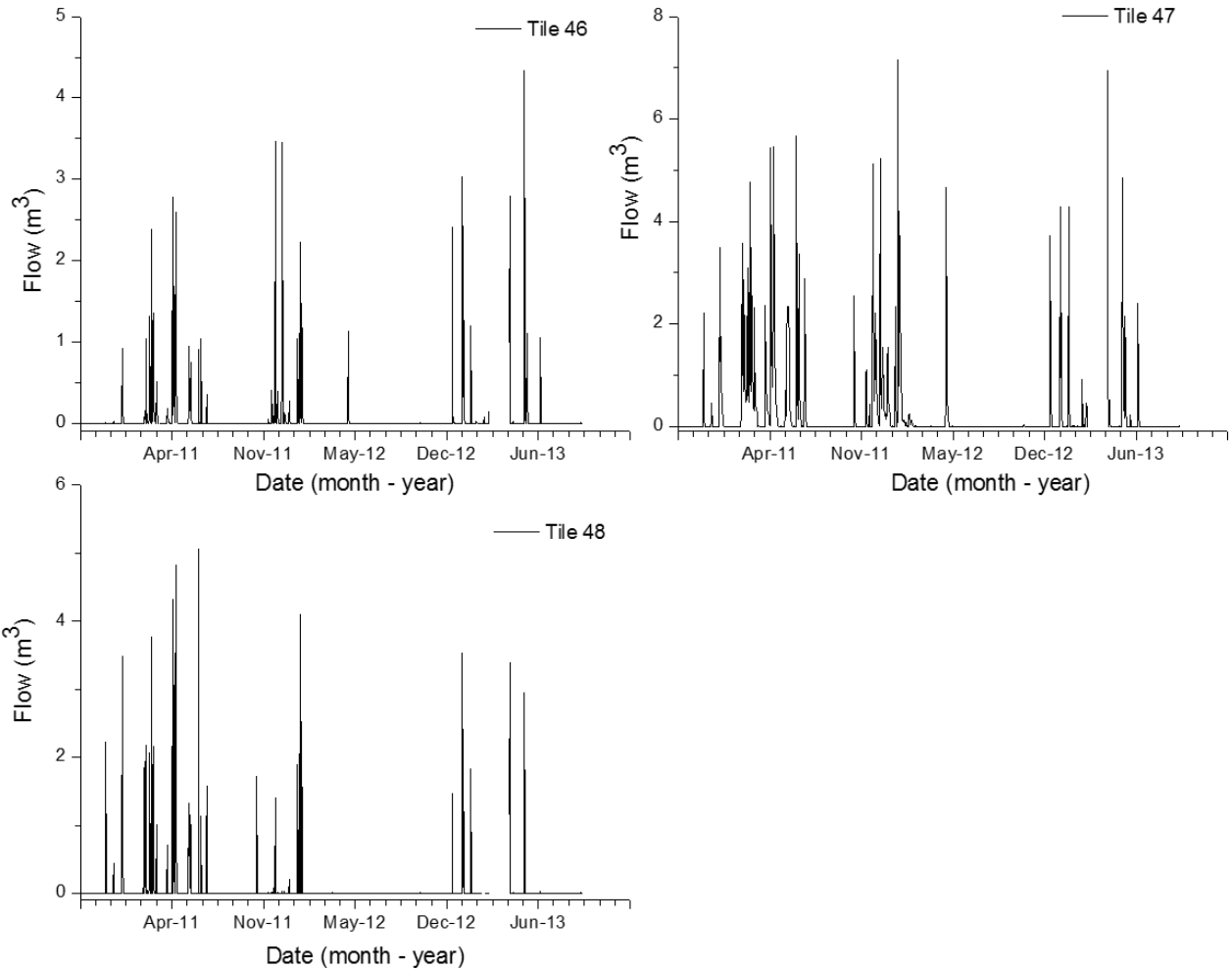


Figure A.4 continued



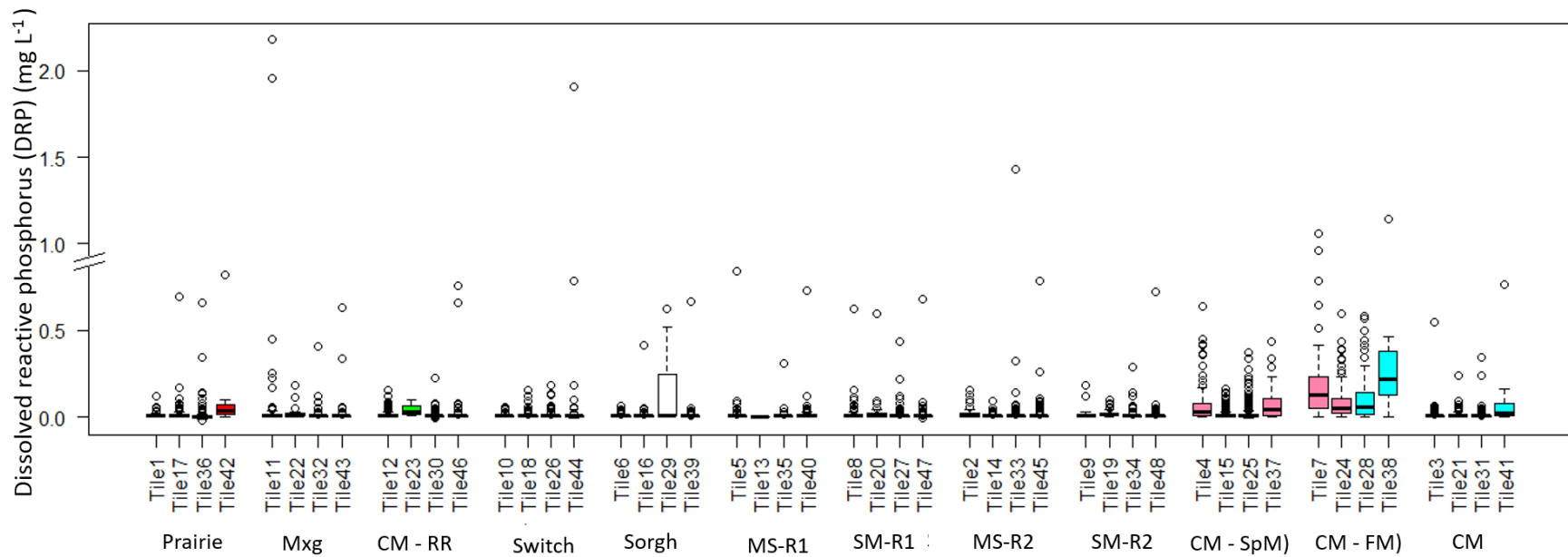


Figure A.5. Boxplots of DRP concentration. Circles represent outliers, whiskers represent the 10th and 90th percentiles, the lower and upper edges of the boxes represent the 25th and 75th percentiles, and the horizontal line inside the boxes represents the median. Tile 42, 22, 23, 13, 2, 9, 38 and, 41, were omitted from the study due to tile failure. Current treatment abbreviations: Prairie, native prairie mixture with residue removed; Mxg, *Miscanthus x giganteus* established in 2008 ; CM -RR, continuous maize with residue removal; Switch, Switchgrass established in spring 2007; Sorgh, continuous sorghum with residue removal established in 2008; MS – R1,maize-soybean rotation trt#1 w/residue return; SM-R1, soybean-maize rotation trt #1 w/residue return; MS – R2, maize-soybean rotation trt#2 w/residue return; SM-R2, soybean-maize rotation trt #1 w/residue return; CM -SpM, continuous maize with residue return and spring manure applications; CM-FM, continuous maize with residue return and fall manure applications; CM, continuous maize with residue return. More details on previous crop, nutrient and tillage management can be found in Table S3 in the main text.

Supplemental references

- Chalmers, J. M. and A. J. Handley. 2006. Inductively coupled plasma spectrometry and its applications analytical chemistry. Steve J. Hill. Blackwell Publishing Ltd, Oxford. <https://onlinelibrary.wiley.com/doi/book/10.1002/9780470988794>.
- Croghan, C. W., and P. P. Egeghy. 2003. Methods of dealing with values below the limit of detection using SAS. Southern SAS User Group, 5.
- Gentry, L. E., M. B. David, T. V. Royer, C. A. Mitchell, and K. M. Starks. 2007. Phosphorus transport pathways to streams in tile-drained agricultural watersheds. *J. Environ. Qual.* 36 (2): 408. <https://doi.org/10.2134/jeq2006.0098>.
- Gotway, C. A., D. R. Helsel, and R. M. Hirsch. 1994. Statistical methods in water resources. *TECHNOMETRICS* 36 (3): 323. <https://doi.org/10.2307/1269385>.
- Hernandez-Ramirez, G., S. M. Brouder, D. R. Smith, and G. E. Van Scoyoc. 2011. Nitrogen partitioning and utilization in corn cropping systems: rotation, N source, and N timing. *Eur. J. Agron.* 34 (3): 190–95. <https://doi.org/10.1016/j.eja.2010.12.002>.
- Hyndman, R. and G. Athanasopoulos. 2014. Forecasting: Principles & Practice. <https://otexts.com/fpp2/>
- Katimon, A., S. Shahid, and M. Mohsenipour. 2017. Modeling Water Quality and Hydrological Variables Using ARIMA: A Case Study of Johor River, Malaysia. *Sustain. Water Resour. Manag.* 4, 991 - 998. <http://link.springer.com/10.1007/s40899-017-0202-8>.
- King, K. W., M. R. Williams, and N. R. Fausey. 2016. Effect of crop type and season on nutrient leaching to tile drainage under a corn-soybean rotation. *J. SOIL WATER CONSERV.* 71 (1): 56–68. <https://doi.org/10.2489/jswc.71.1.56>.
- Loureiro, D., C. Amado, A. Martins, D. Vitorino, A. Mamade, and S. T. Coelho. 2016. Water distribution systems flow monitoring and anomalous event detection: A practical approach. *Urban Water J.* 13, 242–252. <https://doi.org/10.1080/1573062X.2014.988733>
- McLean, E. O. 1982. Soil PH and lime requirement. In: A.L. Page et al., editor, *Methods of Soil Analysis. Part 2.* 2nd Ed. Agron. Monogr. 9. ASA and SSSA, Madison, Wis, 199–224.
- Mehlich, A. 1984. Mehlich 3 soil test extractant: A modification of Mehlich 2 extractant. *Commun. Soil Sci. Plan.* 15 (12): 1409–16. <https://doi.org/10.1080/00103628409367568>.
- Nasir, N., R. Sansudin, and A. Shabri. 2017. Monthly streamflow forecasting with auto-regressive integrated moving average. *J. Phys. Conf. Ser.* 890, 12141. Olsen, S.R., C.V. Cole, F.S.

- Watanabe, and Dean, L.A. 1954. "Estimation of Available Phosphorus in Soils by Extraction with Sodium Bicarbonate." *USDA Circular 939*. U.S. Government Printing Office, Washington D.C.
- Pagano, Thomas C., and David Garen. 2004. "The Recent Increase in Western US Streamflow Variability and Persistence." *Bulletin of the American Meteorological Society*: 4785–89.
- Pagano, T. C. and D. Garen. 2004. The recent increase in Western US streamflow variability and persistence. *Bulletin of the American Meteorological Society*, 4785–89. <https://doi.org/10.1175/JHM410.1>.
- Ruark. 2006. *The Fate of Dissolved Organic Carbon in Tile Drained Agroecosystems*. Ruark. M. D. 2006. The fate of dissolved organic carbon in tile drained agroecosystems. (Order No. 3259974). Available from Agricultural & Environmental Science Collection; Dissertations & Theses @ CIC Institutions; ProQuest Dissertations & Theses Global. (305280542). Retrieved from <https://search.proquest.com/docview/305280542?accountid=13360>
- Ruark, M. D., S. M. Brouder, and R. F. Turco. 2009. Dissolved organic carbon losses from tile drained agroecosystems. *J. Environ. Qual.* 38 (3): 1205. <https://doi.org/10.2134/jeq2008.0121>.
- Scheeringa, K. 2002. About Indiana climate. <https://iclimat.org/about-indiana-climate/>.
- Seo, S. 2006. A Review and Comparison of Methods for Detecting Outliers in Univariate Data Sets. Masters Thesis, University of Pittsburg. <http://d-scholarship.pitt.edu/7948/>.
- Tomer, M. D., D. W. Meek, D. B. Jaynes, and J. L. Hatfield. 2003. Evaluation of nitrate-nitrogen fluxes from a tile-drained watershed in Central Iowa. *J. Environ. Qual.* 32 (2): 642–53. <https://doi.org/10.2134/jeq2003.6420>.
- Trybula, E. 2012. Quantifying Ecohydrologic Impacts of Perennial Rhizomatous Grasses on Tile Discharge: A Plot Level Comparison of Continuous Corn, Upland Switchgrass, Mixed Prairie, and Miscanthus x Giganteus. (Order No. 1535171). Available from Dissertations & Theses @ CIC Institutions; ProQuest Dissertations & Theses Global. (1328160945). Retrieved from <https://search.proquest.com/docview/1328160945?accountid=13360>.
- Tukey, J.W. 1977. *Exploratory Data Analysis*. Addison-Wesely.
- Walkley, A. 1947. A critical examination of a rapid method for determining organic carbon in soils—effect of variations in digestion conditions and of inorganic soil constituents. *Soil Sci.*, no. 63: 251–64.
- Walkley, A., and I. A. Black. 1934. An examination of degtjareff method for determining soil

organic matter and a proposed modification of the chromic acid titration method. *Soil Sci*, no. 37: 29–37.

Watson, M. E. and J. R. Brown. 2011. Chemical soil test procedures for the North Central Region. Program 221 (221). <https://doi.org/10.1007/978-1-4020-6710-5>.

Williams, M. R., K. W. King, and N. R. Fausey. 2015. Drainage water management effects on tile discharge and water quality. *Agr. Water Manage.* 148: 43–51. <https://doi.org/10.1016/j.agwat.2014.09.017>.

SUPPLEMENTAL MATERIALS CHAPTER 3

Table A.9 A brief description of current treatments at the Water Quality Field Station (WQFS) (abbreviations and year of establishment), any previous treatment (cropping system and N rates applied to maize) dating back to 1997, and P, N and tillage management. An estimate of the cumulative P₂O₅ applied from 1997 – 2013 is shown parenthetically. Current N management identifies the N rates applied to perennial crops, sorghum, and continuous and rotated maize. (Table obtained from Welikhe et al. (2020))

Current Treatment (abbrev. /yr. est.) [§]	Previous Treatment (maize N rate, lbs acre ⁻¹ yr ⁻¹) [¶]	Plots [#]	P management (cumulative P ₂ O ₅ applied 1997-2013; lbs acre ⁻¹) ^{††}	Current N management (annual rate, lbs acre ⁻¹ yr ⁻¹)	Tillage
Native prairie mixture (Prairie /1993)	NA	1, 17, 36, 42	No fert. (0)	No fert. (0)	No till since 1993
<i>Miscanthus x giganteus</i> (Mxg /2008)	Annual soybean- maize rotation (148- P)	11, 22 , 32,43	Commercial fertilizer based on STP (148) + starter (66)	Spring broadcast urea (46)	No till since 2008
Continuous maize w/ residue removal (CM-RR /2008)	Continuous maize w/ residue return (166-P)	12, 23 , 30,46	Commercial fertilizer based on STP (218) + starter (224)	Preplant UAN (148) + starter	No till since 2008
Switchgrass var. Shawnee (Switch /2007)	Annual maize- soybean rotation (148-P)	10,18, 26,44	Commercial fertilizer based on STP (148) + starter (66)	Spring broadcast urea (46)	No till since 2007
Continuous sorghum w/ residue removal (Sorgh /2008)	Continuous maize w/ residue return (129-S)	6,16, 29,39	Commercial fertilizer based on STP + starter (145)	Preplant UAN (148)	Till
Maize-soybean rotation trt#1 w/ residue return (MS- R1 /1997)	NA	5,13 , 35,40	Commercial fertilizer based on STP (218) + starter (118)	Preplant UAN (129) + starter	Till
Soybean-maize rotation trt#1 w/ residue return (SM-R1)	NA	8,20, 27,47	Commercial fertilizer based on STP (218) + starter (105)	Preplant UAN (129) + starter	Till
Maize-soybean rotation trt#2 w/ residue return (MS- R2 /1997)	NA	2,14, 33,45	Commercial fertilizer based on STP (218) + starter (118)	Sidedress UAN (111) + starter	Till
Soybean-maize rotation trt#2 w/ residue return (SM- R2 /1997)	NA	9,19 , 34,48	Commercial fertilizer based on STP (218) + starter (105)	Sidedress UAN (111) + starter	Till
Continuous maize w/ residue return & spring manure (CM-SpM /1998)	NA	4,15, 25,37	16 yr annual spring swine effluent (approx. 1201) + starter (224)	Preplant swine effluent (avg. 210) + starter	Till
Continuous maize w/ residue return & fall manure (CM- FM /1998)	NA	7,24, 28, 38	14 yr annual fall swine effluent (approx. 1050) + starter (224)	Post-harvest swine effluent (avg. 210) + starter	Till
Continuous maize w/ residue return (CM /1997)	NA	3,21, 31, 41	Commercial fertilizer based on STP (218) + starter (224)	Preplant UAN (148) + starter	Till

[§] Treatments other than the prairie were variable and not consistently maintained prior to 1997

[¶] N rates are only for the maize year in a rotation with P or S following the rate indicating a preplant or sidedress application. Not application (NA) indicates a treatment was maintained from 1997 – 2013.

[#] An italicized plot number indicates a tile line that ceased to function, and the plot was therefore eliminated from analysis of relationships between soluble P in drainage water and measures of soil P saturation.

^{††} Cumulative P₂O₅ added as commercial fertilizer differs among cropping systems as perennial crops did not receive applications. Cumulative starter P₂O₅ varies reflecting the number of times maize was grown on a specific treatment and includes current and previous systems. Cumulative P₂O₅ applied as manure differs as there were 16 spring applications but only 14 fall applications reflecting weather and termination of both manure treatments in fall 2013; quantities are based on an estimated amount of 75 lbs P₂O₅ acre⁻¹ per application.

Table A.10 Summary for Organic matter (OM) (%), phosphorus (P) (mg kg⁻¹), Aluminum (Al) (mg kg⁻¹), P saturation ratio (PSR) (unitless), Soil P storage capacity (SPSC) (L kg⁻¹), and Annual flow-weighted mean DRP concentrations (fDRP) (mg L⁻¹) obtained from the monitored plots at the Water Quality Field Station (WQFS) for 2011 -2013 water years (e.g. Oct 1, 2010 – Sept 30, 2011 for 2011 water year). Cropping system abbreviation and management histories are provided in supplemental table S1. (Table obtained from Welikhe et al. (2020))

Cropping system	Plot#	2011 water year						2012 water year						2013 water year					
		OM	P	Al	PSR	SPSC	fDRP	OM	P	Al	PSR	SPSC	fDRP	OM	P	Al	PSR	SPSC	fDRP
Prairie	1	4.8	27	846	0.23	-12.02	0.0084	5.1	26	860	0.22	-9.46	0.0055	5.3	29	845	0.23	-14.54	0.0093
	17	4.7	23	758	0.22	-5.55	0.0090	4.7	26	821	0.23	-10.68	0.0299	5.3	24	855	0.22	-5.26	0.0163
	36	4.9	14	788	0.18	19.06	0.0027	4.2	11	785	0.17	28.87	0.0075	5	16	820	0.19	13.31	0.0147
Mxg	11	4.6	26	900	0.22	-10.04	0.0599	5	24	922	0.22	-5.10	0.0217	5.4	25	895	0.22	-6.61	0.0701
	32	3.3	9	734	0.16	35.01	0.0017	3.1	8	798	0.15	41.03	0.0058	3.6	8	753	0.15	41.81	0.0052
	43	4.2	13	767	0.18	20.63	0.0018	3.7	12	811	0.17	23.76	0.0013	4.1	11	770	0.17	28.37	0.0062
CM - RR	12	5.3	27	862	0.23	-10.89	0.0045	5.2	32	969	0.24	-18.34	0.0162	5.6	26	932	0.22	-7.79	0.0214
	30	4.1	11	927	0.17	30.73	0.0020	4.2	12	934	0.17	26.88	0.0068	4.5	21	932	0.21	0.44	0.0064
	46	4.9	22	846	0.21	-1.93	0.0021	4.3	17	916	0.20	10.03	0.0016	5.4	25	906	0.22	-6.50	0.0129
Switch	10	4.8	22	810	0.21	-2.57	0.0036	5	22	883	0.21	-1.30	0.0220	5.4	23	889	0.21	-2.61	0.0031
	18	5	23	810	0.22	-4.30	0.0047	4.9	17	838	0.20	10.41	0.0111	4.9	14	805	0.18	19.31	0.0066
	26	3.6	15	816	0.19	12.91	0.0055	3.8	11	801	0.17	28.04	0.0061	4	10	779	0.16	32.78	0.0086
	44	4.4	16	816	0.19	11.90	0.0043	4.2	11	824	0.17	29.47	0.0017	4.8	13	787	0.18	22.37	0.0000
Sorgh	6	3.7	15	843	0.19	13.55	0.0014	3.9	17	859	0.20	8.31	-	4.6	32	888	0.24	-20.21	0.0018
	16	4.2	25	821	0.22	-9.89	0.0019	4.8	37	806	0.25	-27.60	0.0109	4.7	36	751	0.25	-27.03	0.0029
	39	4.6	34	860	0.24	-23.40	0.0021	4.5	31	916	0.24	-18.62	0.1116	4.8	28	869	0.23	-13.53	0.0029
MS – R1	5	3.8	16	839	0.19	10.69	0.007	3.7	16	875	0.19	10.88	0.0161	4.4	28	944	0.23	-13.64	0.0033
	35	3.7	12	809	0.17	23.73	0.0017	3	12	793	0.18	21.35	0.0079	3.7	16	825	0.19	10.23	0.0050
	40	5.1	33	888	0.24	-20.74	0.0083	5.2	33	840	0.24	-21.03	0.2683	5.1	28	915	0.23	-12.49	0.0106
SM – R1	8	4.9	20	882	0.21	3.10	0.0074	4.8	23	896	0.22	-3.72	0.0131	5.5	27	934	0.22	-9.79	0.0204
	20	5.3	31	886	0.23	-17.37	0.0072	5.7	31	854	0.23	-17.01	0.0274	6	33	839	0.24	-19.75	0.0136
	27	3.7	16	831	0.19	10.31	0.0046	3.4	11	788	0.17	26.68	0.0090	4	11	760	0.17	27.95	0.0028
	47	4.1	20	814	0.21	0.47	0.0023	4.7	15	815	0.19	15.68	0.0054	4.9	19	883	0.20	5.60	0.0030
MS – R2	14	4.8	27	849	0.23	-11.99	0.0029	4.9	24	856	0.22	-6.02	0.0180	4.8	32	846	0.24	-20.22	0.0041
	33	3	10	802	0.16	30.16	0.0023	3.1	11	761	0.17	25.32	0.0054	3.3	12	827	0.18	22.82	0.0082
	45	4.3	25	849	0.22	-9.35	0.0020	3.9	21	809	0.21	-2.43	0.0021	4.6	20	794	0.21	1.38	0.0123
SM – R2	19	4.9	41	904	0.25	-31.51	0.0100	4.6	51	922	0.27	-42.53	0.0185	5.3	52	888	0.27	-42.53	0.0170
	34	3.3	11	811	0.17	26.73	0.0027	3	10	756	0.17	29.42	0.0054	3.5	17	781	0.20	6.19	0.0080
	48	4.6	26	782	0.23	-11.33	0.0061	3.6	25	727	0.23	-12.50	0.1001	5	26	778	0.23	-10.58	0.0115
CM -SpM	4	4.3	59	815	0.28	-50.85	0.1373	4.8	83	811	0.31	-66.38	0.0761	4.6	92	833	0.31	-71.53	0.1368
	15	4.6	89	836	0.31	-69.92	0.1266	4.5	79	769	0.30	-64.76	0.1264	4.7	104	818	0.32	-77.34	0.1617
	25	4.1	74	824	0.30	-62.04	0.1371	4.2	91	763	0.32	-72.07	0.1500	3.9	73	776	0.30	-62.11	0.1251
	37	4.3	56	786	0.28	-48.57	0.0586	3.9	68	774	0.30	-58.74	0.2785	4.9	64	803	0.29	-53.79	0.1718
CM - FM	7	5.4	62	849	0.28	-51.20	0.1928	5.1	88	932	0.31	-68.23	0.1087	5.5	76	995	0.29	-60.27	0.3732
	24	4.9	59	836	0.28	-49.64	0.1194	5.1	73	785	0.30	-59.94	0.1055	5.5	81	827	0.30	-64.18	0.2010
	28	3.4	38	819	0.26	-31.95	0.1609	3.5	41	782	0.26	-35.62	0.1080	4.1	41	813	0.26	-33.87	0.2160
CM	3	3.8	20	846	0.21	0.09	0.0043	4.8	26	967	0.22	-8.96	0.0085	4.4	28	918	0.23	-13.89	0.0055
	21	5.1	43	888	0.26	-33.60	0.0059	5	48	906	0.26	-38.99	0.0123	5.6	50	915	0.27	-39.99	0.0117
	31	3.7	13	819	0.18	20.06	0.0042	3.8	13	774	0.18	19.68	0.0062	4.2	16	822	0.19	11.50	0.0097

Table A.11 Field data (empirical dataset) used to generate the theoretical dataset and for the calculation of PI values. Treatment (cropping system) abbreviation and management histories are provided in supplemental Table S1. Swine manure was applied at rates meant to supply ~ 228 lbs N ha⁻¹ yr.

Plot #	Treatment	Water year	STP (mg kg ⁻¹)	FPR (lbs P ₂ O ₅ A ⁻¹)	FPA (unitless)	OPR (lbs P ₂ O ₅ A ⁻¹)	OPA (unitless)	SE (unitless)	SR (unitless)	SDP (unitless)	DTW (unitless)
1	Prairie	2011	27	0	0	0	0	1	0	4	1
1	Prairie	2012	26	0	0	0	0	1	0	4	1
1	Prairie	2013	29	0	0	0	0	1	0	4	1
2	MS-R2	2011	15	18.96	1	0	0	1	0	4	1
2	MS-R2	2012	17	57.00	4	0	0	1	0	4	1
2	MS-R2	2013	26	18.96	1	0	0	1	0	4	1
3	CM	2011	20	18.96	1	0	0	1	0	4	1
3	CM	2012	26	57.00	4	0	0	1	0	4	1
3	CM	2013	28	18.96	1	0	0	1	0	4	1
4	CM-SpM	2011	59	0	0	81	1	1	0	4	1
4	CM-SpM	2012	83	0	0	81	1	1	0	4	1
4	CM-SpM	2013	92	0	0	81	1	1	0	4	1
5	MS-R1	2011	16	18.96	1	0	0	1	0	4	1
5	MS-R1	2012	16	57.00	4	0	0	1	0	4	1
5	MS-R1	2013	28	18.96	1	0	0	1	0	4	1
6	Sorgh	2011	15	0	0	0	0	1	0	4	1
6	Sorgh	2012	17	57.00	4	0	0	1	0	4	1
6	Sorgh	2013	32	0	0	0	0	1	0	4	1
7	CM-FM	2011	62	0	0	81	1	1	0	4	1
7	CM-FM	2012	88	0	0	81	1	1	0	4	1
7	CM-FM	2013	76	0	0	81	1	1	0	4	1
8	SM-R1	2011	20	18.96	1	0	0	1	0	4	1
8	SM-R1	2012	23	57.00	4	0	0	1	0	4	1
8	SM-R1	2013	27	0	0	0	0	1	0	4	1
10	Switch	2011	22	0	0	0	0	1	0	4	1
10	Switch	2012	22	0	0	0	0	1	0	4	1

Table A.11 continued

Plot #	Treatment	Water year	STP (mg kg ⁻¹)	FPR (lbs P ₂ O ₅ A ⁻¹)	FPA (unitless)	OPR (lbs P ₂ O ₅ A ⁻¹)	OPA (unitless)	SE (unitless)	SR (unitless)	SDP (unitless)	DTW (unitless)
10	Switch	2013	23	0	0	0	0	1	0	4	1
11	Mxg	2011	26	0	0	0	0	1	0	4	1
11	Mxg	2012	24	0	0	0	0	1	0	4	1
11	Mxg	2013	25	0	0	0	0	1	0	4	1
12	CM-RR	2011	27	18.96	1	0	0	1	0	4	1
12	CM-RR	2012	32	0	0	0	0	1	0	4	1
12	CM-RR	2013	26	18.96	1	0	0	1	0	4	1
14	MS-R2	2011	27	18.96	1	0	0	1	0	4	1
14	MS-R2	2012	24	57.00	4	0	0	1	0	4	1
14	MS-R2	2013	32	18.96	1	0	0	1	0	4	1
15	CM-SpM	2011	89	0	0	81	1	1	0	4	1
15	CM-SpM	2012	79	0	0	81	1	1	0	4	1
15	CM-SpM	2013	104	0	0	81	1	1	0	4	1
16	Sorgh	2011	25	0	0	0	0	1	0	4	1
16	Sorgh	2012	37	57.00	4	0	0	1	0	4	1
16	Sorgh	2013	36	0	0	0	0	1	0	4	1
17	Prairie	2011	23	0	0	0	0	1	0	4	1
17	Prairie	2012	26	0	0	0	0	1	0	4	1
17	Prairie	2013	24	0	0	0	0	1	0	4	1
18	Switch	2011	23	0	0	0	0	1	0	4	1
18	Switch	2012	17	0	0	0	0	1	0	4	1
18	Switch	2013	14	0	0	0	0	1	0	4	1
19	SM-R2	2011	41	18.96	1	0	0	1	0	4	1
19	SM-R2	2012	51	57.00	4	0	0	1	0	4	1
19	SM-R2	2013	52	18.96	1	0	0	1	0	4	1
20	SM-R1	2011	31	18.96	1	0	0	1	0	4	1
20	SM-R1	2012	31	57.00	4	0	0	1	0	4	1
20	SM-R1	2013	33	18.96	1	0	0	1	0	4	1

Table A.11 continued

Plot #	Treatment	Water year	STP (mg kg ⁻¹)	FPR (lbs P ₂ O ₅ A ⁻¹)	FPA (unitless)	OPR (lbs P ₂ O ₅ A ⁻¹)	OPA (unitless)	SE (unitless)	SR (unitless)	SDP (unitless)	DTW (unitless)
21	CM	2011	43	18.96	1	0	0	1	0	4	1
21	CM	2012	48	57.00	4	0	0	1	0	4	1
21	CM	2013	50	18.96	1	0	0	1	0	4	1
24	CM-FM	2011	59	0	0	81	1	1	0	4	1
24	CM-FM	2012	73	0	0	81	1	1	0	4	1
24	CM-FM	2013	81	0	0	81	1	1	0	4	1
25	CM-SpM	2011	74	0	0	81	1	1	0	4	1
25	CM-SpM	2012	91	0	0	81	1	1	0	4	1
25	CM-SpM	2013	73	0	0	81	1	1	0	4	1
26	Switch	2011	15	0	0	0	0	1	0	4	1
26	Switch	2012	11	0	0	0	0	1	0	4	1
26	Switch	2013	10	0	0	0	0	1	0	4	1
27	SM-R1	2011	16	18.96	1	0	0	1	0	4	1
27	SM-R1	2012	11	57.00	4	0	0	1	0	4	1
27	SM-R1	2013	11	18.96	1	0	0	1	0	4	1
28	CM-FM	2011	38	0	0	81	1	1	0	4	1
28	CM-FM	2012	41	0	0	81	1	1	0	4	1
28	CM-FM	2013	41	18.96	1	81	1	1	0	4	1
30	CM-RR	2011	11	18.96	1	0	0	1	0	4	1
30	CM-RR	2012	12	57.00	4	0	0	1	0	4	1
30	CM-RR	2013	21	18.96	1	0	0	1	0	4	1
31	CM	2011	13	18.96	1	0	0	1	0	4	1
31	CM	2012	13	57.00	4	0	0	1	0	4	1
31	CM	2013	16	18.96	1	0	0	1	0	4	1
32	Mxg	2011	9	0	0	0	0	1	0	4	1
32	Mxg	2012	8	0	0	0	0	1	0	4	1
32	Mxg	2013	8	0	0	0	0	1	0	4	1
33	MS-R2	2011	10	18.96	1	0	0	1	0	4	1

Table A.11 continued

Plot #	Treatment	Water year	STP (mg kg ⁻¹)	FPR (lbs P ₂ O ₅ A ⁻¹)	FPA (unitless)	OPR (lbs P ₂ O ₅ A ⁻¹)	OPA (unitless)	SE (unitless)	SR (unitless)	SDP (unitless)	DTW (unitless)
33	MS-R2	2012	11	57.00	4	0	0	1	0	4	1
33	MS-R2	2013	12	18.96	1	0	0	1	0	4	1
34	SM-R2	2011	11	18.96	1	0	0	1	0	4	1
34	SM-R2	2012	10	57.00	4	0	0	1	0	4	1
34	SM-R2	2013	17	18.96	1	0	0	1	0	4	1
35	MS-R1	2011	12	18.96	1	0	0	1	0	4	1
35	MS-R1	2012	12	57.00	4	0	0	1	0	4	1
35	MS-R1	2013	16	18.96	1	0	0	1	0	4	1
36	Prairie	2011	14	0	0	0	0	1	0	4	1
36	Prairie	2012	11	0	0	0	0	1	0	4	1
36	Prairie	2013	16	0	0	0	0	1	0	4	1
37	CM-SpM	2011	56	0	0	81	1	1	0	4	1
37	CM-SpM	2012	68	0	0	81	1	1	0	4	1
37	CM-SpM	2013	64	0	0	81	1	1	0	4	1
39	Sorgh	2011	34	0	0	0	0	1	0	4	1
39	Sorgh	2012	31	57.00	4	0	0	1	0	4	1
39	Sorgh	2013	28	0	0	0	0	1	0	4	1
40	MS-R1	2011	33	18.96	1	0	0	1	0	4	1
40	MS-R1	2012	33	57.00	4	0	0	1	0	4	1
40	MS-R1	2013	28	18.96	1	0	0	1	0	4	1
43	Mxg	2011	13	0	0	0	0	1	0	4	1
43	Mxg	2012	12	0	0	0	0	1	0	4	1
43	Mxg	2013	11	0	0	0	0	1	0	4	1
44	Switch	2011	16	0	0	0	0	1	0	4	1
44	Switch	2012	11	0	0	0	0	1	0	4	1
44	Switch	2013	13	0	0	0	0	1	0	4	1
45	MS-R2	2011	25	18.96	1	0	0	1	0	4	1
45	MS-R2	2012	21	57.00	4	0	0	1	0	4	1

Table A.11 continued

Plot #	Treatment	Water year	STP (mg kg⁻¹)	FPR (lbs P₂O₅ A⁻¹)	FPA (unitless)	OPR (lbs P₂O₅ A⁻¹)	OPA (unitless)	SE (unitless)	SR (unitless)	SDP (unitless)	DTW (unitless)
45	MS-R2	2013	20	18.96	1	0	0	1	0	4	1
46	CM-RR	2011	22	18.96	1	0	0	1	0	4	1
46	CM-RR	2012	17	57.00	4	0	0	1	0	4	1
46	CM-RR	2013	25	18.96	1	0	0	1	0	4	1
47	SM-R1	2011	20	18.96	1	0	0	1	0	4	1
47	SM-R1	2012	15	57.00	4	0	0	1	0	4	1
47	SM-R1	2013	19	18.96	1	0	0	1	0	4	1
48	SM-R2	2011	26	18.96	1	0	0	1	0	4	1
48	SM-R2	2012	25	57.00	4	0	0	1	0	4	1
48	SM-R2	2013	26	18.96	1	0	0	1	0	4	1

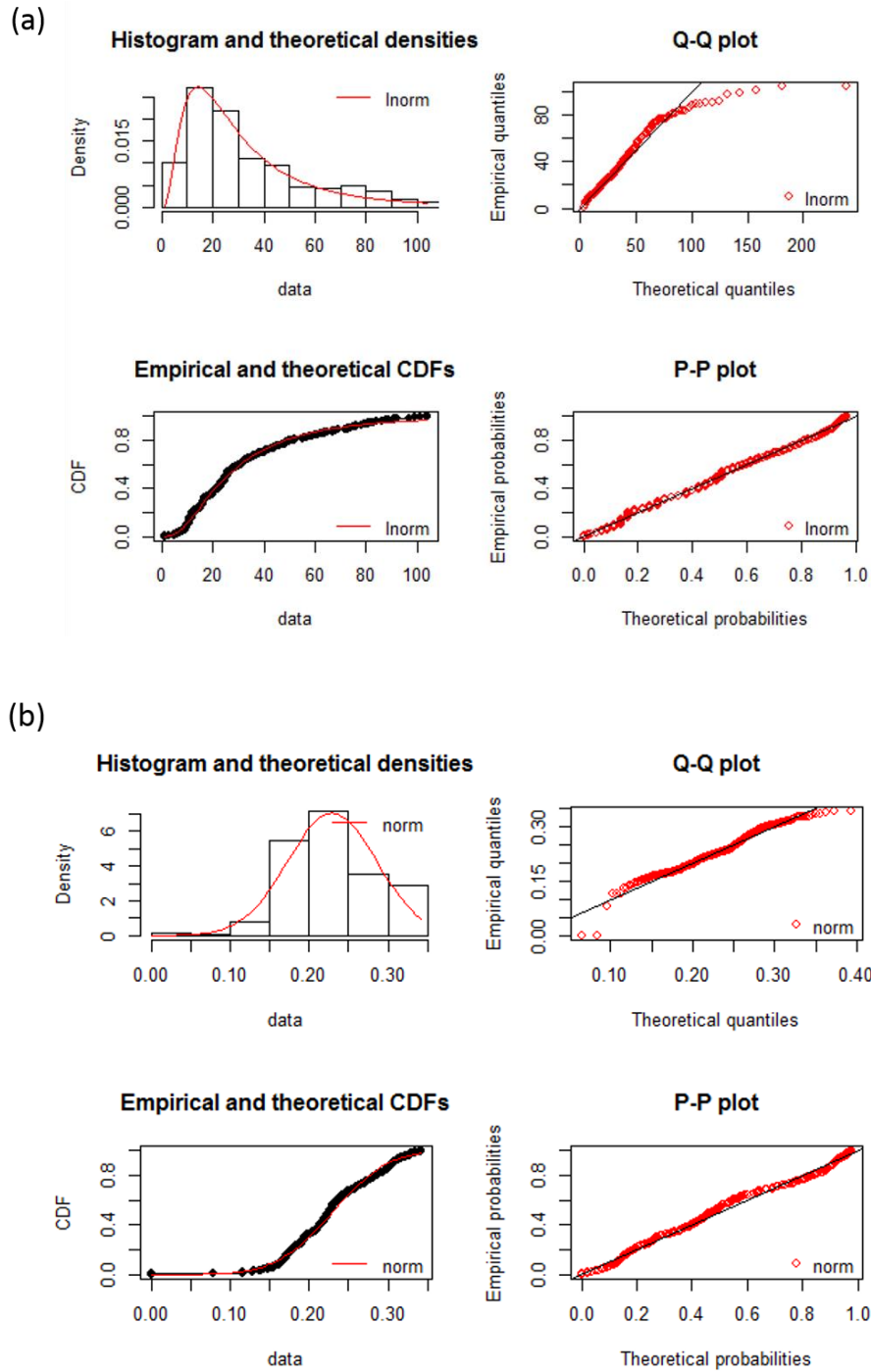


Figure A.6 Histogram and theoretical densities, Q-Q plot, empirical and theoretical cumulative distribution functions and P-P plots for the (a) Mehlich 3 soil test P log-normal (lnorm) distribution, (b) P saturation ratio normal (norm) distribution, and (c) Soil P storage capacity normal (norm) distribution.

Figure continued

(c)

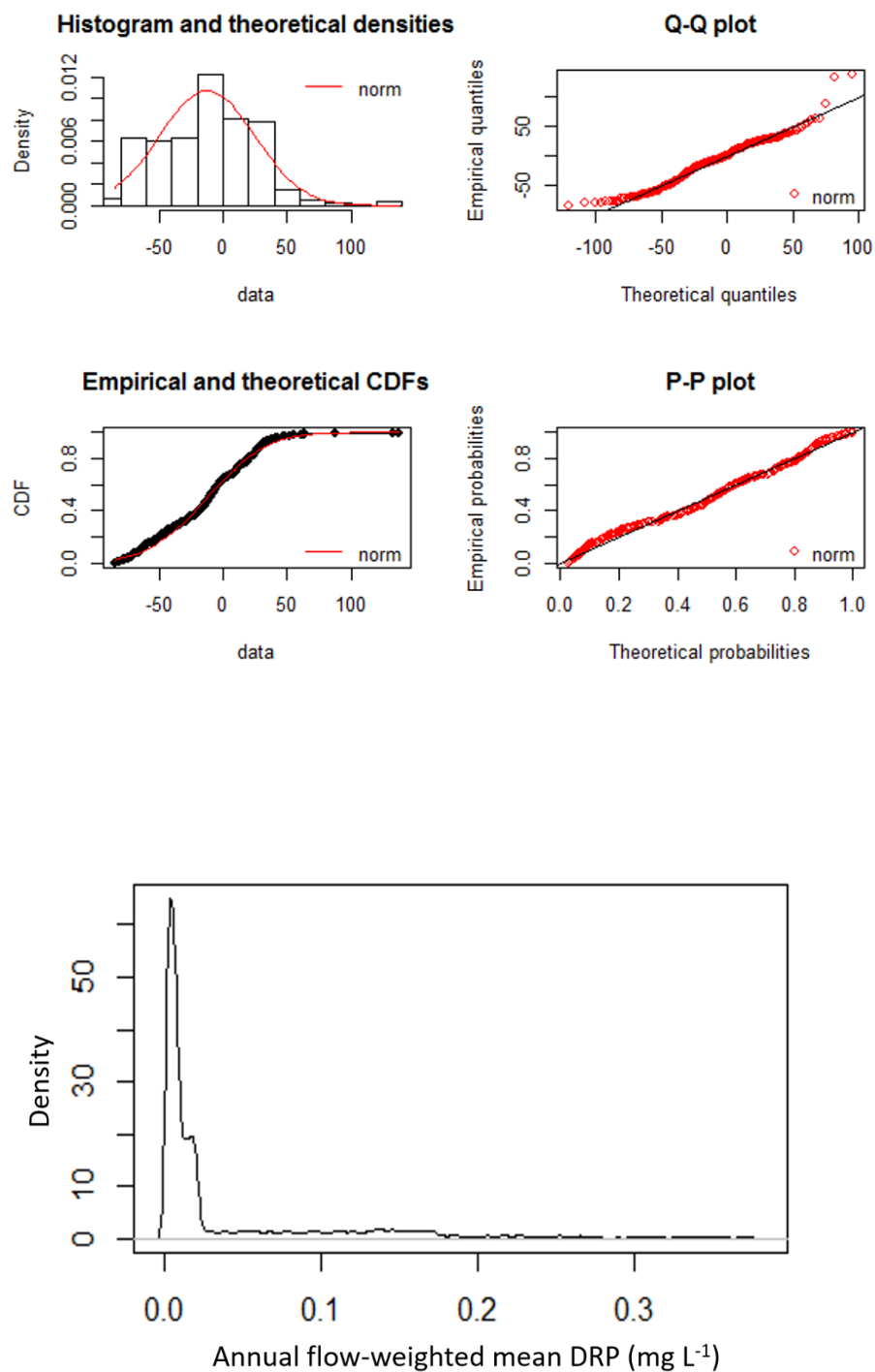


Figure A.7 Density plot showing the distribution of annual flow-weighted mean DRP values.

References

- IN-NRCS. (2013). *Indiana Nutrient and Sediment Transport Risk Assessment Tool (NASTRAT)*. (November), 1–15.
- Welikhe, P., Brouder, S. M., Volenec, J. J., Gitau, M., and Turco, R. F. (2020). Development and Evaluation of Phosphorus Sorption Capacity- based Environmental Indices. *Journal of Environmental Quality* <https://doi.org/10.1002/jeq2.20044>

PUBLICATION

1. Welikhe, P., Brouder, S. M., Volenec, J. J., Gitau, M., & Turco, R. F. (2020). Development of phosphorus sorption capacity – Based environmental indices for Tile-drained systems. *Journal of Environmental Quality*, (January), 1–14. <https://doi.org/10.1002/jeq2.20044>